

DIFFUSION IN REGULAR AND DISORDERED LATTICES

J.W. HAUS

Physics Department, Rensselaer Polytechnic Institute, Troy, New York 12181, U.S.A

and

K.W. KEHR

Institut fuer Festkoerperforschung der Kernforschungsanlage Juelich, D-5170 Juulich, F.R. Germany

Received December 1986

Contents:

1. Introduction	265	6.4. Effective medium approximation	333
2. Poissonian random walk on regular lattices	267	6.5. The percolation problem	338
2.1. Discrete random walk	267	6.6. Renormalization-group methods	340
2.2. Markoffian master equation	269	6.7. Non-Markoffian nature of results	344
2.3. Poissonian random walk with recursion relations	272	7. Lattice models with random traps	348
2.4. Extensions	274	7.1. Introduction to the model	348
2.5. Energetically inequivalent sites	279	7.2. Exact result for the mean-square displacement	349
3. Continuous-time random walks on regular lattices	282	7.3. Exact results: Higher moments	351
3.1. Waiting-time distributions and time homogeneity	282	7.4. Approximate treatments	353
3.2. Continuous-time random walk by recursion relations	284	8. Diffusion on some irregular and fractal structures	356
3.3. Equivalence with generalized master equation	287	8.1. Diffusion on chains with irregular bond lengths	356
3.4. Multistate continuous-time random walks	289	8.2. Random walk on a random walk	359
4. Random walks with correlated jumps	291	8.3. Diffusion in lattices with inaccessible sites	361
4.1. Historical survey; one-dimensional models	291	8.4. Random walks on fractals	364
4.2. Model with reduced reversals/backward jump model	295	9. First-passage time problems	369
4.3. Other models with correlated walks	300	9.1. First passage to a site on a linear chain	369
4.4. Some properties of correlated continuous-time random walks	304	9.2. Relation between first-passage time distribution and conditional probability and applications	372
4.5. Applications of correlated walks	305	9.3. Survival probability of particles diffusing in the presence of traps	376
5. Multiple-trapping models	308	9.4. Reemission and recapture	384
5.1. The two-state model	308	10. Biased random walks	386
5.2. Multiple-trapping models	312	10.1. Introduction	386
5.3. Direct derivation of waiting-time distributions for multistate trapping models	315	10.2. Biased continuous-time random walk models	388
5.4. Decomposition into number of state changes	318	10.3. Random lattices with a constant bias	391
6. Lattice models with random barriers	321	10.4. Models with a random bias	395
6.1. Introduction	321	Acknowledgments	399
6.2. Exact results in one dimension	322	References	399
6.3. The broken-bond model	330	Notes added in proof	405

Single orders for this issue

PHYSICS REPORTS (Review Section of Physics Letters) 150, Nos. 5 & 6 (1987) 263-416.

Copies of this issue may be obtained at the price given below. All orders should be sent directly to the Publisher. Orders must be accompanied by check.

Single issue price Dfl. 101.00, postage included.

DIFFUSION IN REGULAR AND DISORDERED LATTICES

J.W. HAUS

Physics Department, Rensselaer Polytechnic Institute, Troy, New York 12181, U.S.A.

and

K.W. KEHR

Institut fuer Festkoerperforschung der Kernforschungsanlage Juelich, D-5170 Juelich, F.R. Germany



NORTH-HOLLAND – AMSTERDAM

Abstract:

Classical diffusion of single particles on lattices with frozen-in disorder is surveyed. The methods of continuous-time random walk theory are pedagogically developed and applications to solid-state physics are discussed. The first part of the review treats models with regular transition rates; these models possess internal structure or correlations over two jumps and complete solutions are given for each case. The second part of the review covers models with disorder in the transition rates and irregular lattices. For these problems too, explicit calculations and methods are explained and discussed.

1. Introduction

Die Wissenschaft, sie ist und bleibt,
Was einer ab vom andern schreibt.
Doch trotzdem ist, ganz unbestritten,
sie immer weiter fortgeschritten.

Eugen Roth, Roth's Tierleben

This review surveys random walks of single particles in ordered and disordered lattices. These walks may serve as models of classical particle transport in ordered and disordered solids. Random-walk theory on ordered lattices has been extended far beyond uncorrelated walks with constant transition rates. Furthermore, methods of statistical averaging have been developed to deal with random walks on lattices with static disorder. It is the intent of the authors to present a systematic, yet pedagogical, discussion of these methods and to give details of the derivations of the results.

The random-walk models are treated here under the perspective of their applicability to solid-state physics, but the methods presented have applications in many fields. The authors hope that a broad readership will find the presentation useful. There are many results which are not found in any review (some results are new) and the results of several researchers on the same problem are presented in a unified notation. Though the models are motivated by solid-state applications, there have been many parallel pure mathematical and interdisciplinary (biology, chemistry and physics) developments. The authors found it necessary to impose a constraint on the citations. The main criterion for selection was the paper's contribution to the coherence of the presentation. Despite this constraint, over 300 articles are cited and even this list cannot be considered to be complete.

In the review the diffusion of a particle is described by stochastic methods. That is, probability concepts are used and the information about the particle's dynamics is contained in a statistical quantity called a probability distribution on the lattice. The dynamics is formulated either in terms of enumerating the individual transitions of the particle from one site to another (random walk description) or in terms of rate equations for the probability distribution, the so-called master equation. The first formulation requires that the transitions be summed and weighted according to their frequency of occurrence; this powerful method is derived in chapters 2 and 3; first simple models are considered, then more complicated situations are introduced. Of course, the equivalence of this method to the master-equation approach is shown. Most of the review is devoted to continuous-time random walks; however, discrete-time random walks have also been included.

The justification of the stochastic methods must be sought in the complicated Hamiltonian dynamics of the particle. The particle is coupled to the many degrees of freedom of the lattice and it undergoes rapid and irregular momentum changes by its interaction with the atoms in its environment. As this statement implies, there must be a wide separation of time scales between the particle's motion and the lattice vibrations; the host atom then acts as a random heat bath coupled to the particle and the local minima of the potential form a lattice on which the particle moves. This separation of time scales would allow a description of particle diffusion in terms of Fokker-Planck equations. In a solid the particle

remains near a local minimum of the potential energy for a long time and in an event of short duration it passes through a local saddle point of the potential to get into the next local minimum. Thus there is a second separation of time scales between the duration of the transitions and the mean residence time of the particle near the local minima. It is this second separation that allows the passage to a description of particle diffusion in solids as a random walk between lattice points. Often this second separation is not well justified; however, in the framework of the phenomenological formulation the deviations are included in internal states, more complicated time dependencies of the individual processes, etc. It remains then to derive the parameters of the random-walk models from first principles. Theories that deduce the transition rates between local minima from a combination of Hamiltonian mechanics and statistical mechanics have been developed [1, 2]. The success of these theories relies on a knowledge of the atomic interactions between the host crystal atoms and between the diffusing particle and the host crystal atoms [3].

Stochastic modelling is quite powerful and the methods have been used with great success in laser theory [4], biological systems [5] and chemical dynamics [6]. In solid-state physics, they provide a framework for analyzing experimental results on particle diffusion in ordered and disordered materials and testing models for the underlying dynamics. Stochastic models are of practical importance because they are not difficult to formulate and in many circumstances exact results can be derived. The clarification of the particular circumstances in which these results can be derived is a partial goal of this review.

The subject matter treated in the review can be divided into two parts. The first part, chapters 2–5, covers diffusion in ordered structures. Complications arise from non-Bravais lattices (chapter 2), correlation between successive jumps (chapter 4) and internal structure of the lattice sites (chapter 5). All these complexities can be managed by suitable extensions of random-walk theory. Complete solutions of the probability density are given for all these problems and this subject can be considered to be conceptually well understood, as far as diffusion in ordered solids is concerned. The conceptual difficulties appear when these models are used to describe diffusion in disordered solids.

Considerable progress has been achieved in the last years in the direct treatment of random walks in disordered lattices, cf. chapters 6–10. This progress is partially due to the identification of two prototype models of particle diffusion in disordered solids. The random-barrier model is studied in chapter 6 and the random-trap model in chapter 7; each model has its own simplicities and difficulties. Methods have been developed to give approximate solutions for the prototype models. Long-time asymptotic solutions are derived for specific physical quantities. Complete analytic solutions are available only for special cases in one dimension. Despite their obvious simplicity, both models exhibit a signature of disorder; namely, moments of the particle's displacement have non-analytic time dependence. For instance, the non-analytic time dependence is manifest as a long-time tail of the velocity autocorrelation function. These signatures are disorder specific and do not appear when a periodic distribution of transition rates is assumed, instead of a random distribution of the same transition rates. Both models have disorder only in the transition rates and the particle diffuses on a regular lattice. The regular lattice structure is a difficult restriction to relax and only very special models are discussed in chapter 8 and section 6.5. The authors know of no methods available for analytically treating topologically disordered solids. The above models, as well as the more general models of disordered systems with local and global drift (chapter 10) also exhibit signatures of disorder. In chapter 9 trapping of particles by random walks in the presence of random permanent traps is discussed. This is clearly a non-equilibrium phenomenon, but also here the signatures of disorder become visible.

At the time this review was being organized in 1982, diffusion in disordered media was a subject of

active research. Though four years have intervened before the work was completed, research on this subject has not waned. On the contrary, several important achievements have been published; and the activity shows no signs of diminishing. This shall be most apparent to the reader by the large number of articles cited from the years 1983–1985.

There are several other good reviews and books on the subject of random walks. Weiss and Rubin [7] discuss applications with an emphasis on polymers and on solid-state physics. Montroll and West and the book edited by Shlesinger and West [8] treat special mathematical topics in detail, they also contain historical notes which are interesting reading as well. Excellent mathematical works are Stratonovich's and Feller's two volumes [9, 10] and Spitzer's book [11]. Barber and Ninham's book [12] is another useful source of information on random-walk models. Goel and Richter-Dyn [13] cover applications of stochastic processes to biological systems and van Kampen [14] has many applications of stochastic processes.

2. Poissonian random walk on regular lattices

2.1. Discrete random walk

This chapter treats the random walk of a particle on a translation-invariant lattice where the transitions between the sites occur according to a Poisson process. This is a standard textbook problem and it is described here mainly for introductory and reference purposes. Several extensions are made in this chapter; for instance, the inclusion of the case of non-equivalent sites in the unit cells of non-Bravais lattices is handled.

First the discrete random walk (RW) of a particle on a d -dimensional Bravais lattice is considered. It is conveniently formulated in terms of recursion relations. The sites of the Bravais lattice will be denoted by integer vectors \mathbf{n} . A linear, square, cubic, or hypercubic lattice with lattice spacing a is taken for specific examples. In each step of the discrete RW the particle makes a transition from a given site, say \mathbf{m} , to a set of sites \mathbf{n} with probabilities $p_{\mathbf{n},\mathbf{m}}$. The assumption of lattice-translation invariance requires that $p_{\mathbf{n},\mathbf{m}}$ depends on the difference $\mathbf{n} - \mathbf{m}$ only. The simplest example is provided by nearest-neighbor transitions on cubic lattices in d dimensions,

$$p_{\mathbf{n},\mathbf{m}} = \begin{cases} 1/2d & \text{if } \mathbf{n} \text{ is a nearest neighbor of } \mathbf{m}, \\ 0 & \text{otherwise.} \end{cases} \quad (2.1)$$

Of course, $p_{\mathbf{n},\mathbf{m}}$ must be normalized,

$$\sum_{\mathbf{n}} p_{\mathbf{n},\mathbf{m}} = 1. \quad (2.2)$$

The quantity of interest is the conditional probability $P_{\nu}(\mathbf{n}|\mathbf{l})$ of finding the particle at lattice site \mathbf{n} after ν steps when it started at site \mathbf{l} . The following recursion relation is obvious

$$P_{\nu}(\mathbf{n}|\mathbf{l}) = \sum_{\mathbf{m}} p_{\mathbf{n},\mathbf{m}} P_{\nu-1}(\mathbf{m}|\mathbf{l}). \quad (2.3)$$

The probability $P_{\nu}(\mathbf{n}|\mathbf{l})$ can be expressed by iteration as a ν -fold product over the transition probabilities. In the translation-invariant case the recursion relation is simplified by Fourier transforma-

tion. A large but finite lattice composed of $L^d = N$ unit cells is considered and periodic boundary conditions are imposed. The Fourier transformation is defined by

$$P_\nu(\mathbf{k}) = \sum_n \exp[-i\mathbf{k} \cdot (\mathbf{R}_n - \mathbf{R}_l)] P_\nu(\mathbf{n} | \mathbf{l}). \quad (2.4)$$

The Fourier transform of the spatial transition probabilities $p_{n,m}$ is called the 'structure function'; another name is the 'characteristic function'. It is given for nearest-neighbor transitions on the simple-cubic lattices by

$$p(\mathbf{k}) = \frac{1}{d} \sum_{i=1}^d \cos(ak_i), \quad (2.5)$$

where a is the lattice constant. It should be noted that $p(\mathbf{k})$ generally reflects the structure of the reciprocal lattice, e.g., it is periodic with period $2\pi\mathbf{G}$ where \mathbf{G} is a vector of the reciprocal lattice.

In Fourier space the iteration of eq. (2.3) leads to

$$P_\nu(\mathbf{k}) = p^\nu(\mathbf{k}), \quad (2.6)$$

where $p_0(\mathbf{m} | \mathbf{l}) = \delta_{\mathbf{m},\mathbf{l}}$ was used. From this formula the elementary expression for the probability distribution of the 1-dimensional RW after n steps is easily obtained. For symmetric nearest-neighbor jumps $p(k) = \cos(ka)$. Inverse Fourier transformation of eq. (2.6) yields [15, 16]

$$P_\nu(n | m) = \left(\frac{1}{2}\right)^\nu \nu! / \left\{ \left(\frac{\nu + m - n}{2}\right)! \left(\frac{\nu - m + n}{2}\right)! \right\}. \quad (2.7)$$

The generating function $P(\mathbf{n}; \xi)$ of the discrete RW is very useful for general considerations. It is defined by

$$P(\mathbf{n}; \xi) = \sum_{\nu=0}^{\infty} \xi^\nu P_\nu(\mathbf{n}). \quad (2.8)$$

Evidently

$$P_\nu(\mathbf{n}) = \frac{1}{\nu!} \left. \frac{d^\nu P(\mathbf{n}; \xi)}{d\xi^\nu} \right|_{\xi=0}. \quad (2.9)$$

An equation for the generating function is obtained by multiplying the recursion relation eq. (2.3) by ξ^ν and summing from $\nu = 1$ to ∞

$$P(\mathbf{n}; \xi) - \xi \sum_m p_{n,m} P(\mathbf{m}; \xi) = P_0(\mathbf{n}). \quad (2.10)$$

Again this equation is simplified by Fourier transformation. Its solution is

$$P(\mathbf{k}; \xi) = [1 - \xi p(\mathbf{k})]^{-1}. \quad (2.11)$$

ν -fold differentiation of this result according to eq. (2.9) yields the previous result eq. (2.6).

2.2. Markoffian master equation

In this section the RW of a particle on a translation-invariant lattice is considered where the transitions of the particle are assumed to represent a Poisson process in time. The transition rate from a site to a nearest-neighbor site will be called Γ ; further-neighbor jumps will be ignored until section 2.4 for simplicity. As the discrete RW, so too the time-continuous RW is a Markoff process, i.e., the present state is determined by the past state at a particular time, but not by a more detailed sequence of states. The object of interest is now the conditional probability $P(\mathbf{n}, t | \mathbf{l}, 0)$ of finding the particle at site \mathbf{n} at time t when it started at site \mathbf{l} at time 0. It is also assumed that the process is time-homogeneous, i.e., no time point is distinguished. The Markoff property requires that the conditional probability obeys the Chapman–Kolmogoroff equation [17]

$$P(\mathbf{n}, t | \mathbf{l}, 0) = \sum_{\mathbf{m}} P(\mathbf{n}, t | \mathbf{m}, t') P(\mathbf{m}, t' | \mathbf{l}, 0), \tag{2.12}$$

where $t > t' > 0$. If $t = t' + \tau$ is chosen with a small τ then

$$P(\mathbf{n}, t' + \tau | \mathbf{m}, t') = \begin{cases} \Gamma\tau & \mathbf{n}, \mathbf{m} \text{ nearest neighbors,} \\ 1 - z\Gamma\tau & \mathbf{n} = \mathbf{m}, \\ 0 & \text{otherwise.} \end{cases} \tag{2.13}$$

z is the number of nearest-neighbor sites, also called the coordination number. The first and third line are consequences of the assumption of a Poisson process with transition rate Γ , the second line follows from particle conservation. In the limit of infinitesimally small τ , the master equation is found,

$$\frac{d}{dt} P(\mathbf{n}, t | \mathbf{l}, 0) = \Gamma \sum_{\langle \mathbf{m}, \mathbf{n} \rangle} [P(\mathbf{m}, t | \mathbf{l}, 0) - P(\mathbf{n}, t | \mathbf{l}, 0)]. \tag{2.14}$$

The notation $\langle \mathbf{m}, \mathbf{n} \rangle$ designates \mathbf{m} as the nearest-neighbor site of \mathbf{n} .

It is useful to define a transition rate matrix $A_{\mathbf{n}, \mathbf{m}}$. This matrix contains as off-diagonal elements, the negative transition rates from site \mathbf{m} to site \mathbf{n} , the diagonal elements give the total transition rate originating at the sites \mathbf{n} . With this new notation the master equation is

$$\frac{dP(\mathbf{n}, t | \mathbf{l}, 0)}{dt} = - \sum_{\mathbf{m}} A_{\mathbf{n}, \mathbf{m}} P(\mathbf{m}, t | \mathbf{l}, 0). \tag{2.14'}$$

The master equation is easily solved after Fourier and Laplace transformation. The Laplace transformation is defined by

$$\tilde{P}(\mathbf{k}, s) = \int_0^\infty dt \exp(-st) P(\mathbf{k}, t), \tag{2.15}$$

the equation then has the form

$$\{s - z\Gamma[p(\mathbf{k}) - 1]\} \tilde{P}(\mathbf{k}, s) = P(\mathbf{k}, t = 0) = 1, \tag{2.16}$$

where $p(\mathbf{k})$ is the structure function introduced in eq. (2.5) for simple cubic lattices. Thus, it is clear

from this equation that the conditional probability is also the Green function for the master equation. The solution of eq. (2.16) is immediate, and one has in the time domain

$$P(\mathbf{k}, t) = \exp[-\Lambda(\mathbf{k}) t], \quad (2.17)$$

where

$$\Lambda(\mathbf{k}) = z\Gamma[1 - p(\mathbf{k})] \quad (2.18)$$

is the Fourier transform of the previously defined transition-rate matrix.

Moments of the probability distribution are also important physical quantities. From the definition of the Fourier transform, the second moment or mean-square displacement of the particle is:

$$\langle \tilde{r}^2 \rangle(s) = -\nabla_{\mathbf{k}}^2 \tilde{P}(\mathbf{k}, s)|_{\mathbf{k}=\mathbf{0}}, \quad (2.19)$$

in the Laplace-transformed representation and

$$\langle r^2 \rangle(t) = -\nabla_{\mathbf{k}}^2 P(\mathbf{k}, t)|_{\mathbf{k}=\mathbf{0}}, \quad (2.20)$$

using the representation of the conditional probability with the time variable. From eqs. (2.16) and eq. (2.17) the explicit results for the mean-square displacement in these representations and for simple-cubic lattices are:

$$\langle \tilde{r}^2 \rangle(s) = 2d\Gamma a^2/s^2, \quad (2.21)$$

and

$$\langle r^2 \rangle(t) = 2d\Gamma a^2 t. \quad (2.22)$$

From this expression the diffusion coefficient is deduced

$$D = \Gamma a^2 = a^2/2d\tau, \quad (2.23)$$

and $\tau = (2d\Gamma)^{-1}$ is the mean residence time of the particle at a site. The fourth moment of the particle's position also finds application in later chapters. A definition of the fourth moment is:

$$\langle \tilde{r}^4 \rangle(s) = \sum_{i=1}^d \frac{\partial^4}{\partial k_i^4} \tilde{P}(\mathbf{k}, s)|_{\mathbf{k}=\mathbf{0}}, \quad (2.24)$$

in the Laplace-variable representation. For concreteness the expression of this moment for the hypercubic lattices is:

$$\langle \tilde{r}^4 \rangle(s) = 24d\Gamma^2 a^4/s^3 + 2d\Gamma a^4/s^2. \quad (2.25)$$

In the time representation this result is:

$$\langle r^4 \rangle(t) = 12d\Gamma^2 a^4 t^2 + 2d\Gamma a^4 t. \tag{2.26}$$

The probability distribution can be analytically calculated for many lattices in space and time representation. From eq. (2.17) and the inverse Fourier transformation, the result for the hypercubic lattice is:

$$P(\mathbf{n}, t) = \frac{a^d}{(2\pi)^d} \exp(-2d\Gamma t) \int_{-\pi/a}^{\pi/a} d^d k \prod_{i=1}^d [\exp\{ik_i n_i a - 2\Gamma t \cos(k_i a)\}]. \tag{2.27}$$

The symmetry of the integrands allows the replacement $\exp(ik_i n_i)$ with $\cos(k_i n_i)$ and each integral is independent. The integrals are the definitions of the modified Bessel functions, $I_m(2\Gamma t)$, the final expression is:

$$P(\mathbf{n}, t) = \exp(-2d\Gamma t) \prod_{i=1}^d I_{n_i}(2\Gamma t). \tag{2.28}$$

As $t \rightarrow 0$, all the modified Bessel functions approach zero except for $I_0(2\Gamma t)$, which approaches unity. For long times, the asymptotic properties of the Bessel function give:

$$P(\mathbf{0}, t) = (4\pi\Gamma t)^{-d/2}. \tag{2.29}$$

In particular, for $\mathbf{n} = 0$ the particle disappears from the initial site with an inverse power law which depends on the dimension of the lattice.

For completeness the representation of the conditional probability is given for the space and Laplace-variable representation in 1 dimension. The inverse Fourier transform of eq. (2.16) for the linear chain is:

$$\tilde{P}(n, s) = \frac{a}{2\pi} \int_{-\pi/a}^{\pi/a} dk \frac{\exp(inka)}{[s + 2\Gamma(1 - \cos ka)]}. \tag{2.30}$$

The integral can be most simply evaluated by contour integration. Define the variable $Z = \exp(ika)$, then

$$\tilde{P}(n, s) = \frac{1}{2\pi i} \int_C dZ \frac{Z^n}{(s + 2\Gamma)Z - \Gamma - \Gamma Z^2}, \tag{2.31}$$

where the initial site is chosen to be the origin. The contour C is closed on the unit circle. The denominator contains two simple poles:

$$Z_{\pm} = \frac{s + 2\Gamma}{2\Gamma} \pm \frac{\sqrt{s(s + 4\Gamma)}}{2\Gamma}. \tag{2.32}$$

Furthermore, for $n > 0$, there is an n th order pole at infinity and for $n < 0$ there is an n th order pole at the origin. The contour integration is carried out so that these poles are excluded. For short times $s \rightarrow -\infty$, and the pole Z_+ is inside the unit circle, whereas Z_- is outside the unit circle. The result is:

$$\tilde{P}(n, s) = \begin{cases} Z_+^n / \Gamma(Z_+ - Z_-), & n \geq 0, \\ Z_-^n / \Gamma(Z_+ - Z_-), & n \leq 0. \end{cases} \quad (2.33)$$

The definitions of the moments and the probability distributions calculated above are often referred to in the following chapters of this review.

An important application of this result is the derivation of the cross section of incoherent quasielastic scattering on single particles diffusing in crystals. Van Hove [18] showed that this cross section is proportional to the spatial and temporal Fourier transform of a self-correlation function $P_s(\mathbf{r}, t)$. In the classical approximation the self-correlation function is identical to the conditional probability introduced above. The incoherent quasielastic dynamical structure function is related to $\tilde{P}(\mathbf{r}, s)$ by

$$S_{\text{inc}}(\mathbf{k}, \omega) = \frac{1}{\pi} \text{Re}\{\tilde{P}(\mathbf{k}, s = i\omega)\}. \quad (2.34)$$

The quantity $\tilde{P}(\mathbf{k}, s)$ has been derived above for the model of diffusion of a particle on a Bravais lattice. Hence $S_{\text{inc}}(\mathbf{k}, \omega)$ for diffusion of a particle on a regular Bravais lattice is given by

$$S_{\text{inc}}(\mathbf{k}, \omega) = \frac{1}{\pi} \frac{\Lambda(\mathbf{k})}{\omega^2 + \Lambda^2(\mathbf{k})}. \quad (2.35)$$

The Lorentzian appearing in eq. (2.35) is called 'quasielastic line' and its width is given by $\Lambda(\mathbf{k})$. This width function reflects the structure of the reciprocal lattice, $\Lambda(\mathbf{k})$ is periodic modulo $2\pi\mathbf{G}$ and vanishes at the Bragg points. For small \mathbf{k}

$$\Lambda(\mathbf{k}) \xrightarrow[k \rightarrow 0]{} Dk^2 \quad (2.36)$$

where D is the diffusion coefficient introduced in eq. (2.23).

Chudley and Elliott [19] were the first to apply the master equation (2.14) of jump diffusion to the determination of the cross section for quasielastic incoherent neutron scattering. They intended to provide a quasicrystalline model of a liquid; their result found wide application for diffusion of interstitials in solids, in particular of hydrogen in metals. In this field the structure of the lattice of interstitial sites was a key question; an identification of the lattice of octahedral sites for hydrogen diffusing in the FCC lattice of palladium by the determination of $\Lambda(\mathbf{k})$ was achieved by Rowe et al. [20]. The application of quasielastic incoherent neutron scattering to diffusion in solids, especially of hydrogen in metals, has been reviewed by Springer [21], Richter [22] and Springer and Richter [23].

2.3. Poissonian random walk with recursion relations

Instead of introducing a Markoffian master equation, continuous-time random walks (CTRW) can be treated in complete analogy to discrete RW by using recursion relations. This approach has been introduced by Montroll and Weiss [24] with general waiting-time distributions between successive jumps of the particle. In this section the conditional probability for continuous-time random walk with an underlying Poisson process will be derived by this alternative method.

The conditional probability of finding the particle at lattice site \mathbf{n} at time t when it started at site \mathbf{l} at $t = 0$ is decomposed into the contributions of different numbers ν of transitions,

$$P(\mathbf{n}, t | \mathbf{l}, 0) = \sum_{\nu=0}^{\infty} P_{\nu}(\mathbf{n}, t | \mathbf{l}, 0). \quad (2.37)$$

$P_{\nu}(\mathbf{n}, t | \mathbf{l}, 0)$ is the conditional probability of finding the particle at site \mathbf{n} at time t when it performed exactly ν steps. The following separation can be made for a Markoff process where the spatial transition probabilities and the time dependence are separable,

$$P_{\nu}(\mathbf{n}, t | \mathbf{l}, 0) = P_{\nu}(\mathbf{n} | \mathbf{l}) V_{\nu}(t), \quad (2.38)$$

with $P_{\nu}(\mathbf{n} | \mathbf{l})$ the conditional probability of the discrete RW considered in section 2.1 and $V_{\nu}(t)$ the probability that exactly ν steps have been performed until time t . A recursion relation for $V_{\nu}(t)$ is easily obtained. For a Poisson transition process the probability that the particle has not yet performed a transition until time t when it arrived at a site at $t = 0$ is $\exp(-t/\tau)$ where τ is the mean residence time on this site. Hence

$$V_0(t) = \exp(-t/\tau), \quad (2.39)$$

and

$$V_{\nu}(t) = \int_0^t dt' \exp[-(t-t')/\tau] \frac{1}{\tau} V_{\nu-1}(t'). \quad (2.40)$$

$1/\tau$ is the transition rate at an (arbitrary) time point t' , the first factor in the integral is the probability that no further transition occurs between t' and t . The recursion relation is solved to yield

$$V_{\nu}(t) = \frac{1}{\nu!} \left(\frac{t}{\tau}\right)^{\nu} \exp(-t/\tau). \quad (2.41)$$

Equation (2.37) can now be written in Fourier space in the form

$$P(\mathbf{k}, t) = \sum_{\nu=0}^{\infty} p^{\nu}(\mathbf{k}) \frac{1}{\nu!} \left(\frac{t}{\tau}\right)^{\nu} \exp(-t/\tau), \quad (2.42)$$

where eq. (2.6) has been used. Summation of the exponential series gives

$$P(\mathbf{k}, t) = \exp\{-[1 - p(\mathbf{k})]t/\tau\}. \quad (2.43)$$

This result is identical to eq. (2.17). Of course, the recursion relations and the master equation must yield identical results since the underlying assumptions of a Markoff process are the same, as well as the basic transition probabilities.

An approximate correspondence between discrete RW and CTRW at long times can be deduced from the structure of $V_{\nu}(t)$ according to eq. (2.41). The results of discrete RW can often be translated into the results of CTRW, at long times, and vice-versa, by identifying the number of steps with t/τ . For

large numbers ν of steps $V_\nu(t)$ can be represented as

$$V_\nu(t) = \exp[\phi_\nu(t)], \quad (2.44)$$

where the leading terms of $\phi_\nu(t)$ are

$$\phi_\nu(t) \approx -\nu \ln \nu + \nu \ln(t/\tau). \quad (2.45)$$

Thus $\phi_\nu(t)$ has asymptotically a maximum at $\nu = t/\tau$. Its width is determined by the second derivative of $\phi_\nu(t)$ with respect to ν ,

$$\partial^2 \phi_\nu(t) / \partial \nu^2 = -1/\nu. \quad (2.46)$$

The maximum becomes sharp for large ν or t/τ . Hence in sums over ν , such as eq. (2.42), the main contributions come from step numbers ν of the order of t/τ . However, this argument must be applied with caution; it requires that the remaining functions of ν behave sufficiently smoothly. Otherwise the product of $V_\nu(t)$ and these functions must be examined.

2.4. Extensions

i) *Transitions to further-neighbor sites.* Transitions to next-nearest or further-neighbor sites can be included in the derivation of the conditional probability in both formulations. Here the recursion-relation method will be used which was applied to this problem by Gissler and Rother [25]. The spatial transition probabilities p_{n-m} now include transitions to further-neighbor sites, the sum of p_{n-m} over n must be normalized according to eq. (2.2). As before, τ is the mean residence time of a particle on a site. The formal result of the recursion-relation method is eq. (2.43); $p(\mathbf{k})$ is modified by the inclusion of further-neighbor transitions.

In the master-equation formulation the transition rates depend on the distance $n - m$,

$$\frac{d}{dt} P(\mathbf{n}, t | \mathbf{l}, 0) = \sum_{\{\mathbf{m}\}} [\Gamma_{\mathbf{n},\mathbf{m}} P(\mathbf{m}, t | \mathbf{l}, 0) - \Gamma_{\mathbf{m},\mathbf{n}} P(\mathbf{n}, t | \mathbf{l}, 0)]. \quad (2.47)$$

When the transition rates between neighboring sites of order (i) are denoted by Γ_i and the number of neighbor sites of this order by z_i , then

$$p_{n-m} = \Gamma_i / \sum_i z_i \Gamma_i, \quad (2.48)$$

and

$$\sum_i z_i \Gamma_i = \tau^{-1}. \quad (2.49)$$

Equation (2.48) allows to make the connection to the result eq. (2.43). In applications, further-neighbor jumps were introduced to describe results of quasielastic neutron scattering on hydrogen in palladium and niobium at elevated temperatures [26, 27, 28].

ii) *Non-Bravais lattices.* The random walk of a particle in non-Bravais lattices is of practical importance since one of the most commonly encountered lattices of interstitial sites is of this kind: the lattice of tetrahedral sites in a BCC lattice (cf. fig. 2.1). This case will be treated here in detail, using the master-equation formulation developed by Rowe et al. [29]. An earlier derivation was given by Blaesser and Peretti [30]. The derivation may serve as an example for other non-Bravais lattices. There are six tetrahedral sites per metal atom, corresponding to a Bravais lattice (BCC) with basis. Each point of the lattice is characterized by a vector \mathbf{R}_n and a vector \mathbf{a}_α ($\alpha = 1, \dots, 6$), whose vertices connect the origin with the sites in a unit cell.

The basic quantity to be calculated is the conditional probability $P(\mathbf{n}, \alpha, t | \mathbf{l}, \gamma, 0)$ of finding the particle at site \mathbf{n}, α at time t when it was at site \mathbf{l}, γ at $t = 0$. It is convenient to use a different origin for each sublattice, characterized by α , and to define the Fourier transform of $P(\mathbf{n}, \alpha, t | \mathbf{l}, \gamma, 0)$ as follows

$$P_{\alpha\gamma}(\mathbf{k}, t) = \sum_{\mathbf{n}} \exp[-i\mathbf{k} \cdot (\mathbf{R}_{n\alpha} - \mathbf{R}_{l\gamma})] P(\mathbf{n}, \alpha, t | \mathbf{l}, \gamma, 0). \tag{2.50}$$

The initial condition is

$$P_{\alpha\gamma}(\mathbf{k}, t = 0) = \delta_{\alpha\gamma}. \tag{2.51}$$

The master equation for transitions on the lattice of tetrahedral sites reads

$$\frac{dP}{dt}(\mathbf{n}, \alpha, t | \mathbf{l}, \gamma, 0) = \Gamma \sum_{\langle m\beta, n\alpha \rangle} P(\mathbf{m}, \beta, t | \mathbf{l}, \gamma, 0) - 4\Gamma P(\mathbf{n}, \alpha, t | \mathbf{l}, \gamma, 0). \tag{2.52}$$

This set of equations can be brought into a simpler form by Fourier and Laplace transformation. The equations have then the form

$$\sum_{\beta=1}^6 [s\delta_{\alpha\beta} + \Lambda_{\alpha\beta}(\mathbf{k})] \tilde{P}_{\beta\gamma}(\mathbf{k}, s) = \tilde{P}_{\alpha\gamma}(\mathbf{k}, t = 0). \tag{2.53}$$

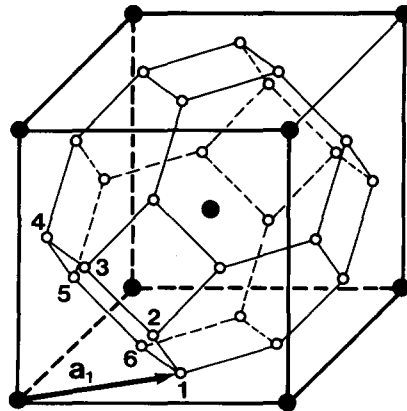


Fig. 2.1. Lattice of the tetrahedral sites (○) in the BCC Lattice (●). The vector \mathbf{a}_1 connects the origin to one of the six sites belonging to the unit cell of the Bravais lattice, these sites are numerated.

The transition rate matrix $\Lambda_{\alpha\beta}$ is given by

$$\Lambda_{\alpha\beta}(\mathbf{k}) = 4\Gamma\delta_{\alpha\beta} - \Gamma \exp(i\mathbf{k} \cdot \mathbf{l}_{\beta\alpha}), \quad (2.54)$$

where $\mathbf{l}_{\alpha\beta}$ is the vector that connects the site on sublattice α to its neighboring sites which are on sublattices β (β may coincide with α). The explicit form of the matrix $\Lambda_{\alpha\beta}(\mathbf{k})$ is

$$\Lambda_{\alpha\beta} = \Gamma \begin{pmatrix} 4 & 0 & -A_1 & -A_2 & -A_5^* & -A_6 \\ 0 & 4 & -A_2^* & -A_1^* & -A_6^* & -A_5 \\ -A_1^* & -A_2 & 4 & 0 & -A_3 & -A_4 \\ -A_2^* & -A_1 & 0 & 4 & -A_4^* & -A_3^* \\ -A_5 & -A_6 & -A_3^* & -A_4 & 4 & 0 \\ -A_6^* & -A_5 & -A_4^* & -A_3 & 0 & 4 \end{pmatrix}, \quad (2.55)$$

where

$$\begin{aligned} A_1 &= \exp\left[-\frac{ia}{4}(k_1 + k_2)\right], & A_2 &= \exp\left[-\frac{ia}{4}(k_1 - k_2)\right], \\ A_3 &= \exp\left[-\frac{ia}{4}(k_2 + k_3)\right], & A_4 &= \exp\left[-\frac{ia}{4}(k_2 - k_3)\right], \\ A_5 &= \exp\left[-\frac{ia}{4}(k_3 + k_1)\right], & A_6 &= \exp\left[-\frac{ia}{4}(k_3 - k_1)\right] \end{aligned} \quad (2.56)$$

and an asterisk superscript denotes complex conjugation.

The master equation can be solved after diagonalization of the matrix $\Lambda_{\alpha\beta}(\mathbf{k})$. Consider the eigenvalue problem

$$\sum_{\beta} \Lambda_{\alpha\beta} v_{\beta\gamma} = \lambda_{\gamma}(\mathbf{k}) v_{\alpha\gamma}. \quad (2.57)$$

Since $\Lambda_{\alpha\beta}(\mathbf{k})$ is Hermitian, the eigenvalues are real, and the $v_{\alpha\beta}$ are orthogonal and complete; after normalization

$$\sum_{\alpha} v_{\alpha\gamma}^* v_{\alpha\delta} = \delta_{\gamma\delta}, \quad \sum_{\gamma} v_{\alpha\gamma}^* v_{\beta\gamma} = \delta_{\alpha\beta}. \quad (2.58)$$

Hence

$$\sum_{\alpha} v_{\alpha\delta}^* \Lambda_{\alpha\beta} = \lambda_{\delta}(\mathbf{k}) v_{\beta\delta}^*. \quad (2.59)$$

Using these relations the solution of the master equation is obtained in the form

$$\tilde{P}_{\alpha\gamma}(\mathbf{k}, s) = \sum_{\beta, \delta} \frac{1}{s + \lambda_{\delta}(\mathbf{k})} v_{\alpha\delta} v_{\beta\delta}^* P_{\beta\gamma}(\mathbf{k}, t=0). \quad (2.60)$$

The diagonalization was carried out explicitly by Blaesser and Peretti [30] for the main symmetry

directions. For instance, they found the following simple expressions for the eigenvalues of $\Lambda_{\alpha\beta}(\mathbf{k})$ in the (100)-direction, cf. also fig. 2.2,

$$\begin{aligned} \lambda_{1,2} &= 4\Gamma, \\ \lambda_{3,4} &= 3\Gamma \pm \Gamma\sqrt{9 - 8\sin^2(ka/4)}, \\ \lambda_{5,6} &= 5\Gamma \pm \Gamma\sqrt{1 + 8\sin^2(ka/4)}. \end{aligned} \tag{2.61}$$

For general \mathbf{k} the matrix must be diagonalized by numerical methods.

In the application to quasielastic scattering on hydrogen in metals the total conditional probability is required as a sum over the probabilities of finding the particle at a specific sublattice,

$$\tilde{P}(\mathbf{k}, s) = \sum_{\alpha=1}^6 \tilde{P}_{\alpha}(\mathbf{k}, s). \tag{2.62}$$

The quantity $\tilde{P}_{\alpha}(\mathbf{k}, s)$ is defined as the conditional probability of finding the particle on sublattice α , when the particle started with equal probabilities at each sublattice or

$$\tilde{P}_{\alpha}(\mathbf{k}, s) = \frac{1}{6} \sum_{\gamma=1}^6 \tilde{P}_{\alpha\gamma}(\mathbf{k}, s), \tag{2.63}$$

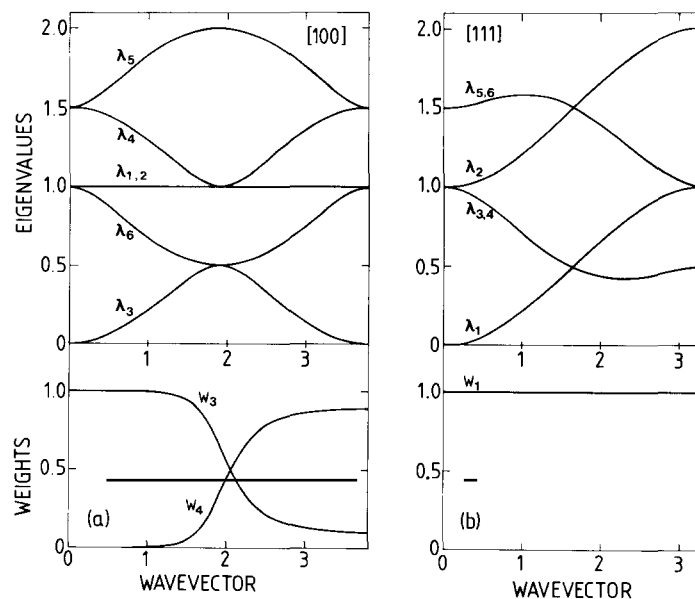


Fig. 2.2. Widths λ_i and weights w_i of the incoherent quasielastic structure function for diffusion on the lattice of tetrahedral sites as a function of wavevector \mathbf{Q} in the (a) [100] and (b) [111]-directions. The weights w_3, w_4 continue mirror-symmetric with respect to the Bragg point in the [100]-direction. Weights not shown are zero.

where the initial condition eq. (2.51) was used for $\tilde{P}_{\alpha\gamma}(\mathbf{k}, s)$. Using eq. (2.60) the total conditional probability can be expressed in the form

$$\tilde{P}(\mathbf{k}, s) = \sum_{\delta=1}^6 W_{\delta} \frac{1}{s + \lambda_{\delta}(\mathbf{k})}, \quad (2.64)$$

with

$$W_{\delta} = \frac{1}{6} \sum_{\alpha, \beta=1}^6 v_{\alpha\delta} v_{\beta\delta}^* = \frac{1}{6} \left| \sum_{\alpha=1}^6 v_{\alpha\delta} \right|^2. \quad (2.65)$$

The incoherent dynamical structure function follows from eq. (2.64) by using eq. (2.34),

$$S_{\text{inc}}(\mathbf{k}, \omega) = \sum_{\delta=1}^6 \frac{W_{\delta}}{\pi} \frac{\lambda_{\delta}(\mathbf{k})}{\omega^2 + \lambda_{\delta}^2(\mathbf{k})}. \quad (2.66)$$

Thus it is a weighted sum of (normalized) Lorentzians; the weights are denoted by W_{δ} . Also the weights can be found in the example considered above for the main symmetry directions by analytical calculations. In the (100)-direction $W_1 = W_2 = W_5 = W_6 = 0$; explicit expressions for W_3, W_4 can be found in ref. [30]. The behavior of the eigenvalues and weights as a function of the wavevector in two main symmetry directions is shown in fig. 2.2.

In the non-Bravais case there is no direct periodicity of the weights with $2\pi\mathbf{G}$ where \mathbf{G} is a vector of the reciprocal lattice. (However, there appears a periodicity with higher multiples of $2\pi\mathbf{G}$.) If one chooses a particular reciprocal lattice vector, e.g. $2\pi/a(2, 0, 0)$, an eigenvalue can approach zero without the corresponding weight approaching unity. The weight can be considered to be a generalized structure factor of the lattice under consideration. Important information about the lattice for interstitial diffusion can be drawn from an experimental determination of these weights. In this way Lottner et al. [31] have established the lattice of tetrahedral sites as the interstitial for hydrogen diffusion in niobium.

iii) *Two independent stochastic processes.* A further possible extension is the combination of two independent stochastic processes. The problem will be exemplified by the Chudley–Elliott model in its complete form which was designed to describe oscillatory diffusion in a quasicrystalline liquid [19]. The basic assumption is the independence of the oscillatory motion and the diffusion; alternating transitions between the oscillatory and diffusive state require a more complicated model, as discussed later (cf. section 5.4). Consider the dynamical incoherent structure function of a particle in the classical approximation, in the time domain,

$$I(\mathbf{k}, t) = \langle \exp\{i\mathbf{k} \cdot [\mathbf{r}(t) - \mathbf{r}(0)]\} \rangle. \quad (2.67)$$

The motion of the particle is decomposed into jumps between equilibrium sites with coordinates $\mathbf{R}(t)$, and oscillations about each equilibrium site with coordinates $\mathbf{u}(t)$, independent of the positions $\mathbf{R}(t)$,

$$\mathbf{r}(t) = \mathbf{R}(t) + \mathbf{u}(t). \quad (2.68)$$

If both motional processes are independent, the average in eq. (2.67) can be factorized,

$$I(\mathbf{k}, t) = \langle \exp\{i\mathbf{k} \cdot [\mathbf{R}(t) - \mathbf{R}(0)]\} \rangle \langle \exp\{i\mathbf{k} \cdot [\mathbf{u}(t) - \mathbf{u}(0)]\} \rangle. \quad (2.69)$$

The two terms can now be treated separately. The first average can be evaluated by the methods of sections 2.2–2.3, if the particle performs a RW on a translation-invariant Bravais lattice. The result will then be an exponential decay. The evaluation of the second term depends on the detailed dynamics of the particle. For instance, a hydrogen atom would perform localized vibrations with frequency ω_0 well above the lattice frequencies or the transition rates. Restricting the discussion to frequencies of the order of the transition rate, the second term can be replaced, for this particular problem, by a ‘Debye–Waller factor’ $\exp(-k^2 \langle u^2 \rangle / 6)$. The incoherent dynamical structure function will then have the form

$$I(\mathbf{k}, t) = \exp\{-\Lambda(\mathbf{k}) t\} \exp(-k^2 \langle u^2 \rangle / 6), \quad (2.70)$$

and it will be a Lorentzian with reduced intensity in the frequency domain. For a more detailed discussion see ref. [21]. Also other time dependencies of $\mathbf{u}(t)$ might be considered. The main point to be made here is the factorization into two independent expressions when the two motional processes are assumed to be independent.

2.5. Energetically inequivalent sites

In this section the diffusion of a particle on a linear chain with periodically distributed temporary traps is investigated. This model typifies the case of several, energetically inequivalent sites per unit cell of a Bravais lattice. Hence the method to be described is representative for this case. From a more general point of view, the problem is an example of RW of a particle with internal states, to be discussed in the next chapter. It is useful, however, to treat this problem separately in view of its importance in applications. The derivation follows ref. [32]; similar results were obtained by Kutner and Sosnowska [33]. Here the quantity of interest is the conditional probability of the diffusing particle. Periodically distributed traps were also treated by Wu and Montroll [8, 34]. They elaborated mainly properties associated with the first passage to the trapping sites.

A pictorial representation of a one-dimensional model with periodic trapping sites is given in fig. 2.3. As suggested by the figure, the particle can be released from the trapping sites by thermal excitation. The period of the traps is L , and unit cells of length La are introduced. The equilibrium sites are

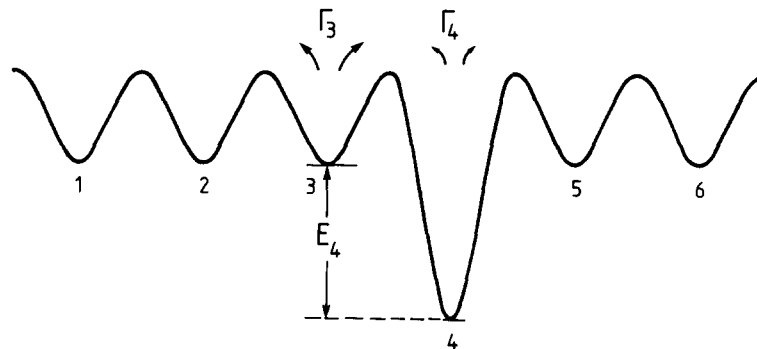


Fig. 2.3. Periodic trapping model. The potential indicates the transition rates and the equilibrium energies of the sites. The energy of the sites $\alpha \neq 4$ is taken as reference energy. The model is periodically continued ($L = 6$).

enumerated by $\alpha = 1, \dots, 6$. Abstractly the periodic models are characterized by sets of transition rates between nearest-neighbor sites within a unit cell, and between adjacent cells. For the trapping model of fig. 2.3 the transition rates F_α depend only on the index α of the initial site, not on the final site.

It is illustrative to consider the conditional probability for the diffusion of a particle in the periodic trapping model on a one-dimensional lattice. It was calculated in [32] by numerical solution of the master equation, for specific initial conditions. An example is given in fig. 2.4a where the particle starts on site 2 of fig. 2.3. Averaging over different initial conditions with weights corresponding to the mean thermal occupation of the sites (see also below) results in a much less structured averaged probability

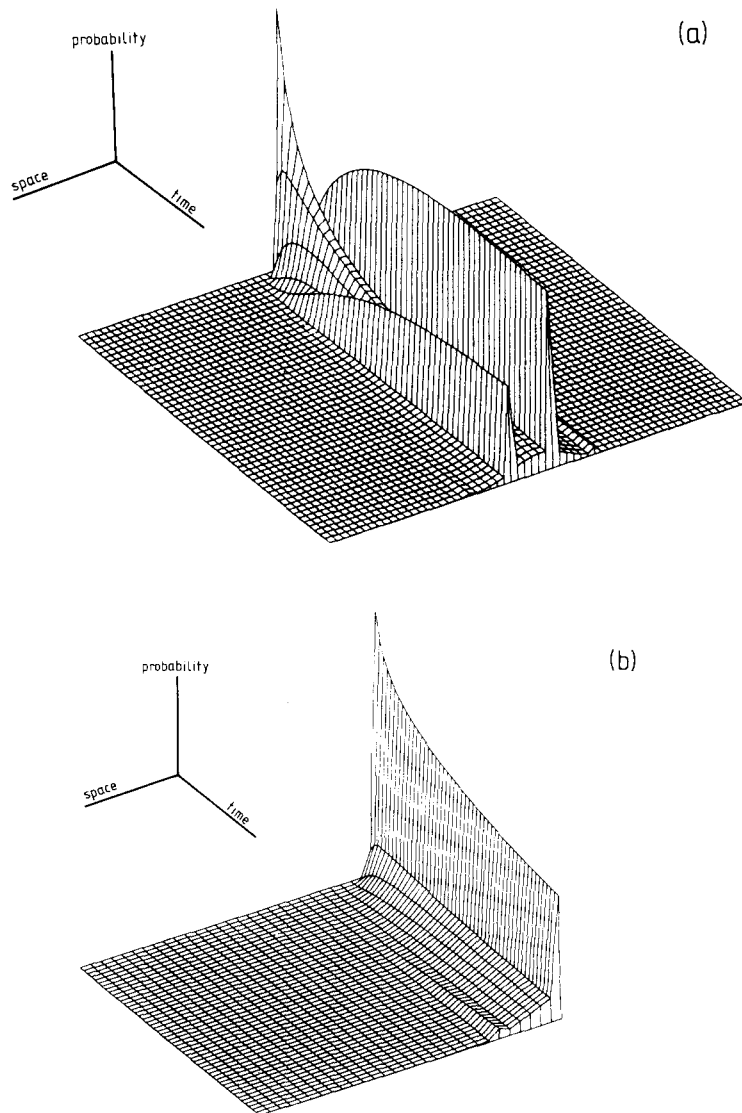


Fig. 2.4. (a) Conditional probability in the periodic one-dimensional trapping model as a function of position and time, the particle initially starts at site 2, two sites from the trapping site. (See fig. 2.3.) (b) Averaged probability distribution for thermal equilibrium initial conditions, the space coordinate is counted relative to the initial sites. Figure adapted from [32].

distribution, cf. fig. 2.4b. Also the mean-square displacement of a particle for starting at specific sites, and for starting at different sites with the appropriate thermal equilibrium weights was studied in [32]. It was found that $\langle x^2 \rangle(t)$ divided by t increases or decreases with t , depending on the start in the trap or outside of the traps, while the averaged quantity $\langle x^2 \rangle(t)/t$ is independent of time. This result will also be derived, for the general case of disordered configurations of traps, in section 7.2.

The periodic models can be dealt with by the formalism of the previous section, when the initial condition of starting at a specific site is used, or starting at each site with equal probabilities. The appropriate master equation is formulated in analogy to eq. (2.52) and after Fourier transformation the transition-rate matrix $\Lambda_{\alpha\beta}(\mathbf{k})$ is identified. The matrix $\Lambda_{\alpha\beta}(\mathbf{k})$ is non-Hermitian in the case of energetically inequivalent sites, however, it is diagonalizable.

A complication arises through the requirement that the average conditional probability of the periodic trap model be derived in a stationary ensemble. In this case the equilibrium occupation of the different sites influences the result. A large chain with NL sites will be considered. It is evident and can be deduced from the master equation that a stationary solution exists with

$$\sum_n P(\mathbf{n}, \alpha, t | I, \gamma, 0) \xrightarrow{t \rightarrow \infty} \rho_\alpha = \left[\Gamma_\alpha \sum_{\beta=1}^L \Gamma_\beta^{-1} \right]^{-1}. \quad (2.71)$$

The condition of detailed balance can be used to relate the rates Γ_α to a reference rate Γ_0

$$\Gamma_\alpha / \Gamma_0 = \exp(-E_\alpha / k_B T), \quad (2.72)$$

where E_α is the energy difference between site α and the reference site. In the stationary situation the probability of finding the particle on a site with index α is given by the expression

$$\rho_\alpha = \frac{\exp(E_\alpha / k_B T)}{\sum_{\beta=1}^L \exp(E_\beta / k_B T)}; \quad (2.73)$$

hence it should be used as a weighting factor in the initial conditions, when calculating the averaged conditional probability. The transition-rate matrix is transformed into a Hermitian form by

$$\Lambda'_{\alpha\beta} = \rho_\alpha^{-1/2} \Lambda_{\alpha\beta} \rho_\beta^{1/2}. \quad (2.74)$$

A similar transformation can be performed in the general case of inequivalent sites in the unit cell. The eigenvectors of Λ' will be denoted by \mathbf{v}' ,

$$\sum_\beta \Lambda'_{\alpha\beta} v'_{\beta\gamma} = \lambda_\gamma v'_{\alpha\gamma}. \quad (2.75)$$

The eigenvalues are identical with those of $\Lambda_{\alpha\beta}(\mathbf{k})$. A little algebra gives

$$\tilde{P}_{\alpha\gamma}(\mathbf{k}, s) = \sum_{\beta, \delta} \frac{1}{s - \lambda_\delta} \rho_\alpha^{1/2} v'_{\alpha\delta} v'_{\beta\delta}{}^* \rho_\beta^{-1/2} P_{\beta\gamma}(\mathbf{k}, t=0). \quad (2.76)$$

If one sums over the initial sites with the weighting factors ρ_γ , and over the final sites, one obtains the *average* conditional probability in a stationary ensemble, in the Laplace domain

$$\tilde{P}(\mathbf{k}, s) = \sum_{\alpha\gamma} \tilde{P}_{\alpha\gamma} \rho_\gamma = \sum_{\delta} W_{\delta} (s + \lambda_{\delta})^{-1}, \quad (2.77)$$

where the weights $W_{\delta}(\mathbf{k})$ are given by

$$W_{\delta} = \left| \sum_{\alpha=1}^L \rho_{\alpha}^{1/2} v'_{\alpha\delta} \right|^2. \quad (2.78)$$

Explicit results for the eigenvalues $\lambda_{\alpha}(\mathbf{k})$ and weights $W_{\alpha}(\mathbf{k})$ for several periodic models can be found in ref. [32]. They will not be reproduced here. Since the traps of the model of fig. 2.3 are periodically arranged, one of the eigenvalues vanishes not only at the Bragg points of the original lattice (multiples of $2\pi/a$), but also at the Bragg points of the superlattice with period La . This means a vanishing of an eigenvalue at several points (multiples of $2\pi/6a$ in the example) of the reciprocal lattice. The associated weight generally does not vanish at these points. These features are not found for the eigenvalues and weights of models with random trap distributions. Hence the periodic trapping models cannot be applied to the calculation of the incoherent dynamical structure function of diffusion in the presence of *random* traps. More appropriate models will be described in chapter 7. Nevertheless, the derivations presented above are valuable in the case of diffusion with inequivalent sites. For instance, Anderson [35] has described diffusion of hydrogen in yttrium with alternating transitions between inequivalent sites.

3. Continuous-time random walks on regular lattices

In this chapter the discussion of the previous chapter is generalized to allow the possibility of non-Poissonian waiting-time distributions of the particle between the transitions. The lattices considered generally shall be translation-invariant, with one exception considered in the last section. This chapter will appear rather abstract; applications of the formalism to physically motivated models will appear in the subsequent two chapters. In the last section the formulation will be extended to include the availability of different *states* that the particle can acquire at the sites of the lattice.

3.1. Waiting-time distributions and time homogeneity

A particle performs a random walk on a Bravais lattice; in this section only the stochastic process of the transition of the particle in time will be considered. The waiting-time distribution (WTD) $\psi(t)$ of the particle is defined as follows. Let the particle have performed its last transition at $t = 0$. Then $\psi(t)$ is the probability density that it performs *its next* transition at time t after it waited until t . The simplest example is provided by the WTD of a Poisson process, $\psi(t) = \exp(-t/\tau)/\tau$. The factor $(1/\tau)$ is the probability density or 'rate' of a transition to another site, the second factor is the probability that no transition has occurred until time t . Of course, the concept of WTD allows for more general time dependencies. General WTD were introduced into the theory of random walks on lattices by Montroll and Weiss [24].

The waiting-time distribution $\psi(t)$ must be positive semidefinite, and when integrated over all time, its value must be normalized. If not positive, $\psi(t)$ is not a probability density and should $\psi(t)$ not be normalized then the particle number is not conserved in the system. It is useful to introduce the sojourn probability $\Psi(t)$ that the particle remains on the lattice site until t without a transition,

$$\Psi(t) = 1 - \int_0^t dt' \psi(t'). \quad (3.1)$$

In the Laplace domain the sojourn probability is:

$$\tilde{\Psi}(s) = [1 - \tilde{\psi}(s)]/s. \quad (3.1')$$

In the case of a Poisson process the sojourn probability is $\Psi(t) = \exp(-t/\tau)$. It is assumed here that the first moment of the WTD exists,

$$\bar{t} = \int_0^{\infty} dt' t' \psi(t') < \infty. \quad (3.2)$$

The *renewal theorem* [36] states that for large times the transitions of the particle occur, on the average, at a constant rate \bar{t}^{-1} . For shorter times, however, the time homogeneity of the process is destroyed when the transitions begin at $t = 0$ and are all described by the WTD $\psi(t)$. If a system is considered in a stationary state, then a constant rate of transitions should occur, on the average, at all times. The point is that the time origin can be chosen arbitrarily in the stationary situation; the last transition of the particle may have occurred some time before $t = 0$. To incorporate this possibility into the theory, the *first* transition of the particle needs a special treatment; it will be characterized by the waiting-time distribution $h(t)$. It is plausible that the correct WTD of the *first* transition in a stationary ensemble is obtained by averaging the WTD $\psi(t)$ over all time differences t' between the time origin and the last transition,

$$h_{\text{eq}}(t) = \int_0^{\infty} dt' \psi(t+t') / \int_0^{\infty} dt \int_0^{\infty} dt' \psi(t+t'). \quad (3.3)$$

The denominator is required for normalization. An equivalent expression is

$$h_{\text{eq}}(t) = \Psi(t)/\bar{t}. \quad (3.4)$$

It is easily seen that for a Poisson process $h_{\text{eq}}(t) = \psi(t)$, but in general both quantities are different. Figure 3.1 illustrates this difference for a particular example.

Feller [36] derived eq. (3.3) from the requirement that the stochastic process described by $h(t)$, $\psi(t)$ be stationary. A different derivation of eq. (3.3) was given by Lax and Scher [37] using conditional probabilities. It should be stressed that the correct choice of $h(t)$ depends on the initial conditions, in particular whether a stationary situation is given or not. Equation (3.3) is the correct form for a stationary or equilibrium ensemble. If the system is prepared at $t = 0$ in a state from which it develops according to $\psi(t)$ (for instance, by implantation of a particle at $t = 0$) then $\psi(t) = h(t)$ is the correct assignment.

Tunaley recognized that the above considerations on time homogeneity are relevant for the CTRW theory [38] which will be described in the following section.

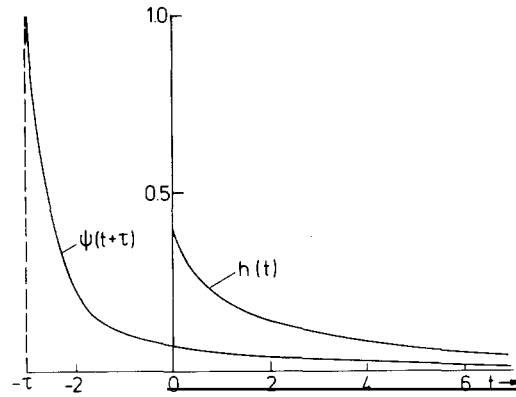


Fig. 3.1. The waiting-time distribution $\psi(t)$ and the first-jump waiting-time distribution $h(t)$ determined from eq. (3.3). The WTD $\psi(t)$ is derived from a two-state model, cf. section 5.1.

3.2. Continuous-time random walk by recursion relations

The theory of CTRW of a particle on a lattice with general WTD was developed by Montroll and Weiss [24]. Tunaley extended their work by incorporating a distinct WTD for the first jump $h(t)$ into the formal CTRW theory [39]. The theory is most conveniently developed by introducing recursion relations [40]. A slight generalization, which will be made here, is the introduction of ‘non-separable’ CTRW [40]. The transitions of a particle are then characterized by the WTD $\psi_{n,m}(t)$, the probability density of transition to site n at time t when it arrived at site m at $t = 0$. These WTD are normalized according to

$$\sum_n \int_0^\infty dt' \psi_{n,m}(t') = 1. \quad (3.5)$$

The CTRW will be called ‘separable’ when

$$\psi_{n,m}(t) = p_{n,m} \psi(t), \quad (3.6)$$

where $p_{n,m}$ and $\psi(t)$ were introduced in previous sections.

The quantity of interest is the conditional probability $P(n, t | l, 0)$ of finding the particle at site n at time t when it was at site l at time $t = 0$. Let $Q_\nu(n, t)$ be the probability density that the particle has performed its ν th transition at time t and thereby reached site n . Evidently

$$Q_\nu(n, t) = \sum_m \int_0^t dt' \psi_{n,m}(t-t') Q_{\nu-1}(m, t'). \quad (3.7)$$

The recursion relation is only valid for $\nu \geq 2$ since the first transition has to be treated differently,

$$Q_1(n, t) = \sum_m h_{n,m}(t) P(m, t=0). \quad (3.8)$$

Here $h_{n,m}(t)$ is the WTD for the first transition from site m to site n , the normalization is analogous to eq. (3.5). These WTD will not be specified for the moment. The probability density that site n is occupied by a transition at time t is given by

$$Q(\mathbf{n}, t) = \sum_{\nu=1}^{\infty} Q_{\nu}(\mathbf{n}, t). \tag{3.9}$$

Resummation of the recursion relations yields

$$Q(\mathbf{n}, t) = \sum_{\mathbf{m}} \int_0^t dt' \psi_{n,m}(t-t') Q(\mathbf{m}, t') + Q_1(\mathbf{n}, t). \tag{3.10}$$

The convolutions appearing in eq. (3.10) become simple products after Fourier and Laplace transformation. The result is

$$\tilde{Q}(\mathbf{k}, s) = \frac{\tilde{h}(\mathbf{k}, s) P(\mathbf{k}, t=0)}{1 - \tilde{\psi}(\mathbf{k}, s)}. \tag{3.11}$$

The conditional probability $P(\mathbf{n}, t|I, 0)$ is related to $Q(\mathbf{n}, t')$ by the probability that no further transition occurs between t' and t , but there is also the probability that no transition occurred at all. Hence

$$P(\mathbf{n}, t|I, 0) = \int_0^t dt' \Psi(t-t') Q(\mathbf{n}, t') + H(t) P(\mathbf{n}, t=0), \tag{3.12}$$

where $\Psi(t)$ and $H(t)$ are given by

$$\Psi(t) = 1 - \sum_{\mathbf{n}} \int_0^t dt' \psi_{n,m}(t'), \quad H(t) = 1 - \sum_{\mathbf{n}} \int_0^t dt' h_{n,m}(t'). \tag{3.13}$$

Equation (3.12) is written in the Fourier–Laplace domain and $\Psi(t)$, $H(t)$ are substituted by the analogues of eq. (3.1'). The final result is

$$\tilde{P}(\mathbf{k}, s) = s^{-1} [1 - \tilde{\psi}(\mathbf{k}, s)]^{-1} [1 - \tilde{h}(\mathbf{0}, s) + \tilde{h}(\mathbf{k}, s) - \tilde{\psi}(\mathbf{k}, s) + \tilde{h}(\mathbf{0}, s) \tilde{\psi}(\mathbf{k}, s) - \tilde{h}(\mathbf{k}, s) \tilde{\psi}(\mathbf{0}, s)]. \tag{3.14}$$

The result simplifies for separable CTRW

$$\tilde{P}(\mathbf{k}, s) = s^{-1} [1 - p(\mathbf{k}) \tilde{\psi}(s)]^{-1} \{1 - \tilde{h}(s) + p(\mathbf{k}) [\tilde{h}(s) - \tilde{\psi}(s)]\}. \tag{3.15}$$

This is the form of $\tilde{P}(\mathbf{k}, s)$ derived by Tunaley [39].

When a stationary ensemble is considered, the WTD for the first transition is given by a generalization of eq. (3.3)

$$h_{n,m}^{\text{eq}}(t) = \frac{\int_0^{\infty} dt' \psi_{n,m}(t+t')}{\sum_{\mathbf{n}} \int_0^{\infty} dt \int_0^{\infty} dt' \psi_{n,m}(t+t')}. \tag{3.16}$$

The Fourier–Laplace transform of eq. (3.16) is

$$\tilde{h}(\mathbf{k}, s) = [\tilde{\psi}(\mathbf{k}, s) - \tilde{\psi}(\mathbf{k}, 0)] / (\bar{t}s),$$

where

$$\bar{t} = \sum_{\mathbf{n}} \int_0^{\infty} dt' t' \psi_{\mathbf{n},m}(t'). \quad (3.17)$$

The conditional probability for a stationary ensemble is then given by

$$\tilde{P}(\mathbf{k}, s) = \left\{ \frac{1}{s} + \frac{1}{\bar{t}s^2} \frac{[1 - \tilde{\psi}(\mathbf{0}, s)][\tilde{\psi}(\mathbf{k}, 0) - 1]}{1 - \tilde{\psi}(\mathbf{k}, s)} \right\}. \quad (3.18)$$

It was assumed that $P(\mathbf{k}, 0) = 1$, i.e., the particle is assumed to be at the origin at $t = 0$. The specialization of eq. (3.18) to a separable walk is obvious.

It is interesting to consider the lowest moments of $P(\mathbf{n}, t)$ which can be found by expansion of $\tilde{P}(\mathbf{k}, s)$ for small k and inverse Laplace transformation. It will be assumed that an expansion of $\tilde{\psi}(\mathbf{k}, s)$ about $\mathbf{k} = 0$ is possible uniformly in s ,

$$\tilde{\psi}(\mathbf{k}, s) = \tilde{\psi}(\mathbf{0}, s) + O(k^2). \quad (3.19)$$

It is then found that the conditional probability for a stationary ensemble has the following behavior for small k and arbitrary s

$$\tilde{P}(\mathbf{k}, s) \xrightarrow{k \rightarrow 0} \frac{1}{s} + \frac{\text{const } k^2}{\bar{t}s^2}. \quad (3.20)$$

It is recommended to repeat this derivation for the case of separable CTRW, where the argument is more direct. The zeroth moment of the conditional probability is $1/s$, corresponding to particle number conservation. The second moment of $P(\mathbf{k}, t)$ is found to be independent of the precise form of the waiting-time distributions; it is proportional to t and the second moment of the structure function $p(k)$. The second moment of $P(\mathbf{n}, t)$ represents the mean-square displacement and the coefficient of t is proportional to the diffusion coefficient. Thus CTRW, in the form presented, yields a time-independent diffusion coefficient, corresponding to a frequency-independent mobility.

Though it is not seen directly from eq. (3.18) the result on the strict linearity of the mean-square displacement with time is a consequence of the inclusion of the WTD for the first transition according to eq. (3.3). If no distinct $h(t)$ is introduced, or $h(t)$ is chosen which does not correspond to the stationary ensemble, a non-linear mean-square displacement and thus a frequency-dependent mobility is obtained. The consequences of the inclusion of $h_{\mathbf{n},m}^{\text{eq}}(t)$ on the diffusion coefficient, or equivalently, on the mobility of a particle under the influence of a small force, were drawn by Tunaley [39]. He considered only separable CTRW, but the conclusions are equally valid for the non-separable case, as the above derivations show. These results aroused a debate whether $h_{\mathbf{n},m}(t)$ should be included in CTRW theory when it is applied to model transport in disordered systems. A discussion of this controversy will be deferred to section 6.7, until transport in disordered systems has been reviewed too.

CTRW theory with inclusion of a distinct WTD for the first transition in equilibrium seems to be intrinsically correct. This opinion is shared in other reviews [7, 41]. Less formal, but perhaps more physical arguments can be given by considering the velocity correlations of the particle executing CTRW. The second derivative of the mean-square displacement with respect to time is obtained in a thermal equilibrium ensemble from the velocity correlation function. This amounts to a multiplication with $s^2/2$ in the Laplace domain. From eq. (3.20) a constant is found in the Laplace domain, corresponding to a velocity correlation function proportional to $\delta(t)$ in the time domain. The velocity correlation function ought to be a delta function in the CTRW considered here. There is no reason why backward (or forward) correlations in the transitions of the particle should appear, no matter how complicated the time dependence of the stochastic transition process is. Since the Fourier transform of the velocity correlation function is the frequency-dependent diffusion coefficient, it is frequency-independent in the equilibrium CTRW model studied here.

3.3. Equivalence with generalized master equation

It was shown by Bedeaux et al. [42] that the solution of the separable CTRW problem and that of the corresponding master equation approach each other at long times when all moments of the waiting-time distribution exist. The spatial transition probabilities $p_{n,m}$ are identical in both formulations, the transition rate is \bar{t}^{-1} where \bar{t} is the first moment of the waiting-time distribution (for simplicity separable CTRW is considered) and the times must be large compared to the maximum of $(\tau_n)^{1/n}$, where τ_n is the n th moment of the WTD. Kenkre et al. [43] pointed out that at arbitrary times a correspondence exists between (separable) CTRW and a generalized master equation. This equivalence will be described here for the case of single-state non-separable CTRW on ideal lattices.

The starting point is the form (3.12) of the solution of the CTRW problem, where (3.11) is inserted,

$$\tilde{P}(\mathbf{k}, s) = \{ \tilde{\Psi}(s) [1 - \tilde{\psi}(\mathbf{k}, s)]^{-1} \tilde{h}(\mathbf{k}, s) + \tilde{H}(s) \} P(\mathbf{k}, 0). \quad (3.21)$$

It can be written in the form

$$[1 - \tilde{\psi}(\mathbf{k}, s)] \tilde{\Psi}^{-1}(s) \tilde{P}(\mathbf{k}, s) = \{ \tilde{h}(\mathbf{k}, s) - [1 - \tilde{\psi}(\mathbf{k}, s)] \tilde{\Psi}^{-1}(s) \tilde{H}(s) \} P(\mathbf{k}, 0); \quad (3.22)$$

this can be compactly expressed as:

$$[s - \tilde{\phi}(\mathbf{k}, s)] \tilde{P}(\mathbf{k}, s) = P(\mathbf{k}, 0) + \tilde{I}(\mathbf{k}, s), \quad (3.23)$$

where

$$\tilde{\phi}(\mathbf{k}, s) = s [\tilde{\psi}(\mathbf{k}, s) - \tilde{\psi}(\mathbf{0}, s)] / [1 - \tilde{\psi}(\mathbf{0}, s)] \quad (3.24)$$

and

$$\tilde{I}(\mathbf{k}, s) = \frac{\tilde{h}(\mathbf{k}, s) - \tilde{\psi}(\mathbf{k}, s) - [\tilde{h}(\mathbf{0}, s) - \tilde{\psi}(\mathbf{0}, s)] + \tilde{h}(\mathbf{0}, s) \tilde{\psi}(\mathbf{k}, s) - \tilde{h}(\mathbf{k}, s) \tilde{\psi}(\mathbf{0}, s)}{1 - \tilde{\psi}(\mathbf{0}, s)} P(\mathbf{k}, 0). \quad (3.25)$$

In the time domain, eq. (3.23) yields the generalized master equation (GME) with an inhomogeneous term,

$$\frac{d}{dt} P(\mathbf{k}, t) = \int_0^t dt' \phi(\mathbf{k}, t-t') P(\mathbf{k}, t') + I(\mathbf{k}, t). \quad (3.26)$$

$\phi(\mathbf{k}, t)$ and $I(\mathbf{k}, t)$ are the inverse Laplace transforms of eqs. (3.24) and (3.25), respectively. The transformation of the GME to direct space is obvious.

One disturbing feature of eq. (3.26) is the presence of the inhomogeneous term. It is a consequence of the introduction of a different WTD for the first step, and thus of the requirement of time homogeneity.¹ It will be discussed further in the context of specific models, cf. section 5.2, where using specific models it is shown explicitly how to obtain $h(t)$ and under what initial conditions $h(t)$ agrees with or differs from $\psi(t)$.

The kernel $\phi(\mathbf{k}, t)$ and the inhomogeneity $I(\mathbf{k}, t)$ are somewhat simpler for separable CTRW,

$$\tilde{\phi}(\mathbf{k}, s) = [p(\mathbf{k}) - 1] \tilde{\phi}(s), \quad (3.27)$$

where

$$\tilde{\phi}(s) = s \tilde{\psi}(s) / [1 - \tilde{\psi}(s)], \quad (3.28)$$

and

$$\tilde{I}(\mathbf{k}, s) = [p(\mathbf{k}) - 1] \frac{\tilde{h}(s) - \tilde{\psi}(s)}{1 - \tilde{\psi}(s)} P(\mathbf{k}, 0). \quad (3.29)$$

The equivalence of CTRW with the GME was originally given [43] through these relations, except the inhomogeneity. In an equilibrium ensemble, where $h(t)$ is given by eq. (3.3), the inhomogeneity acquires the simple form

$$\tilde{I}(\mathbf{k}, s) = [p(\mathbf{k}) - 1] \frac{1}{s} [t^{-1} - \tilde{\phi}(s)]. \quad (3.29')$$

It is illustrative to consider two simple cases. i) Kernel without memory, $\phi(t) = \gamma \delta(t)$. Equation (3.27) gives an exponential WTD, $\psi(t) = \gamma \exp(-\gamma t)$. This kernel corresponds to the ordinary master equation with total transition rate γ ; hence the ordinary master equation corresponds to CTRW with exponential WTD, as discussed in the previous chapter. ii) Kernel with exponential memory, $\phi(t) = a \exp(-\lambda t)$. The resulting WTD is the sum of two exponentials,

$$\psi(t) = (2a/\rho) \exp(-\lambda t/2) \sinh(\rho t/2) \quad (3.30)$$

where $\rho = \sqrt{\lambda^2 - 4a^2}$. The GME can be transcribed in this case to a variant of the telegrapher's equation, cf. [43].

¹ An inhomogeneous term appears also in the GME resulting from the Liouville-von Neumann equation. It may vanish if appropriate initial conditions are given. See the discussion of Kenkre [44] for the case of exciton transport. The existence of an inhomogeneous term in the GME is not generally appreciated and this point is taken up again in section 6.7.

3.4. Multistate continuous-time random walks

The derivations of the last sections will now be generalized to include the availability of different states of the particle at each site of the lattice. A physical motivation for such a generalization may be the existence of several internal states of the particle at each lattice site. For instance, a non-spherical molecule diffusing on a surface of a crystal may take on different orientations at each site. In this section a rather general formulation of multistate CTRW will be given; possible applications will be mentioned in the context of more specialized models. However, one particular extension will be mentioned here. Namely, when the states are identified with the sites themselves, the formulation includes the case of different WTD at each site of the system (which may not even form a lattice). References to previous work will be deferred to the end of this section.

The quantity of interest is $P(\mathbf{n}, \beta, t | \mathbf{l}, \alpha, 0)$, the conditional probability of finding the particle at site \mathbf{n} in state β at time t when it was at site \mathbf{l} , in state α , at time 0. The WTD for a transition to site \mathbf{n} and state β at time t , when the particle arrived at site \mathbf{m} and state α at $t = 0$ is $\psi_{\mathbf{n}\beta, \mathbf{m}\alpha}(t)$. Normalization is required,

$$\sum_{\mathbf{n}\beta} \int_0^{\infty} dt' \psi_{\mathbf{n}\beta, \mathbf{m}\alpha}(t') = 1. \quad (3.31)$$

A vector/matrix notation with respect to the state indices will be adopted henceforth. For instance, the Fourier–Laplace transform of the WTD will be denoted by $\tilde{\psi}(\mathbf{k}, s)$.

The derivations of the previous two sections are easily extended to the general case. The result for the conditional probability is

$$\tilde{P}(\mathbf{k}, s) = \{\tilde{\Psi}(s) \cdot [\mathbf{E} - \tilde{\Psi}(\mathbf{k}, s)]^{-1} \cdot \tilde{\mathbf{h}}(\mathbf{k}, s) + \tilde{\mathbf{H}}(s)\} \cdot P(\mathbf{k}, 0), \quad (3.32)$$

in complete correspondence to eq. (3.22). \mathbf{E} is the unit matrix and the quantity $\tilde{\mathbf{h}}(\mathbf{k}, s)$ is the Fourier–Laplace transform of the WTD for the first transition. $\tilde{\Psi}(s)$ is the Laplace transform of the probability that no further transition occurs after the last one. It is a diagonal matrix with the elements in the Fourier/Laplace domain

$$\tilde{\Psi}_{\alpha\alpha}(s) = \frac{1}{s} \left[1 - \sum_{\gamma} \tilde{\psi}_{\gamma\alpha}(\mathbf{0}, s) \right]. \quad (3.33)$$

$\tilde{\mathbf{H}}(s)$ is the Laplace transform of the probability that the first transition has not yet occurred until time t . It is also a diagonal matrix of the same structure as eq. (3.33) where $\tilde{\psi}(0, s)$ is replaced by $\tilde{h}(0, s)$.

Equation (3.32) constitutes the general solution of the multistate CTRW problem. The further simplification of this expression, in analogy to eq. (3.15), is not possible unless $\tilde{\Psi}$ and $\tilde{\mathbf{h}}$ are diagonal. However, it is possible to deduce a coupled set of GMEs. The algebra runs as in the preceding section; some care is necessary with the matrix manipulations. The result is

$$[s\mathbf{E} - \tilde{\Phi}(\mathbf{k}, s)] \cdot \tilde{P}(\mathbf{k}, s) = P(\mathbf{k}, 0) + \tilde{I}(\mathbf{k}, s). \quad (3.34)$$

The matrix elements of the kernel are given by

$$\tilde{\phi}_{\alpha\beta}(\mathbf{k}, s) = \frac{s[\tilde{\psi}_{\alpha\beta}(\mathbf{k}, s) - \delta_{\alpha\beta} \sum_{\gamma} \tilde{\psi}_{\gamma\beta}(\mathbf{0}, s)]}{1 - \sum_{\gamma} \tilde{\psi}_{\gamma\beta}(\mathbf{0}, s)}. \quad (3.35)$$

The inhomogeneity is given by

$$\tilde{\mathbf{I}}(\mathbf{k}, s) = \tilde{\mathbf{M}}(\mathbf{k}, s) \cdot \mathbf{P}(\mathbf{k}, 0),$$

where the matrix elements of $\tilde{\mathbf{M}}$ are given by

$$\begin{aligned} \tilde{M}_{\alpha\beta}(\mathbf{k}, s) = & \left[1 - \sum_{\gamma} \tilde{\psi}_{\gamma\beta}(\mathbf{0}, s) \right]^{-1} \left\{ \tilde{h}_{\alpha\beta}(\mathbf{k}, s) - \tilde{\psi}_{\alpha\beta}(\mathbf{k}, s) - \delta_{\alpha\beta} \sum_{\gamma} [\tilde{h}_{\gamma\beta}(\mathbf{0}, s) - \tilde{\psi}_{\gamma\beta}(\mathbf{0}, s)] \right. \\ & \left. + \tilde{\psi}_{\alpha\beta}(\mathbf{k}, s) \sum_{\gamma} \tilde{h}_{\gamma\beta}(\mathbf{0}, s) - \tilde{h}_{\alpha\beta}(\mathbf{k}, s) \sum_{\gamma} \tilde{\psi}_{\gamma\beta}(\mathbf{0}, s) \right\}. \end{aligned} \quad (3.36)$$

As a special case the ‘separable’ multistate CTRW will be considered,

$$\tilde{\psi}(\mathbf{k}, s) = \mathbf{p}(\mathbf{k}) \tilde{\Psi}(s), \quad (3.37)$$

where $\mathbf{p}(\mathbf{k})$ includes transition probabilities between sites and states and where $\tilde{\Psi}(s)$ is a diagonal matrix with elements $\tilde{\psi}_{\alpha}(s)$. \mathbf{p} and $\tilde{\Psi}$ must be normalized separately,

$$\sum_{\beta} p_{\beta\alpha}(\mathbf{k} = \mathbf{0}) = 1, \quad \tilde{\psi}_{\alpha}(s = 0) = 1. \quad (3.38)$$

It is further assumed that

$$\tilde{\mathbf{h}}(\mathbf{k}, s) = \mathbf{p}(\mathbf{k}) \cdot \tilde{\mathbf{h}}(s), \quad (3.39)$$

with the same transition matrix \mathbf{p} and a diagonal matrix $\tilde{\mathbf{h}}$. The kernel of the GME is now given by the matrix elements

$$\tilde{\phi}_{\alpha\beta}(\mathbf{k}, s) = \frac{s[p_{\alpha\beta}(\mathbf{k}) - \delta_{\alpha\beta}] \tilde{\psi}_{\beta}(s)}{1 - \tilde{\psi}_{\beta}(s)}, \quad (3.40)$$

and the elements of the matrix appearing in the inhomogeneity

$$\tilde{M}_{\alpha\beta}(\mathbf{k}, s) = \frac{[p_{\alpha\beta}(\mathbf{k}) - \delta_{\alpha\beta}] [\tilde{h}_{\beta}(s) - \tilde{\psi}_{\beta}(s)]}{1 - \tilde{\psi}_{\beta}(s)}. \quad (3.41)$$

So far a rather general formulation of continuous-time random walk of a particle between different states and sites has been given, and the equivalence with the GME established. Note that the inhomogeneous term in the GME is always present when a different WTD for the first transition is introduced, i.e., when $h(t) \neq \psi(t)$. The multistate CTRW of a particle will generally yield frequency-dependent diffusion coefficients, although this is not yet evident from the present formulation. This will

be demonstrated in the particular application of the general formulation in the next chapter. The solution of the set of coupled GME requires the diagonalization of matrices, hence it is practical only when a small number of states is taken into account. Although the expressions eq. (3.32) and eq. (3.33) provide a solution of the problem of CTRW on a lattice (or even on a general set of sites) with different WTD at each vertex, the solution is only formal when, say, 10^3 sites are involved.

The earliest publications on multistate CTRW were made by Kenkre and several collaborators [45]. They considered sites with a different WTD at each site and established the correspondence between CTRW and the GME. Research with a similar theme was published by Shugard and Reiss [46]. The general formulation of CTRW, including the equivalence with the GME, was developed by Landman et al. [47] and the present authors also obtained similar results [48]. Landman and Shlesinger made applications of the formalism, especially to surface diffusion [49]. A compact derivation of multistate CTRW and its equivalence with the GME was given by Gillespie [50], in this work states are equivalent to sites. Multistate CTRW was also treated in ref. [51] with the aim to include energy dependence of the RW process. More references will be given in the next two chapters when special cases of the general formalism are considered. There are presumably more applications of CTRW with internal states than hitherto considered. For instance, the combined spatial and spectral diffusion of an excitation in a crystal could provide a case in point.

4. Random walks with correlated jumps

Correlated random walks are a class of random walks where memory is not lost after each step, but only after a finite number of steps. This chapter treats mainly correlations over two successive steps and it is shown that correlated walks are a special case of multistate random walks. However, they deserve a separate treatment since they represent an important class of random walks with many significant applications. They are more easily treated directly than by using the full formalism of the last chapter. Also, their distinct features tend to be hidden by the general formalism.

4.1. *Historical survey; one-dimensional models*

Correlated walks were invented in the course of the discussion of ‘persistence of motion’ of particles in fluids. The first calculation, using kinetic theory arguments, showing that a particle persists to move in the same direction after a collision is attributed to Jeans [52]. Smoluchowski [53] in his investigation of the kinematic justification of Brownian motion, extended the calculation of Jeans by determining the mean-square displacement. This was evidently the impetus for Fuerth [54] to work out a detailed one-dimensional random-walk theory with persistence. As an application of his formula for the mean-square displacement, he studied the diffusion of infusoria in solution (actually, he measured the average time it required an infusor to make a first passage across a predetermined segment). The mean-square displacement showed a definite non-linear time evolution; in this case, the correlation or memory accounts for the fact that the particles possess an inertia and thus, they persisted to move in the same direction for a time which is not negligible compared to observation time. Independently, Taylor [55] developed an equivalent theory in an attempt to explain the correlations of particle diffusion in a turbulent medium.

Since then, correlated random walks were rediscovered in various physical applications. The two most prominent applications are i) conformation of polymers, and ii) tracer diffusion in metals. One is

interested in the squared end-to-end distance of a polymer chain of n segments (monomers), or in the mean-squared displacement of a tagged particle after n steps. The simple model of a freely rotating chain fixes the polar angle $\alpha = \cos \theta$ between two consecutive segments, and allows arbitrary azimuthal angles ϕ [56]. For tracer diffusion a correlation between successive steps appears since, after one step of the tracer, the vacancy that promoted this step is with certainty behind the tracer [57]. It then effects more easily a backward step of the tracer than a forward or sideward step, resulting in a negative average angle $\langle \cos \theta \rangle$ between two steps. In both problems the square of the sum of all displacements \mathbf{d}_i is considered,

$$\langle (\mathbf{R}_n - \mathbf{R}_0)^2 \rangle = \left\langle \left(\sum_{i=1}^n \mathbf{d}_i \right) \left(\sum_{j=1}^n \mathbf{d}_j \right) \right\rangle. \quad (4.1)$$

In RW with correlations between two successive steps \mathbf{d}_i is related to \mathbf{d}_j indirectly through the intermediate steps, and $\langle \mathbf{d}_i \cdot \mathbf{d}_j \rangle$ is $\propto \alpha^{|i-j|}$ in the first case and $\propto \langle \cos \theta \rangle^{|i-j|}$ in the second one (some restrictive assumptions are necessary in the case of diffusion in crystals [58]). This fact is sufficient to allow an evaluation of eq. (4.1) with the result

$$\frac{\langle (\mathbf{R}_n - \mathbf{R}_0)^2 \rangle}{\langle (\mathbf{R}_n - \mathbf{R}_0)^2 \rangle_{uc}} \xrightarrow{n \rightarrow \infty} f, \quad (4.2)$$

where the denominator is the mean-square displacement for uncorrelated random walks and f the correlation factor, in application i) [56]

$$f = (1 + \alpha)/(1 - \alpha), \quad (4.3a)$$

where α is the fixed value of the polar angle, or in application ii) [58]

$$f = (1 + \langle \cos \theta \rangle)/(1 - \langle \cos \theta \rangle). \quad (4.3b)$$

Thus there appears a modification of the static diffusion coefficient, which constitutes the most conspicuous effect of correlated random walks. This chapter is concerned with a more detailed description of correlated walks, for instance in the derivation of the complete conditional probability for correlated walks.

As a particularly simple example, a correlated walk on the linear chain with constant transition rates is considered [59]. The rate for a transition in the same direction as the previous one is denoted by Γ_f and the rate for a transition in the opposite direction is denoted by Γ_b . The conditional probability $P(n, t)$ of finding the particle at site n at time t when it originated at site 0 at $t = 0$ is split up into two contributions $P_+(n, t)$ and $P_-(n, t)$, where $+$ and $-$ indicates that the particle came from site $n + 1$ or $n - 1$, respectively. These quantities obey the coupled master equations:

$$\frac{d}{dt} P_+(n, t) = \Gamma_f [P_+(n + 1, t) - P_+(n, t)] + \Gamma_b [P_-(n + 1, t) - P_+(n, t)], \quad (4.4)$$

$$\frac{d}{dt} P_-(n, t) = \Gamma_f [P_-(n - 1, t) - P_-(n, t)] + \Gamma_b [P_+(n - 1, t) - P_-(n, t)].$$

This set of master equations is transformed into a set of coupled algebraic equations by Fourier and Laplace transformations,

$$\begin{aligned}
 [s + \Gamma_f(1 - e^{ika}) + \Gamma_b] \tilde{P}_+(k, s) - \Gamma_b e^{ika} \tilde{P}_-(k, s) &= P_+(k, 0), \\
 -\Gamma_b e^{-ika} \tilde{P}_+(k, s) + [s + \Gamma_f(1 - e^{-ika}) + \Gamma_b] \tilde{P}_-(k, s) &= P_-(k, 0).
 \end{aligned}
 \tag{4.5}$$

The initial conditions are $P_+(k, 0) = P_-(k, 0) = \frac{1}{2}$. The summary conditional probability is obtained from the solution of eq. (4.5) as

$$\tilde{P}(k, s) = \frac{s + \gamma + (\Gamma_b - \Gamma_f) \cos ka}{s^2 + 2s[\Gamma_b + \Gamma_f(1 - \cos ka)] + 2\Gamma_f \gamma (1 - \cos ka)},
 \tag{4.6}$$

where $\gamma = \Gamma_f + \Gamma_b$ is the total transition rate.

The small- k expansion of $\tilde{P}(k, s)$ is

$$\tilde{P}(k, s) \rightarrow \frac{1}{s} - \frac{(s + \gamma) \Gamma_f (ka)^2}{s^2(s + 2\Gamma_b)} + \dots
 \tag{4.7}$$

The time-dependent mean-square displacement or the frequency-dependent diffusion coefficient shall be discussed later when this model is generalized to arbitrary dimensions. Here only the asymptotic mean-square displacement is given, which follows from the small- s behavior of eq. (4.7),

$$\langle x^2 \rangle(t) \xrightarrow{t \rightarrow \infty} \frac{\Gamma_f}{\Gamma_b} \gamma a^2 t.
 \tag{4.8}$$

The resulting static diffusion coefficient is the product of the diffusion coefficient of the uncorrelated random walk, $\gamma a^2/2$, times the correlation factor $f = \Gamma_f/\Gamma_b$.

The conditional probability can be easily transformed back into real space,

$$\tilde{P}(n, s) = \int_{-\pi}^{+\pi} \frac{dk}{2\pi} e^{ikn} \tilde{P}(k, s).
 \tag{4.9}$$

The lattice constant a was set to unity. This integral is evaluated by the technique explained in section 2.2, of eqs. (2.30)–(2.33). The final result is

$$\begin{aligned}
 \tilde{P}(n, s) &= (A^2 - B^2)^{-1/2} \{ (s + \gamma) [(A^2 - B^2)^{1/2} - A]^{|n|} B^{-|n|} \\
 &\quad + \frac{1}{2}(\Gamma_b - \Gamma_f) [(A^2 - B^2)^{1/2} - A]^{|n+1|} B^{-|n+1|} \\
 &\quad + \frac{1}{2}(\Gamma_b - \Gamma_f) [(A^2 - B^2)^{1/2} - A]^{|n-1|} B^{-|n-1|} \},
 \end{aligned}
 \tag{4.10}$$

where

$$A(s) = s^2 + 2s\gamma + 2\Gamma_f\gamma,$$

and

$$B(s) = -2\Gamma_f(s + \gamma).$$

When the result is transformed into the conditional probability $P(n, t)$ in lattice space and time, it is found [60, 61] that side peaks develop at intermediate times, cf. fig. 4.1. These side peaks are clearly visible for $\Gamma_f \gg \Gamma_b$; and they correspond to the fraction of particles, in an ensemble, that have not yet suffered backward transitions. In this limit the particles move in the forward direction with an apparent velocity $a\Gamma_f \approx a\gamma$. However, these apparent manifestations of a 'persistence of motion' are transient as long as Γ_f/Γ_b is finite. Eventually, each particle will be scattered in the backward direction, and asymptotically diffusive behavior is obtained. The conditional probability approaches asymptotically a Gaussian distribution, cf. also the discussion in section 4.4.

The conditional probability, eq. (4.6) can be decomposed into partial fractions, and the dynamical incoherent structure function obtained by using eq. (2.34). The zeroes of the denominator in eq. (4.6) are given by

$$s_{1,2} = -[\Gamma_b + \Gamma_f(1 - \cos ka)] \pm SQ, \quad (4.11)$$

$$SQ = (\Gamma_b^2 - \Gamma_f^2 \sin^2 ka)^{1/2}.$$

Only when $\Gamma_b > \Gamma_f$ the two poles are always real. In the opposite case $\Gamma_f > \Gamma_b$ there appear complex poles for larger k values. The consequences of complex poles in the conditional probability in real space and time are the side peaks discussed above. The structure function is only discussed for backward correlations $\Gamma_b > \Gamma_f$. In this case it is the sum of two Lorentzians

$$S_{\text{inc}}(k, \omega) = W_1 \frac{\omega_1/\pi}{\omega_1^2 + \omega^2} + W_2 \frac{\omega_2/\pi}{\omega_2^2 + \omega^2}, \quad (4.12)$$

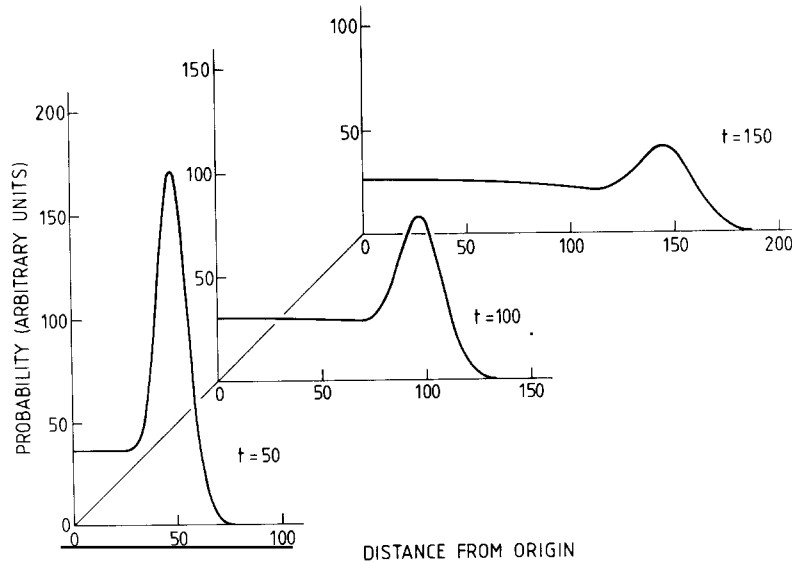


Fig. 4.1. Conditional probability for the forward-correlated random-walk model with $\Gamma_f = 0.99\gamma$ at three different times plotted as a function of distance from the origin. A continuous curve was drawn through simulation results for 450 000 particles and the time is given in Monte-Carlo steps per particle.

where $\omega_{1,2} = -s_{1,2}$ are the widths of the Lorentzian and the weights are given by

$$W_1 = (SQ + I_b \cos ka)/(2SQ), \quad W_2 = 1 - R_1. \tag{4.13}$$

In the limit $k \rightarrow 0$ there is only one Lorentzian and its width is proportional to the diffusion coefficient,

$$W_1 \xrightarrow{k \rightarrow 0} 1, \quad W_2 \xrightarrow{k \rightarrow 0} 0, \quad \omega_1 \xrightarrow{k \rightarrow 0} \frac{1}{2} f\gamma(ka)^2. \tag{4.14}$$

The behavior for general k is given by the formulae above. For instance, at the zone boundary $k = \pi/a$ the first weight vanishes,

$$W_1 \xrightarrow{k \rightarrow \pi/a} 0, \quad W_2 \xrightarrow{k \rightarrow \pi/a} 1,$$

and the second pole gives the summary transition rate,

$$\omega_2 \xrightarrow{k \rightarrow \pi/a} 2\gamma. \tag{4.14'}$$

The widths and weights of this one-dimensional correlated-walk model will be represented in fig. 5.2b, to facilitate comparison with the results for the two-state model.

4.2. Model with reduced reversals/backward jump model

This section describes a simple model of a RW of a particle with correlations over two successive steps that can be solved explicitly in arbitrary dimensions. There are two special cases of this model that are discussed here, i) the particle has a less-than-average probability of returning to the site visited by the preceding step (model with reduced reversals), and ii) the particle has a larger-than-average probability of returning to the previous site (backward jump model). Of course, both models differ only in the sign of the correlations, not in their physical content. The discrete RW with the correlations described above was treated by Domb and Fisher [62] following earlier work of Gillis [63]. They obtained the solution for the generating function, the derivations were quite complicated. The CTRW of a particle including the correlations described above was considered by the authors [59].

Here the direct approach of ref. [59] will be followed. It is a generalization of the treatment of RW by recursion relations in section 3.2. The probability density $Q_\nu(\mathbf{n}, t)$ of a transition of the particle to site \mathbf{n} at time t by step number ν is now related to this quantity taken with one *and* two steps less ($\nu \geq 3$)

$$Q_\nu(\mathbf{n}, t) = (1 - \varepsilon) \sum_m \int_0^t dt' \psi(t - t') p_{\mathbf{n},m} Q_{\nu-1}(\mathbf{m}, t') + \varepsilon \sum_m \int_0^t dt' \int_0^{t'} dt'' \psi(t - t') \psi(t' - t'') q_{\mathbf{n},m} Q_{\nu-2}(\mathbf{m}, t''). \tag{4.15}$$

The parameter ε determines the strength of the memory to the previous step ($\nu - 2$). For the special case $\varepsilon = 0$ the single-state CTRW is recovered. Separable CTRW is used, and $p_{\mathbf{n},m}$, $q_{\mathbf{n},m}$ are normalized

spatial transition probabilities. A simple choice is nearest-neighbor transitions for $p_{n,m}$, as described by eq. (2.1), and

$$q_{n,m} = \delta_{n,m}. \quad (4.16)$$

With this particular choice and $\varepsilon > 0$ the particle has a preference to return to a visited site by two consecutive transitions, while for $\varepsilon < 0$ the particle tends to avoid this site (model with reduced reversals).

The further derivations parallel those of sections 3.2 and 3.3. It is convenient to introduce Fourier and Laplace transformations. The Fourier transform of $q_{n,m}$ is denoted by $q(\mathbf{k})$; it is unity for the case eq. (4.16). The initial condition is $P(\mathbf{k}, t = 0)$. It is assumed that no memory is effective at the first step, either by preparation or by using a stationary ensemble. Let $h(t)$ be the appropriate WTD for the first step. Then

$$\begin{aligned} \tilde{Q}_1(\mathbf{k}, s) &= p(\mathbf{k}) \tilde{h}(s) P(\mathbf{k}, 0), \\ \tilde{Q}_2(\mathbf{k}, s) &= (1 - \varepsilon) p(\mathbf{k}) \tilde{\psi}(s) \tilde{Q}_1(\mathbf{k}, s) + \varepsilon q(\mathbf{k}) \tilde{\psi}(s) \tilde{h}(s) P(\mathbf{k}, 0). \end{aligned} \quad (4.17)$$

Resummation of the recursion relation yields

$$\tilde{Q}(\mathbf{k}, s) = \frac{p(\mathbf{k}) + \varepsilon q(\mathbf{k}) \tilde{\psi}(s)}{1 - (1 - \varepsilon) \frac{p(\mathbf{k}) \tilde{\psi}(s)}{p(\mathbf{k}) \tilde{\psi}(s)} - \varepsilon q(\mathbf{k}) \tilde{\psi}^2(s)} \tilde{h}(s) P(\mathbf{k}, 0). \quad (4.18)$$

The Green function $\tilde{P}(\mathbf{k}, s)$ in the Fourier and Laplace domain is obtained from eq. (4.18) by using a relation analogous to eq. (3.12),

$$\begin{aligned} \tilde{P}(\mathbf{k}, s) &= \{ \tilde{\Psi}(s) [1 - (1 - \varepsilon) p(\mathbf{k}) \tilde{\psi}(s) - \varepsilon q(\mathbf{k}) \tilde{\psi}^2(s)]^{-1} \\ &\quad \cdot [p(\mathbf{k}) + \varepsilon q(\mathbf{k}) \tilde{\psi}(s)] \tilde{h}(s) + \tilde{H}(s) \} P(\mathbf{k}, 0). \end{aligned} \quad (4.19)$$

Substitution of $\tilde{\Psi}(s)$ and $\tilde{H}(s)$ leads to the form

$$\tilde{P}(\mathbf{k}, s) = \frac{[1 + \varepsilon p(\mathbf{k}) \tilde{\psi}(s)][1 - \tilde{h}(s)] + [p(\mathbf{k}) + \varepsilon q(\mathbf{k}) \tilde{\psi}(s)] [\tilde{h}(s) - \tilde{\psi}(s)]}{s [1 - (1 - \varepsilon) \frac{p(\mathbf{k}) \tilde{\psi}(s)}{p(\mathbf{k}) \tilde{\psi}(s)} - \varepsilon \frac{q(\mathbf{k}) \tilde{\psi}^2(s)}{q(\mathbf{k}) \tilde{\psi}^2(s)}]} P(\mathbf{k}, 0). \quad (4.20)$$

This is the generalization of Tunaley's result eq. (3.15) to the model with reduced reversals, his result is recovered for $\varepsilon = 0$.

Simpler expressions are obtained for the special case of a Poisson process. In this case $\tilde{\psi}(s) = \gamma/(s + \gamma)$ and the WTD for the first jump $\tilde{h}(s) \equiv \tilde{\psi}(s)$. Also $P(\mathbf{k}, 0) = 1$ will be used. The conditional probability is then given by

$$\tilde{P}(\mathbf{k}, s) = \frac{s + \gamma + \varepsilon \gamma p(\mathbf{k})}{(s + \gamma)^2 - (1 - \varepsilon) \gamma (s + \gamma) p(\mathbf{k}) - \varepsilon \gamma^2}. \quad (4.21)$$

Here the special case eq. (4.16) was used and $p(\mathbf{k})$ is given by eq. (2.5) for the square, simple-cubic,

and hypercubic lattices. The result eq. (4.21) is equivalent to the result of Domb and Fisher when $(s + \gamma)$ is substituted with z^{-1} , the variable used in their generating functions, and ε identified with $-\delta$.

It is easy to deduce the frequency-dependent diffusion coefficient from eq. (4.21) by calculating the mean-square displacement and multiplying with $s^2/2d$. The result is, in Laplace space

$$\tilde{D}(s) = \frac{a^2 \gamma}{2d} \frac{s + (1 - \varepsilon)\gamma}{s + (1 + \varepsilon)\gamma}. \quad (4.22)$$

The frequency-dependent diffusion coefficient is obtained by substituting $s = i\omega$ and taking the real part. The high-frequency limit is given by $D(\infty) = a^2\gamma/2d$, thus the correlations do not enter in this limit. The diffusion coefficient in the static limit is related to the high-frequency limit by a proportionality constant f :

$$D = D(\infty) f; \quad (4.23)$$

the constant f , called the correlation factor, is given for this model by

$$f = (1 - \varepsilon)/(1 + \varepsilon). \quad (4.24)$$

The behavior of the frequency-dependent diffusion coefficient, $D(\omega)$, is shown in fig. 4.2 for two values of f . Positive ε corresponds to the backward jump model, $\varepsilon = 1$ or $f = 0$ is the limiting case where diffusion ceases to exist. Negative ε corresponds to the model with reduced reversals. There is a smallest admissible value of ε . A particle at site n that came from site m has the combined probability $(1 - \varepsilon) p_{m,n} + \varepsilon$ of return to site m . This quantity must be non-negative, hence it is required that $(1 - \varepsilon)/2d + \varepsilon \geq 0$. Thus ε can approach -1 in $d = 1$, but is restricted to $\varepsilon \geq -\frac{1}{3}$ on the square lattice in $d = 2$. The case $\varepsilon = -\frac{1}{3}$ in $d = 2$ is the one where no backward transitions occur at all, and the maximal correlation factor is $f = 2$. Analogous restrictions hold in higher dimensions.

It may be of interest to give the explicit expression for the mean-square displacement in the time domain which results from eq. (4.21)

$$\langle [R(t) - R(0)]^2 \rangle = \gamma a^2 \frac{1 - \varepsilon}{1 + \varepsilon} t - \frac{2\varepsilon a^2}{(1 + \varepsilon)^2} [e^{-\gamma(1+\varepsilon)t} - 1]. \quad (4.25)$$

Equation (4.25) is a generalization of Fuerth's result [54] for the discrete RW in $d = 1$ to a CTRW in arbitrary dimensions. The mean-square displacement is given in fig. 4.3 for the model with reduced reversals, for the uncorrelated random walk and for the backward jump model.

The model of correlated walks under consideration can be brought into correspondence with a second-order integro-differential equation [59]. To establish this correspondence eq. (4.19) is written in the form

$$\tilde{F}(\mathbf{k}, s) \tilde{P}(\mathbf{k}, s) = \left\{ \left[\frac{\gamma}{\tilde{\psi}(s)} p(\mathbf{k}) + \varepsilon \gamma q(\mathbf{k}) \right] \tilde{h}(s) + \tilde{F}(\mathbf{k}, s) \tilde{H}(s) \right\} P(\mathbf{k}, 0), \quad (4.26)$$

where

$$\tilde{F}(\mathbf{k}, s) = \frac{\gamma s}{\tilde{\psi}(s) [1 - \tilde{\psi}(s)]} [1 - (1 - \varepsilon) p(\mathbf{k}) \tilde{\psi}(s) - \varepsilon q(\mathbf{k}) \tilde{\psi}^2(s)],$$

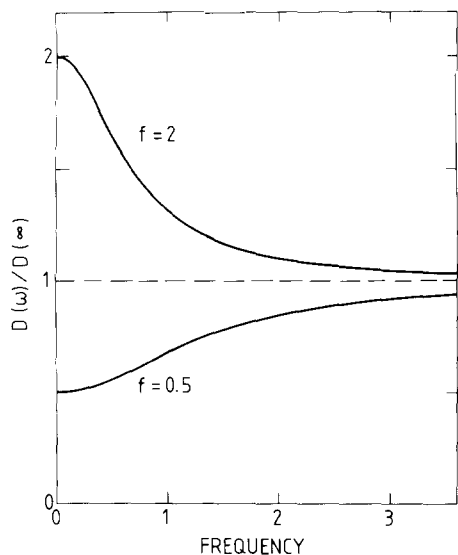


Fig. 4.2. The real part of the frequency-dependent diffusion coefficient from eq. (4.22). Results are scaled to $\tilde{D}(\infty)$ and f is defined in eq. (4.24).

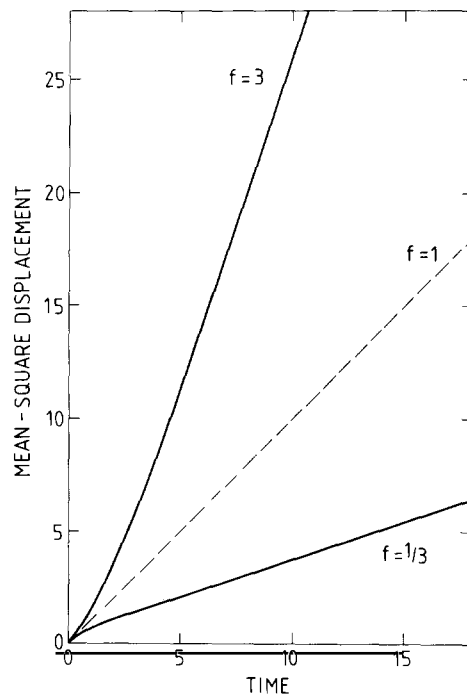


Fig. 4.3. Mean-square displacement of particles that perform correlated random walks with $f=3$ and $f=1/3$. The dashed curve is the result for uncorrelated random walks.

and

$$\gamma^{-1} = - \left. \frac{\partial \tilde{\psi}}{\partial s} \right|_{s=0}$$

is the inverse of the first moment of $\psi(t)$. The quantity $\tilde{F}(\mathbf{k}, s)$ can be brought into the form

$$\tilde{F}(\mathbf{k}, s) = s^2 + [1 - (1 - \varepsilon) p(\mathbf{k})] \gamma s + s \tilde{\chi}(s) + J(\mathbf{k}) \tilde{\eta}(s),$$

where

$$\tilde{\chi}(s) = \gamma / \tilde{\psi}(s) - s, \quad \tilde{\eta}(s) = \gamma s \tilde{\psi}(s) / [1 - \tilde{\psi}(s)]$$

and

$$J(\mathbf{k}) = 1 - (1 - \varepsilon) p(\mathbf{k}) - \varepsilon q(\mathbf{k}). \quad (4.27)$$

It is clear from the structure of $\tilde{F}(\mathbf{k}, s)$ in eq. (4.27) that a second derivative appears in the time domain. There appear initial-time terms when the transformation from the time to the Laplace domain is made. These initial-time terms are particularly simple when a stationary ensemble is considered where

$$\left. \frac{dP}{dt}(\mathbf{k}, t) \right|_{t=0} = -\gamma[1 - p(\mathbf{k})] P(\mathbf{k}, 0). \quad (4.28)$$

In the case of stationary initial conditions eq. (4.26) can be represented in the form

$$\tilde{F}(\mathbf{k}, s) \tilde{P}(\mathbf{k}, s) = [\gamma \tilde{\psi}^{-1}(s) + \varepsilon p(\mathbf{k}) \gamma] P(\mathbf{k}, 0) + \tilde{I}(\mathbf{k}, s). \quad (4.29)$$

The first terms on the right-hand side are the initial terms mentioned above and

$$\tilde{I}(\mathbf{k}, s) = \gamma [\tilde{\psi}(s) (1 - \tilde{\psi}(s))]^{-1} \{ [1 - p(\mathbf{k}) + \varepsilon \tilde{\psi}(s) (p(\mathbf{k}) - q(\mathbf{k}))] [\tilde{\psi}(s) - \tilde{h}(s)] \} P(\mathbf{k}, 0). \quad (4.30)$$

Transformation of eq. (4.29) to the time domain leads to the following equation

$$\begin{aligned} \frac{d^2 P}{dt^2}(\mathbf{k}, t) + \gamma [1 - (1 - \varepsilon) p(\mathbf{k})] \frac{dP}{dt}(\mathbf{k}, t) \\ + \int_0^t dt' \chi(t-t') \frac{dP}{dt}(\mathbf{k}, t') + J(\mathbf{k}) \int_0^t dt' \eta(t-t') P(\mathbf{k}, t') = I(\mathbf{k}, t). \end{aligned} \quad (4.31)$$

The kernels $\chi(t)$, $\eta(t)$ appearing in this equation are the inverse Laplace transforms of $\tilde{\chi}(s)$ and $\tilde{\eta}(s)$, respectively, cf. eq. (4.27). The inhomogeneity $I(\mathbf{k}, t)$ is the inverse Laplace transform of eq. (4.30).

The expressions simplify considerably for a WTD corresponding to a Poisson process. The kernels are then given by

$$\chi(t-t') = \gamma \delta(t-t'), \quad \eta(t-t') = \gamma^2 \delta(t-t'), \quad (4.32)$$

and the inhomogeneity eq. (4.30) vanishes since in this case $\psi(t) \equiv h(t)$. There remains the following second-order differential equation

$$d^2 P/dt^2 + [2\gamma - (1 - \varepsilon) p(\mathbf{k})] dP/dt + \gamma^2 J(\mathbf{k}) P = 0. \quad (4.33)$$

This second-order differential equation is solved by the usual Laplace–Fourier transformation methods. For Bravais lattices the equations are completely diagonalized by these methods. However, as demonstrated in chapter 2 for uncorrelated walks, the correlated-walk problem is not completely diagonalized for non-Bravais lattices; there are as many coupled equations as inequivalent sublattices. For instance, the tetrahedral lattice of interstitial sites in a body-centered cubic lattice has six inequivalent sites, therefore, the corresponding master equation is reduced to six coupled equations.

Equation (4.33) has the following continuum limit

$$\frac{d^2 P}{dt^2}(\mathbf{r}, t) + (1 + \varepsilon) \gamma \frac{dP}{dt}(\mathbf{r}, t) + (1 - \varepsilon) \gamma a^2 \nabla^2 \frac{dP}{dt}(\mathbf{r}, t) + \gamma^2 a^2 (1 - \varepsilon) \nabla^2 P = 0. \quad (4.34)$$

In the formal limit $\gamma \rightarrow \infty$, $\varepsilon \rightarrow -1$, $a \rightarrow 0$, such that $\gamma a = V$ and $(1 + \varepsilon)\gamma = \Gamma$ this equation is the

well-known telegraph equation

$$d^2P/dt^2 + \Gamma dP/dt + 2V^2 \nabla^2 P = 0, \quad (4.35)$$

which has been studied in connection with correlated random walks by Goldstein [64].

In this limit the particle moves mainly in the radial direction from its center and the particle moves in this direction with a velocity V . Every now and then a change of direction can occur, this event has a rate Γ ; were it not for a change of directions the particle would propagate in the medium without a loss of memory of its initial state.

4.3. Other models with correlated walks

There are many more models with correlated walks than the one considered, especially in higher dimensions, even if only memory to one previous step is included. Perhaps the simplest one is the *forward jump model* where the particle has a larger than average probability to make a transition in the same direction as the previous transition while the probability for a transition in any other direction is reduced compared to the average value. In $d = 1$ the forward jump model is identical with the model of reduced reversals while in higher dimensions they are different. This is illustrated in fig. 4.4 for both models on a square lattice and parameters such that the same diffusion coefficient obtains.

The models with memory over two consecutive steps are analytically treated by using the correspondence with multistate random walk discussed in chapter 3. The conditional probability is indexed by the previously occupied site \mathbf{n}' , as well as the presently occupied site, \mathbf{n} : $P(\mathbf{n}, \mathbf{n}', t)$. This index \mathbf{n}' specifies the prehistory of the particles. Since the transition probabilities extend to a finite set of neighbors of \mathbf{n} , the number of states, specified by \mathbf{n}' , is finite. The general procedure is exemplified by the forward jump model on a Bravais lattice with constant transition rates (corresponding to Poisson processes) Γ_f in forward and Γ' in the other directions. The resulting master equation for $P(\mathbf{n}, \mathbf{n}', t)$ is

$$\frac{d}{dt} P(\mathbf{n}, \mathbf{n}', t) = \Gamma_f [P(\mathbf{n}', 2\mathbf{n}' - \mathbf{n}, t) - P(\mathbf{n}, \mathbf{n}', t)] + \Gamma' \sum'_{\mathbf{n}'' \neq 2\mathbf{n}' - \mathbf{n}} [P(\mathbf{n}', \mathbf{n}'', t) - P(\mathbf{n}, \mathbf{n}', t)]. \quad (4.36)$$

For this model it is somewhat more convenient to introduce the directions of the transitions as the state index. Equation (4.36) can be transformed into a set of z coupled algebraic equations by Fourier and Laplace transformation. As can be verified on the explicit solution for the square lattice, no reduction to a set of two coupled equations appears possible for general directions in k -space. Hence one has to work with eq. (4.36) for the forward model in $d \geq 2$, or analogous equations for other models. In

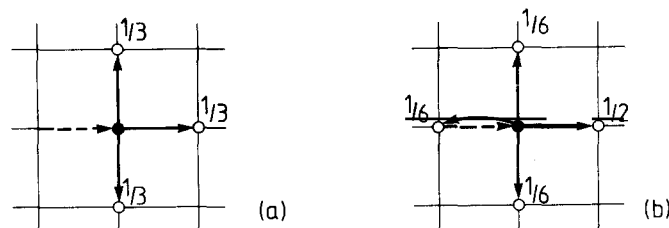


Fig. 4.4. Illustration of (a) model with reduced reversals and (b) forward jump model. The dashed arrows indicate the preceding steps and the full arrows indicate the consecutive steps. Probabilities for the transitions which give a correlation factor $f = 2$ are indicated in the figure.

contrast, the simple backward jump model or model with reduced reversals *are* reducible to two coupled or one second-order master equation. For this model the following master equation can be set up

$$\frac{d}{dt} P(\mathbf{n}, \mathbf{n}', t) = \Gamma_b [P(\mathbf{n}', \mathbf{n}, t) - P(\mathbf{n}, \mathbf{n}', t)] + \Gamma' \sum'_{\mathbf{n}'' \neq \mathbf{n}} [P(\mathbf{n}', \mathbf{n}'', t) - P(\mathbf{n}, \mathbf{n}', t)], \quad (4.37)$$

where Γ_b is the transition rate to the previous site \mathbf{n}' and Γ' the transition rate to arrive at a site which was not occupied in the previous step. In order to reduce the master equation eq. (4.37) to the results of the previous section, a summation over all previous histories is performed,

$$P(\mathbf{n}, t) = \sum_{\langle \mathbf{n}': \mathbf{n} \rangle} P(\mathbf{n}, \mathbf{n}', t). \quad (4.38)$$

The quantity $P(\mathbf{n}, t)$ then obeys the second-order differential equation eq. (4.33) where the following identifications are made

$$\gamma = \Gamma_b + (z - 1) \Gamma', \quad \varepsilon = (\Gamma_b - \Gamma') / \gamma. \quad (4.39)$$

The spatial transition probabilities $p_{n,m}$ and $q_{n,m}$ are given by eq. (2.1) and eq. (4.16), respectively.

The impossibility of reduction of the forward-jump model to the results of the previous section, related to the backward-jump model, is connected with the different symmetry of the correlated transitions in both models. In the backward-jump model, two correlated jumps lead to the initial site with strength ε , that is to a situation with the same symmetry as before. In the forward-jump model, two correlated jumps introduce a particular direction with a symmetry lower than the original symmetry. In $d = 1$ the forward-jump model and the model with reduced reversals are identical. The solution is provided by eq. (4.21) with $p(k) = \cos ka$. Of course, this solution is easily deduced from either eq. (4.36) with $\Gamma' = \Gamma_b$ or eq. (4.37) with $\Gamma' = \Gamma_f$ [59].

The forward- and backward-jump models were investigated by the authors [59b] for non-Bravais lattices; in particular, they considered the tetrahedral interstitial sites in a BCC lattice, which is relevant for hydrogen diffusion. In this work a set of coupled master equations with constant transition rates was formulated, extending eqs. (4.36) and (4.37) to the non-Bravais case. Also the case of 'planar jumps' in the lattice of tetrahedral sites was studied, cf. fig. 4.5. These types of jumps were suggested by molecular-dynamics studies of hydrogen motion in metals [65]. The coupled set of master equations was solved numerically in the Fourier-Laplace domain, it amounts to determining eigenvalues and eigenvectors of appropriate matrices, similar to the derivations in chapter 2. The eigenvalues determine the widths of the corresponding Lorentzians in the dynamical structure function, the eigenvectors their weights. Details are given in ref. [59b]. Okamura et al. [66] studied correlated discrete RW of a particle on the SC lattice with different probabilities for forward, backward and sideward steps, and a probability of sojourn on a lattice site. Thus their model includes also temporary trapping effects and the asymptotic diffusion coefficient contains both the features of correlated walk and of the trapping model to be discussed in the next chapter. Extensions to the BCC and FCC lattices were also considered. Godoy [67] considered the influence of an external field in correlated RW in $d = 1$, using a continuous-time formulation with WTD corresponding to a Poisson process in time. He observed that the introduction of an external field suppresses the divergence in the mean-square displacement of a particle for $\Gamma_f \rightarrow \gamma$ if the limits are taken appropriately.

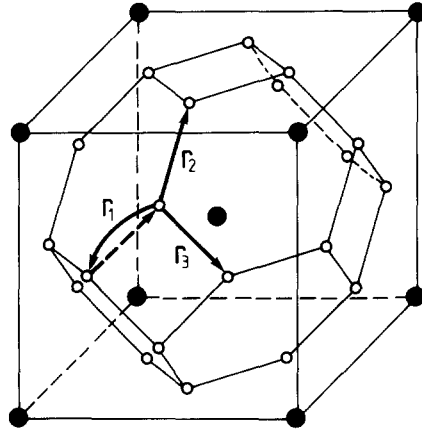


Fig. 4.5. Illustration of planar jump model on tetrahedral sites of a BCC lattice. The preceding step of the particle is indicated by the dashed arrow. In this model $r_3 \geq r_1 \geq r_2$ for preferred in-the-plane transitions.

The models referred to in this section regarded correlated RW either as a discrete process or as a continuous-time process with exponential WTD, representing a Poisson process. The extension of correlated walk to CTRW with general WTD was given by the authors [59] for the model with reduced reversals. (The introduction of a distinct WTD for the first transition was omitted in this work.) The model with reduced reversals is characterized by one WTD $\psi(t)$ for the temporal development, the correlations enter through the parameter ε . However, in a general multistate CTRW each transition (e.g. forward and backward in $d = 1$) can be characterized by a separate WTD, and only the sum of all transitions need be normalized according to eq. (3.31). An example of correlated walk with WTD that were not simple exponentials was studied by Landman and Shlesinger [47] in the context of their discussion of multistate CTRW. Correlated CTRW on the linear chain with general WTD $\psi_f(t)$ for forward and $\psi_b(t)$ for backward transitions was discussed by Zwerger and Kehr [68]. They obtained $\tilde{Q}(k, s)$ the Fourier–Laplace transform of the probability of a transition of the particle to site n at time t as

$$\tilde{Q}(k, s) = \frac{\tilde{\psi}_b(s) - \tilde{\psi}_f(s) + \cos(ak)}{1 - 2\tilde{\psi}_f(s)\cos(ak) + \tilde{\psi}_f^2(s) - \tilde{\psi}_b^2(s)} \tilde{h}(s) P(k, 0), \quad (4.40)$$

where $\tilde{h}(s)$ is the WTD for the first transition (see below).

Zwerger and Kehr also studied an explicit one-dimensional model with internal states that can be mapped exactly on the backward-jump model. This model is shown pictorially in fig. 4.6a. The particle may arrive at say level 1 at site i from the left, the WTD for a transition to level 3 at site $i - 1$ ($\psi_b(t)$) and a transition to level 1 at site $i + 1$ ($\psi_f(t)$) are different. They are derived explicitly from the first-passage problem on a finite chain, depicted in fig. 4.6b. The levels 1, 2, 3 correspond to levels, 1, 2, 3 at site i , 0 corresponds to $(3, i - 1)$ and 4 to $(1, i + 1)$. $\psi_b(t)$ is identical to the probability of the first transition at time t from 1 to 0, and $\psi_f(t)$ is identical to the probability of first transition to site 4 with 1 as the starting site. It is interesting to point out that the WTD for the *first* transition $h(t)$ in the stationary ensemble can be determined in two ways.

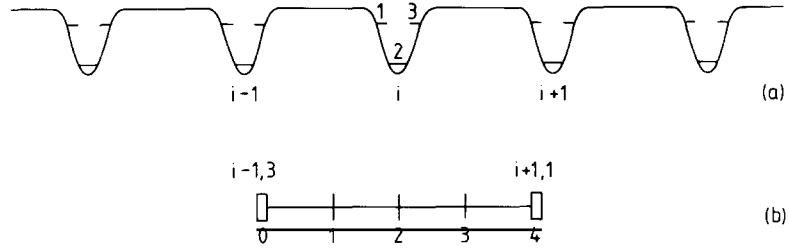


Fig. 4.6. (a) Random-walk model with internal states. (b) Diagram exhibiting the first-passage problem on a finite chain corresponding to the internal-state model.

(i) *The time average* of $\psi_f(t) + \psi_b(t)$ is taken, in analogy to eq. (3.3),

$$h_{\text{eq}}(t) = \frac{1}{t} \int_0^{\infty} dt' [\psi_f(t+t') + \psi_b(t+t')] ; \quad (4.41)$$

(ii) *the thermal average* of $\psi_f(t)$, $\psi_b(t)$ and the first-passage time distribution $\chi_{02}(t)$ of a transition from the inner level 2 to an adjacent site is taken

$$h_{\text{eq}}(t) = [P_{1,\text{eq}} + P_{3,\text{eq}}] [\psi_f(t) + \psi_b(t)] + P_{2,\text{eq}} \chi_{02}(t) . \quad (4.42)$$

Both determinations of $h_{\text{eq}}(t)$ give the same result. Further, the authors worked out the linear-response theory for this simple model and corroborated in this way the results of the CTRW description. The frequency-dependent diffusion coefficient of the one-dimensional backward-jump model is obtained as

$$D(\omega) = \frac{a^2}{2t} f(\omega) , \quad (4.43)$$

where the frequency-dependent correlation factor is given by

$$f(\omega) = \text{Re} \left\{ \frac{1 + \langle \cos \theta \rangle(s)}{1 - \langle \cos \theta \rangle(s)} \right\}_{s=i\omega} ,$$

where

$$\langle \cos \theta \rangle(s) = \tilde{\psi}_f(s) - \tilde{\psi}_b(s) . \quad (4.44)$$

Hence the frequency dependence of $D(\omega)$ is determined by the Fourier transforms of the WTD, in the combination indicated above. The static result is obtained by setting $s = 0$.

A three-dimensional correlated-jump model with general WTD was investigated by Kehr et al. [69] in the context of diffusion in lattice gases, see the following section. The authors derive the conditional probability $\tilde{P}(\mathbf{k}, s)$ in Fourier–Laplace space for correlated diffusion of a tagged particle in a FCC lattice with 5 different WTD for forward, backward, and 3 types for sideward transitions. Explicit expressions for $\tilde{P}(\mathbf{k}, s)$ were obtained in the main symmetry directions. Again the frequency-dependent diffusion coefficient is obtained in the form eqs. (4.43, 44) where

$$\langle \cos \theta \rangle(s) = \sum_{i=1}^5 n_i \cos \theta_i \tilde{\psi}_i(s), \quad (4.45)$$

and n_i are the numbers of equivalent transitions for one type of transition. Distinct WTD for the first transition were taken into account in these derivations.

4.4. Some properties of correlated continuous-time random walks

In this section some properties of correlated CTRW will be discussed in more detail.

i) *Markoffian nature.* This property of correlated walks was discussed by Montroll [70], who admitted correlations over an arbitrary but finite number of steps, and infinite correlations with sufficiently rapid decay with distance in the step numbers. Montroll was interested in the dependence of the squared end-to-end distance of polymer chains on the number n of monomers and the probability distribution of this distance. He considered explicitly a RW model of a polymer where the enumeration of monomers corresponds to the step number of a discrete walk. In his RW model on a square lattice only sideward transitions (90°) were allowed and first-order overlaps after four steps (corresponding to 4 monomers forming a square) were excluded. The essence of his argument can be formulated more abstractly by considering k consecutive steps $\mathbf{a}_{n-k}, \mathbf{a}_{n-k+1}, \dots, \mathbf{a}_n$ as a $k \times d$ dimensional matrix. Evidently this matrix at $n+1$ steps can be entirely deduced from the matrix at n steps if a memory to k steps is assumed. Consequently a Markov process occurs, described in terms of these matrices. All conclusions pertaining to such processes can be drawn, in particular that the growth of the mean-squared end-to-end distance is proportional to the step number (number of monomers). A singular case is the limit of strong correlations, i.e., when the next step is uniquely determined by the previous one, rendering the complete evolution deterministic. This is realized, for instance, in the forward model when $p_i = 1$ and the particle moves in a straight line.

ii) *Frequency dependence of diffusion coefficient.* As has been shown by the examples of the model with reduced reversals and the backward-jump model with general WTD, the diffusion coefficient of these models is frequency dependent. These examples are sufficient to establish the generic nature of the frequency dependence. The frequency dependence appears even when distinct WTD for the first transition corresponding to stationary ensembles are introduced. In more physical terms, this class of models has, by their design, taken into account the possibility of forward or backward correlations in the *velocity* of a particle; this is necessary to give frequency dependence to the diffusion coefficient. Alternatively formulated, the models with correlated jumps yield non-linear time-dependent mean-square displacements of a particle. Only at long times does the asymptotic diffusional behavior appear, which then contains the effect of the correlations. Hence, when the need arises of modelling a system with frequency dependence of the diffusion coefficient, the class of models with correlated CTRW offers a relatively simple possibility to include these effects.

iii) *Correspondence with single-state CTRW.* Correlated CTRW can be considered as a special case of multistate CTRW. Even the simple model of reduced reversals, which involves only one WTD and a memory between two steps, is equivalent to the multistate CTRW. One may inquire whether the result of a correlated-walk model can be mapped onto single-state CTRW models with possibly more complicated waiting-time distributions. To be specific, the discussion will be based on the model with reduced reversals with constant transition rates, whose Green function is given by eq. (4.21). This expression will be compared with the result of single-state CTRW eq. (3.15) including a distinct WTD for the first transition. One has to identify

$$\tilde{\psi}(s) = \frac{(1 - \varepsilon) \gamma (s + \gamma)}{(s + \gamma)^2 - \varepsilon \gamma^2}. \quad (4.46)$$

The WTD is normalized and its first moment is $\bar{t} = (1 + \varepsilon)/[(1 - \varepsilon)\gamma]$. The WTD $\tilde{h}_{\text{eq}}(s)$ corresponding to a stationary ensemble is deduced from eq. (4.46) according to eq. (3.3) or eq. (3.4). It is easily seen that eq. (3.15) cannot be brought into correspondence, if the WTD $\tilde{h}_{\text{eq}}(s)$ is used in this comparison. However, a correspondence can be established by identifying

$$\tilde{h}(s) = \frac{\gamma s + (1 - \varepsilon) \gamma^2}{(s + \gamma)^2 - \varepsilon \gamma^2}. \quad (4.47)$$

Hence correlated CTRW can be mapped, in this example, onto a single-state CTRW with a particularly chosen WTD for the first transition. This WTD does not represent an equilibrium ensemble and its physical meaning is not obvious.

iv) *Higher-order partial correlations.* Tchen [71] studied systematically the case of a RW with multiple partial correlations, i.e. specified partial correlations between two steps which are an arbitrary number apart. Let c_i describe a partial correlation over i steps ($c_1 = \langle \cos \theta \rangle$ of the previous case), then a simple final result can be obtained, if some third-order terms are neglected,

$$\langle (\mathbf{R}_n - \mathbf{R}_0)^2 \rangle / \langle (\mathbf{R}_n - \mathbf{R}_0)^2 \rangle_{\text{uc}} \xrightarrow{n \rightarrow \infty} \prod_{i=1}^k (1 + c_i) / \prod_{j=1}^k (1 - c_j), \quad (4.48)$$

where k is an arbitrary finite number. Further studies of higher-order partial correlations were made by Kutner [72] in the context of self-diffusion in lattice gases, see below. Rubin [73] studied the influence of correlations between step i and step $i + j$ of a RW where the step separation j can be large. He considered the dependence of the mean-square displacement on j in different dimensions, in order to understand the influence of repulsive interactions on the end-to-end distance of polymers.

4.5. Applications of correlated walks

Various applications of correlated random walks were made, some of the earlier applications were already mentioned. This section reviews other applications in a rather cursory way, except the tracer diffusion in metals, which will be discussed more thoroughly.

One important application is the description of conformations of polymers, initiated by Kuhn [56]. The details of this application are reviewed e.g. by Flory [74]. More recent work on polymer conformations using correlated-walk models was done by Fujita et al. [75], Thorpe and Schroll [76] and Schroll et al. [77]. Schroll et al. were particularly interested in the case of stiff chains, corresponding to strong forward correlations. The main point with respect to these applications is that a correlated walk with a memory over a finite number of steps does not allow a proper treatment of the effects of self-avoiding walks. The treatment of these effects requires quite different methods from the one discussed here and is outside the scope of this review. See [78] for an overview. The combined effects of self-avoiding walks and strong forward correlations were considered by Halley et al. [79].

Strongly correlated walks were also used by Argyrakis and Kopelman to describe coherent transport of excitons at low temperatures [80]. Coherent transport of excitons should be described by generalized master equations [44]. A rough physical picture is that an exciton propagates in one direction in a

wave-like fashion until it suffers a scattering event, it then continues to propagate in another direction until another scattering event occurs. This process was modelled by Argyrakis and Kopelman [80a] by a correlated walk where the exciton makes transitions over L sites in a straight line and L was taken from a Gaussian distribution with mean value $L \gg 1$ and standard deviation σ . After L steps the particle chooses another direction at random. Hence the model differs somewhat from the forward jump model of section 4.3, but the results of both models are rather similar if L and $p_f = \Gamma_f/\gamma$ are chosen appropriately.¹

Further applications of correlated walks comprise a description of superionic conductance [81], transport in a Lorentz gas [82], and the helix-coil transition of polypeptides [83].

The application of correlated walks to the diffusion of tracer particles in metals deserves special interest. Abstractly this is the problem of diffusion of a tagged particle in a lattice gas where the transition process is mediated by a small concentration of vacancies. In the limit of vanishingly small vacancy concentration, the correlations in the transitions of the tagged particle that are caused by one vacancy can only extend over two steps of the tagged particle [84]. This observation is the basis of the application of eq. (4.3b) to tracer diffusion in metals. The average angle $\langle \cos \theta \rangle$ between successive transitions of the tracer is commonly derived from lattice Green functions for diffusion of the vacancy [85, 86]. However, there are problems associated with the proper normalization of the weights used for calculating $\langle \cos \theta \rangle$. It is important to calculate the probabilities for the *first* return of the vacancy to the starting site only. A correct theory was given by Benoist et al. [87]. Another problem appears through the possibility of escape of the vacancy to infinity in three- and higher-dimensional crystals. Kidson [88] and Koiwa [89] showed in careful analyses how these processes can be taken into account. A third problem is the possibility of interference of the vacancy responsible for the first transition with other vacancies. Also this problem has been resolved by careful considerations [90].

All these derivations relate to long-range diffusion in the limit of large times or numbers of steps. Not much work has been done on the detailed time dependence of tracer diffusion in metals. There exists the phenomenological 'encounter model' which describes the net effect of correlated exchanges of one vacancy with the tagged particle [91, 92]. In $d = 1$ the WTD for an exchange of a vacancy with the tagged particle are known in the limit of vanishing vacancy concentration $c_v \rightarrow 0$ [93]. The extension of these results to higher dimensions seems straightforward, although it has not yet been worked out. It is necessary to employ the CTRW formulation of the model with correlated jumps where general WTD are used, and to express these WTD in terms of the time or frequency-dependent Green functions for the diffusion of a single vacancy, in a manner analogous to ref. [87]. The time dependence of correlated diffusion of tagged particles was also treated by Bender and Schroeder [94] using a hierarchy of master equations; they were interested in the application to the Moessbauer lineshape.

While the description of tagged particle diffusion in lattice gases as a RW with correlations over two successive steps is exact in the limit of vanishing vacancy concentration, the correlated RW is an approximation at higher vacancy concentrations. Much work has been devoted to lattice gases at arbitrary concentrations, both numerically (see the reviews [95, 96]) and theoretically (see [93, 97–102]). In the context of correlated CTRW, the waiting-time distributions of a tagged particle were estimated by Monte-Carlo simulations for diffusion of a lattice gas on an FCC lattice and analyzed by semiphenomenological considerations [69]. The WTD were classified according to forward, 3 types of sideward, and backward transitions, cf. fig. 4.7. The results at 4 different concentrations are reproduced in fig. 4.8. It is seen that the WTD for backward transitions begins for small times with the unblocked

¹ In the forward-jump model the distribution of straight paths p_L of length L is approximately Poissonian for $p_f \rightarrow 1$, $p_L \approx (1 - p_f) \exp[-(1 - p_f)L]$. The average length of a straight path in the forward model is $\bar{L} = (1 - p_f)^{-1}$.

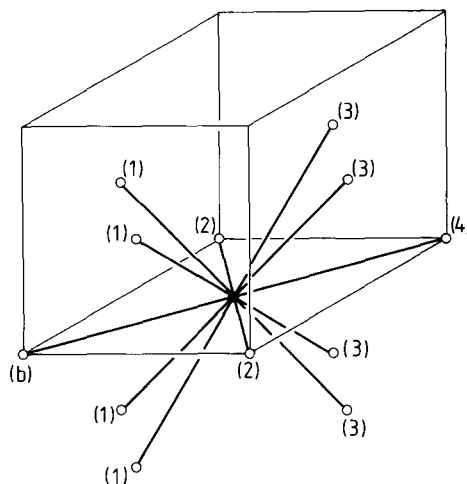


Fig. 4.7. Classification of consecutive transitions on an FCC lattice. The preceding step of the particle was from site (b) to the center of the bottom plane. The subsequent transitions can be designated as b (for backward) and by numbers indicating the order of the neighbor shell from site b.

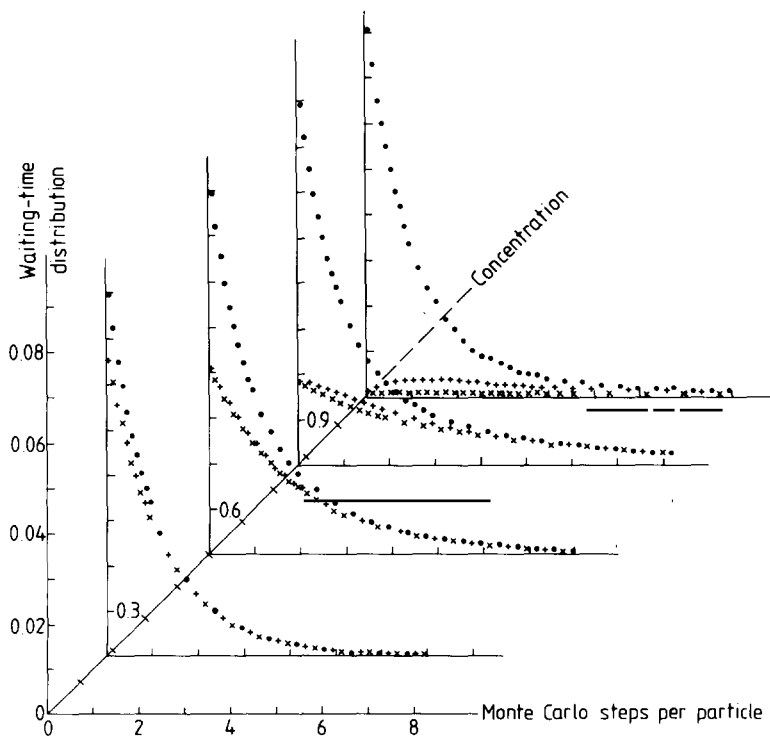


Fig. 4.8. The waiting-time distributions for four different concentrations of particles on the FCC lattice. The full circles indicate backward transitions, the plus signs, +, indicate transitions to sites labeled 1 in fig. 4.7 and the crosses, ×, indicate transitions to the site labeled 4.

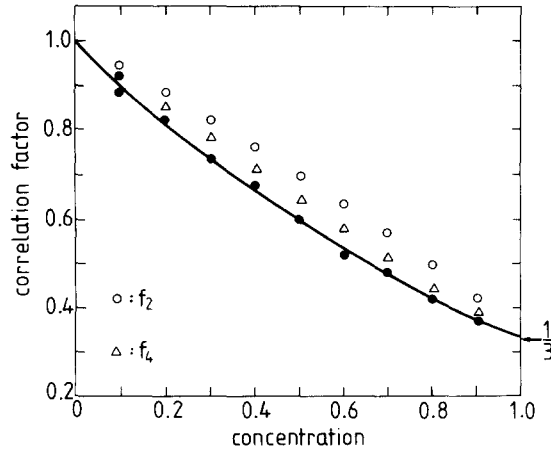


Fig. 4.9. Correlation factor f for tagged particle diffusion on a honeycomb lattice gas. Full circles: Monte-Carlo simulations; full line: theory of ref. [98]; open circles: f -factors where correlations over two jumps are included; open triangles: f -factors for four-step correlations. Figure adapted from [72].

transition rate Γ and decays to the forward WTD. The forward WTD begins with the blocked transition rate $(1 - c)\Gamma$ where c is the concentration of the lattice gas. The forward WTD behaves approximately exponentially. The WTD for sideward transitions shows an initial increase at small times, for small vacancy concentrations, due to the possibility that the initial vacancy enables a sideward transition. For more details see ref. [69]. This work appears to be the first simulation of WTD in a nontrivial physical context.

As a test on the validity of the assumption of correlations over two successive steps, one can derive the static diffusion coefficient by using the formula eq. (4.43) $\omega = 0$. As eqs. (4.44, 45) show this requires the determination of the areas of the WTD. One observes that the model is indeed a good approximation for tracer diffusion in an FCC lattice gas [69]. Kutner [72] made a similar investigation of tagged particle diffusion in a lattice gas on a honeycomb lattice. Due to the small coordination number ($z = 3$) correlation effects are expected to be more pronounced than in the FCC lattice. For instance, the correlation factor $f = \frac{1}{3}$ in this lattice in the limit $c_v \rightarrow 0$ whereas $f = 0.78145 \dots$ for the FCC lattice in this limit. As fig. 4.9 demonstrates the model of RW with correlations over two steps is clearly insufficient at general vacancy concentrations, and the correlation factor determined in the above-mentioned way differs markedly from the one directly determined from the reduction of the diffusion coefficient [72]. Inclusion of higher-order correlations remedies the discrepancy, but even when correlations over 4 steps are taken into account, the ensuing theoretical correlation factor differs still from the simulated value. Hence, CTRW with correlation over two successive steps is only a rough approximation for lattice gases at arbitrary concentrations whose quality depends on the type of lattice considered.

5. Multi-trapping models

5.1. The two-state model

In this chapter another class of random-walk models on ideal lattices is considered, namely the ‘multiple-trapping models’. They are characterized as random-walk models with internal states. In one of these states the particle can perform ordinary random walk on the lattice, but there are one or several trapping states associated with each site, the particle being immobile in these states. Release of

the particle from the trapping state(s) to the mobile state is possible; thus the trapping is temporary in these models. Although the multiple-trapping models are a subclass of the multistate models, they also deserve a separate discussion because of their simplicity and of their importance in applications. One advantage is that the multiple-trapping models with constant transition rates are explicitly solvable (analytically on Bravais lattices when only a few states are included). These solutions allow to pass explicitly to a contracted description and to study the correspondence with single-state CTRW.

The concept of two-state behavior in diffusive transport developed gradually in the past. An early reference is the work of Lennard-Jones [103, 104] who considered surface diffusion and attributed two states to a diffusing particle: (1) the vibrating state where it is immobile, and (2) the diffusive state. Let τ be the lifetime in the mobile state, D_f the diffusion coefficient of the particle in the mobile state, and τ^* the lifetime of the immobile states. Lennard-Jones deduced the effective diffusion coefficient D in the form

$$D = D_f \tau / (\tau^* + \tau) . \tag{5.1}$$

This form is highly plausible: it describes the reduction of the free diffusion coefficient by the mean time spent in the immobile state.

Subsequently, multistate trapping models were introduced in various fields of the natural sciences. Only a selected choice of references can be given. They were proposed to describe in a phenomenological manner transport processes in chemical systems [105–107], the transport of excited charge carriers across amorphous materials [108–116], self-diffusion in liquids [117], the motion of interstitials in metals [118–122], and $1/f$ noise [123]. Also the depolarization of muon-spin rotation caused by the interplay between diffusion and trapping was treated in the framework of multistate trapping [124–125].

To demonstrate the ease with which multistate behavior is discussed and to give an indication of its potential for applications, the Green function of the two-state model with constant transition rates is discussed in the remainder of this section. The model is depicted schematically in $d = 1$ in fig. 5.1. Three parameters characterize this model, γ the summary transition rate to neighbor sites in the free state ($\gamma = 2\Gamma$ for nearest-neighbor transitions), γ_t the capture rate into the trapped state and γ_r the release rate from the trapped state. For simplicity nearest-neighbor transitions on a Bravais lattice are assumed, as in eq. (2.1). The conditional probability is decomposed according to

$$P(\mathbf{n}, t) = P_f(\mathbf{n}, t) + P_t(\mathbf{n}, t) , \tag{5.2}$$

where the index indicates the state that is occupied by the particle. The master equations obeyed by a particle diffusing according to this model are

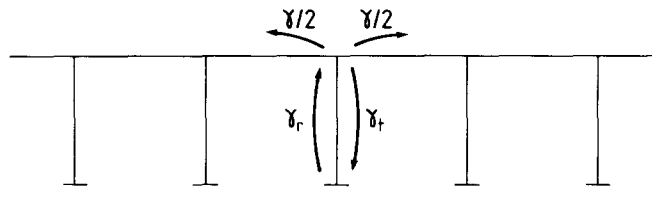


Fig. 5.1. The two-state model in one dimension with transition rate to nearest-neighbor sites $\gamma/2$, trapping rate γ_t and release rate γ_r .

$$\begin{aligned} \frac{d}{dt} P_i(\mathbf{n}, t) &= -\sum_{\mathbf{n}'} \Lambda_{\mathbf{n}, \mathbf{n}'} P_i(\mathbf{n}', t) - \gamma_t P_i(\mathbf{n}, t) + \gamma_r P_i(\mathbf{n}, t), \\ \frac{d}{dt} P_t(\mathbf{n}, t) &= -\gamma_r P_t(\mathbf{n}, t) + \gamma_t P_t(\mathbf{n}, t). \end{aligned} \quad (5.3)$$

$\Lambda_{\mathbf{n}, \mathbf{n}'}$ is the transition-rate matrix introduced in eq. (2.14'). To solve these equations they are transformed into the Fourier–Laplace domain,

$$\begin{aligned} [s + \Lambda(\mathbf{k}) + \gamma_t] \tilde{P}_i(\mathbf{k}, s) - \gamma_r \tilde{P}_i(\mathbf{k}, s) &= P_i(\mathbf{k}, 0), \\ [s + \gamma_r] \tilde{P}_t(\mathbf{k}, s) - \gamma_t \tilde{P}_t(\mathbf{k}, s) &= P_t(\mathbf{k}, 0), \end{aligned} \quad (5.4)$$

where $\Lambda(\mathbf{k}) = \gamma[1 - p(\mathbf{k})]$, cf. eq. (2.18).

Here the question of the appropriate initial conditions arises. The particle is assumed to start at the origin at $t = 0$. It may be further assumed that the probabilities of originating in the free or trapped state are given by the stationary solution of the master equation, i.e., by the asymptotic probabilities of finding the particle in either of the two states. The assumption reads explicitly

$$P_f(\mathbf{k}, 0) = \gamma_r / (\gamma_t + \gamma_r), \quad P_t(\mathbf{k}, 0) = \gamma_t / (\gamma_t + \gamma_r). \quad (5.5)$$

With this assumption the solution of eq. (5.4) is

$$\tilde{P}(\mathbf{k}, s) = \frac{s + \overline{\gamma_r} + \gamma_t + [\gamma_t / (\gamma_t + \gamma_r)] \Lambda(\mathbf{k})}{s^2 + s[\Lambda(\mathbf{k}) + \gamma_t + \gamma_r] + \gamma_r \Lambda(\mathbf{k})}. \quad (5.6)$$

For the square, simple-cubic lattices in d dimensions

$$\tilde{P}(\mathbf{k}, s) \xrightarrow{k \rightarrow 0} \frac{1}{s} - \frac{\overline{\gamma_r}}{\gamma_t + \gamma_r} \frac{\gamma}{s^2} \frac{(ka)^2}{2d} + \dots \quad (5.7)$$

The mean-square displacement follows from eq. (5.7) by using eq. (2.19) in the time domain

$$\langle [R(t) - R(0)]^2 \rangle = \frac{\gamma_r}{\gamma_t + \gamma_r} \gamma a^2 t, \quad t \geq 0. \quad (5.8)$$

The result contains the diffusion coefficient

$$D = D_f \gamma_r / (\gamma_t + \gamma_r). \quad (5.9)$$

This expression is in accordance with the form given by Lennard-Jones, cf. (5.1); note that τ^* corresponds to γ_r^{-1} , and the diffusion coefficient in the mobile state is $D_f = \gamma a^2 / 2d$, cf. eq. (2.23).

The mean-square displacement eq. (5.8) is strictly linear for all times, not only asymptotically. Hence, in this model and with the initial conditions assumed, the diffusion coefficient is frequency-independent,

$$D(\omega) = D . \tag{5.10}$$

In particular, $D(\infty) = D(0)$. The reduction factor in eq. (5.9) is interpreted differently at high and low frequencies. At high frequencies it represents the fraction of particles in the mobile state, at low frequencies the reduction through the average time spent in the immobile state.

While diffusion is simple in the two-state model, the structure of the Green function at general k is more complicated. The dynamical incoherent structure function $S_{\text{inc}}(\mathbf{k}, \omega)$ will be considered which is obtained from $\tilde{P}(\mathbf{k}, s)$ by application of eq. (2.34). The structure function can be decomposed into two Lorentzians

$$S_{\text{inc}}(\mathbf{k}, \omega) = \frac{W_1 \omega_1 / \pi}{\omega^2 + \omega_1^2} + \frac{W_2 \omega_2 / \pi}{\omega^2 + \omega_2^2} , \tag{5.11}$$

where the widths are given by

$$\begin{aligned} \omega_{1,2} &= \frac{1}{2} [A(\mathbf{k}) + \gamma_t + \gamma_r] \mp \frac{1}{2} SQ , \\ SQ &= [(A(\mathbf{k}) + \gamma_t + \gamma_r)^2 - 4\gamma_r A(\mathbf{k})]^{1/2} , \end{aligned} \tag{5.12}$$

and the weights by

$$W_1 = \frac{1}{2} + \frac{1}{2} [\gamma_t + \gamma_r + A(\mathbf{k}) (\gamma_t - \gamma_r) / (\gamma_t + \gamma_r)] / SQ , \quad W_2 = 1 - W_1 . \tag{5.13}$$

The widths and weights of a one-dimensional two-state model are given in fig. 5.2a. For comparison, the widths and weights of a one-dimensional correlated-walk model are given in fig. 5.2b. In the limit

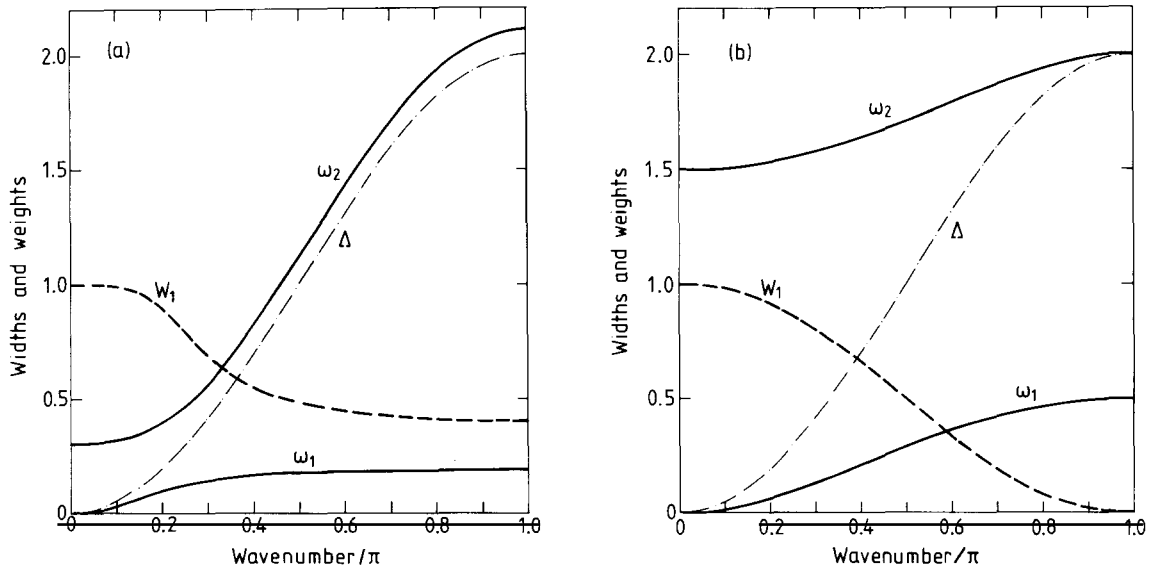


Fig. 5.2. (a) The widths and weights for the two-state model in one dimension. The dash-dotted line represents the width of the Lorentzian in the free state. The trapping rate is $\gamma_t = 0.2$, the release rate is $\gamma_r = 0.1$ and the transition rate is $\gamma = 1$. (b) Widths and weights for the correlated random walk in one dimension. The rate for forward transitions is $\gamma_f = 0.25$ and for the backwards transitions it is $\gamma_b = 0.75$. The dash-dotted line corresponds to the uncorrelated random walk.

$k \rightarrow 0$ only the diffusive component remains,

$$\begin{aligned} A(k) &\rightarrow Dk^2, \\ W_1 &= 1 - O(k^4), \quad W_2 = O(k^4). \end{aligned} \tag{5.14}$$

Generally, however, there are two components. Their interpretation becomes especially simple near the zone boundary under the condition $\gamma \gg \gamma_t, \gamma_r$

$$\begin{aligned} \omega_1 &\approx \gamma_r, \quad \omega_2 \approx 2\gamma, \\ W_1 &\approx \gamma_t / (\gamma_t + \gamma_r), \quad W_2 \approx \gamma_r / (\gamma_t + \gamma_r). \end{aligned} \tag{5.15}$$

It is seen that for these k values one component exhibits the effect of release from the traps with the appropriate weight of trap occupation. The other component exhibits essentially the free transitions to neighbor sites, again with the correct weight. The results of the two-state model for general k, ω were applied to an interpretation of the diffusion of hydrogen in metals with trapping centers by Richter and Springer [121]. They could verify the above-mentioned features in their experiments. For further details see ref. [121].

5.2. Multiple-trapping models

In this section the multiple-trapping models are considered in more detail. A particle may assume N different states at each lattice site, state N is the mobile state, the other $N - 1$ ones are immobile states. Constant transition rates between the states are assumed in this section; this leads naturally to a formulation in terms of master equations. Starting from the master equations, also the transformation to a generalized master equation will be examined. Special attention will be given to the role of the initial conditions. Two variants of multiple-trapping models will be considered,

i) *The direct-access trapping model.* This model has one mobile state N with a total transition rate γ to neighbor sites. For simplicity only nearest-neighbor transitions are assumed, characterized by the spatial transition probabilities $p_{n,m}$, eq. (2.1). The $N - 1$ trapping states are reached directly from the mobile state. The transition rate into the trapping state α is called γ_α , the escape rate from this state to the mobile state r_α . The model is schematically shown in fig. 5.3 for $d = 1$. The behavior of a particle according to this model is described by $P_\alpha(\mathbf{n}, t)$ the conditional probability of finding the particle at site \mathbf{n} in state α at time t . The initial conditions are specified later. The Green functions $P_\alpha(\mathbf{n}, t)$ develop according to the master equations

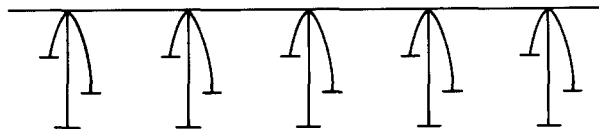


Fig. 5.3. A multiple-trapping model with direct transitions from the mobile state to each of the trap states.

$$\begin{aligned} \frac{d}{dt} P_N(\mathbf{n}, t) &= -\sum_m \Lambda_{n,m} P_N(\mathbf{m}, t) - \sum_{\alpha=1}^{N-1} \gamma_\alpha P_N(\mathbf{n}, t) + \sum_{\alpha=1}^{N-1} r_\alpha P_\alpha(\mathbf{n}, t), \\ \frac{d}{dt} P_\alpha(\mathbf{n}, t) &= -r_\alpha P_\alpha(\mathbf{n}, t) + \gamma_\alpha P_N(\mathbf{n}, t), \quad \alpha = 1, \dots, N-1. \end{aligned} \tag{5.16}$$

After Fourier and Laplace transformation the master equations read

$$\begin{aligned} \left[s + \Lambda(\mathbf{k}) + \sum_{\alpha=1}^{N-1} \gamma_\alpha \right] \tilde{P}_N(\mathbf{k}, s) - \sum_{\alpha=1}^{N-1} r_\alpha \tilde{P}_\alpha(\mathbf{k}, s) &= P_N(\mathbf{k}, 0), \\ (s + r_\alpha) \tilde{P}_\alpha(\mathbf{k}, s) - \gamma_\alpha \tilde{P}_N(\mathbf{k}, s) &= P_\alpha(\mathbf{k}, 0), \quad \alpha = 1, \dots, N-1. \end{aligned} \tag{5.17}$$

Thus the random-walk problem for the trapping model is reduced to a set of N coupled algebraic equations. Explicit solutions are easily obtained for smaller N , cf. the case $N = 2$ in the last section.

ii) *Ladder-trapping model.* Also this model has one mobile state (N) and $N - 1$ trapping states. However, the trapping states form a ‘ladder’ such that state α is connected to states $\alpha + 1$ and $\alpha - 1$. The transition rate to state $\alpha + 1$ is called ζ_α and the transition rate to state $\alpha - 1$ is ν_α . The ladder shall be finite, hence $\nu_1 = 0$. The rate ζ_N is replaced by γ , the total transition rate to neighbor sites. A pictorial representation of the ladder-trapping model in $d = 1$ is given in fig. 5.4. The ladder-trapping model is described by the master equations

$$\begin{aligned} \frac{d}{dt} P_N(\mathbf{n}, t) &= -\sum_m \Lambda_{n,m} P_N(\mathbf{m}, t) - \nu_N P_N(\mathbf{n}, t) + \zeta_{N-1} P_{N-1}(\mathbf{n}, t), \\ \frac{d}{dt} P_\alpha(\mathbf{n}, t) &= \nu_{\alpha+1} P_{\alpha+1}(\mathbf{n}, t) + \zeta_{\alpha-1} P_{\alpha-1}(\mathbf{n}, t) - (\nu_\alpha + \zeta_\alpha) P_\alpha(\mathbf{n}, t), \quad \alpha = 2, \dots, N-1, \\ \frac{d}{dt} P_1(\mathbf{n}, t) &= \nu_2 P_2(\mathbf{n}, t) - \zeta_1 P_1(\mathbf{n}, t). \end{aligned} \tag{5.18}$$

This set of master equations is transformed into a set of N coupled algebraic equations by Fourier and Laplace transformation. Hence also this model is solved in principle.

Often one is only interested in the summary quantity

$$P(\mathbf{n}, t) = \sum_{\alpha=1}^N P_\alpha(\mathbf{n}, t). \tag{5.19}$$

An experiment, for instance neutron scattering, may only allow to determine the time-dependent position of the particle, not its state. The question arises whether this summary quantity can be derived

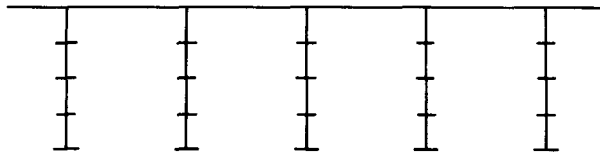


Fig. 5.4. A ladder-trapping model with a hierarchy of deeper traps.

for the trapping models more directly than by solving eq. (5.16) or eq. (5.18). Indeed, it will be shown that the trapping models, in this 'contracted' level, are completely equivalent to single-state CTRW, or to the generalized master equation.

The derivation will be made for the direct-access trapping model; it can be equally given for the ladder model. All equations of (5.17) are added with the result

$$\tilde{P}(\mathbf{k}, s) + \Lambda(\mathbf{k}) \tilde{P}_N(\mathbf{k}, s) = P(\mathbf{k}, 0). \quad (5.20)$$

The quantity \tilde{P}_N is eliminated from this equation by using the second group of equations (5.11) ($\alpha = 1, \dots, N-1$). The result can be written in the form

$$[s - \tilde{\phi}(\mathbf{k}, s)] \tilde{P}(\mathbf{k}, s) = P(\mathbf{k}, 0) + \tilde{I}(\mathbf{k}, s),$$

where

$$\begin{aligned} \tilde{\phi}(\mathbf{k}, s) &= -\Lambda(\mathbf{k}) \left(1 + \sum_{\alpha=1}^{N-1} \frac{\gamma_{\alpha}}{s + r_{\alpha}} \right)^{-1}, \\ \tilde{I}(\mathbf{k}, s) &= \Lambda(\mathbf{k}) \left[\left(1 + \sum_{\alpha=1}^{N-1} \frac{\gamma_{\alpha}}{s + r_{\alpha}} \right) \right]^{-1} \sum_{\beta=1}^{N-1} \frac{1}{s + r_{\beta}} P_{\beta}(\mathbf{k}, 0). \end{aligned} \quad (5.21)$$

This equation is precisely of the form of a generalized master equation, cf. (3.23). Here the case of 'separable' CTRW appears, hence the kernel ϕ and the inhomogeneity I should be compared with eqs. (3.28) and (3.29), respectively. The comparison gives the WTD

$$\tilde{\psi}(s) = \gamma \left[\gamma + s \left(1 + \sum_{\alpha=1}^{N-1} \frac{\gamma_{\alpha}}{s + r_{\alpha}} \right) \right]^{-1}. \quad (5.22)$$

A discussion of the initial state of the system has been deferred to this point. The inverse Laplace transform of eq. (5.21) would have the form of a homogeneous generalized master equation were $P_{\alpha} = 0$ for $\alpha = 1, 2, \dots, N-1$. This is the case when the initial state of the system is so prepared that the particle finds itself always in the transport state. This situation is realized in photoconductivity experiments where the electrons are initially excited on the surface of an amorphous semiconductor or polymer; also this is a good approximation when muons are implanted at random in a metal with a dilute concentration of traps. In other situations the system is not specially prepared and the equilibrium occupation of the various states on a particular lattice site is appropriate; this is the case, for instance, in neutron scattering experiments on hydrogen in metals.

The equilibrium occupation probabilities are easily obtained from eq. (5.16)

$$\begin{aligned} \rho_{\alpha} &= \sum_{\mathbf{n}} P_{\alpha}(\mathbf{n}, \infty) = \frac{\gamma_{\alpha}}{r_{\alpha}} \left(1 + \sum_{\beta=1}^{N-1} \frac{\gamma_{\beta}}{r_{\beta}} \right)^{-1}, \quad \alpha = 1, \dots, N-1, \\ \rho_N &= \sum_{\mathbf{n}} P_N(\mathbf{n}, \infty) = \left(1 + \sum_{\beta=1}^{N-1} \frac{\gamma_{\beta}}{r_{\beta}} \right)^{-1}. \end{aligned} \quad (5.23)$$

With these initial conditions, the comparison of eq. (5.21) with eqs. (3.28, 29) allows to identify

$$\tilde{h}(s) = \frac{\gamma[1 + \sum_{\alpha=1}^{N-1} \gamma_{\alpha}/(s + r_{\alpha})]}{(1 + \sum_{\alpha=1}^{N-1} \gamma_{\alpha}/r_{\alpha})(\gamma + \gamma[1 + \sum_{\beta=1}^{N-1} \gamma_{\beta}/(s + r_{\beta})])}. \quad (5.24)$$

This is the Laplace transform of $h_{\text{eq}}(t)$ determined according to eq. (3.3) and eq. (3.4). Namely, $\tilde{h}(s) = [1 - \tilde{\psi}(s)]/s$, where $\tilde{\psi}(s)$ is given by eq. (5.22) and

$$\bar{t} = \gamma^{-1} \left(1 + \sum_{\alpha=1}^{N-1} \frac{\gamma_{\alpha}}{r_{\alpha}} \right), \quad (5.25)$$

is the first moment of the WTD $\psi(t)$, as follows from eq. (5.22).

Thus it is shown that the contracted description of the multiple-trapping model is equivalent to single-state CTRW with a distinct WTD for the first transition. The WTD for the first transition depends on the initial conditions; for start in the mobile state $h(t) \equiv \psi(t)$, in the stationary situation $h(t)$ is determined from the time average of $\psi(t)$. The conclusions concerning the frequency independence of the diffusion coefficient in a stationary situation, which were given in chapter 3, hold in this model, and are easily verified directly. Analogous derivations, with identical conclusions, can be made for the ladder-trapping model.

The equivalence between multistate trapping models and single-state CTRW was established by Schmidlin [112] and Noolandi [113] for the initial conditions $P(\mathbf{k}, 0) = P_N(\mathbf{k}, 0)$ where no distinct WTD for the first transition appears. The equivalence was extended to include the case of stationary initial condition by the authors [126].

5.3. Direct derivation of waiting-time distributions for multistate trapping models

In the last section the WTD for the direct-access multistate trapping model was obtained by comparison of the CTRW theory with the results of the master-equation formulation. It should be possible to derive directly the WTD of the multistate trapping models, once it is accepted that these models are describable by CTRW. It is pointed out in this section how this can be done. Although only constant transition rates for the elementary transitions will be used, the derivations can be easily generalized to include more general WTD. First the direct-access trapping model will be studied.

The key to the WTD of the multistate trapping models is the observation that they are identical to the first-passage time distributions to the set of neighbor sites at time t when the particle arrived at the starting site at time zero. Thus the problem of determining the WTD for the direct-access multistate trapping model is equivalent to the first-passage time problem depicted in fig. 5.5a. The set of neighbor sites is replaced by a fictitious level $N + 1$, and $\psi(t)$ is identical to the first-passage probability density to level $N + 1$ given that the particle arrived at level N at $t = 0$. The following integral equation is obeyed by $\psi(t)$

$$\begin{aligned} \psi(t) = & \gamma \exp \left[- \left(\gamma + \sum_{\alpha=1}^{N-1} \gamma_{\alpha} \right) t \right] \\ & + \int_0^t dt' \int_0^{t'} dt'' \sum_{\beta=1}^{N-1} \gamma_{\beta} \exp \left[- \left(\gamma + \sum_{\alpha=1}^{N-1} \gamma_{\alpha} \right) t'' \right] r_{\beta} \exp[-r_{\beta}(t' - t'')] \psi(t - t'). \end{aligned} \quad (5.26)$$

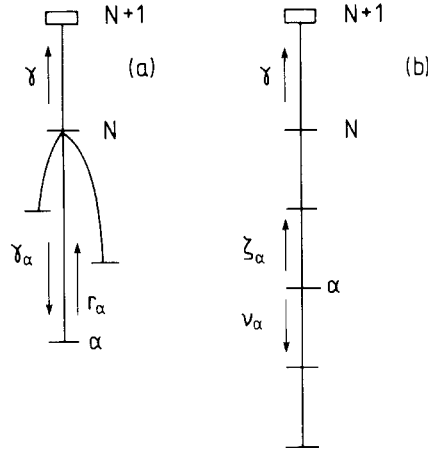


Fig. 5.5. The states needed to calculate the WTDs as first-passage time distributions: (a) for the direct-access trapping model and (b) for the ladder-trapping model. The absorbing site is shown as an open box.

The first term represents the WTD for a direct transition to the level $N + 1$; it is not normalized since the particle can also fall into the trapping levels. The second term represents the sum of possible transitions to trapping levels β with rates γ_β ; from these levels the particle can be released with rates r_β to make a first transition to the level $N + 1$ after a time lapse $t - t'$. The Laplace transform of the integral equation (5.26) is

$$\tilde{\psi}(s) = \left(s + \gamma + \sum_{\alpha=1}^{N-1} \gamma_\alpha \right)^{-1} \left[\gamma + \sum_{\beta=1}^{N-1} \frac{\gamma_\beta r_\beta}{s + r_\beta} \tilde{\psi}(s) \right]. \quad (5.27)$$

It follows straightforwardly that $\tilde{\psi}(s)$ is identical to eq. (5.22).

The derivation of the WTD for the ladder-trapping model is made in an analogous way. In this case the equivalent first-passage time problem can be given by introducing a finite chain with $N + 1$ states, see fig. 5.5b, the state $N + 1$ corresponding to the set of neighbor sites. The first-passage time distribution is required for the first transition of the particle to state $N + 1$ at time t given that it arrived at state N at $t = 0$. This WTD fulfils the integral equation

$$\begin{aligned} \psi(t) &= \gamma \exp[-(\gamma + \nu_N)t] \\ &+ \int_0^t dt' \int_0^{t'} dt'' \nu_N \exp[-(\gamma + \nu_N)t''] \chi_{N,N-1}(t' - t'') \psi(t - t'). \end{aligned} \quad (5.28)$$

The quantity $\chi_{N,N-1}(t)$ is the WTD for the first transition of the particle to state N when it arrived at state $N - 1$ at $t = 0$. Again the first term represents the direct transition from level N to level $N + 1$. Iteration of this equation leads to a series that describes repeated transitions between the levels $N - 1$ and N , with possible excursions of the particle to lower levels included in the WTD $\chi_{N,N-1}$. The solution of eq. (5.28) is obtained in the Laplace domain

$$\tilde{\psi}(s) = \frac{\gamma}{s + \gamma + \nu_N - \nu_N \tilde{\chi}_{N,N-1}(s)}. \quad (5.29)$$

Similar considerations as made above lead to the relation between the WTD $\tilde{\chi}_{\alpha+1,\alpha}$ and $\tilde{\chi}_{\alpha,\alpha-1}$ for the first transitions from α to $\alpha + 1$ and from $\alpha - 1$ to α ,

$$\tilde{\chi}_{\alpha+1,\alpha}(s) = \frac{\zeta_\alpha}{s + \zeta_\alpha + \nu_\alpha - \nu_\alpha \tilde{\chi}_{\alpha,\alpha-1}(s)}, \quad N - 1 \geq \alpha \geq 2. \quad (5.30)$$

Repeated substitution of $\tilde{\chi}_{\alpha+1,\alpha}$ in eq. (5.29) leads to a continued-fraction representation of the WTD $\tilde{\psi}(s)$ of the ladder-trapping model. This continued fraction will terminate for finite ladders, since for the lowest level

$$\tilde{\chi}_{21}(s) = \zeta_1 / (s + \zeta_1). \quad (5.31)$$

Hence also the WTD of the ladder-trapping model is obtained rather directly.

It is interesting to calculate the mean time the particle spends at given site according to the ladder-trapping model. The mean time \bar{t} can be essentially derived from the continued-fraction representation of $\tilde{\psi}(s)$, for details see ref. [68]. The result is

$$\bar{t} = \gamma^{-1} \left(1 + \frac{\nu_N}{\zeta_{N-1}} + \frac{\nu_N \nu_{N-1}}{\zeta_{N-1} \zeta_{N-2}} + \dots + \frac{\nu_N \dots \nu_2}{\zeta_{N-1} \dots \zeta_1} \right). \quad (5.32)$$

When the transition rates between levels α and $\alpha - 1$ are not symmetric, then their quotient may be interpreted as due to an energy difference between levels α and $\alpha - 1$, according to

$$\nu_\alpha / \zeta_{\alpha-1} = \exp[\beta(\varepsilon_\alpha - \varepsilon_{\alpha-1})], \quad (5.33)$$

where $\beta = (k_B T)^{-1}$. Using this expression the mean time \bar{t} can be given in the simple form

$$\bar{t} = \gamma^{-1} [1 + \exp\{\beta(\varepsilon_N - \varepsilon_{N-1})\} + \exp\{\beta(\varepsilon_N - \varepsilon_{N-2})\} + \dots + \exp\{\beta(\varepsilon_N - \varepsilon_1)\}]. \quad (5.34)$$

As an illustration, the WTD for the ladder trapping model with $N = 10$ and 20 levels will be shown in fig. 5.6. The rates are uniform, $\nu_\alpha + \zeta_\alpha = \gamma$, and $\nu_\alpha / \zeta_\alpha = \exp(\beta \Delta\varepsilon)$, and $\beta \Delta\varepsilon = 0.5$ was chosen. The WTD show a shoulder, which is essentially caused by the escape processes from the lowest levels. In fact, the WTD of the ladder model can be approximated by the WTD of a two-state model when the trapping rate is chosen as $\gamma_t = [1 + \exp(-\beta \Delta\varepsilon)]^{-1} \gamma$ and the release rate is $\gamma_r = \bar{t}^{-1}$ (cf. the dashed lines in the figure). However, quite different behavior of $\psi(t)$ can be obtained by other choices of the transition rates ν_α, ζ_α on the ladder.

The WTD for the first transition to a neighbor site, in the multiple-trapping model, can be derived as a thermal average by utilizing these methods. This will be exemplified for the direct-access trapping models. The WTD for the transition to level $N + 1$ at time t when the particle is in trapping level α ($\alpha = 1, \dots, N - 1$) at $t = 0$ will be called $\psi_\alpha(t)$. It is related to $\psi(t)$ by

$$\psi_\alpha(t) = \int_0^t dt' r_\alpha \exp(-r_\alpha t') \psi(t - t'). \quad (5.35)$$

The thermal average of all $\tilde{\psi}_\alpha(s)$, including $\tilde{\psi}(s)$ will be determined as

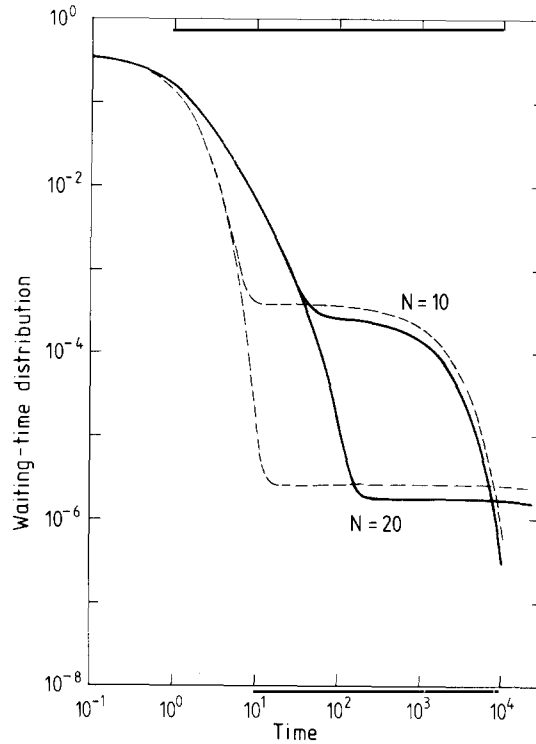


Fig. 5.6. The waiting-time distributions of the ladder-trapping model for $N=10$ and 20 levels. The dashed lines show the WTD of the corresponding two-state model with trapping and release rates as described in the text.

$$\langle \tilde{\psi}(s) \rangle = \sum_{\alpha=1}^{N-1} \rho_{\alpha} \tilde{\psi}_{\alpha}(s) + \rho_N \tilde{\psi}(s). \quad (5.36)$$

The weights ρ_{α} , ρ_N will be taken according to the stationary solution of the master equation, cf. eq. (5.23). The result is

$$\langle \tilde{\psi}(s) \rangle = \tilde{h}_{\text{eq}}(s) = \frac{1}{\bar{t}s} [1 - \tilde{\psi}(s)], \quad (5.37)$$

with \bar{t} as given in eq. (5.25) and $\tilde{h}_{\text{eq}}(s)$ represents the time average of the WTD $\tilde{\psi}(s)$. Hence the WTD for the first transition in a stationary situation can be introduced either as the time average of $\psi(t)$, cf. eqs. (3.3–4), or as the thermal average, cf. eq. (5.36).

The same conclusions can be drawn for the ladder-trapping model. Also in this model the WTD $\psi_{\alpha}(t)$ can be introduced and recursion relations obtained for them. It turns out [68] that also for this model the thermal average $\langle \tilde{\psi}(s) \rangle$ according to eq. (5.36) with the appropriate weights is identical to $\tilde{h}_{\text{eq}}(s)$, derived from the time average of $\psi(t)$.

5.4. Decomposition into number of state changes

There is an especially appealing way of treating multiple-trapping models, namely the method of decomposition into the number of state changes. Suppose a particle can be in either one of two states 1,

2. The conditional probability $P_1(\mathbf{n}, t)$ of finding the particle at site \mathbf{n} in state 1 at time t can be decomposed into an expression where no state change has occurred at all in the time interval $(0, t)$ plus an expression where the particle made one state change from 2 to 1 at an intermediate time t' , plus the terms representing repeated state changes. The decomposition is graphically shown in fig. 5.7, a similar picture can be drawn for the conditional probability $P_2(\mathbf{n}, t)$.

Let $R_\alpha(\mathbf{n}, t)$ be the Green functions for random walks in a single state where the particle remains *all the time* in state α ($\alpha = 1$ or 2), and $\phi_\alpha(t)$ the WTDs for the transitions to the other state. $R_\alpha(\mathbf{n}, t)$ is not the conditional probability of finding the particle on site \mathbf{n} in state α at time t , the latter quantity is determined below. The corresponding sojourn probabilities in the state α are $\Phi_\alpha(t)$. No distinct WTD for the first state changes are introduced to keep the formalism more transparent. Hence the following derivations are strictly valid i) for exponential WTD, as used for instance in the two-state model of section 5.1, ii) for arbitrary WTD if the first transition can be described by the same WTD as all further transitions. It is assumed that the $\phi_\alpha(t)$ are normalized and have finite first moments. Fourier transforms of the conditional probabilities will be employed to avoid convolutions in direct space. The conditional probability of finding the particle in state α at time t when it started in state β will be called $P_{\alpha\beta}(\mathbf{k}, t)$. Evidently, see fig. 5.7

$$\begin{aligned}
 P_{11}(\mathbf{k}, t) &= R_1(\mathbf{k}, t) \Phi_1(t) \\
 &+ \int_0^t dt' \int_0^{t'} dt'' R_1(\mathbf{k}, t'') \phi_1(t'') R_2(\mathbf{k}, t' - t'') \phi_2(t' - t'') R_1(\mathbf{k}, t - t') \Phi_1(t - t') + \dots
 \end{aligned}
 \tag{5.38}$$

The convolutions in eq. (5.38) become simple products in the Laplace domain. The Laplace transforms of the products $R_\alpha \Phi_\alpha$ and $R_\alpha \phi_\alpha$ appear and they will be designated by brackets, e.g.,

$$[R_\alpha \phi_\alpha]_s = \int_0^\infty dt \exp(-st) R_\alpha(k, t) \phi_\alpha(t).
 \tag{5.39}$$

If the WTDs are exponential, then the Laplace transform of R_α appears with a shifted argument, e.g.,

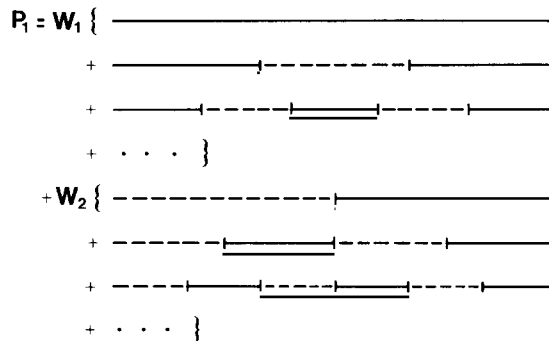


Fig. 5.7. Graph describing the conditional probability of finding a particle in state 1 at time t . The Green function of the particle being exclusively in state 1 is represented by the solid line, the same quantity for state 2 is represented by the dashed line.

$$\tilde{\phi}_\alpha(s) = \frac{\gamma_\alpha}{\gamma_\alpha + s} \Rightarrow [R_\alpha \phi_\alpha]_s = \gamma_\alpha \tilde{R}_\alpha(s + \gamma_\alpha). \quad (5.40)$$

The geometric series eq. (5.38) can be resummed with the result

$$\tilde{P}_{11}(\mathbf{k}, s) = \frac{[R_1 \Phi_1]_s}{1 - [R_1 \phi_1]_s [R_2 \phi_2]_s}. \quad (5.41)$$

Similarly, for the other states,

$$\begin{aligned} \tilde{P}_{12}(\mathbf{k}, s) &= D^{-1} [R_2 \phi_2]_s [R_1 \Phi_1]_s, \\ \tilde{P}_{21}(\mathbf{k}, s) &= D^{-1} [R_1 \phi_1]_s [R_2 \Phi_2]_s, \\ \tilde{P}_{22}(\mathbf{k}, s) &= D^{-1} [R_2 \Phi_2]_s, \\ D &= 1 - [R_1 \phi_1]_s [R_2 \phi_2]_s. \end{aligned} \quad (5.42)$$

The summary conditional probability is given by

$$\tilde{P}(\mathbf{k}, s) = W_1 [\tilde{P}_{11}(\mathbf{k}, s) + \tilde{P}_{21}(\mathbf{k}, s)] + W_2 [\tilde{P}_{12}(\mathbf{k}, s) + \tilde{P}_{22}(\mathbf{k}, s)], \quad (5.43)$$

where W_1, W_2 are the weights of the initial states 1 and 2. In the stationary situation these weights can be obtained from the behavior of eqs. (5.41–42) for small s , corresponding to long times. It is seen that the summary conditional probability is normalized, and

$$\begin{aligned} \tilde{P}_{11}(0, s), \tilde{P}_{12}(0, s) &\xrightarrow{s \rightarrow 0} \frac{1}{s} \frac{\bar{t}_1}{\bar{t}_1 + \bar{t}_2}, \\ \tilde{P}_{21}(0, s), \tilde{P}_{22}(0, s) &\xrightarrow{s \rightarrow 0} \frac{1}{s} \frac{\bar{t}_2}{\bar{t}_1 + \bar{t}_2}, \end{aligned} \quad (5.44)$$

where

$$\bar{t}_\alpha = -\partial \tilde{\phi}_\alpha / \partial s|_{s=0}.$$

The coefficients of eq. (5.44) can now serve as the weights in eq. (5.43). The final results for exponential WTD $\phi_\alpha(t)$ can be brought into the form

$$\tilde{P}(\mathbf{k}, s) = [D(\bar{t}_1 + \bar{t}_2)]^{-1} \{ \bar{t}_1 [R_1 \Phi_1]_s + 2[R_1 \Phi_1]_s [R_2 \Phi_2]_s + \bar{t}_2 [R_2 \Phi_2]_s \}. \quad (5.45)$$

It is instructive to work out the case of the simple two-state model with exponential WTD, $\tilde{R}_1(\mathbf{k}, s) \equiv \tilde{P}(\mathbf{k}, s)$ for simple random walk (cf. section 2.2) and $\tilde{R}_2(\mathbf{k}, s) = 1/s$ corresponding to a trapped particle. Of course, the results of section 5.1 are recovered.

The treatment of the two-state model by decomposition into the number of state changes and

resummation of the series was given by Singwi and Sjolander [117]. They applied this formalism to a description of oscillatory diffusion in liquids. The mathematical description of two-state renewal processes was reviewed by Cox [127]. The two-state random walk with general WTD, including distinct WTD for the first transition, was treated by Weiss [128, 129] who also included biased random walks. Weiss was mainly interested in the derivation of asymptotic properties, such as the Gaussian form of the conditional probability and the mean time spent in the two states. The advantage of the treatment of the two-state model by decomposition into the number of state changes is that the Green functions of the individual states $R_\alpha(\mathbf{k}, t)$ are considered to be known, it is not necessary to derive them simultaneously. This may save much labor. Expressed differently, in a multistate CTRW all site and state changes are treated on the same footing. In the approach presented in this section the transitions between sites, within the *same* state, are already summed up to the Green functions $R_\alpha(\mathbf{k}, t)$. It is obvious that the formalism can be extended to a larger number of states, although the calculational efforts are increased. It should be noted [129] that the ordinary random walk can be considered as a special case of the two-state random walk, with one state corresponding to the instantaneous transitions to neighbor sites and the other one to the sojourn at a site. It is also worth mentioning that a decomposition into the number of state changes is useful in other stochastic problems, for example in chemical kinetics and its investigation by NMR (for a review see [130]), rotational diffusion of molecules [131] and in the strong collision model of the depolarisation of rotating spins [125, 132].

6. Lattice models with random barriers

6.1. Introduction

Beginning with this chapter a new aspect of diffusion in disordered media is treated. In all the previous chapters, the models were solvable by Fourier transform methods alone because the models possessed translational invariance. With a degree of disorder in the medium averaging methods must be developed to restore the translational invariance to averaged quantities. Perhaps the most intensively studied lattice models possessing random transition rates are the random barrier models. One compelling reason for studying this model is its simplicity and as a consequence, there is a wealth of exact results that have been obtained [133–140]. These results can be used as benchmark tests of the validity of approximate or more simply expressed solutions. The reader should not be discouraged from investigating such models, because the solution remains incomplete; most results have been obtained in one dimension and even for this case, a complete solution has been given only for the case when the barriers are infinitely high. In higher dimensions the solution of the infinite barrier problem must be at least as difficult as solving the bond percolation problem to be discussed below. Hence, there is a clear need to develop useful and accurate approximations for application to higher dimensional systems. These models, simple as they may be, find application in explaining frequency-dependent conductivity experiments of disordered quasi-one-dimensional electronic conductors, conductive polymers, semiconductor glasses and transport through composite materials.

The model is depicted in fig. 6.1. The sites are at the potential minima and the barriers over which the particles jump have heights which are randomly and independently placed on the lattice. The transition rate from site n to site $n + 1$ is the same as the transition rate from site $n + 1$ to n ; this feature is present because all the minima lie at the same energy. As might be expected from the pictorial representation, the equilibrium solution corresponds to all sites having the same occupation probability.

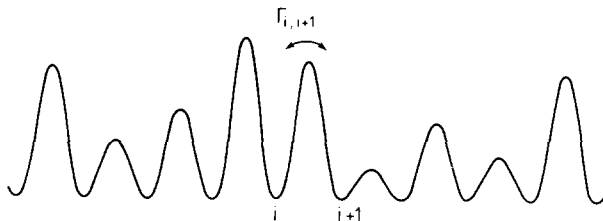


Fig. 6.1. Schematic representation of the random barrier (or mountain) model. All valleys are equally spaced and have the same energy.

6.2. Exact results in one dimension

The presentation is restricted in this portion of the chapter to one dimension. The dynamics of the particle on a linear chain is described by the master equation:

$$dP(n, t)/dt = \Gamma_n [P(n-1, t) - P(n, t)] + \Gamma_{n+1} [P(n+1, t) - P(n, t)], \quad (6.1)$$

where the nearest-neighbor transition rates are labeled according to the larger site index of the pair. The treatment outlined below is due to Zwanzig [138] and the results were extended by Denteneer and Ernst [139, 140].

Consider a lattice of N sites with periodic boundary conditions; the lattice constant, a , is chosen to be unity. The method of Zwanzig introduces the Laplace transform of the time variable and the Fourier transform of the space variable to express the conditional probability.

The solution of the master equation, eq. (6.1), is formally written as:

$$\tilde{P}(k, s) = \sum_{k'} (s\mathbf{E} + \mathbf{f} \cdot \mathbf{U} \cdot \mathbf{f}^*)^{-1} P(k', 0), \quad (6.2)$$

where the following matrices have been defined:

$$f_{kk'} = \delta_{kk'} (e^{ik} - 1), \quad (6.3)$$

and

$$U_{kk'} = \frac{1}{N} \sum_n e^{i(k-k')n} \Gamma_n. \quad (6.4)$$

The matrix \mathbf{f} has been defined so that it has an inverse. \mathbf{E} is the previously defined unit matrix. The matrix multiplying $P(k', 0)$ in eq. (6.2) is the Green function for the dynamical process; it is denoted by $\tilde{G}_{k,k'}(s)$.

From the Green function a connection can be made between the density of eigenvalues, which is simply called the density of states, and the averaged Green function. The density of states is the sum of delta functions having the eigenvalues in the argument averaged over the ensemble of configurations of the system. This is called a spectral property of the model. The normalized density of states is:

$$\rho(u) = \frac{1}{N} \sum_\nu \langle \delta(u - \lambda_\nu) \rangle, \quad (6.5)$$

where the brackets denote an average over all configurations of transition rates. We note here that the average is taken over the distribution of disordered transition rates in the medium. In previous chapters averages have been implicitly taken over realizations of random walks and over thermally weighted initial conditions. Here these averages are not distinguished with different notations and the meaning of the brackets will be clear from the accompanying text. The eigenvalues belong to the spectrum of the matrix of transition rates; from eq. (6.2) the relation between the eigenvalues and the matrix can be written as:

$$\lambda_\nu V_\nu = \mathbf{f} \cdot \mathbf{U} \cdot \mathbf{f}^* \cdot V_\nu, \tag{6.6}$$

where the eigenfunctions V are not further necessary for the density of states. The identity

$$\frac{1}{u - \lambda_\nu - i\varepsilon} = P \frac{1}{u - \lambda_\nu} + i\pi \delta(u - \lambda_\nu), \tag{6.7}$$

where P denotes the principal part, is useful for making the connection between the density of states and the Green function. Using eq. (6.7) in eq. (6.5) gives:

$$\rho(u) = \frac{\text{Im}}{\pi} \left\langle \frac{1}{N} \sum_\nu \frac{1}{u - i\varepsilon - \lambda_\nu} \right\rangle, \tag{6.8}$$

where Im is the imaginary part of the quantity and N is the number of sites introduced earlier. The eigenvalues are replaced by the full matrix using eq. (6.6),

$$\begin{aligned} \rho(u) &= \frac{-\text{Im}}{\pi} \sum_k \frac{1}{N} \left\langle \frac{1}{-(u - i\varepsilon)\mathbf{E} + \mathbf{f} \cdot \mathbf{U} \cdot \mathbf{f}^*} \right\rangle_{kk} \\ &= \frac{-\text{Im}}{\pi} \sum_k \langle \tilde{G}_{kk}(s) \rangle = \frac{-\text{Im}}{\pi} \langle \tilde{P}(0, s) \rangle. \end{aligned} \tag{6.9}$$

The sum over ν has been replaced by the sum over wave numbers k . Invariance of trace has been used. $s = -(u - i\varepsilon)$ and the last equality shows that the density of states is related to the probability that the particle is found on the initial site. This expression is generally valid. Using the matrix notation the average Green function from eq. (6.2) is written as:

$$\langle \tilde{\mathbf{G}}(s) \rangle = \langle \mathbf{f}^{*-1} \cdot (s\mathbf{E} + \mathbf{f}^* \cdot \mathbf{f} \cdot \mathbf{U})^{-1} \cdot \mathbf{f}^* \rangle. \tag{6.10}$$

This function is used as the basis for the derivation of the short-time and long-time properties of the model.

The short-time properties of the Green function are found by expanding this function in powers of $1/s$. To do this separate the matrix $U_{k,k'}$ into diagonal and off-diagonal contributions:

$$U_{kk'} = \Gamma_\infty \delta_{kk'} + \Delta_{kk'}, \tag{6.11}$$

with

$$\Gamma_\infty = \frac{1}{N} \sum_n \Gamma_n \tag{6.12}$$

and

$$\Delta_{kk'} = \frac{1}{N} \sum_n \delta \Gamma_n e^{i(k-k')n}, \quad (6.13)$$

where $\delta \Gamma_n = \Gamma_n - \Gamma_\infty$, and Γ_∞ is the average jump rate expected for the short-time particle diffusion. The off-diagonal contribution Δ is treated as a perturbation; the unperturbed Green function is

$$\tilde{G}_{kk'}^\infty(s) = \delta_{kk'} [s + 2\Gamma_\infty(1 - \cos k)]^{-1} = \delta_{kk'} \tilde{g}_k^\infty(s). \quad (6.14)$$

The diagonal portion of $\tilde{G}_{k,k'}^\infty(s)$ is dominant, since the sums with $k \neq k'$ oscillate; the law of large numbers for independently and identically distributed random numbers averages out the off-diagonal terms and they are negligible in the limit $N \rightarrow \infty$. The Green function is rewritten in the form introducing an average over all transition rate configurations. For this the following operator identity for operators A and B is useful

$$(A + B)^{-1} = A^{-1} - A^{-1}BA^{-1} + A^{-1}B(A + B)^{-1}BA^{-1}, \quad (6.15)$$

and the result is

$$\langle \tilde{G}_{kk}^\infty(s) \rangle = \tilde{g}_k^\infty - \langle \tilde{g}_k^\infty f_{kk} \Delta_{kk} f_{kk}^* \tilde{g}_k^\infty \rangle + \langle \tilde{g}_k^\infty f_{kk} [\mathbf{\Delta} \cdot \mathbf{f}^* ((\tilde{\mathbf{G}}^\infty)^{-1} + \mathbf{f} \cdot \mathbf{\Delta} \cdot \mathbf{f}^*)^{-1} \mathbf{f} \cdot \mathbf{\Delta}]_{kk} f_{kk}^* \tilde{g}_k^\infty \rangle. \quad (6.16)$$

Using eq. (6.13) it is easily seen that the second term in eq. (6.16) vanishes since $\Delta_{k,k} = \sum_n \delta \Gamma_n / N$. This equation is further expanded with respect to Δ to obtain the short-time corrections. The mean-square displacement is:

$$\begin{aligned} \langle x^2 \rangle(s) &= \frac{-d^2}{dk^2} \langle \tilde{G}_{kk}^\infty(s) \rangle \Big|_{k=0} \\ &= \frac{2\Gamma_\infty}{s^2} - \frac{1}{s^2} \left\langle \left[\mathbf{\Delta} \cdot \mathbf{f}^* \cdot \tilde{\mathbf{G}}^\infty \sum_{l=0}^{\infty} (-\mathbf{f} \cdot \mathbf{\Delta} \cdot \mathbf{f}^* \tilde{\mathbf{G}}^\infty)^l \cdot \mathbf{f} \cdot \mathbf{\Delta} \right]_{00} \right\rangle. \end{aligned} \quad (6.17)$$

From $l=0$, the first correction to the leading term in eq. (6.17) is:

$$\frac{1}{s^2} \left\langle \sum_{k'} \Delta_{0k'} \tilde{g}_{k'}^\infty(s) 2(1 - \cos k') \Delta_{k'0} \right\rangle = \frac{2\langle \delta \Gamma^2 \rangle}{s^3} + O(s^{-2}). \quad (6.18)$$

This short-time correction is proportional to t^2 . The correction is negative and reduces the mean-square displacement found by using only the leading term. The mean-square displacement following from a systematic expansion has the form

$$\langle x^2 \rangle(s) = 2\tilde{D}_\infty(s)/s^2, \quad (6.19)$$

where

$$\tilde{D}_\infty(s) = \Gamma_\infty [1 + \Delta_1(\Gamma_\infty/s) + \Delta_2(\Gamma_\infty/s)^2 + \Delta_3(\Gamma_\infty/s)^3 + \dots].$$

The coefficients $\Delta_1, \dots, \Delta_3$ can be derived by this method and they are given in table 1. The real part of $\tilde{D}_\infty(i\omega)$ is the frequency-dependent diffusion coefficient, derived here in a high-frequency expansion. The ensuing short-time behavior of the mean-square displacement is:

$$\langle x^2 \rangle(t) = 2\Gamma_\infty t [1 + \frac{1}{2}\Delta_1 \Gamma_\infty t + \frac{1}{6}\Delta_2 (\Gamma_\infty t)^2 + \frac{1}{24}\Delta_3 (\Gamma_\infty t)^3 + \dots]. \tag{6.20}$$

The comparison of the exact results for the coefficients $\Delta_1, \dots, \Delta_3$ with numerical simulations of $\langle x^2 \rangle(s)$ is deferred to section 6.4.2. Unfortunately, the short-time expansion breaks down for times of order unity; for larger times the long-time asymptotic regime must be developed.

The formalism introduced above can be used to discuss the long-time regime. The development needs only to be slightly modified. In this regime the limit $s \rightarrow 0$ is taken; therefore it is necessary that the matrix \mathbf{U} in eq. (6.4) has an inverse. This inverse exists as long as $\Gamma_n \neq 0$ for all n . The Green function is written as:

$$\langle \tilde{\mathbf{G}} \rangle = \mathbf{f}^*{}^{-1} \langle \mathbf{U}^{-1} (\mathbf{f}^* \mathbf{f} + s \mathbf{U}^{-1})^{-1} \rangle \mathbf{f}^*. \tag{6.21}$$

The matrix \mathbf{U}^{-1} is expressed in its diagonal and off-diagonal elements:

$$U_{kk'}^{-1} = \delta_{kk'} / \bar{\Gamma}_0 + \Delta_{kk'}, \tag{6.22}$$

where $\bar{\Gamma}_0$ is the following average inverse transition rate:

Table 1
Coefficients of the diffusion

$\tilde{D}_x(s)$	Δ_1	Δ_2	Δ_3
Exact	$-\frac{2\langle \delta \Gamma^2 \rangle}{\Gamma_\infty^2}$	$\frac{4\langle \delta \Gamma^3 \rangle}{\Gamma_\infty^3} - 3\Delta_1$	$-8 \frac{\langle \delta \Gamma^4 \rangle}{\Gamma_\infty^4} - 6\Delta_2 - 4\Delta_1 + \frac{3\Delta_1^2}{2}$
EMA			$-8 \frac{\langle \delta \Gamma^4 \rangle}{\Gamma_\infty^4} - 6\Delta_2 - 8\Delta_1 + \Delta_1^2$
$\tilde{D}_0(s)$	θ_1	θ_2	θ_3
Exact	$\frac{\kappa_2}{2}$	$\frac{-\kappa_3}{4} + \frac{11\kappa_2^2}{24}$	$\frac{\kappa_4}{8} - \frac{\kappa_2}{16} - \frac{61\kappa_2\kappa_3}{96} + \frac{1345\kappa_2^3}{2304}$
EMA		$\frac{-\kappa_3}{4} + \frac{3\kappa_2^2}{8}$	$\frac{\kappa_4}{8} - \frac{\kappa_2}{16} - \frac{7\kappa_2\kappa_3}{16} + \frac{21\kappa_2^3}{64}$
$\tilde{D}_2(s)$	ϕ_1		ϕ_2
Exact	$\frac{1}{12} + \frac{\kappa_2^2}{108}$		$\frac{\kappa_2}{24} - \frac{\kappa_2\kappa_3}{54} + \frac{\kappa_2^3}{27}$
EMA	$\frac{1}{12}$		$\frac{\kappa_2}{24}$

The coefficients κ_n are cumulants; those shown here are:

$$\kappa_2 = \left\langle \left(\frac{1}{\Gamma} - \left\langle \frac{1}{\Gamma} \right\rangle \right)^2 \right\rangle / \left\langle \frac{1}{\Gamma} \right\rangle^2, \quad \kappa_3 = \left\langle \left(\frac{1}{\Gamma} - \left\langle \frac{1}{\Gamma} \right\rangle \right)^3 \right\rangle / \left\langle \frac{1}{\Gamma} \right\rangle^3, \quad \kappa_4 = \left\langle \left(\frac{1}{\Gamma} - \left\langle \frac{1}{\Gamma} \right\rangle \right)^4 \right\rangle / \left\langle \frac{1}{\Gamma} \right\rangle^4.$$

$$\bar{\Gamma}_0^{-1} = \frac{1}{N} \sum_n \frac{1}{\Gamma_n} \quad (6.23)$$

and

$$\Delta_{kk'} = \frac{1}{N} \sum_n \left(\frac{1}{\Gamma_n} - \frac{1}{\bar{\Gamma}_0} \right) e^{i(k-k')n} = \frac{1}{N} \sum_n \delta \frac{1}{\Gamma_n} e^{i(k-k')n}. \quad (6.24)$$

Neglecting for the moment, the off-diagonal contribution in eq. (6.21), the Green function for the uniform lattice is:

$$\tilde{G}_{kk'}^0(s) = \tilde{g}_k^0(s) \delta_{kk'} = \delta_{kk'} [s + 2\bar{\Gamma}_0(1 - \cos k)]^{-1}. \quad (6.25)$$

The mean-square displacement derived from eq. (6.25) is a linear function of time as in the simple random walk and $\bar{\Gamma}_0$ expresses the exact result for the average transition rate at long times. The diffusion coefficient of the random barrier model is thus given by $D = \bar{\Gamma}_0 a^2$ and the average transition rate in the expression is the inverse of the average of the inverse transition rates. This is a general result in $d = 1$, valid for more complicated models. The diffusion coefficient is related to the mobility by the familiar Einstein relation and it is intuitively obvious that the mobility is limited by the small transition rates or equivalently the large barriers, as expressed in fig. 6.2. The perturbation theory generating the exact corrections to the Green function, eq. (6.21), can be systematically developed.

The Green function, $\tilde{G}_{k,k}(s)$, for long times is derived in a manner similar to the short-time expansion. This function is expressed in the following long-wavelength limit ($k \rightarrow 0$):

$$\langle \tilde{G}_{kk}(s) \rangle = \{s + k^2[\tilde{D}_0(s) - k^2 \tilde{D}_2(s) + \dots]\}^{-1}. \quad (6.26)$$

The most extensive results have been published by Denteneer and Ernst [139, 140]. They derive corrections for the diffusion coefficient, $\tilde{D}_0(s)$, and the so-called super Burnett coefficient, $\tilde{D}_2(s)$; these coefficients appear in the expressions for the moments of the displacement. Some moments of special interest are the mean-square displacement:

$$\langle x^2 \rangle(s) = 2\tilde{D}_0(s)/s^2; \quad (6.27)$$

the fourth moment of the displacement:

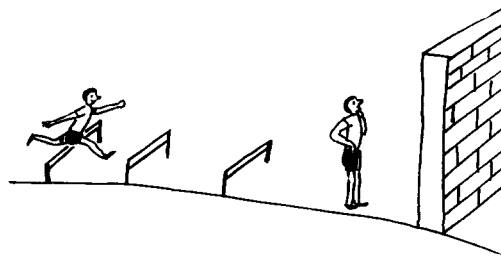


Fig. 6.2. The effect of high barriers on the average mobility as perceived by J. Villain.

$$\langle x^4 \rangle(s) = 24(D_2(s)/s^2 + D_0^2(s)/s^3), \quad (6.28)$$

and the velocity autocorrelation function:

$$\tilde{C}(s) = \frac{s^2}{2} \langle x^2 \rangle(s). \quad (6.29)$$

The results will not be derived in detail, they are quoted to $s^{3/2}$ for $\tilde{D}_0(s)$:

$$\tilde{D}_0(s) = \bar{\Gamma}_0 \{1 + \theta_1(s/\bar{\Gamma}_0)^{1/2} + \theta_2(s/\bar{\Gamma}_0) + \theta_3(s/\bar{\Gamma}_0)^{3/2}\}, \quad (6.30)$$

and to $s^{1/2}$ for $\tilde{D}_2(s)$:

$$\tilde{D}_2(s) = \bar{\Gamma}_0 \{ \phi_0 + \phi_1(s/\bar{\Gamma}_0)^{1/2} \}. \quad (6.31)$$

The coefficients are given in table 1. More details can be found in Denteneer and Ernst [139, 140].

Since the real part of $\tilde{D}_0(i\omega)$ represents the low-frequency diffusion coefficient, the result eq. (6.30) implies a correction term proportional to $\omega^{1/2}$ at low frequencies. Further remarks on the significance of this result will be made in section 6.7. The corresponding behavior of the mean-square displacement in the time domain is:

$$\langle x^2 \rangle(t) = 2\bar{\Gamma}_0 t \left[1 + \frac{2}{\sqrt{\pi}} \theta_1(\bar{\Gamma}_0 t)^{-1/2} + \theta_2(\bar{\Gamma}_0 t)^{-1} + \frac{\theta_3}{\sqrt{\pi}} (\bar{\Gamma}_0 t)^{-3/2} + \dots \right]. \quad (6.32)$$

Hence for this model corrections to the asymptotic mean-square displacement appear, which begin with a $t^{1/2}$ term. See section 6.4.2 for comparison with numerical simulations.

The previous analysis remains sensible for a transition rate distribution $\rho(\Gamma)$ which vanishes sufficiently rapidly as $\Gamma \rightarrow 0$:

$$\mu_{-m} = \langle 1/\Gamma^m \rangle = \int d\Gamma \rho(\Gamma)/\Gamma^m < \infty, \quad (6.33)$$

where m may be arbitrarily large. The case where eq. (6.33) is assumed is sometimes called the *weak disorder limit*. This language is not used here since it may cause confusion later; instead, the weak disorder limit is used to denote an expansion in powers of $\delta\Gamma$. Other distributions with divergent inverse moments were considered by Alexander et al. [133–137]. Their method of solution using integral equations has been formulated to determine the exact asymptotic behavior of $\tilde{P}(0, s)$ even under conditions where eq. (6.33) is violated. If the particle is initially placed at site $n = 0$, the occupation of this site, after taking the Laplace transform of eq. (6.1), can be formally expressed as:

$$\tilde{P}(0, s) = [s + \tilde{\phi}_0^-(s) + \tilde{\phi}_0^+(s)]^{-1}, \quad (6.34)$$

where

$$\tilde{\phi}_0^-(s) = \Gamma_0 \frac{\tilde{P}(0, s) - \tilde{P}(-1, s)}{\tilde{P}(0, s)} \quad \text{and} \quad \tilde{\phi}_0^+(s) = \Gamma_1 \frac{\tilde{P}(0, s) - \tilde{P}(1, s)}{\tilde{P}(0, s)}. \quad (6.35)$$

The functions $\tilde{\phi}_0^\pm(s)$ can in turn be considered to be functions of their neighboring conditional probabilities by using the master equation and repetition of this procedure develops a continued fraction for the functions $\tilde{P}(0, s)$

$$\tilde{\phi}_n^+(s) = \left(\frac{1}{\Gamma_{n+1}} + \frac{1}{s + \tilde{\phi}_{n+1}^+(s)} \right)^{-1} \quad (6.36)$$

and

$$\tilde{\phi}_{-n}^-(s) = \left(\frac{1}{\Gamma_{-n}} + \frac{1}{s + \tilde{\phi}_{-n-1}^-(s)} \right)^{-1}, \quad (6.37)$$

where

$$\tilde{\phi}_n^+(s) = \Gamma_{n+1} [\tilde{P}(n+1, s) - \tilde{P}(n, s)] / \tilde{P}(n, s) \quad (6.38)$$

and

$$\tilde{\phi}_{-n}^-(s) = \Gamma_{-n} [\tilde{P}(-n, s) - \tilde{P}(-n-1, s)] / \tilde{P}(-n, s), \quad (6.39)$$

The further development follows the method developed by Dyson and Schmidt for finding the density of states of disordered one-dimensional systems [141].

The functions $\tilde{\phi}_n^\pm(s)$ are themselves random variables and are distributed according to the distribution functions:

$$f_s(x) = \int_0^\infty dx' f_s(x') \int_0^\infty d\Gamma \rho(\Gamma) \delta\left(x - \left(\frac{1}{\Gamma} + \frac{1}{s+x'}\right)^{-1}\right), \quad (6.40)$$

where, again, the translation invariance of the model has been invoked so that the distributions for $\tilde{\phi}^\pm(s)$ are assumed to be independent of n . Also, since $\tilde{\phi}^+(s)$ and $\tilde{\phi}^-(s)$ have no common transition rates, they are independently distributed with the same distribution function $f_s(x)$. $\tilde{P}(0, s)$ has been previously expressed, eq. (6.34), as a function of $\tilde{\phi}^\pm(s)$; therefore, the ensemble average of $\tilde{P}(0, s)$ is:

$$\langle \tilde{P}(0, s) \rangle = \int_0^\infty dx' f_s(x') \int_0^\infty dx'' f_s(x'') \frac{1}{s \mp x' \mp x''}. \quad (6.41)$$

This approach to the problem makes no assumption about the distribution $\rho(\Gamma)$. In fact, even the first inverse moment may diverge. This is a situation where no diffusion exists. Alexander et al. [136] considered several classes of distributions and analyzed these distributions based on the asymptotic form of the function $f_s(x)$ ($s \rightarrow 0$):

$$f_s(x) = \frac{1}{\varepsilon(s)} h_s(x). \quad (6.42)$$

For the case discussed in eq. (6.33), Stieltjes transforms and inequalities can be used to deduce the scaled function $h_s(x)$; the details can be found in ref. [135]. The result is:

$$h_s(x) = \delta(x/\varepsilon(s) - 1), \tag{6.43}$$

and the parameter $\varepsilon(s)$ is:

$$\varepsilon^{-1}(s) = \sqrt{\mu_{-1}/s}. \tag{6.44}$$

The expansion parameter which determines the long-time properties is proportional to $s^{1/2}$. From the above equations, the expression for $\langle \tilde{P}(0, s) \rangle$ is:

$$\langle \tilde{P}(0, s) \rangle = 1/[s + 2\varepsilon(s)]. \tag{6.45}$$

Recently Igarashi [142] considered corrections to this leading behavior and expressed $\tilde{P}(0, s)$ as:

$$\begin{aligned} \langle \tilde{P}(0, s) \rangle = \frac{1}{\varepsilon(s)} \left[\frac{1}{2} + \mu_{-1} \frac{\varepsilon(s)}{8} \left(1 - \frac{\mu_{-2}}{\mu_{-1}^2} \right) \right. \\ \left. + \mu_{-1}^2 \varepsilon(s)^2 \left(\frac{1}{16} \frac{\mu_{-3}}{\mu_{-1}^3} + \frac{1}{256} - \frac{9}{128} \frac{\mu_{-2}}{\mu_{-1}^2} - \frac{15}{256} \left(\frac{\mu_{-2}}{\mu_{-1}^2} \right)^2 \right) \right]. \end{aligned} \tag{6.46}$$

Corrections to order $\varepsilon(s)$ were determined using the replica method by Stephen and Kariotis [143]; this method is not further explained here. The interested reader is referred to their paper for details.

The real advantage of the Dyson–Schmidt method is realized when the inverse moments diverge. One such distribution used in refs. [135–136] is

$$\rho(\Gamma) = \begin{cases} (1 - \alpha) \Gamma^{-\alpha}, & 0 \leq \Gamma \leq 1, \\ 0, & \text{otherwise} \end{cases} \tag{6.47}$$

with $0 < \alpha < 1$. Using Stieltjes transforms [135], the scaling variable can be determined to be $\varepsilon(s) = s^{1/(2-\alpha)}$. Furthermore, $h_s(\varepsilon)$ can be determined by using Mellin transforms [135,144]. This method gives the asymptotic properties of the density of states, i.e. eq. (6.9). The diffusion coefficient is calculated by assuming a scaling relation between $\tilde{P}(n, s)$ and $\tilde{P}(0, s)$:

$$\langle \tilde{P}(n, s) \rangle = \langle \tilde{P}(0, s) \rangle F(n/\xi(s)). \tag{6.48}$$

Requiring normalization of the sum over all the probabilities, the correlation length, $\tilde{\xi}(s)$, is:

$$\tilde{\xi}^{-1}(s) = 2s \langle \tilde{P}(0, s) \rangle. \tag{6.49}$$

Numerical simulations [135, 145] have provided the function $F(z)$:

$$F(z) = e^{-|z|}. \tag{6.50}$$

This result is used to calculate the diffusion coefficient as:

$$\tilde{D}(s) = D_0^\alpha C_0^{(\alpha)-2} s^{\alpha/(2-\alpha)}, \quad (6.51)$$

with

$$C_0^{(\alpha)} = \frac{1}{2} [\pi(1-\alpha)/\sin \pi\alpha]^{1/(2-\alpha)}. \quad (6.52)$$

This expression can also be calculated by the effective medium theory (see section 6.4) [135, 144]; the result is:

$$C_0^{(\alpha)}(\text{EMA}) = \frac{1}{2} [\pi(1-\alpha)2^\alpha/\sin \pi\alpha]^{1/(2-\alpha)}. \quad (6.53)$$

There is a speculation in ref. [144] that eq. (6.53) is exact. At any rate for α small, the effective medium is in very good agreement with the result derived from the Dyson–Schmidt method and the scaling relation.

In the time domain the mean-square displacement is:

$$\langle x^2 \rangle(t) = 2D_0^\alpha C_0^{(\alpha)-2} \frac{t^{2(1-\alpha)/(2-\alpha)}}{\Gamma((4-3\alpha)/(2-\alpha))}. \quad (6.54)$$

6.3. The broken-bond model

A special case of interest is the distribution:

$$\rho(\Gamma') = (1-c) \delta(\Gamma' - \Gamma) + c \delta(\Gamma'). \quad (6.55)$$

For this distribution all the inverse moments of the jump rate diverge. Moreover, the lattice is broken up into chains of finite lengths. On each of these chains the transition rates are constant and equal to Γ . This problem was analyzed by Heinrichs [146] using periodic boundary conditions on each chain. This deficiency was corrected and the boundary sites were properly treated by Odagaki and Lax [147]. In a manner similar to eqs. (6.19) and (6.29) $\tilde{D}(s)$ is related to the mean-square displacement by $\langle \tilde{x}^2 \rangle(s) = 2\tilde{D}(s)/s^2$ for equilibrium ensembles. In the time domain $D(t)$ is proportional to the second derivative of $\langle x^2 \rangle(t)$. For this model as $t \rightarrow \infty$ $D(t) \rightarrow 0$. The static diffusion coefficient vanishes, but the frequency dependence of this quantity is of interest here. They consider the average frequency-dependent diffusion coefficient expressed as a weighted sum of the ‘diffusion’ coefficients for the finite segments $\tilde{D}_N(s)$:

$$\tilde{D}(s) = \sum_{N=1}^{\infty} N C_N \tilde{D}_N(s), \quad (6.56)$$

where

$$\tilde{D}_N(s) = \frac{s^2}{2N^2} \sum_{n, n_0=1}^N (n - n_0)^2 \tilde{P}_N(n, s | n_0, 0), \quad (6.57)$$

and C_N is:

$$C_N = c^2(1-c)^{N-1}. \quad (6.58)$$

$$\begin{aligned}\tilde{D}_N(s) &= \frac{N^2 - 1}{-12F^2} s - \frac{s^2}{2N^2F} \sum_{\nu=1}^{N-1} \frac{[1 - (-1)^\nu] (1 + C_{2\nu})}{(1 - C_{2\nu})^2 [2F(1 - C_{2\nu}) + s]} \\ &= 1 + \frac{(1 + 4F/s)^{1/2}}{N} \left(\frac{1}{Z_+^{2N} + 1} - \frac{1}{Z_-^{2N} + 1} \right),\end{aligned}\quad (6.65)$$

where $Z_{\pm} = (\sqrt{s} \pm \sqrt{s + 4F})/2\sqrt{F}$. For the short-time regime the asymptotic result for $\tilde{D}(s)$ was given by Odagaki and Lax as ($s \rightarrow \infty$):

$$\tilde{D}(s) = (1 - c)F - 2c(1 - c)F^2/s + 2c(1 + c)(1 - c)F^3/s^2 + \dots, \quad (6.66)$$

and for the long-time regime the asymptotic result obtained by them is ($s \rightarrow 0$):

$$\tilde{D}(s) = \frac{(1 - c)}{2c^2} s - \frac{(1 - c)(1 + c)^2}{4c^2} \frac{s^2}{F}. \quad (6.67)$$

The last expression reveals that the static diffusion coefficient vanishes, as required, for this model. It should be remarked that the derivation of Odagaki and Lax does not include the possibility of effects deriving from strong fluctuations in the segment lengths. These fluctuations may lead to a non-analytic behavior of the diffusivities at low frequencies. Analogous nonanalytic effects appear in the survival probability against trapping and they are discussed in chapter 9.

The probability of finding the particle on the initial site at time t exhibits an interesting time dependence. This is related to the previous development by the series:

$$\langle P(0, t) \rangle = \sum_{N=1}^{\infty} N C_N \langle P(0, t) \rangle_N. \quad (6.68)$$

Using eq. (6.64) this quantity can be written in the form [148]:

$$\langle P(0, t) \rangle = c[1 + I(t)]. \quad (6.69)$$

The time-independent contribution in eq. (6.69) is derived from the stationary solution. The time-dependent part is simplified using the disorder-independent initial occupation of site 0 and the normalization of the eigenvectors as well as the inverse Laplace transform of eq. (6.64):

$$c I(t) = c^2 \sum_{N=2}^{\infty} (1 - c)^{N-1} \sum_{l=1}^{N-1} \exp\left[-2Ft\left(1 - \cos \frac{\pi l}{N}\right)\right]. \quad (6.70)$$

$I(t)$ is an integral over the density of states $\rho(u)$:

$$c I(t) = \int_0^{\infty} du \rho(u) e^{-uFt}, \quad (6.71)$$

with the density of states from eq. (6.64) and eq. (6.9) given by:

$$\begin{aligned}\rho(u) &= \frac{c^2}{(1-c)} \sum_{N=2}^{\infty} \exp[N \ln(1-c)] \sum_{l=1}^{N-1} \delta\left(u - 2\left(1 - \cos \frac{\pi l}{N}\right)\right) \\ &\approx \frac{c^2}{1-c} \sum_{N=2}^{\infty} N \ln(1-c) \sum_{l=1}^{N-1} \frac{N}{2\pi\sqrt{u}} \delta\left(l - \frac{\sqrt{u}N}{\pi}\right).\end{aligned}\quad (6.72)$$

The dominant contributions from the sum over l are the first few terms and the sum over N can be transformed to a continuous Poisson distribution with $|\ln(1-c)|^{-1}$ as the correlation number ($c < 1$). The density of states, expressing the sum over l as a Heavyside function and using this to give the integral over N a finite lower bound, is:

$$\rho(u) \approx \frac{\alpha^2}{2\pi\sqrt{u}} \left[1 + \frac{\pi\alpha}{\sqrt{u}}\right] \exp(-\pi\alpha/\sqrt{u}). \quad (6.73)$$

This is used to evaluate eq. (6.71) using a saddle-point approximation; the result is:

$$c I(t) = \frac{1}{(3\pi Ft)^{1/2}} [1 + \tau^{2/3}] \exp(-3/2\tau^{1/3}), \quad (6.74)$$

where

$$\tau = \sqrt{2\pi} Ft \ln^2(1-c). \quad (6.75)$$

The probability of finding the particle on the initial site exhibits an unusual decay:

$$\langle P(0, t) \rangle - c \approx \exp(-at^{1/3}). \quad (6.76)$$

This behavior has been found in a number of other models of diffusion on disordered lattices; therefore, further discussion of this behavior will be deferred to chapter 9.

6.4. Effective medium approximation

6.4.1. Discussion and general formalism

The exact results of the previous section have demonstrated the interesting frequency-dependent properties capable of being derived from simple models with static disorder. The methods employed to obtain those results are, with the exception of the replica method, only suited to deal with one dimension; in order to make progress on the problem of transport in higher dimensions, other methods must be sought. One simple method which can give reasonable results in any dimension for large disorder and high concentrations of the defects is the effective-medium approximation (EMA) [149–156]. The EMA is exact in the limit of high and low concentrations of defects and it provides a smooth interpolation between the two limits. The reliability of the EMA can be gauged by comparison with exact results and by checking the solutions against Monte Carlo simulations. The effective-medium theories have been formulated in the spirit of multiple scattering formalisms. Their merit lies in the ease of calculating explicit results within the formalism. However, extensions beyond the simplest approximations are quite tedious and there is no procedure to estimate the expected error in the procedure.

In the EMA the effects of disorder are replaced by an average medium. To begin assume that the conditional probability $G(\mathbf{n}, t)$ in the average medium satisfies a generalized master equation:

$$\frac{d}{dt} G(\mathbf{n}, t) = \int_0^t dt' \Gamma(t-t') \sum_{\langle \mathbf{n}', \mathbf{n} \rangle} [G(\mathbf{n}', t') - G(\mathbf{n}, t')], \quad (6.77)$$

where the sum is over all nearest-neighbor sites around the site \mathbf{n} . $\Gamma(t)$ is an associated transition rate for the effective medium; it contains the non-Poissonian properties of the disordered medium.

The formulation of the EMA provides a connection between the distribution of transition rates $\rho(\Gamma)$ and the associated transition rate for the effective medium $\Gamma(t)$. This is done by considering a cluster of bonds whose transition rates are taken from the original configuration of rates and embedding it into the effective medium (fig. 6.3). For sites which are not connected to bonds of the embedded cluster, eq. (6.77) holds. However, for sites within or contiguous with the embedded cluster, the transition rates are random functions.

The system with the embedded cluster is described by the set of equations:

$$\begin{aligned} \frac{d}{dt} P(\mathbf{n}, t) = \sum_{\langle \mathbf{n}', \mathbf{n} \rangle} \left\{ \Gamma_{\mathbf{n}, \mathbf{n}'} \Delta_{\mathbf{n}, \mathbf{n}'} [P(\mathbf{n}', t) - P(\mathbf{n}, t)] \right. \\ \left. + \int_0^t dt' \Gamma(t-t') (1 - \Delta_{\mathbf{n}, \mathbf{n}'})[P(\mathbf{n}', t') - P(\mathbf{n}, t')] \right\}, \end{aligned} \quad (6.78)$$

where

$$\Delta_{\mathbf{n}, \mathbf{n}'} = \begin{cases} 1 & \text{if } \mathbf{n} \text{ and } \mathbf{n}' \text{ are nearest neighbor members of the cluster sites,} \\ 0 & \text{otherwise.} \end{cases} \quad (6.79)$$

These equations are solved by introducing the Laplace transform of the time variable. The Fourier transformation of the site index does not completely diagonalize the equations, but only elements for those sites connected to the random bonds of the cluster appear as inhomogeneous terms in the expression for $\tilde{P}(k, s)$. The final set of linear equations can be solved by algebraic methods. The function $\tilde{\Gamma}(s)$ is determined by a self-consistency requirement; namely, averaging over the remainder of the transition rates in the cluster should give the same expressions for $\tilde{G}(0, s)$ as given by the solution of the generalized master equation, eq. (6.77).

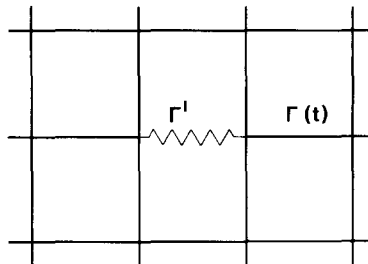


Fig. 6.3. In the effective-medium approximation all but a small cluster of transition rates is replaced by an effective value. Here a cluster of one bond Γ' between two sites is chosen.

For a single random transition rate, $\Gamma_{0,1}$, the self-consistency condition is:

$$\left\langle \frac{\tilde{\Gamma}(s) - \Gamma_{0,1}}{1 - (2/z)\{[1 - s \tilde{G}(\mathbf{0}, s)]/\tilde{\Gamma}(s)\}(\tilde{\Gamma}(s) - \Gamma_{0,1})} \right\rangle = 0; \tag{6.80}$$

$\tilde{G}(\mathbf{0}, s)$ is the initial site occupation probability in the EMA:

$$\tilde{G}(\mathbf{0}, s) = \frac{1}{(2\pi)^d} \int \frac{d^d k}{s + z \tilde{\Gamma}(s) [1 - p(\mathbf{k})]}. \tag{6.81}$$

The function $p(\mathbf{k})$ depends on the lattice type. For the d -dimensional hypercubic lattices (i.e. linear chain, square, simple cubic, etc.) the transition probability is given by eq. (2.5). The function $\tilde{G}(\mathbf{0}, s)$ with $\tilde{\Gamma}(s)$ as a parameter has been extensively studied for other lattices in the literature [156–157].

6.4.2. Transport in one dimension

In one dimension the EMA results can be compared with those in section 6.2. For the case where the moments are finite, the following asymptotic behavior for large s is found [153, 155]:

$$\tilde{\Gamma}(s) = \Gamma_\infty [1 + \Delta_1(\Gamma_\infty/s) + \Delta_2(\Gamma_\infty/s)^2 + \Delta_3(\Gamma_\infty/s)^3 + \dots]; \tag{6.82}$$

i.e., $\tilde{\Gamma}(s)$ is of the same form as $\tilde{D}_\infty(s)$ in eq. (6.19), the coefficients derived in the EMA are given in table 1.

Γ_∞ and Δ_1 were derived in section 6.2 and they are exact. The coefficient Δ_2 can be found in [136] and it is also exact in the EMA.

In the limit $s \rightarrow 0$, $\tilde{\Gamma}(s)$ has the same form as $\tilde{D}_0(s)$ in eq. (6.30),

$$\tilde{\Gamma}(s) = \bar{\Gamma}_0 [1 + \theta_1(s/\bar{\Gamma}_0)^{1/2} + \theta_2(s/\bar{\Gamma}_0) + \theta_3(s/\bar{\Gamma}_0)^{3/2} + \dots]. \tag{6.83}$$

The coefficients can be found in table 1 and they are compared to the exact results. $\bar{\Gamma}_0$ and θ_1 are exact, see eq. (6.30). The results for the coefficients θ_i and Δ_i have been compared with Monte-Carlo simulations of the master equation using the distribution:

$$\rho(\Gamma') = (1 - c) \delta(\Gamma' - \Gamma) + c \delta(\Gamma' - \Gamma^<). \tag{6.84}$$

The results are shown in figs. 6.4 and 6.5 for the mean-square displacement and fourth moment, respectively. One finds generally very good agreement between the simulations and the short-time and long-time expansions. It is seen that it is necessary to include the coefficients θ_2 and θ_3 in order to get agreement at long times. The EMA expressions have been used in the figures, but the difference between exact results and EMA is not visible in the simulation. As mentioned previously the EMA also gives results when the inverse moments diverge; this case will be discussed in section 6.5.

6.4.3. Transport in higher dimensions

It is an easy task within the EMA to derive explicit results in higher dimensions. The d -dimensional results for the hypercubic lattices are available. In the limit $s \rightarrow \infty$, $\tilde{\Gamma}(s)$ is of the same form as eq. (6.82) with slightly modified coefficients.

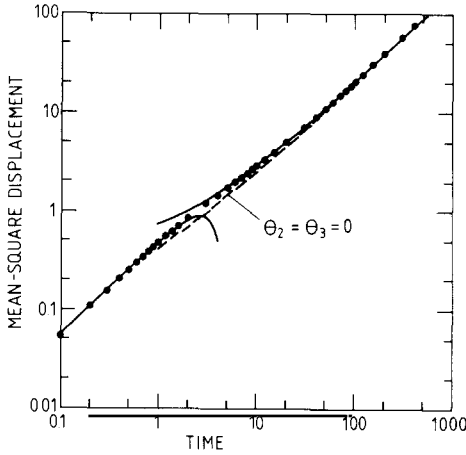


Fig. 6.4. The mean-square displacement versus time for the dichotomic random-barrier model in $d = 1$ with $c = 0.5$ and $\Gamma^* = 0.1\Gamma$. The solid curves represent the EMA for the short- and long-time behavior.

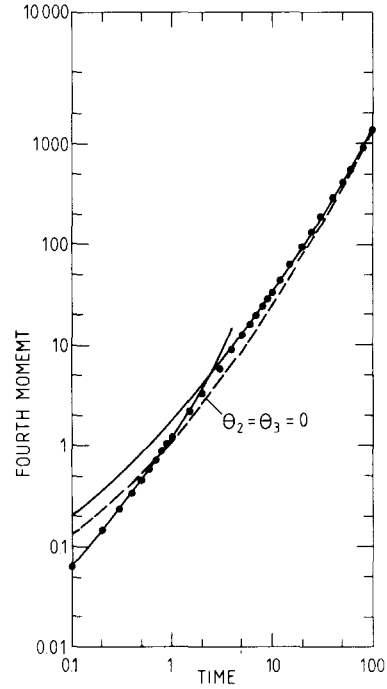


Fig. 6.5. The fourth moment of the displacement versus time for the random-barrier model. See fig. 6.4 for details.

The coefficients Γ_x and Δ_1 are identical to those given in 1 dimension. The higher coefficients are given by:

$$\Delta_2 = 4\langle(\Gamma - \Gamma_x)^3\rangle/\Gamma_x^3 - (2d + 1)\Delta_1$$

and

$$\Delta_3 = -8\langle(\Gamma - \Gamma_x)^4\rangle/\Gamma_x^4 + \Delta_1^2 - 6\Delta_2 + 12(\frac{1}{3} - d)\Delta_1. \quad (6.85)$$

A comparison of these results with Monte-Carlo simulations reveals that the short-time expansion breaks down at a later time in higher dimensions than in one dimension (see figs. 6.6 and 6.7).

The expansion for small s requires that each dimension be separately treated, since the asymptotic behavior of $\tilde{G}(\mathbf{0}, s)$ in eq. (6.80) determines the precise behavior of $\tilde{F}(s)$. The average transition rate, $\bar{\Gamma}_0$, in d dimensions follows generally in the limit $s \rightarrow 0$ from:

$$\left\langle \frac{\bar{\Gamma}_0 - \Gamma'}{1 - (\bar{\Gamma}_0 - \Gamma')/d\bar{\Gamma}_0} \right\rangle = 0. \quad (6.86)$$

For $\rho(\Gamma)$ given by eq. (6.84), this average rate is:

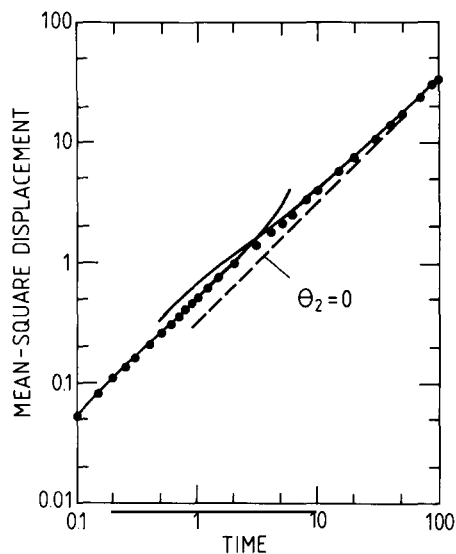


Fig. 6.6. The mean-square displacement versus time for the dichotomic random-barrier model in two dimensions. The parameters are as described in fig. 6.4 and the curves have analogous meaning.

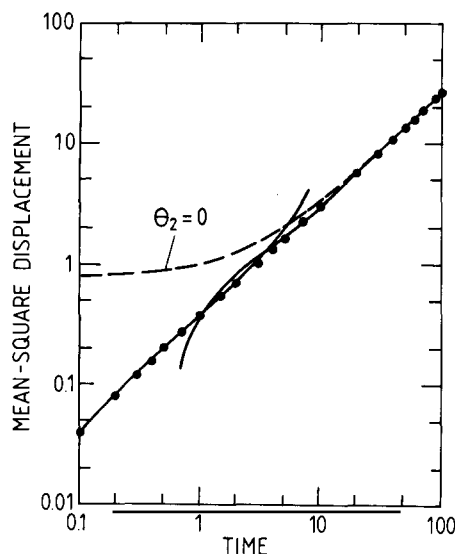


Fig. 6.7. The mean-square displacement versus time for the dichotomic random-barrier model in three dimensions. The parameters are given in fig. 6.4 and the curves have analogous meaning.

$$\bar{\Gamma}_0 = \frac{q}{2(d-1)} + \frac{1}{2(d-1)} \sqrt{q^2 + 4(d-1)\Gamma\Gamma^<} \quad (6.87)$$

defining $q = (d-1)[(1-c)\Gamma + c\Gamma^<] - c\Gamma - (1-c)\Gamma^<$.

In two dimensions $\Gamma(s)$ is:

$$\tilde{\Gamma}(s) = \bar{\Gamma}_0 [1 + \theta_2 s \ln(32\bar{\Gamma}_0/s) + \dots]; \quad (6.88)$$

and in three dimensions the corresponding expression is:

$$\tilde{\Gamma}(s) = \bar{\Gamma}_0 [1 + \theta_1 (s/\bar{\Gamma}_0) + \theta_2 (s/\bar{\Gamma}_0)^{3/2} + \dots]. \quad (6.89)$$

The structure of the coefficients θ_i is independent of the dimensionality:

$$\theta_i = A_i(d) \left\langle \frac{\Gamma_0 - \Gamma'}{[1 - (\Gamma_0 - \Gamma')/d\Gamma_0]^2} \right\rangle \left/ \left\langle \frac{\Gamma'}{[1 - (\Gamma_0 - \Gamma')/d\Gamma_0]^2} \right\rangle \right. \quad (6.90)$$

The coefficients $A_i(d)$ depend on the dimension and they are

$$\begin{aligned} A_2(2) &= 1/4\pi \\ A_1(3) &= G(0) \approx \frac{1}{4} \quad \text{and} \quad A_2(3) \approx -1/4\pi. \end{aligned} \quad (6.91)$$

As a consequence of this expansion, the velocity autocorrelation functions have negative long-time tails proportional to $t^{-(d+2)/2}$. Figures 6.6 and 6.7 illustrate the behavior of the mean-square displacement

ments. The solid curves show the EMA results for long and short times, and one recognizes very good agreement between the simulations and the EMA results.

The renormalization group method [158] and the replica method [159] have been applied to this model in $d = 2$ and 3. The results are qualitatively the same as that found by the EMA; however, in both cases the results would not provide accurate representations of the Monte Carlo simulations. The renormalization group method is discussed in section 6.6.

6.5. The percolation problem

Another aspect of the random lattice is the random removal of bonds from an otherwise perfect lattice in higher dimensions than one. This is the bond percolation problem, which has been intensively investigated and finds application in a variety of experimental situations [160–162]. The lattice with the removed bonds is like a board with a matrix of resistors some of which have been removed. After the random removal of each resistor a voltmeter measuring the resistance across the matrix is used to test whether there is still a closed circuit. After a certain fraction of resistors has been removed, the board no longer conducts from one side to the other, i.e. there is an open circuit. If the board is large enough (i.e. the number of resistors approaches infinity), the fraction at which the conductivity vanishes is a constant. This fraction is called the percolation concentration. Another way of understanding this phenomenon is that above the percolation concentration, in the limit of an infinite number of resistors, there are no infinite clusters of connected resistors; whereas, below this concentration there is certainly an infinite cluster. Even though all sites are not contained in the infinite cluster, it does connect the opposite sides of the matrix as the number of sites goes to infinity.

The infinite cluster can have a very complicated structure with multiple paths and dead-end branches. This is properly a critical phenomenon and the methods of that field have been extensively applied to percolation problems. However, giving more details lies out of the scope of this review and the reader interested in more details is referred to the following articles [161–164]. The results presented below refer to the physical quantities derived from the EMA. This approximation is properly called the mean-field approximation in the critical phenomena literature and as such, it cannot be relied upon to yield accurate behavior of physical quantities close to the percolation concentration. Nevertheless, the quantities do have the proper qualitative behavior and because the frequency behavior is easily derived in the EMA, dynamical phenomena are worth investigating to obtain new insights.

The distribution of transition rates is represented in eq. (6.55); the calculation of the diffusion in the EMA using the self-consistency condition, eq. (6.86) gives the result:

$$D_0 = \bar{I}_0 a^2 = \begin{cases} \frac{z\Gamma}{z-2} \left(\frac{z-2}{z} - c \right), & \frac{z-2}{z} \geq c \\ 0, & \text{otherwise} \end{cases} \quad (6.92)$$

The diffusion coefficient is a linear function of concentration and vanishes at the percolation concentration $c_p = (z-2)/z$. This value is exact for one and two dimensions on the square lattice, but for three dimensions the value $c_p = \frac{3}{4}$ [165], rather than $\frac{2}{3}$, is closer to the numerical value of the percolation concentration. Furthermore, the EMA does not give the exact result for the percolation concentration on other two-dimensional lattices, such as the triangular lattice.

Frequency-dependent corrections to the diffusion coefficient can also be derived from the self-consistency condition. Only the low-frequency behavior is quoted here. In one dimension the static

diffusion coefficient always vanishes and the corrections are ($\Gamma = 1$) [151]:

$$D(\omega) = \frac{(1-c)(1+c)}{4c^2} i\omega + \frac{(1-c)(1+c)}{8c^4} \omega^2. \quad (6.93)$$

These results are only in qualitative agreement with the exact results, eq. (6.67).

In two and three dimensions, three regions must be considered and each dimension treated separately. For $d = 2$ [151]:

$$\tilde{D}(\omega) = \begin{cases} D_0 - \frac{ic\omega \ln \omega}{4\pi(c_p - c)} + c \frac{[\pi/2 + i \ln 64(c_p - c)]\omega}{4\pi(c_p - c)}, & c < c_p \\ \frac{1}{4\sqrt{\pi}} (1+i)(-\omega \ln \omega)^{1/2}, & c = c_p \\ \alpha i\omega + \frac{32c\alpha^4 \omega^2}{32(c - c_p)\alpha^2 + F'(1 + (4\alpha)^{-1})}, & c > c_p, \end{cases} \quad (6.94)$$

where α is the solution of the equation:

$$F(1 + (4\alpha)^{-1}) = 8(c - c_p)\alpha \quad (6.95)$$

and $F(z)$ is related to the Green function $\tilde{G}(s)$ defined in eq. (6.81):

$$F\left(1 + \frac{s}{z\tilde{G}(s)}\right) = z\tilde{F}(s)\tilde{G}(s). \quad (6.96)$$

$F'(z)$ is the derivative of $F(z)$ with respect to the argument. Although the percolation concentration is exact for this model, the frequency behavior of the diffusion coefficient need not be accurate. It would be interesting to observe where the EMA result breaks down.

In $d = 3$ the following behavior has been computed for the diffusion coefficient [151]:

$$\tilde{D}(\omega) = \begin{cases} D_0 + \frac{F(1)c}{12(c_p - c)} i\omega + \frac{cC(1-i)\omega^{3/2}}{36\sqrt{2}(c_p - c)^{3/2}}, & c < c_p \\ \sqrt{\frac{F(1)}{12}} i\omega, & c = c_p \\ \frac{1 - \sqrt{3(c - c_p)}}{9(c - c_p)} i\omega + \frac{[2 + 3(c - c_p) - \sqrt{27(c - c_p)}]c\omega^2}{3^4 \times 2(c - c_p)^3}, & c > c_p, \end{cases} \quad (6.97)$$

where $F(1) = 8 G(0)/3 = 1.51638 \dots$ [166] and $C = 3\sqrt{6}/2\pi$. These results have not yet been critically analyzed and there is a need for more precise theoretical determination of these quantities.

Another quantity of interest is the average occupation probability of the initial site for long times, $\langle P(0, \infty) \rangle$. Of course, if $c = 1$ the particle has no possibility of moving to another site; also if all the

clusters have a finite extent, then the particle will never completely vanish from its initial site; this is precisely the situation in the percolation regime $c > c_p$. Thus the quantity $\langle P(0, \infty) \rangle$ can be used as a definition of the localization, when it vanished the particle is not localized, otherwise it is localized. This has been referred to as the strong localization condition [147].

Using the knowledge of the equilibrium state, i.e., the probability of occupying a site in a cluster of size N is $1/N$, the value of $\langle P(0, \infty) \rangle$ is an average of the inverse of the cluster size:

$$\langle P(0, \infty) \rangle = \langle 1/N \rangle . \quad (6.98)$$

The self-consistency condition solved for this quantity gives the result:

$$\langle P(0, \infty) \rangle = \begin{cases} \frac{z}{2} (c - c_p), & c_p \leq c \\ 0, & \text{otherwise} . \end{cases} \quad (6.99)$$

This linear function of concentration resembles the behavior of the diffusion coefficient in the regime $c < c_p$. The two properties are complementary to one another.

In one dimension the result in eq. (6.99) is exact [155]. In higher dimensions there appear significant deviations close to the percolation concentration.

6.6. Renormalization-group methods

The renormalization-group (RG) method has been already mentioned in the previous sections and was developed to high precision to study systems near criticality. Dynamical systems have been investigated using field-theoretic methods [167, 168] and lattice methods [169]. The methods discussed here will be those developed to analyze diffusion in disordered media [170–172]. The authors feel that the potential of this method has not yet been achieved; this section outlines three of the methods which have been applied to the problem with the hope that this will stir the imagination of the reader to develop the method further.

The RG developed in each of the references differ greatly from one another. Visscher [158, 171] defines a space-time coarsening transformation which acts on a discrete set of equations of motion. Under repeated RG transformations, the system approaches a fixed point which is described by the usual diffusion equation:

$$\partial \rho / \partial t = D \nabla^2 \rho . \quad (6.100)$$

Corrections to this equation are obtained in an expansion of the disorder. This method, although only applied to systems with weak disorder, is the only RG method to give results in Euclidean d dimensions.

Guyot developed another RG method of studying one-dimensional disorder lattices. His method is based on a decimation procedure acting on the master equation; in this procedure every other site on the lattice is eliminated [172]. The master equation is written in the following form:

$$s \tilde{P}(n, s) = \delta_{n,0} - V_n \tilde{P}(n, s) + \Gamma_n \tilde{P}(n+1, s) + \Gamma_{n-1} \tilde{P}(n-1, s) . \quad (6.101)$$

The quantity $V_n = \Gamma_n + \Gamma_{n-1}$ before the renormalization procedure is implemented. After the RG transformation is applied, this quantity is no longer a simple function of the renormalized transition rates. The sites $n = \pm 1, \pm 3, \pm 5, \dots$ are eliminated and the new equations of motion are:

$$s \tilde{P}(2n, s) = \delta_{2n,0} - V'_{2n}(s) \tilde{P}(2n, s) + \Gamma'_{2n}(s) \tilde{P}(2n+2, s) + \Gamma'_{2n-2}(s) \tilde{P}(2n-2, s), \quad (6.102)$$

where the coefficients have been renormalized according to the decimation procedure to:

$$\begin{aligned} \tilde{V}'_{2n}(s) &= \tilde{V}_{2n}(s) - \tilde{I}_{2n}^2(s) \tilde{D}_{2n+1}(s) - \tilde{I}_{2n-1}^2(s) \tilde{D}_{2n-1}(s), \\ \tilde{I}'_{2n}(s) &= \tilde{I}_{2n}(s) \tilde{I}_{2n+1}(s) \tilde{D}_{2n+1}(s), \\ \tilde{I}'_{2n-2}(s) &= \tilde{I}_{2n-1}(s) \tilde{I}_{2n-2}(s) \tilde{D}_{2n-1}(s), \\ \tilde{D}_m^{-1}(s) &= s + \tilde{V}_m(s). \end{aligned} \quad (6.103)$$

At this point the master equation no longer conserves probability, but by simply renumbering the lattice sites $2n \rightarrow n$, $\tilde{P}(2n, s) \rightarrow \tilde{P}'(n, s)$, the equation recovers its original form and the RG transformation can be successively applied.

The central simplifying feature of this procedure appears when the successive transformations become so large in number that the effective coarsening of the lattice has become larger than the diffusion length. In this regime the particle is bound to the central site and the jump rates to nearest-neighbor sites approach zero. In this limit the equations reduce to:

$$\tilde{P}^{(m)}(0, s) \approx \frac{1}{1 + \tilde{V}_0^{(m)}(s)}. \quad (6.104)$$

The method could be numerically implemented and is especially suited to determining the density of states [173]. Guyer approximated the RG transformations, but these approximations did not reliably reproduce the diffusion coefficient or the long-time asymptotic corrections.

The RG method closest to the CTRW formalism was developed by Machta [170]. He also uses the decimation procedure in one dimension. The fixed point in his case, as in the method of Visscher, corresponds to diffusion of the particle on a regular lattice. The long-time properties are determined by the fixed point, the approach to the fixed point determines the effect of the disorder on the diffusing particle.

The waiting-time distributions for transitions from the site n to $n+1$ or $n-1$ are:

$$\begin{aligned} \psi_n^+(t) &= \Gamma_{n+1} \exp[-(\Gamma_n + \Gamma_{n+1})t], \\ \psi_n^-(t) &= \Gamma_n \exp[-(\Gamma_n + \Gamma_{n+1})t]. \end{aligned} \quad (6.105)$$

The plus sign denotes a jump to the right from site n and the minus sign denotes a transition from n in the opposite direction.

The reduction of the lattice sites through the decimation procedure is accomplished by considering a lattice site $2n$; the waiting-time distribution for the particle to reach site $2n+2$ without jumping to site

$2n - 2$ is a series of convolutions involving products of the waiting-time distributions. The result is expressed as a geometric series whose terms are physically interpreted as the elementary transitions between sites $2n - 1$, $2n$ and $2n + 2$:

$$\tilde{\psi}'_{2n}{}^{+}(s) = \frac{\tilde{\psi}_{2n}^{+}(s) \tilde{\psi}_{2n+1}^{+}(s)}{(1 - \tilde{\psi}_{2n}^{+}(s) \tilde{\psi}_{2n+1}^{-}(s) - \tilde{\psi}_{2n}^{-}(s) \tilde{\psi}_{2n-1}^{+}(s))} \quad (6.106)$$

and

$$\tilde{\psi}'_{2n}{}^{-}(s) = \frac{\tilde{\psi}_{2n}^{-}(s) \tilde{\psi}_{2n-1}^{-}(s)}{(1 - \tilde{\psi}_{2n}^{+}(s) \tilde{\psi}_{2n+1}^{-}(s) - \tilde{\psi}_{2n}^{-}(s) \tilde{\psi}_{2n-1}^{+}(s))}. \quad (6.107)$$

The new functions $\tilde{\psi}^{\pm}(s)$ differ from the previously defined functions, but when $s = 0$ their sum is normalized to unity. The new lattice has a length that is twice as long as the old one and rescaling the length requires an additional factor λ to rescale the time; let $2n \rightarrow n$ and define:

$$\tilde{\psi}'_n{}^{\pm}(s) = \tilde{\psi}_{2n}^{\pm}(s/\lambda). \quad (6.108)$$

The fixed point equation for this transformation is:

$$\tilde{\psi}^*(s) = \frac{\tilde{\psi}^*(s/\lambda)^2}{1 - 2\tilde{\psi}^*(s/\lambda)^2}. \quad (6.109)$$

The asymptotic behavior of this function in the case where diffusion is present is:

$$\tilde{\psi}^*(s) \xrightarrow{s \rightarrow 0} \frac{1}{2}(1 - Ts). \quad (6.110)$$

From eq. (6.109) $\lambda = 4$ is the only solution. This result is easily interpreted using the mean-square displacement. This quantity remains invariant under the RG transformation;

$$\langle x^2 \rangle(t) = \Gamma l^2 t = \Gamma l'^2 t'. \quad (6.111)$$

Since, $l' = 2l$ and $t' = t/\lambda$, invariance requires that $\lambda = 4$. Γ is related to the inverse of the average stay time T , approaches a fixed point value and does not change under further RG transformations. The fixed-point equation for the waiting-time distribution has the solution:

$$\tilde{\psi}^*(s) = \frac{1}{2} \operatorname{sech}(2\sqrt{sT}). \quad (6.112)$$

This result does not correspond to a Poisson process and the result is the same whether or not disorder is present on the lattice.

The effective transition rates associated with the waiting-time distributions become frequency dependent under the action of the RG transformation. It is easier to use the transition rates in the RG transformation since they express the disorder in the master equation. To do this some knowledge of the perturbation theory developed in section 6.2 is used and the parameter

$$\tau_n = \frac{1/\Gamma_n}{\langle 1/F \rangle} \tag{6.113}$$

is chosen for the RG method. This parameter is related to the waiting-time distributions at $s=0$ through the equations:

$$\tilde{\psi}_n^+(0) = \tilde{\Gamma}_n(0)/[\tilde{\Gamma}_n(0) + \tilde{\Gamma}_{n-1}(0)] \tag{6.114}$$

and

$$\tilde{\psi}_n^-(0) = \tilde{\Gamma}_{n-1}(0)/[\tilde{\Gamma}_n(0) + \tilde{\Gamma}_{n-1}(0)]. \tag{6.115}$$

The quantity q_n can be defined:

$$q_n = \frac{\Gamma_0}{\Gamma_n} = \begin{cases} \frac{\tilde{\psi}_n^-(0)}{\tilde{\psi}_n^+(0)} \frac{\tilde{\psi}_{n-1}^-(0)}{\tilde{\psi}_{n-1}^+(0)} \dots \frac{\tilde{\psi}_1^-(0)}{\tilde{\psi}_1^+(0)}, & n > 0 \\ 1, & n = 0 \\ \frac{\tilde{\psi}_{n+1}^+(0)}{\tilde{\psi}_{n+1}^-(0)} \frac{\tilde{\psi}_{n+2}^+(0)}{\tilde{\psi}_{n+2}^-(0)} \dots \frac{\tilde{\psi}_0^+(0)}{\tilde{\psi}_0^-(0)}, & n < 0 \end{cases} \tag{6.116}$$

with the property that the sum is

$$\frac{1}{2N} \sum_{n=-N+1}^N q_n = \Gamma_0 \left\langle \frac{1}{\Gamma} \right\rangle. \tag{6.117}$$

The quantity of interest is defined as:

$$\tau_n = \frac{q_n}{(1/2N) \sum_{n=-N+1}^N q_n}, \tag{6.118}$$

and it is related to the waiting-time distributions through eqs. (6.114–115). The quantity has a simple recursion relation:

$$\tau'_n = (\tau_n + \tau_{n+1})/2. \tag{6.119}$$

At the fixed point $\tau^* = 1$. For further details the reader is referred to the original papers. The master equation with nearest-neighbor transition rates is expanded as previously done using the method of Zwanzig. The generalized diffusion coefficient is:

$$\tilde{D}(s) = \tilde{D}(4^N s) = \langle \Gamma_n \rangle^{(N)} \left\{ 1 - \frac{\langle (\delta \Gamma_n)^2 \rangle^{(N)}}{\langle \Gamma_n \rangle^{(N)2}} \left[1 + \left(\frac{4^N s}{4 \langle \Gamma_n \rangle^{(N)}} \right)^{1/2} \right] \right\}. \tag{6.120}$$

Note the factor 4^N from rescaling the time N times. As $N \rightarrow \infty$, the moments in eq. (6.120) have the following behavior:

$$\langle \Gamma_m \rangle^{(N)} = \frac{1}{\langle 1/\Gamma \rangle} \left\langle \frac{1}{\tau_n} \right\rangle^{(N)} = \frac{1}{2\langle 1/\Gamma \rangle} \left(\left\langle \frac{1}{\tau_n} \right\rangle^{(N-1)} + \left\langle \frac{1}{\tau_{n-1}} \right\rangle^{(N-1)} \right) = \left\langle \frac{1}{\Gamma} \right\rangle^{-1} \quad (6.121)$$

and

$$\langle \delta \Gamma_m^2 \rangle^{(N)} = \frac{1}{\langle 1/\Gamma \rangle^2} \langle \delta \tau_m^2 \rangle^{(N)} = \frac{1}{\langle 1/\Gamma \rangle^2} \left\langle \left(\frac{\delta \tau_m + \delta \tau_{m-1}}{2} \right)^2 \right\rangle^{(N-1)} = \left\langle \frac{1}{\Gamma} \right\rangle^{-2} \frac{1}{2} \langle (\delta \tau_m)^2 \rangle^{(N-1)}. \quad (6.122)$$

Under repetitions of the RG transformation, the fluctuations are reduced by a factor of 2; the solution for the diffusion equation is:

$$\tilde{D}(s) = D_0 \left(1 + \frac{\langle (\delta \tau)^2 \rangle}{2} (s D_0)^{1/2} \right). \quad (6.123)$$

Thus the result of Zwanzig's method is recovered, cf. eq. (6.30) and table 1.

6.7. Non-Markoffian nature of results

Particle transport in the random-barrier model exhibits non-Markoffian behavior when it is considered in the ensemble average. This is evident in $d=1$ from the frequency dependencies of the diffusion coefficient and the modified Burnett coefficient, see section 6.2, and in general dimensions from the frequency dependence of the effective transition rate $\tilde{\Gamma}(s)$, see section 6.4. In this section the non-Markoffian nature is discussed in more detail, and also the correspondence with a single-state CTRW description is examined.

The main result can be summarized as long-time tail behavior which shows up in the corrections to the asymptotic mean-square displacements, as well as in the algebraic decay of the velocity autocorrelation function (VAF). The coefficients of these corrections, or of the asymptotic VAF, are *disorder-specific*, i.e., they are present when there is disorder and vanish only in its absence. Note that the coefficients are present for quite regular distributions of transition rates where all inverse moments exist. Thus the long-time tail behavior in the mean-square displacement can be regarded as a signature of disorder. It is interesting to note that this behavior can be obtained in perturbation theory, or by effective-medium methods. For these problems, the situation is not as extreme as discussed by Anderson [174].

In $d=1$ the presence of a correction term $\propto \omega^{1/2}$ in the VAF $\tilde{C}(\omega)$ means that the frequency-dependent diffusivity $\tilde{D}(\omega)$ of a particle rises as $\omega^{1/2}$ for small frequencies, above the static diffusion coefficient $\tilde{D}(0)$. It is plausible that a strong increase of the diffusivity with frequency, for small frequencies, appears in the random-barrier model as a consequence of the disorder. Consider a random-barrier model with two barriers, Γ , $\Gamma^<$ and $\Gamma^< \ll \Gamma$ and the high barriers have a concentration $c \ll 1$. There are then segments of consecutive low barriers of varying lengths. The diffusion coefficient at finite frequencies gives an estimate for the mean-square displacement of a particle in the time interval $2\pi/\omega$. If the frequency is increased, and thus the time interval reduced, the number of available segments with squared lengths equal or larger than the new, reduced mean-square displacement increases. Of course, the qualitative result does not yet give the quantitative result $\tilde{D}(\omega) - \tilde{D}(0) \propto \omega^{1/2}$.

It will now be discussed whether the averaged random walk of a particle according to the

random-barrier model can be brought into correspondence with a continuous-time random walk. The first problem is the determination of the average waiting-time distributions. There are two rather different answers to this problem.

i) *The literal WTD.* The average WTD of a particle can be determined by applying literally the definition of a WTD. Given a particle arrived at a site at $t = 0$, the average WTD will be defined as the probability density, in the ensemble average, that the particle makes its next transition to another site at time t . The elementary WTD for transitions to nearest-neighbor sites according to the random-barrier model are given in eq. (6.105). For simplicity a dichotomic distribution of transition rates is chosen, eq. (6.84). An ensemble of linear chains with the distribution eq. (6.84) is introduced. It is assumed that the ensemble is in equilibrium and the time origin is chosen arbitrarily. The average WTD for the *first* transition after $t = 0$ is obtained as the ensemble average of the elementary WTD with the distribution eq. (6.84). The result is

$$h(t) = c^2 2\Gamma^< \exp(-2\Gamma^<t) + (1-c)^2 2\Gamma \exp(-2\Gamma t) + 2c(1-c)(\Gamma + \Gamma^<) \exp[-(\Gamma + \Gamma^<)t]. \quad (6.124)$$

The average WTD $\psi(t)$ for all successive transitions is obtained by inverting the relation eq. (3.3) between $h(t)$ and $\psi(t)$ which applies for a stationary situation,

$$\psi(t) = -\bar{t} dh(t)/dt. \quad (6.125)$$

The resulting average WTD is

$$\psi(t) = \bar{t} \{ c^2 (2\Gamma^<)^2 \exp(-2\Gamma^<t) + (1-c)^2 (2\Gamma)^2 \exp(-2\Gamma t) + 2c(1-c)(\Gamma + \Gamma^<)^2 \exp[-(\Gamma + \Gamma^<)t] \}. \quad (6.126)$$

The mean residence time \bar{t} on a site is given by the inverse of the transition rate in equilibrium,

$$\bar{t} = [2c\Gamma^< + 2(1-c)\Gamma]^{-1}. \quad (6.127)$$

It is also possible to derive the WTD for forward and backward transitions, relative to the preceding transition. If the particle is found between two low (Γ) or two high ($\Gamma^<$) barriers, it will make the transition in forward or backward direction with equal probabilities. If the particle is found between a low and a high barrier, it arrived there with probability $\Gamma/(\Gamma + \Gamma^<)$ by a transition over the low barrier, and with probability $\Gamma^</(\Gamma + \Gamma^<)$ by a transition over the high barrier. The probabilities of leaving the site via the low or high barrier are given by the same factors, hence

$$\psi_b(t) = \frac{1}{2}\psi(t) + \bar{t} c(1-c)(\Gamma - \Gamma^<)^2 \exp[-(\Gamma + \Gamma^<)t], \quad (6.128)$$

$$\psi_f(t) = \psi(t) - \psi_b(t). \quad (6.129)$$

It is evident that a determination of the WTD by numerical simulations gives the *literal* WTD. In these simulations, the definition of the WTD given above is implemented; details are given in [176]. Figure 6.8 contains the above results on the WTD, together with the results of the simulations. As

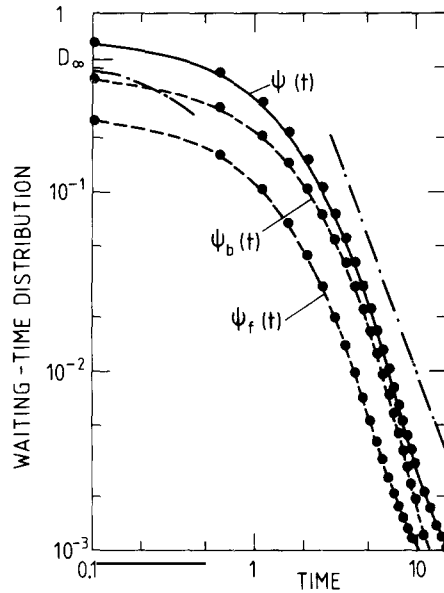


Fig. 6.8. The literal waiting-time distributions of the random-barrier model in $d = 1$ calculated from Monte-Carlo simulations (dots) and analytically (lines). The dash-dotted curves are the asymptotic results for the associated waiting-time distribution.

expected, the numerical simulations verify the correctness of the simple derivation given above. It should be emphasized that renewal theory was instrumental in this derivation.

Unfortunately, the literal average WTDs give incorrect results when used in the CTRW formalism. Only the short-time behavior is obtained correctly. In single-state CTRW the predicted diffusion coefficient is incorrect and its frequency dependence is missing. The correlated CTRW according to section 4.3, where $\psi_b(t)$ and $\psi_f(t)$ are used, also gives an incorrect static diffusion coefficient. A frequency dependence of $\tilde{D}(\omega)$ is obtained, however, it is analytic and does not show the expected $\omega^{1/2}$ behavior. Hence the major features of the random-barrier model are not obtained from single-state or correlated CTRW with the literal WTD.

ii) *The associated WTD.* An associated WTD can be obtained by comparing the results of section 6.4 on the associated transition rate of the effective-medium approximation with the single-state CTRW of sections 3.2–3.3. The form of the kernel used in the EMA section 6.4 corresponds to separable CTRW. Comparison with the exact results of section 6.2 shows that the first two leading terms of the mean-square displacement and of the fourth moment at long times are given correctly by the EMA. Hence the correspondence eq. (3.28) between the kernel of the generalized master equation and the WTD can be used to determine the associated WTD $\tilde{\psi}_a(s)$ from the kernel $\tilde{I}(s)$ of the EMA,

$$\tilde{\psi}_a(s) = \tilde{I}(s) / [s + \tilde{I}(s)]. \quad (6.130)$$

Insertion of the large- s expansion of $\tilde{I}(s)$ according to eq. (6.82) up to $O(s^{-1})$ and inverse Laplace transformation shows that the short-time behavior of the associated WTD is given by

$$\psi_a(t) = \Gamma_z [1 - (1 - \Delta_1) \Gamma_z t + \dots]. \quad (6.131)$$

Substitution of $\Gamma(s)$ by its small- s expansion eq. (6.83) up to $O(s^{1/2})$ and inverse Laplace transformation yields the long-time behavior of the associated WTD,

$$\psi_a(t) = \frac{3}{4\sqrt{\pi}} \theta_1 \bar{\Gamma}_0(\bar{\Gamma}_0 t)^{-5/2}. \quad (6.132)$$

The asymptotic behavior of the associated WTD is indicated in the figure. Since no inhomogeneous term is present in the EMA for the random-barrier model it is only consistent to assume that no distinct associate WTD for the first transition must be introduced, which would correspond to an inhomogeneous term in the generalized master equation. This point will also be discussed below.

The initial transition rate following from the associated WTD is given by $\Gamma_\infty = (2t)^{-1}$. It corresponds to the average transition rate, whereas the literal WTD gives a slightly increased initial transition rate, cf. fig. 6.8. The long-time behavior of $\psi_a(t)$ is such that no second moment exists; this can also be deduced directly from eq. (6.130) by using the small- s expansion of $\tilde{\Gamma}(s)$. In contrast, all moments of the literal WTD exist, since it decays exponentially.

The associated WTD has been determined in such a way that it reproduces, when used in a single-state CTRW, the correct long-time and short-time behavior of the random barrier model for the leading terms of the mean-square displacement and fourth moment. In order to obtain this associated WTD, a solution of the random-barrier problem by other means (perturbation theory; EMA) was used. Once such a solution is found, there is no apparent need to reconstruct the corresponding associated WTD. On the other hand, no direct derivation of the associated WTD appears possible, at least at present. Hence its usefulness is rather questionable.

A formal equivalence between averaged particle transport in disordered systems and the generalized master equation or CTRW theory was established by Klafter and Silbey [177]. They assumed that the random walks of the particle in the individual disordered systems are described by Markoffian master equations. They referred explicitly to a lattice model with inaccessible sites, however, their derivations are applicable to the random-barrier model as well. They used the Zwanzig–Nakajima projection operation formalism [178, 179] and the projection operator D is defined as leading from a non-averaged quantity A to the disorder-averaged quantity, $DA = \langle A \rangle$. The result of Klafter and Silbey is that the master equation, when averaged over the disorder, is of the form of a generalized master equation. Since the GME can be brought into correspondence with CTRW, also the correspondence of the averaged master equation with CTRW is shown.

In the course of their derivations they omitted an inhomogeneous term proportional to $(1 - D) \times P(\mathbf{n}, 0)$ where $P(\mathbf{n}, 0)$ represents the initial condition (see ref. [179]). This omission is justified for the case of the random-barrier model where uniform initial conditions are adequate. However, in the case of the random-trapping model (cf. chapter 7) or of the model with inaccessible sites (as described by Klafter and Silbey) an inhomogeneous term should be included in the derivations.

The explicit realization of the correspondence between average transport in the random-barrier model and the ensuing CTRW description was given above. The correspondence leads to the associated WTD which cannot be interpreted as the average WTD of the particle in the literal sense. Moreover, it is not obvious from the general formalism that the associated WTD are always positive semidefinite as is necessary for a probabilistic interpretation. Since no inhomogeneous term appears for the random-barrier model, no distinct WTD for the first transition is necessary. This means that the associated WTD of the random-barrier model cannot be interpreted as describing a renewal process. Since the presence or absence of an inhomogeneous term depends on the model, the question of the interpretation of these associated WTD as describing renewal processes is still open.

7. Lattice models with random traps

7.1. Introduction to the model

The random-trap model is defined on a regular lattice, as was the random barrier model of chapter 6. In this model detailed balance is also required, the transition rates to neighboring sites are symmetric:

$$\Gamma_n = \Gamma_{n,n+d}, \quad (7.1)$$

where $n+d$ is any nearest-neighbor site to n . The random variables $\{\Gamma_n\}$ are independent from one another. A pictorial representation of the random-trap model in one dimension is shown in fig. 7.1. As this figure suggests, the average stationary occupation of the deep traps, i.e. deep minima, should be greater than that of the shallower traps because more energy is required for the particle to escape over the barrier. From this picture is derived a colloquial name for this model, coined by Kitahara, 'the valley model'. In this same spirit, the model of the last chapter is called 'the mountain model'. The model discussed in this chapter is restricted to valleys of finite depth; this insures that a unique equilibrium state is obtained at long times. Another aspect of the random trap model expressed in the figure is its symmetry; there is no tendency for the particle to drift to the right or to the left from any configuration of traps. Traps extending over several sites, where on the average the particle is pulled deeper into them is a topic reserved for chapter 10.

Another manifestation of the simplicity of this model is observed in the elementary WTD of the particle on site n . It has the form:

$$\psi_n(t) = \tau_n^{-1} \exp[-t/\tau_n], \quad (7.2)$$

where

$$\tau_n^{-1} = \sum_d \Gamma_{n,n+d}, \quad (7.3)$$

and τ_n is the sojourn time of the particle on the site n . For this model the averaging of the WTD for a single site, as proposed by Scher and Lax [40, 180]:

$$\psi(t) = \int d\tau_n \rho(\tau_n) \psi_n(t), \quad (7.4)$$

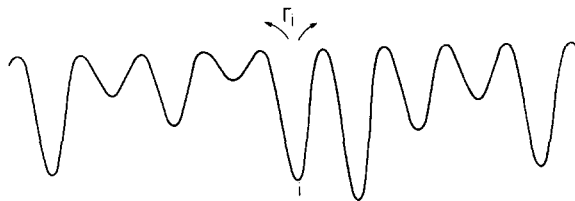


Fig. 7.1. A schematic representation of the random-trap or valley model. All valleys are equally spaced, but have different depths. The mountain peaks are all at the same energy.

where $\rho(\tau_n)$ is the distribution of sojourn times, does not account for the different equilibrium weights given to each trap; the stationary weights, as derived below, depend on the configuration of transition rates on the lattice [181].

In the following section a simple proof is given that the diffusion coefficient is frequency independent, when the initial conditions correspond to the stationary state. While this result, and other moments of the probability distribution have been derived, the complete solution for the probability distribution is unknown. In section 7.4 approximation techniques are used to calculate the probability distribution and the results are interpreted by analogy with the CTRW models of chapter 5.

7.2. Exact result for the mean-square displacement

The mean-square displacement of a particle in the random-trap model is a linear function of time for all times, provided that the initial probability distribution corresponds to a stationary distribution. In ref. [32] it has been shown that the mean-square displacement is the same linear function of time at short and long times and a proof suggested; the proof has been completed in ref. [182]. The main ingredient of the formal proof is the symmetry condition eq. (7.1). Another requirement of the proof is the positivity of all transition rates of eq. (7.1), as will be evident below. If these conditions hold, the proof can be carried out.

An equivalent form of the result is the statement that the velocity correlation function of the hopping particle contains a δ -function at the time origin only. This means that each jump is only correlated with itself; different jumps are uncorrelated on the average. In fact, when a particle has made a transition to a particular site, it will jump with equal probability in any possible direction, hence forward or backward correlations cannot appear due to the symmetry.

However, if one starts with a non-equilibrium situation, the mean-square displacement is not a linear function of time. For example, with equal occupation of all sites, a particle is more likely to make a transition into a trap than out of a trap, resulting in a net decrease of the mean-square displacement with time. It is not justified to infer that the velocity autocorrelation function now has a more complicated time behavior; in fact, this quantity remains delta-function correlated. The connection between the velocity autocorrelation function and the second derivative of the mean-square displacement makes explicit use of the stationary property.

The master equation for this model, using eq. (7.1), is:

$$\frac{d}{dt} P(\mathbf{n}, t | \mathbf{m}, 0) = \sum_{\langle l, n \rangle} \Gamma_{n+l} P(\mathbf{n} + \mathbf{l}, t | \mathbf{m}, 0) - z \Gamma_n P(\mathbf{n}, t | \mathbf{m}, 0). \quad (7.5)$$

The initial condition is explicitly retained in the notation of the conditional probability and the sum over l is over the nearest neighbors of n .

The mean-square displacement of the particle from its initial site is:

$$\langle |\mathbf{n} - \mathbf{m}|^2 \rangle_m = \sum_n |\mathbf{n} - \mathbf{m}|^2 P(\mathbf{n}, t | \mathbf{m}, 0), \quad (7.6)$$

The left-hand side indicates with a subscript that the initial conditions have not yet been inserted. The stationary solution for the master equation needs to be included in the average and this quantity is:

$$P^{\text{eq}}(\mathbf{m}) = \eta \Gamma_m^{-1}, \quad (7.7)$$

where η is a normalization constant. For N lattice sites and one particle per lattice, the normalization constant is:

$$1 = \sum_{\mathbf{m}} P^{\text{eq}}(\mathbf{m}) = \eta \frac{1}{N} \sum_{\mathbf{m}} \Gamma_{\mathbf{m}}^{-1}. \quad (7.8)$$

Letting the number of sites on the lattice approach infinity, the normalization constant is identified as the inverse of the average sojourn time:

$$\eta^{-1} = \langle \Gamma^{-1} \rangle. \quad (7.9)$$

The equation of motion for the mean-square displacement is:

$$\frac{d}{dt} \langle |\mathbf{n} - \mathbf{m}|^2 \rangle_{\mathbf{m}} = \sum_{\mathbf{l}} \sum_{\mathbf{n}} |\mathbf{n} - \mathbf{m}|^2 \Gamma_{\mathbf{n}+\mathbf{l}} P(\mathbf{n} + \mathbf{l}, t | \mathbf{m}, 0) - z \sum_{\mathbf{n}} |\mathbf{n} - \mathbf{m}|^2 \Gamma_{\mathbf{n}} P(\mathbf{n}, t | \mathbf{m}, 0). \quad (7.10)$$

The first term can be rewritten using the identity:

$$|\mathbf{n} - \mathbf{m}|^2 = |\mathbf{l}|^2 - 2\mathbf{l} \cdot (\mathbf{n} + \mathbf{l} - \mathbf{n}) + |\mathbf{n} + \mathbf{l} - \mathbf{m}|^2. \quad (7.11)$$

The last term in eq. (7.11) cancels when inserted into (7.10); the second term in eq. (7.11) also cancels because there is no tendency to drift along a particular axis for any configuration of traps. Multiplying by the stationary distribution eq. (7.7), and summing over all sites \mathbf{m} the average mean-square displacement (for simplicity, cubic symmetry and $|\mathbf{l}|^2 = 1$ is assumed):

$$\frac{d}{dt} \langle r^2 \rangle(t) = z\eta = z \left\langle \frac{1}{\Gamma} \right\rangle^{-1}. \quad (7.12)$$

Hence, the anticipated result has been proven, namely, the mean-square displacement is strictly proportional to time for all times when stationary initial conditions are taken. From this expression the diffusion coefficient is:

$$D_0 = 1/2d\bar{t}, \quad (7.13)$$

where

$$\bar{t}^{-1} = z \langle 1/\Gamma \rangle^{-1} \quad (7.14)$$

and the lattice constant is unity.

The results in eqs. (7.12–13) are exact for any dimensionality and can be generalized to non-cubic and non-Bravais lattices. In d dimensions the expression for the long-time value of the diffusion coefficient was derived by Schroeder [183] using scattering theory methods. In refs. [139, 140] the following argument was given. From the stationary solution, eq. (7.7), the average jump rates, weighted according to the occupation probabilities, are:

$$\bar{t}^{-1} = z \langle\langle \Gamma_n \rangle\rangle, \quad (7.15)$$

where the double bracket indicates this average. Inserting eq. (7.7) shows that eq. (7.15) is equivalent to eq. (7.14). The result, eq. (7.15), can also be obtained by noting that the long- and short-time behavior of the mean-square displacement are identical for stationary initial conditions; hence, the diffusion coefficient can be deduced from a short-time expansion of the master equation, i.e. eq. (7.15).

The Laplace transform of eq. (7.12) has a simple relation to the velocity autocorrelation function, eq. (6.29), $\tilde{C}(s)$. Since, $\langle r^2 \rangle(s) \propto s^{-2}$, then $\tilde{C}(s) = D_0$. The velocity autocorrelation function is a delta function, which proves the earlier statement that the velocities for unequal times are uncorrelated in their second moments. This is plausible in view of the symmetry in the transition rates (fig. 7.1). This does not mean that the model has no disorder specific transport properties, but they must be found in the higher moments, such as the super Burnett coefficient.

7.3. Exact results: Higher moments

The diffusion coefficient in the last section has precisely the same form as the diffusion coefficient for the random-barrier model in one dimension. However, now the diffusion coefficient for the random-trap model is known in all dimensions. This result can be used to develop a systematic perturbation theory for the probability distribution in d dimensions. There is one essential difference from the random-barrier model that must be considered; namely, the equilibrium condition needs to be included in the derivation.

There are two quantities which can be discussed in this model and they do not have a simple relationship to one another. One quantity, used in chapter 6, is the average Green function or more explicitly, the average value of the conditional probability (averaged over the random transition rates). This quantity determines the spectral properties of the model, such as the density of states already discussed in chapter 6. The other quantity is the average probability, where the initial conditions are included in the average, also called the response function in refs. [139, 140]:

$$\langle P(\mathbf{n}, t) \rangle = \left\langle \sum_{\mathbf{m}} P(\mathbf{n} + \mathbf{m}, t | \mathbf{m}, 0) P^0(\mathbf{m}) \right\rangle, \quad (7.16)$$

where $P^0(\mathbf{m})$ is a predetermined initial condition. For the stationary state the expression in eq. (7.7) is used for $P^0(\mathbf{m})$.

The perturbation method discussed in chapter 6 has been generalized by Denteneer and Ernst [139, 140] to apply to the random-trap model in d dimensions. Their method uses the Fourier–Laplace transform of the probability distribution:

$$\langle \tilde{P}(\mathbf{k}, s) \rangle = \frac{1}{N} \sum_{\mathbf{n}, \mathbf{m}} \exp(i\mathbf{k} \cdot \mathbf{n}) \tilde{P}(\mathbf{n}, s | \mathbf{m}, 0) P^0(\mathbf{m}); \quad (7.17)$$

using the master equation, eq. (7.5), it is expressed as:

$$s \langle \tilde{P}(\mathbf{k}, s) \rangle = \frac{1}{N} \sum_{\mathbf{m}} \exp(i\mathbf{k} \cdot \mathbf{m}) P^0(\mathbf{m}) - z \frac{1}{N} \sum_{\mathbf{n}, \mathbf{m}} \Gamma_{\mathbf{n}} \exp(i\mathbf{k} \cdot \mathbf{n}) \tilde{P}(\mathbf{n} + \mathbf{m}, s | \mathbf{m}, 0) P^0(\mathbf{m}) \\ + \left(2 \sum_{\alpha=1}^d \cos k_{\alpha} \right) \frac{1}{N} \sum_{\mathbf{n}', \mathbf{m}} \Gamma_{\mathbf{n}'} \exp(i\mathbf{k} \cdot \mathbf{n}') \tilde{P}(\mathbf{n}' + \mathbf{m}, s | \mathbf{m}, 0) P^0(\mathbf{m}). \quad (7.18)$$

The last term in eq. (7.18) has been simplified by a change of variables $\mathbf{n}' = \mathbf{n} + \mathbf{d}$ and the hypercubic lattice has been assumed. The expression eq. (7.18) is written in a matrix form. The diagonal elements of the matrix are simplified to the compact form:

$$\langle \tilde{P}(\mathbf{k}, s) \rangle = \langle [s\mathbf{E} + z(1 - p(\mathbf{k}))\mathbf{U}]^{-1} \mathbf{P}^0 \rangle_{\mathbf{k}, \mathbf{k}}, \quad (7.19)$$

and

$$U_{\mathbf{k}, \mathbf{k}'} = \frac{1}{N} \sum_{\mathbf{n}} \Gamma_{\mathbf{n}} \exp[i\mathbf{n} \cdot (\mathbf{k} - \mathbf{k}')]. \quad (7.20)$$

Now the previous notation can be followed, the inverse of \mathbf{U} is written as a diagonal and an off-diagonal contribution:

$$\mathbf{U}^{-1} = \bar{\Gamma}(\mathbf{E} + \mathbf{\Delta}). \quad (7.21)$$

$\bar{\Gamma}$ is the exact expression for the average transition rate and the off-diagonal contribution is

$$\Delta_{\mathbf{k}, \mathbf{k}'} = \frac{\bar{\Gamma}}{N} \sum_{\mathbf{n}} \left(\frac{1}{\Gamma_{\mathbf{n}}} - \left\langle \frac{1}{\Gamma} \right\rangle \right) \exp[i(\mathbf{k} - \mathbf{k}') \cdot \mathbf{n}]. \quad (7.22)$$

In this notation the initial conditions are expressed in matrix form as:

$$\mathbf{P}^0 = (\mathbf{E} + \mathbf{\Delta}). \quad (7.23)$$

When these expressions are reinserted into eq. (7.19) the average probability is:

$$\langle \tilde{P}_{\mathbf{k}}(s) \rangle = \langle (\mathbf{E} + \mathbf{\Delta})[(s + \bar{\Gamma}z(1 - p(\mathbf{k}))\mathbf{E} + s\mathbf{\Delta})^{-1} (\mathbf{E} + \mathbf{\Delta})] \rangle_{\mathbf{k}, \mathbf{k}}. \quad (7.24)$$

The Green function giving the long-time transport properties now in d dimensions is:

$$\tilde{g}_{\mathbf{k}}^0(s) = [s + \bar{\Gamma}z(1 - p(\mathbf{k}))]^{-1}, \quad (7.25)$$

and a systematic expansion can be carried out for eq. (7.24).

Denteneer and Ernst [139, 140] find a constant diffusion coefficient for all dimensions as required. The super Burnett coefficient, $\tilde{D}_2(s)$, contains the effect of the random disorder. In one dimension the result is:

$$\tilde{D}_2(s) = \frac{\bar{\Gamma}}{12} + \frac{\bar{\Gamma}}{2} \kappa_2 \left(\frac{\bar{\Gamma}}{s} \right)^{1/2} + \theta_2 \bar{\Gamma} + \theta_3 \left(\frac{s}{\bar{\Gamma}} \right)^{1/2} + \dots, \quad (7.26)$$

where the constants κ_2 , θ_2 and θ_3 have been defined in table 1 in chapter 6. From eq. (7.26) the asymptotic long-time limit for the fourth moment is:

$$\langle r^4 \rangle(t) = 4! \left[\frac{\bar{\Gamma}^2}{2} t^2 + \frac{2}{3\sqrt{\pi}} \kappa_2 (\bar{\Gamma}t)^{3/2} + \left(\frac{1}{12} + \theta_2 \right) \bar{\Gamma}t + 2\theta_3 (\bar{\Gamma}t/\pi)^{1/2} + \dots \right]. \quad (7.27)$$

The term proportional to $t^{3/2}$ is due solely to the fluctuations in the transition rates. This creates a long-time tail in the higher-order correlation function.

In higher dimensions, the corrections to second order in the fluctuations are derived. The second derivative of the fourth moment exhibits the effect of disorder in the form:

$$\frac{d^2}{dt^2} \langle r^4 \rangle(t) \simeq 4! \bar{\Gamma}^2 (1 + \kappa_2 P(\mathbf{0}, t)), \quad (7.28)$$

where $P(\mathbf{0}, t)$ is the probability that the particle is found on site $\mathbf{0}$ as derived from the perfect lattice Green function (see eq. (2.31)). For the hypercubic lattices, this function is a simple product of exponential and modified Bessel functions. The asymptotic decay of the fluctuation contribution in eq. (7.28) is proportional to $t^{-d/2}$.

The spectral and transport properties of the 1-dimensional model have been published by Nieuwenhuizen and Ernst [184] for transition rate distributions with divergent inverse moments (but still insisting that the diffusion coefficient exists). They used the Dyson–Schmidt functional equation method to calculate the density of states, localization length and Burnett coefficient.

7.4. Approximate treatments

The exact results of sections 7.2–3 do not give an explicit expression for the averaged probability (or response function) of the particle in space and time. Hence approximation methods are required to determine this quantity. The effective-medium approximation for the random-trap model has not yet been worked out. One specific difficulty is the correct incorporation of the equilibrium initial conditions. The standard multiple-scattering methods assume uniform initial conditions. These are the correct initial conditions when the equilibrium state is uniform, as it is for the random-barrier model. In the random-trap model the occupation of sites according to equilibrium is a random quantity itself, and it is correlated with the random transition rates.

The random-trap model was treated for small trap concentrations in the average T -matrix approximation (ATA) in [185] and the correct equilibrium initial conditions were taken into account. In a first step the non-uniform initial conditions were removed by transforming the conditional probabilities. The master equation for the thermally weighted probability $P(\mathbf{m}, t | \mathbf{n}, 0)$ was considered with the initial condition

$$P(\mathbf{n}, 0 | \mathbf{m}, 0) = N \rho_n \delta_{\mathbf{n}, \mathbf{m}}, \quad (7.29)$$

where ρ_n is the equilibrium occupation of site \mathbf{n} according to eqs. (7.7) and (7.9) and an explicit factor N is introduced since $\rho_n \propto N^{-1}$. In the Laplace domain the master equation for $\tilde{P}(\mathbf{n}, s | \mathbf{m})$ reads

$$\sum_l (s\delta_{\mathbf{n}, l} + A_{\mathbf{n}, l}) \tilde{P}(l, s | \mathbf{m}) = N\rho_n \delta_{\mathbf{n}, \mathbf{m}}. \quad (7.30)$$

$A_{\mathbf{n}, l}$ is the transition-rate matrix for the trapping model. In the translation-invariant case the Fourier transform of A is $\Lambda(\mathbf{k})$ in eq. (2.18). In the trapping model studied the elements of A are either Γ (transition rate from a normal site) or $\Gamma^<$ (transition rate from a trap site) and the traps occur with concentration c . Uniform initial conditions are obtained by multiplication of eq. (7.30) with $(N\rho_n)^{-1}$,

$$\sum_l [(N\rho_n)^{-1}s\delta_{n,l} + (N\rho_n)^{-1}A_{n,l}] \tilde{P}(l, s | \mathbf{m}) = \delta_{n,m}. \quad (7.31)$$

It is easily seen from the condition of detailed balance that the matrix $(N\rho_n)^{-1}A_{n,l}$ is symmetric. Note that the transformation used here is different from the one employed in section 2.5, cf. eq. (2.74). After the transformation, the master equation (7.31) is analogous to a vibrational problem on a lattice with mass *and* force constant defects.

The calculation of the average probability from the master equation (7.31) can now be carried out explicitly in the average T -matrix approximation. The defects are randomly distributed with concentration $c \ll 1$ over the sites of a simple cubic (SC) lattice. The concentration should be so small that overlap effects of different traps can be neglected (note that after transformation to eq. (7.31) also transition rates between neighboring sites and the defects are modified). The ATA in the low-concentration limit, which is used here, takes a crystal with uniform transition rates Γ as the undisturbed system. In the first step, a single-site T -matrix t for a single trap is calculated; this step can be done completely. The actual calculation relies on group-theoretical simplifications, these technical details can be found in [186]. The T -matrix for a single trap is equivalent to an effective defect, where repeated absorption and emission processes on this particular trap have been included. Explicit expressions are given in refs. [185, 187]. Only the pole which appears in t , for deep traps ($\exp(\beta E) \gg 1$ with E the energy reduction in the traps) will be given,

$$s_r = -\{\exp(\beta E) - 1\} \tilde{P}_0(\mathbf{0}, 0 | \mathbf{0})^{-1}, \quad (7.32)$$

where $\tilde{P}_0(\mathbf{0}, 0 | \mathbf{0})$ is the Green function to return to the origin of a particle in the undisturbed lattice, at $s = 0$. The determination of the pole eq. (7.32) also assumed a 3-dimensional lattice. The pole is the analogue of a resonance pole of a heavy mass defect in a lattice. As is seen below, it describes effectively the escape processes out of the traps.

In the second part of the ATA at low concentrations the propagator of the particle between the different effective defects is treated in an approximate way, whereby the propagation in the undisturbed regions is described by the undisturbed Green function. An explicit form for the self-energy of the defect-averaged probability is given in refs. [185, 187]. It turned out that the expansion parameter is $\varepsilon = c[\exp(\beta E) - 1]$, i.e., the traps cannot be too deep in order that the derivations be valid. This means that the fraction of time spent in the traps must be small.

In the limit of deep traps (but small ε), the resulting averaged probability can be represented in the form

$$\langle \tilde{P}(\mathbf{k}, s) \rangle = \frac{s + \gamma_r + \gamma_t + A(\mathbf{k}) \gamma_t \gamma_r^{-1}}{s^2 + s[\gamma_r + \gamma_t + A(\mathbf{k})] + \gamma_r A(\mathbf{k})}, \quad (7.33)$$

where

$$\gamma_r = -(1 + c)s_r + \varepsilon[6\Gamma - A(\mathbf{k})] \quad (7.34)$$

and

$$\gamma_t = c \tilde{P}_0^{-1}(\mathbf{0}, 0 | \mathbf{0}). \quad (7.35)$$

Expression eq. (7.33) is nothing else than the result of a two-state model describing diffusion in the presence of traps, cf. eq. (5.6). (The last term of the numerator of eq. (7.33) is different from the corresponding term of the two-state model; however, the difference is of relative order ε and is thus negligible.) Equations (7.34–35) provide microscopic expressions for the parameters of this model. The leading term of the release rate γ_t is independent of the trap concentration c , as it should be and given by the pole eq. (7.32). For deep traps it is given by $\Gamma^< = \Gamma \exp(-\beta E)$, apart from a numerical factor which results from the lattice Green function. The capture rate is proportional to the concentration, as it should be; the simple expression found above coincides with the result of the Rosenstock approximation for diffusion-controlled capture, see section 9.3. The diffusion coefficient which follows from eq. (7.33) is of the form required by the two-state model, cf. section 5.1.

It is very satisfactory that the ATA of the random-trap model at low concentrations of the traps (more precisely $\varepsilon \ll 1$) justifies the phenomenological two-state model, and leads to physically reasonable values of its parameters in three dimensions. Moreover, the usual derivation of the capture rate of a particle in a trap assumes that the trap is permanent, i.e., that the particle is never reemitted. The random-trap model, on the other hand, includes capture and release processes, and leads, at least within the approximations described above, to the same result on the capture rate.

Fedders [188] has generalized the ATA treatment of the random-trap model by considering extended traps where the transition rate into the trap sites is larger than the transition rate in the free lattice. He is also restricted to low concentrations of these extended traps which are not allowed to overlap. Fedders applies his theory of motions of a finite yet small concentration of particles on the lattice with random transition rates. He is able to overcome the limitation of small parameter ε , i.e., his traps are also allowed to be very deep, and the result for the diffusion coefficient appears in the form required by the two-state model.

A discussion of the different behavior of random-barrier and random-trapping models was made by Halpern [189]. However, this author only used uniform initial conditions at the time origin, corresponding to equal probabilities of start at any site. An extension of the random trap model has been made, for example, by Machta et al. [190]; they combine the two-state model of chapter 5 with random transition rates into and out of the traps. These models will not be discussed in detail here, the interested reader is referred to their work where additional references are given.

The random-trapping model has also been studied for the case of WTDs whose *first moments* do not exist. Alexander [191] gave a heuristic discussion of the behavior of random-trapping models in general dimensions, and contrasted it with the behavior of random-barrier models under analogous circumstances. He concluded that random-trapping models will exhibit anomalous diffusion with $\langle R^2 \rangle(t) \propto t^{2\nu}$, $\nu < \frac{1}{2}$ at $d \geq 2$. Machta [192] investigated the random-trapping model in arbitrary dimension by renormalization-group (RG) methods. His methods are similar to the ones applied by him to the random-barrier case, see section 6.6. Although approximations are involved, his conclusions seem to be valid. He finds anomalous diffusion in all dimensions. The dimension $d = 2$ is a borderline dimension. For $d > 2$ and class c disorder (see [192]) the fixed-point WTD is non-analytic; it is characterized by an exponent α and $\nu = \alpha/2$. For $d < 2$ the fixed points are disordered random walks themselves. The exponent $\nu = (2 + d_f - d)^{-1}$ where d_f is a fractal dimension and $d_f = d/\alpha$. The fractal dimension d_f for the class c random trapping models can hence be larger than the Euclidean dimension. See [192] for further details.

8. Diffusion on some irregular and fractal structures

Up to now diffusion on regular (mainly Bravais) lattices was considered and the disorder was introduced in the form of random transition rates. In this chapter more irregular structures will be admitted that are, however, derived from regular lattices, either by deformation or by blocking of a subset of the sites. One special case is the diffusion on percolation clusters near the percolation threshold of site blocking. This case will be disregarded for the reasons given in chapter 6. Diffusion on topologically disordered structures will not be included in this chapter, because this topic is not yet well developed. However, diffusion on fractal lattices that are constructed in a regular manner will be included here.

8.1. Diffusion on chains with irregular bond lengths

A model of a linear chain will be considered where the distances between the sites d are distributed according to a given probability distribution $\mu(d)$, and where the hopping process of a particle on that chain is characterized by a Poissonian WTD $\psi(t) = (1/\tau) \exp(-t/\tau)$ at each site. This model was introduced by van Beijeren [193] and has been named ‘waiting-time model’ by him. It is a special case of a stochastic Lorentz model and it gives a nice example of a solvable model with fixed spatial disorder. Its solution is possible since the temporal development is simply solvable, and the combination with the spatial disorder is tractable. The consequences of disorder can be followed explicitly, especially the appearance of long-time tails in the velocity autocorrelation function or mean-square displacement. Figure 8.1 gives a pictorial representation of the waiting-time model. The random walk of one particle on this linear chain where the sites are characterized by the integer index m can be treated by the methods of chapter 2. For the Poissonian WTD the conditional probability $P(m, t)$ of finding the particle at site m at time t when it started at $m = 0$ at $t = 0$ is given by eq. (2.28) for $d = 1$

$$P(m, t) = \exp(-t/\tau) I_m(t/\tau), \quad (8.1)$$

where $I_m(x)$ is the modified Bessel function with index m . The probability density of finding the particle at the coordinate x at time t , when it started at the origin at $t = 0$, in an ensemble of linear chains, is given by

$$\hat{P}(x, t) = \delta(x) P(0, t) + \sum_{m=1}^{\infty} \left\langle \delta\left(x - \sum_{i=0}^{m-1} d_i\right) \right\rangle P(m, t) + \sum_{m=-1}^{-\infty} \left\langle \delta\left(x + \sum_{i=-1}^{-m} d_i\right) \right\rangle P(m, t). \quad (8.2)$$

The brackets $\langle \dots \rangle$ denote the average over the spatial disorder, i.e., over an ensemble characterized by the probability distribution $\mu(d)$ of the d_i . Equation (8.2) could serve as the starting point of further

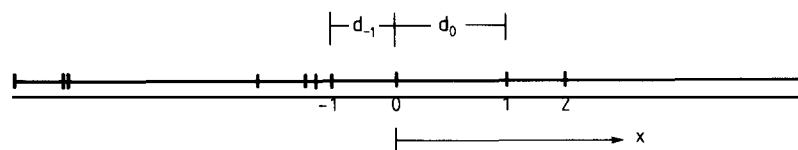


Fig. 8.1. Waiting-time model of van Beijeren. The vertical lines are the lattice sites at which the particle resides. They are Poisson distributed and the particle performs a random walk between nearest-neighbor sites.

derivations. Van Beijeren proceeds to deduce directly the velocity autocorrelation function $C(t)$, cf. [193]. It is given by

$$C(t) = \sum_{m=-\infty}^{+\infty} \frac{1}{4\tau^2} \langle (x_{-1} - x_0)(x_m - x_{m-1}) \rangle P(m, t) + \frac{1}{2\tau^2} \langle x_0^2 + x_{-1}^2 \rangle \delta\left(\frac{t}{\tau}\right). \quad (8.3)$$

The first term describes the correlation of a jump at $t = 0$ with another jump at t . It contains the product of the average initial velocity $(x_{-1} - x_0)/2\tau$ with the average final velocity $(x_m - x_{m-1})/2\tau$. Some careful considerations are necessary to establish the correctness of the first term [193]. The second term represents the correlation of the jump at $t = 0$ with itself. This contribution can be derived by considering jumps that have a duration ε and letting ε go to zero. Let l be the mean value and Δ^2 the variance of $\mu(d)$. Since all d_i are independent random variables, $\langle d_i^2 \rangle = \Delta^2 + l^2$ and $\langle d_i d_j \rangle = l^2$ for $i \neq j$. The velocity autocorrelation function is explicitly given by

$$C(t) = \frac{\Delta^2}{2\tau^2} \exp\left(\frac{-t}{\tau}\right) \left[I_1\left(\frac{t}{\tau}\right) - I_0\left(\frac{t}{\tau}\right) \right] + \frac{\Delta^2 + l^2}{\tau^2} \delta\left(\frac{t}{\tau}\right). \quad (8.4)$$

The long-time behavior of the velocity autocorrelation function is easily found from the asymptotic behavior of the modified Bessel functions (cf. Abramowitz and Stegun [194])

$$C(t) \xrightarrow{t \rightarrow \infty} - \frac{\Delta^2}{4\tau^2(2\pi)^{1/2}} \left(\frac{t}{\tau}\right)^{-3/2}. \quad (8.5)$$

This ‘long-time tail’ in the velocity autocorrelation function is evidently caused by the disorder since it is absent in the case $\Delta = 0$. Its physical origin has been discussed in great detail in the review [193] to which the reader is referred.

The mean-square displacement is found either from eq. (8.4) by double integration, or directly from eq. (8.2) by calculation of the second moment. One obtains

$$\langle x^2 \rangle(t) = l^2 \frac{t}{\tau} + \Delta^2 \frac{t}{\tau} \exp\left(\frac{-t}{\tau}\right) \left[I_0\left(\frac{t}{\tau}\right) + I_1\left(\frac{t}{\tau}\right) \right]. \quad (8.6)$$

The asymptotic behavior is

$$\langle x^2 \rangle(t) \xrightarrow{t \rightarrow \infty} l^2 \frac{t}{\tau} + \frac{2\Delta^2}{(2\pi)^{1/2}} \left(\frac{t}{\tau}\right)^{1/2} + \dots \quad (8.7)$$

The diffusion coefficient of the particle is $D = l^2/2\tau$. There appears a long-time tail $\propto t^{1/2}$ whose coefficient is directly associated with the disorder. This derivation was the first one that demonstrated the existence of a disorder-specific long-time tail in a stochastic random-walk model.

The derivations of van Beijeren can be extended to a simple solvable model for bond distortions of a lattice in d dimensions. Consider a regular lattice dressed with several sites at each vertex, cf. fig. 8.2. The physical origin of such a model might be a regular attachment of an atom to each vertex, but the placement of this atom is random. An interstitially diffusing particle could be preferably attached to these shifted atoms and at high temperatures the irregularities in the transition rates due to the different bond lengths could be negligible.

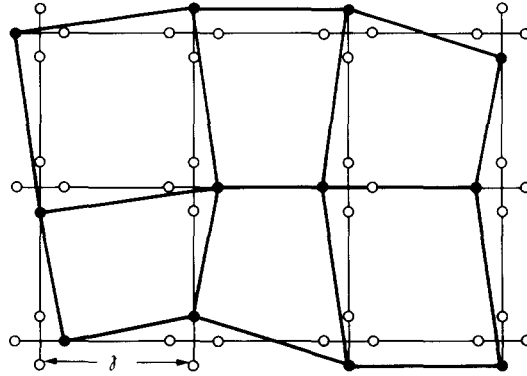


Fig. 8.2. A dressed lattice which has a single chosen site at each vertex on which the particle can reside. The thick solid lines show the deformation of the perfect lattice.

The particle starts at position \mathbf{R}_0 and moves along each bond with the *same* transition rate. This model is thus isomorphic to the regular lattice, since each point is displaced from the vertex n by an amount δn . The $\{\delta n\}$ are a set of independent random variables. Let $|\delta| < \frac{1}{2}$. The calculation of the mean-square displacement is simple. The conditional probabilities are the same as for a regular lattice. $P(\mathbf{m}, t)$ is the probability that the particle is on site \mathbf{R}_m when it started at \mathbf{R}_0

$$\begin{aligned} \langle [\mathbf{R}(t) - \mathbf{R}_0]^2 \rangle &= \sum_{\mathbf{m}} \langle [\mathbf{R}_m - \mathbf{R}_0]^2 \rangle P(\mathbf{m}, t) \\ &= \sum_{\mathbf{m}} \langle [\mathbf{m} + \delta \mathbf{m} - \delta \mathbf{0}]^2 \rangle P(\mathbf{m}, t). \end{aligned} \quad (8.8)$$

Using the result for the mean-square displacement of random walk eq. (2.22) and

$$\langle |\delta \mathbf{0}|^2 \rangle = \langle |\delta \mathbf{m}|^2 \rangle = \delta^2, \quad \langle \delta \mathbf{m} \cdot \delta \mathbf{0} \rangle = \delta^2 \delta_{\mathbf{m}, \mathbf{0}}, \quad (8.9)$$

it follows that

$$\langle \mathbf{R} \rangle^2 = 2dD_0 t + 2\delta^2 [1 - P(\mathbf{0}, t)] \quad (8.10a)$$

where D_0 is the diffusion coefficient of the regular lattice and

$$\frac{d^2}{dt^2} \langle \mathbf{R}^2 \rangle = 2dD_0 \delta(t) - 2\delta^2 \frac{d^2 P(\mathbf{0}, t)}{dt^2}. \quad (8.10b)$$

The ensuing asymptotic behavior of the VAF is

i) in $d = 1$, since $P(\mathbf{0}, t) \propto t^{-1/2}$

$$C(t) = d^2 \langle x^2 \rangle / dt^2 \sim t^{-5/2}; \quad (8.11)$$

ii) in d -dimensional lattices, where $P(\mathbf{0}, t) \propto t^{-d/2}$

$$C(t) \sim t^{-(d+4)/2}. \quad (8.12)$$

Again a disorder-specific long-time tail appears in the velocity autocorrelation function. In $d = 1$ the decay is faster than in the waiting-time model of van Beijeren. This may be related to a different behavior of the mean-square displacement in both models. In the former model, the individual distances d_i add up to a value that deviates from its mean value nl after n steps by $\Delta n^{1/2}$ on the average. The mean-square displacement of a particle in this model has a correction term $\propto t^{1/2}$, cf. eq. (8.7). In the present model, in $d = 1$ the individual distances add up to $0 \pm \delta n$, and the mean-square displacement of a particle shows only a correction term $\propto t^{-1/2}$. Hence the differing behavior in both models is quite plausible.

8.2. Random walk on a random walk

A second example of the superposition of random walk on a linear chain with a spatially disordered structure is provided by the 'random walk on a random walk' which was investigated in ref. [195]. Again the problem can be solved completely by using generating function techniques, or in CTRW. The spatially disordered structure is given as a random walk itself, as indicated in fig. 8.3. These structures need not be one dimensional; generalizations to random walks in arbitrary dimensions are possible. However, the spatial structure thus constructed must be topologically equivalent to a linear chain. The discussion will be restricted to the one-dimensional case. An ensemble of such spatial random walks is characterized by the probability $p_\nu(x)$ of finding a distance x after ν steps. It has been discussed in section 2.1 and $p_\nu(x)$ can be taken from it, cf. eq. (2.7). The probability of finding the particle at site ν

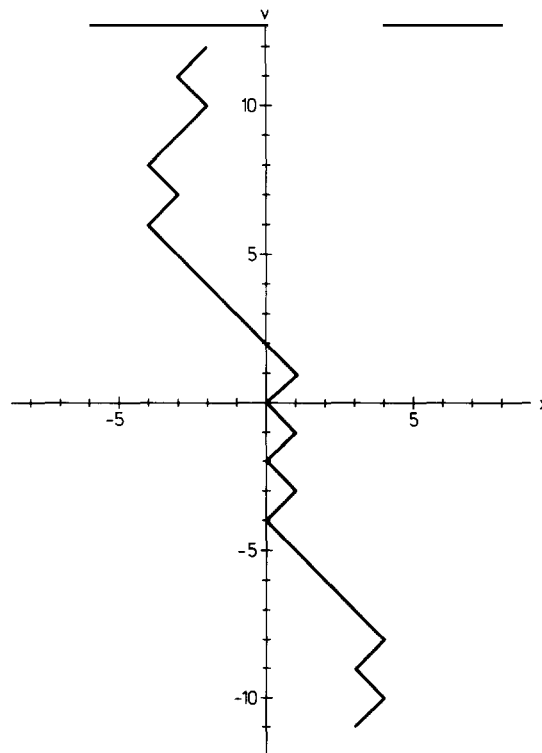


Fig. 8.3. A segment of a chain resulting from a random walk with position x , versus step, ν . The particle performs a nearest-neighbor random walk on this chain.

of the spatial structure is given by

$$p_n(\nu) = \left(\frac{1}{2}\right)^\nu \nu! / \left[\left(\frac{\nu-n}{2}\right)! \left(\frac{\nu+n}{2}\right)! \right], \quad (2.7)$$

for a discrete random walk of n steps, or by

$$p(\nu, t) = \exp(-t/\tau) I_\nu(t/\tau), \quad (8.13)$$

for a Poissonian continuous-time random walk of duration t . The average of the temporal development over an ensemble of basic random walks, i.e., over the spatial disorder, is given by

$$P_n(x) = \sum_\nu p_n(\nu) p_\nu(x) \quad (8.14)$$

or by

$$P(x, t) = \sum_\nu p(\nu, t) p_\nu(x). \quad (8.15)$$

No simple closed-form expression for $P_n(x)$ is obtained, although the generating function for $P_n(k)$ can be derived in Fourier space. The moments of P_n are easily found, e.g.,

$$\langle x^2 \rangle_n = 2 \sum_{\nu>0} \nu p_n(\nu) \quad (8.16)$$

and

$$\langle x^4 \rangle_n = 2 \sum_{\nu>0} (3\nu^2 - 2\nu) p_n(\nu). \quad (8.17)$$

Their asymptotic behavior is

$$\langle x^2 \rangle_n \xrightarrow{n \rightarrow \infty} \left(\frac{2n}{\pi}\right)^{1/2}, \quad (8.18)$$

and

$$\langle x^4 \rangle_n \xrightarrow{n \rightarrow \infty} 3n. \quad (8.19)$$

The proportionality of the mean-square displacement with $n^{1/2}$ is intuitively obvious, since two random walks are superimposed in this model. As is already evident from these moments, the probability distribution is not Gaussian for large n . A saddle-point integration shows that it is roughly given by

$$P_n(x) \approx \frac{2^{2/3}}{(3\pi)^{1/2}} \frac{x^{1/3}}{n^{1/6}} \exp\left(-\frac{3x^{4/3}}{2^{5/3} n^{1/3}}\right). \quad (8.20)$$

The continuous-time version of the random walk on a random walk leads to a closed-form expression for the Fourier and Laplace transform of $P(x, t)$,

$$\tilde{P}(k, s) = \left\{ [s(s + 4\Gamma)]^{-1/2} \frac{2\Gamma - \tilde{A}(s) \cos k}{2\Gamma + \tilde{A}(s) \cos k} \right\},$$

where

$$\tilde{A}(s) = [s(s + 4\Gamma)]^{1/2} - s - 2\Gamma. \quad (8.21)$$

From eq. (8.21) follows the incoherent dynamical structure factor $S_{\text{inc}}(k, \omega)$ of this model by application of eq. (2.34). Also the frequency-dependent mean-square displacement is easily derived from eq. (8.21). The expression for the velocity autocorrelation function will be given in the Laplace domain,

$$\tilde{C}(s) = - \frac{2\Gamma s^2 \tilde{A}(s)}{[s(s + 4\Gamma)]^{1/2} \{[s(s + 4\Gamma)]^{1/2} - s\}^2}. \quad (8.22)$$

It is easily seen that $\lim_{s \rightarrow 0} \tilde{C}(s) = 0$, i.e., no diffusion coefficient exists. $\tilde{C}(s)$ is proportional to $s^{1/2}$ for small s , corresponding to a long-time tail behavior

$$C(t) \xrightarrow{t \rightarrow \infty} - \frac{1}{4} \left(\frac{\Gamma}{\pi} \right)^{1/2} t^{-3/2}. \quad (8.23)$$

The asymptotic mean-square displacement in the time domain is

$$\langle x^2 \rangle(t) \xrightarrow{t \rightarrow \infty} 2 \left(\frac{\Gamma t}{\pi} \right)^{1/2}. \quad (8.24)$$

The $t^{1/2}$ -law is expected as the continuous-time analog of eq. (8.18). Since no static diffusion coefficient exists, in linear response no static mobility under an applied field exists [196].

Both the waiting-time model and the random walk on a random walk are examples of transport in disordered systems where the temporal development of the stochastic process is known exactly, and can be combined with the probability distribution of the spatial disorder in order to obtain the complete time-dependent probability distributions. If an effective, averaged medium would be introduced before the random-walk average is done, the specific results due to disorder would be missed.

8.3. Diffusion in lattices with inaccessible sites

In this section diffusion of a particle is discussed on lattices where some sites are not accessible to the particle. See fig. 8.4 for a pictorial representation. The random walk on the accessible (or 'open') sites is the same as on a regular lattice. It is assumed that the density of the blocking sites is so low that long-range diffusion is possible, i.e., that an infinite cluster of accessible sites exists. As said above, the behavior near the percolation threshold where the infinite cluster ceases to exist will not be considered. The motion of particles in finite clusters in two and higher dimensions will be ignored. In one-dimensional chains only finite clusters exist at arbitrarily small concentrations of blocked sites. However, the one-dimensional case is very similar to the one-dimensional model with broken bonds which has been treated in section 6.3. Hence this case will be completely disregarded. There are several physical examples of the model studied here, notably exciton transport in isotopically mixed crystals. One species of molecules supports the transport of excitons ('guest' or 'trap' sites), whereas the

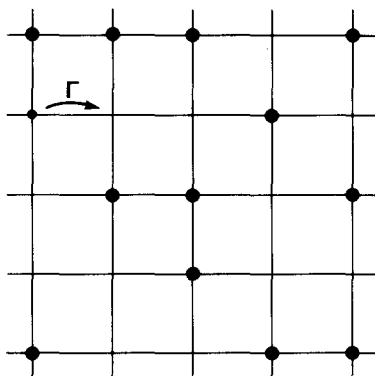


Fig. 8.4. A lattice where some sites are blocked (shown with solid circles) in a random manner. A particle (small solid circle) performs a random walk on this incomplete lattice.

isotopically substituted species cannot participate in the transport ('host' sites). The problem discussed in this section is identical to the one addressed by Klafter and Silbey in [177]. However, Klafter and Silbey outlined only the general solution of the problem and no explicit expressions were given.

The main quantities of interest are the diffusion coefficient and, more generally, the averaged probability of finding the particle at site n at time t . The simplest description of diffusion in a partially blocked lattice is provided by a mean-field theory where the transition rate Γ is replaced by $(1 - c)\Gamma$ where $1 - c$ is the mean number of accessible sites with c the concentration of blocked sites. The diffusion coefficient is given in this mean-field description by

$$D_{\text{MF}} = D_0(1 - c), \quad (8.25)$$

where D_0 is the diffusion coefficient in the lattice without blocked sites. Evidently eq. (8.25) disregards the backward correlations which are present in the random walk of the particle. Namely, when a particle attempts to jump to a blocked site, it cannot perform this transition; this is equivalent to an immediate return to the original site.

An expression for the diffusion coefficient beyond the mean-field expression eq. (8.25) can be taken from the theory of Nakazato and Kitahara [98] for tracer diffusion in a lattice gas where the tracer has a different transition rate than the other (background) particles, cf. also [197, 198]. It is convenient to introduce a correlation factor by defining

$$D = D_{\text{MF}} f_{\text{R}}(c). \quad (8.26)$$

This correlation factor is obtained from [98] by letting the transition rate of the background particles go to zero,

$$f_{\text{R}}^{\text{NK}}(c) = \left[1 + \frac{(1-f)c}{f(1-c)} \right]^{-1}. \quad (8.27)$$

Here f is the correlation factor for diffusion of a tagged particle with equal transition rate in a lattice gas with concentration $c \rightarrow 1$. The expression eq. (8.27) vanishes for $c \rightarrow 1$, hence it does not predict the

percolation concentrations in real lattices. Nevertheless, it is an improvement over the mean-field theory and it compares well with numerical simulations at lower concentrations, see fig. 8.5.

An effective-medium description of particle diffusion in a lattice with partially inaccessible sites was given by Kaski et al. [199], using multiple-scattering methods. They derived the diffusion coefficient and the incoherent dynamical structure function $S_{\text{inc}}(\mathbf{k}, \omega)$. The diffusion coefficient was found to depend linearly on the particle concentration above the percolation threshold of the vacant sites,

$$D_{\text{KTE}} = \begin{cases} \Gamma a^2 (1 - c/c_p), & c \leq c_p, \\ 0, & c > c_p; \end{cases} \quad (8.28)$$

where the percolation threshold is given by

$$c_p = (1 - 2/z). \quad (8.29)$$

For small c there is a similarity between this expression and the one provided by Nakazato and Kitahara, since in a mean-field theory of the correlation factor $f \approx 1 - 2/z$. The agreement of eq. (8.30) with numerical simulations is similar to a result of Tahir-Kheli described below. To obtain $S_{\text{inc}}(\mathbf{k}, \omega)$ Kaski et al. had to determine a function $\eta(\omega)$ self-consistently, $S_{\text{inc}}(\mathbf{k}, \omega)$ is a functional of $\eta(\omega)$ and no more a Lorentzian. The first four frequency moments of the spectral density are exactly given by this effective-medium theory for the SC and BCC lattices.

A different approach to the problem of diffusion in a lattice with blocked sites is the mode-coupling theory of Keyes and Lyklema [200]. They obtain an integral equation for a diffusion kernel and their expression contains a percolation threshold. They have to solve the integral equation numerically to obtain the diffusion coefficient for arbitrary c . The results have the desired qualitative features, although a quantitative verification is lacking.

Recently Loring et al. [201] performed a diagrammatic analysis of this problem. Their work is an extension of the work by Gochanour et al. [202] on transport between completely randomly located 'guest' molecules; this work in turn was based on Haan and Zwanzig [203]. They represented the self-energy for the conditional probability $G_s(t)$ of still finding the particle (excitation in their

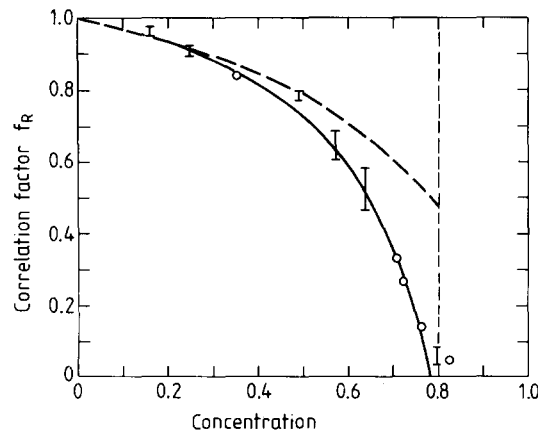


Fig. 8.5. The correlation factor for diffusion on a lattice with inaccessible sites as calculated by Nakazato and Kitahara (dashed line) and Tahir-Kheli (solid line). The data is from Monte-Carlo simulations of the model on an FCC lattice. The vertical dashed line indicates the percolation concentration.

terminology) at the starting site at time t in terms of diagrams and perform a partial summation. An approximate conditional probability can be deduced from this partial sum; also here an implicit equation has to be solved numerically. The results for the diffusion coefficient obtained from those solutions appear reasonable. With the assumption of only nearest-neighbor transfer rates percolation thresholds are obtained as a function of vacancy ('guest') concentrations, which compare well with the known values in simple cubic, FCC and BCC lattices. For long-range transfer rates of the Foerster type no percolation threshold is obtained, in agreement with the expectations.

The most advanced theoretical description of random walk of a particle on a lattice with blocked sites has been developed recently by Tahir-Kheli [204]. His theory describes diffusion of tagged atoms in a multicomponent alloy consisting of several species of atoms with different transition rates, and vacancies. Tahir-Kheli investigated the hierarchy of master equations obeyed by this problem and neglects third-order fluctuations, as in [198]. He then improves two rate parameters of this theory by self-consistent treatment. The case of one immobile species with concentration c , one mobile tagged particle, and the rest vacancies is obtained as a special case in his theory. The following correlation factor is obtained

$$f_{\text{R}}^{\text{TK}}(c) = 1 - \frac{c(1-f)}{f(1-c)}, \quad c \leq f. \quad (8.30)$$

The expression eq. (8.30) is very similar to the result of Kaski et al. in eq. (8.28) and it has the appearance of an expansion of the result of Nakazato and Kitahara eq. (8.27). However, it predicts a percolation concentration for vacancy percolation, expressed in terms of the particle concentration $c_{\text{p}} = f$. For example, in the simple cubic lattice $f = 0.653 \dots$ whereas the critical concentration for vacancy percolation, expressed as particle concentration, is $c_{\text{p}} = 0.689 \dots$ [205]. The result of Tahir-Kheli agrees well with the computer simulations [206] over the full concentration range, cf. fig. 8.5.

8.4. *Random walks on fractals*

A way of breaking translational invariance, but retaining *scale invariance* is to model the transport properties on fractal lattices. A two-dimensional example of these lattices, called the Sierpinski gasket, is shown in fig. 8.6 [207]. In fig. 8.6a the basic building block of this fractal lattice is shown (think of this as an organism under a microscope with a small field of view). When the field of view is widened, as shown in fig. 8.6b, the shape of the object looks similar to the first view; however, a hole appears in the center. Widening the field of view by another factor of two reveals a larger hole cut into the lattice (fig. 8.6c). Each time the field of view is widened a hole twice the size of the previous largest hole is observed. Thus, on each scale the magnification could be set such that the structure looks just like the structure that was previously observed. This is called *scale invariance*.

There are many interesting phenomena which have the property of scale invariance and a detailed discussion can be found in Mandelbrot's book [207]. Of special interest to the reader may be its application to disordered solids [208], non-linear dynamical systems [209] and random walks on percolating clusters already mentioned in section 6.5 [210–212].

From the reader's own experience and from the above discussion it is obvious that below some magnification, the fractal structure disappears for physical objects. Certainly a plastic or a piece of glass, observed with the naked eye, appears to be homogeneous and the fractal structure is not

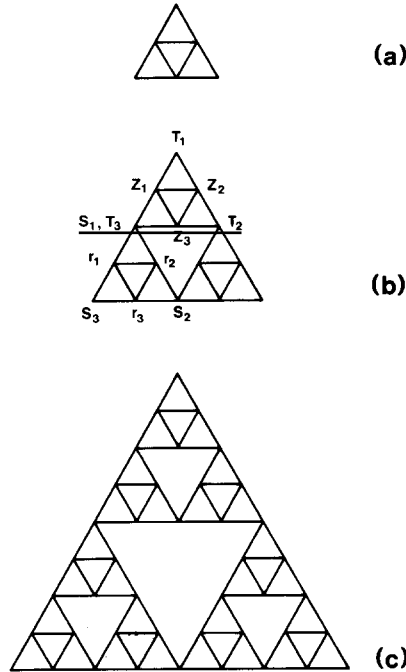


Fig. 8.6. (a) The basic building block of the Sierpinski gasket, (b) three basic building blocks are used to form the magnified view of the lattice and (c) the view is magnified again by using three composite building blocks from (b).

revealed. It is important to analyze in each physical situation where the regime with special fractal properties can appear.

A discussion of fractals cannot be complete without defining some important dimensions. One obvious dimension is the Euclidean dimension in which the fractal lattice is embedded. For fig. 8.6 the Euclidean dimension is $d = 2$. There are two further dimensions which can be defined and they are not necessarily integers (or rational numbers). One is the Hausdorff (or fractal) dimension [207], which is denoted in this review as \bar{d} ; and the second new dimension is called the spectral (or fracton) dimension, which is denoted by d_s .

The fractal dimension for fig. 8.6 can be introduced as follows. The number of points on the lattice of size L is proportional to L raised to the Hausdorff dimension

$$N_L = S_{\bar{d}} L^{\bar{d}}, \tag{8.31}$$

where $S_{\bar{d}}$ is a shape factor for the volume.

In fig. 8.6a, the length scale is set by the base length $L_1 = b = 2$ segments. The number of lattice sites is $N_2 = 6$. In fig. 8.6b the length is doubled $L_2 = 2^2$ and the total number of sites is $N_4 = 3 \cdot 6 - 3$. Finally in fig. 8.6c $L_3 = 2^3$ and $N_{2^3} = 3(3 \cdot 6 - 3) - 3$. This process can be continued and in general

$$L_{n+1} = 2^{n+1} \quad \text{and} \quad N_{2^{n+1}} = 3^n \cdot [6 - 3(1 - (\frac{1}{3})^n)/2]. \tag{8.32}$$

Inserting these expressions into eq. (8.31) and taking the limit $n \rightarrow \infty$, the Hausdorff dimension for the

$d = 2$ Sierpinski gasket with base $b = 2$ is:

$$\bar{d} = \ln 3 / \ln 2 \approx 1.585. \quad (8.33)$$

Gefen et al. [210] noted that this value is quite close to the Hausdorff dimension computed for the backbone cluster in a percolating lattice in $d = 2$. The backbone cluster is the infinite cluster at the percolation concentration with the dead-end branches removed. Gefen et al. compared the Hausdorff dimensions in each Euclidean dimension with the fractal dimension of the backbone cluster. Furthermore, they calculated the asymptotic properties of the conductivity (here the diffusion coefficient) on the fractal lattice and compared these to the corresponding results for the percolating cluster. They found the numerical values were close for $1 \ll d < 4$. This led them to the conclusion that the fractal lattice may already include the predominant features of the percolation problem.

In d dimensions and for general base length b of the elementary building blocks, Hilfer and Blumen [213] have calculated the Hausdorff dimension for the Sierpinski gaskets:

$$\bar{d} = \ln(b + d^{-1}) / \ln b, \quad (8.34)$$

where $\binom{N}{M} = N! / M!(N - M)!$ is the binomial coefficient.

The spectral dimension, as the name suggests, is intimately connected with the dynamical properties of the model [208, 214–215]. As in the calculation of the Hausdorff dimension, the spectral dimension is calculated using scaling arguments. One word of warning, the arguments given below are modified to the diffusion problem, where the relation between frequency and wavenumber is $\omega \approx k^2$. In the quoted literature the derivations are given for elastic vibrations where frequency and wavenumber are related by $\omega \approx k$.

One definition of the spectral dimension (see Rammal and Toulouse [215] for this and another relation for d_s) is given by the asymptotic expression for the probability of the particle to return to the origin:

$$P(\mathbf{0}, t | \mathbf{0}, 0) \sim t^{-d_s/2}. \quad (8.35)$$

This is a natural generalization of the asymptotic properties of $P(\mathbf{0}, t | \mathbf{0}, 0)$ on a Euclidean lattice where $d_s = d$. The Laplace transform of eq. (8.35) can be related by eq. (6.9) to the spectrum of eigenvalues. The asymptotic dependence is

$$\tilde{P}(\mathbf{0}, s | \mathbf{0}) \sim s^{d_s/2-1}. \quad (8.36)$$

For $s = -i\omega$, the density of states is:

$$\rho(\omega) \sim \omega^{d_s/2-1}. \quad (8.37)$$

From eq. (8.31), when the lattice size is scaled by b , then the number of sites scales as:

$$N_L = b^{\bar{d}} N_{L/b}. \quad (8.38)$$

Similarly, since the density of states is related to the length scale by:

$$\rho_L(\omega) d\omega \propto k^{\bar{d}-1} dk, \tag{8.39}$$

then the scaling $L \rightarrow L/b$ implies $k \rightarrow bk$. Hence, the density of states scales as

$$\rho_L(\omega) = b^{\bar{d}} \rho_{L/b}(\omega'); \tag{8.40}$$

ω' is the frequency at the lattice scale L/b . The frequencies on two different lattice scales are also related to one another by a scaling relationship:

$$\omega' = b^a \omega, \tag{8.41}$$

where the exponent a must be calculated for each specific model. With this assumption, the density of states are related on each scale by

$$\rho_{L/b}(\omega') = \frac{d\omega}{d\omega'} \rho_L(\omega'/b^a) = b^{-a} \rho_L(\omega'/b^a). \tag{8.42}$$

Choose the scale so that the argument of the density of states on the right-hand side is a constant, $b = \omega^{1/a}$. Replace this result in eq. (8.40) to find

$$\rho_L(\omega) = \omega^{\bar{d}/a-1} \rho_L(1). \tag{8.43}$$

The exponent in eq. (8.43) can be related to the spectral dimension defined in eq. (8.37):

$$d_s = 2\bar{d}/a. \tag{8.44}$$

The exponent a can be calculated for specific fractal lattices. Consider again the Sierpinski gasket, in particular fig. 8.6b. The calculation follows Rammal and Toulouse [215]. The method of calculating the exponent a is similar to the renormalization group procedure of Guyer [172]. In the figure a cluster of sites is eliminated from the lattice, e.g. $\{r_1, r_2, r_3\}$. The topology of this lattice does not introduce any transitions to further neighbor sites on the renormalized lattice; for instance, S_1 is coupled only to its four nearest neighbors on the new lattice $\{S_2, S_3, T_1, T_2\}$. The new lattice resembles fig. 8.6a.

The Laplace transform of the master equations for the clusters of sites which are to be eliminated (only homogeneous equations here) are:

$$(s + 4) \tilde{P}(r_i, s) = \tilde{P}(S_i, s) + \tilde{P}(S_k, s) + \tilde{P}(r_j, s) + \tilde{P}(r_k, s), \tag{8.45}$$

where (i, j, k) are cyclic permutations of the triple $(1, 2, 3)$. The analysis focuses on site S_1 , but it should be clear by the symmetry of the lattice ($z = 4$ for all sites), that the same results are derived for all remaining lattice sites. The equation governing the evolution of $\tilde{P}(S_1, s)$ is:

$$(s + 4) \tilde{P}(S_1, s) = \tilde{P}(r_1, s) + \tilde{P}(r_2, s) + \tilde{P}(Z_1, s) + \tilde{P}(Z_3, s). \tag{8.46}$$

Equations (8.45) can be directly solved for $\tilde{P}(r_1, s) + \tilde{P}(r_2, s)$ with the result:

$$[(s+4)(s+3)-2](\tilde{P}(r_1, s) + \tilde{P}(r_2, s)) = 2(s+4)\tilde{P}(S_1, s) + (s+6)[\tilde{P}(S_2, s) + \tilde{P}(S_3, s)]. \quad (8.47)$$

This result and a similar result for $\tilde{P}(Z_1, s) + \tilde{P}(Z_3, s)$ can be substituted into eq. (8.46). After factoring the quadratic polynomial, the result is:

$$(s+4)(s+1)(s+6)\tilde{P}(S_1, s) = (s+6)\{\tilde{P}(S_2, s) + \tilde{P}(S_3, s) + \tilde{P}(T_1, s) + \tilde{P}(T_2, s)\}. \quad (8.48)$$

This equation has the same form as eq. (8.45) with a scaling of the frequency scale:

$$s' = s(s+5). \quad (8.49)$$

In the asymptotic limit $s \rightarrow 0$, this corresponds to (recall $s = -i\omega$):

$$\omega' = 2^a \omega = 5\omega;$$

the exponent a is:

$$a = \ln 5 / \ln 2. \quad (8.50)$$

This is substituted into eq. (8.44) to obtain the spectral dimension. A more detailed calculation for d dimensions (but $b = 2$) [215] gives:

$$d_s = 2 \ln(d+1) / \ln(d+3). \quad (8.51)$$

Results for $b = 3$ can be found in ref. [213].

The fractal properties of the underlying lattice can also be expected to be manifest in the particle's mobility. Since the particle is forced to move in a reduced volume on the fractal lattices, a slower growth rate for the mean-square displacement can be expected:

$$\langle r^2 \rangle(t) \sim t^{2\nu}. \quad (8.52)$$

For ordinary Euclidean lattices, the exponent $\nu = \frac{1}{2}$. This exponent is related to the Hausdorff and spectral dimensions by the following heuristic arguments. The volume that the particle covers in time t is:

$$V(t) \sim \langle r^2 \rangle^{d/2}. \quad (8.53)$$

The particle also escapes from the initial site inversely proportional to the volume that the particle has covered:

$$P(\mathbf{0}, t | \mathbf{0}, 0) \sim V(t)^{-1}. \quad (8.54)$$

Using eq. (8.35) and eqs. (8.52–8.54) the exponent ν is:

$$\nu = d_s / 2\bar{d}. \quad (8.55)$$

Thus, the diffusion properties contain both topological and dynamical properties of the model. Guyer has used renormalization group calculations on various fractal lattices [216] to obtain the spectral dimension for these lattices. Another complication can be added by using master equations with memory kernels. This has been discussed by Blumen et al. [217]; they use a WTD with the asymptotic time dependence,

$$\psi(t) \sim t^{-1-\gamma}, \quad (8.56)$$

and find that the mean-square displacement behaves as:

$$\langle r^2 \rangle(t) \sim t^{d_s \gamma / \bar{d}}. \quad (8.57)$$

Finally, Derrida et al. [218] have evaluated the density of states for the d -dimensional bond percolation model using the effective medium approximation as in section 6.5. Their results show that the density of states exhibits a crossover from a low-frequency regime, where results are consistent with Euclidean dimensionality, to a high-frequency regime, where fractal behavior is found. The crossover frequency is shifted to lower frequencies as the percolation concentration is approached. They have used this crossover behavior to explain anomalous conductivity observed in experiments on amorphous materials [219]. However, this interpretation is controversial and more work needs to be done.

9. First-passage time problems

In this chapter problems are described where the probability of the *first* transition of a particle to a specified lattice site (or group of sites) is required. Numerous physical applications of these problems exist, notably capture of particles that perform random walks on lattices with traps. The first-passage problem on a discrete line is closely related to the corresponding problem of diffusion on a continuous line. See, e.g., [220] for some pertinent references.

9.1. First passage to a site on a linear chain

This problem has already been considered in chapter 5, where traps with internal states were modelled as linear chains and the waiting-time distribution was derived for first passage to a final site on this chain that represented the transition to a different site in the lattice. Here the first-passage problem on a linear chain is considered in a more general manner. For instance, infinite chains are admitted.

In section 5.3 the probability density of a first passage to a site i at time t when the particle arrived at site $i-1$ at $t=0$ was derived by setting up a recursion relation which relates this probability density to the probability density for first passage from site $i-2$ to site $i-1$. If the linear chain is finite, the repeated application of the recursion relation terminates and one obtains the expressions studied in section 5.3. It is useful for many applications to treat the infinite uniform linear chain in the same manner.

A particle performs Poissonian random walk on an infinite linear chain, with transition rates Γ between nearest-neighbor sites and it is assumed that the particle arrived at site i at $t=0$. The probability density is required for the first passage to site $i+1$, $\chi_{i+1,i}(t)$. Similar to section 5.3, an infinite series for the Laplace transform $\tilde{\chi}_{i+1,i}(s)$ is set up and resummed, resulting in

$$\bar{\chi}_{i+1,i}(s) = \frac{\Gamma}{s + 2\Gamma - \Gamma\tilde{\chi}_{i,i-1}(s)}. \quad (9.1)$$

If $\tilde{\chi}_{i,i-1}(0) = 1$, then also $\tilde{\chi}_{i+1,i}(0) = 1$. Now, in the infinite uniform chain $\tilde{\chi}_{i+1,i}(s)$ depends on the difference between $i + 1$ and i only, and is identical to $\tilde{\chi}_{i,i-1}(s)$. Hence

$$\tilde{\chi}_{1,0}(s) = \frac{\Gamma}{s + 2\Gamma - \Gamma\tilde{\chi}_{1,0}(s)}. \quad (9.2)$$

The solution of this equation is

$$\tilde{\chi}_{1,0}(\zeta) = \zeta + 1 - \sqrt{\zeta(\zeta + 2)}, \quad (9.3)$$

where $\zeta = s/2\Gamma$. Only the negative sign of the root is admissible, to ensure the correct short-time behavior. In the time domain $\tilde{\chi}_{1,0}(s)$ is a modified Bessel function [221]

$$\chi_{1,0}(t) = \frac{1}{t} I_1(2\Gamma t) \exp(-2\Gamma t). \quad (9.4)$$

By expanding eq. (9.3) for small s it is seen that the first moment of $\tilde{\chi}_{1,0}(s)$ diverges, i.e., the mean first-passage time to a neighbor site diverges in the infinite chain.

The above derivation of the first-passage time distribution is rather direct. There are other methods that deduce the quantity from the conditional probability of finding the particle at a given site at time t . The general relation between both quantities will be discussed in the next section. In this section the method of images will be reviewed for one dimension. It is described in detail in [15] for one absorbing site and discrete RW and in [7] also for two absorbing sites. Here the CTRW formulation will be given.

Consider an absorbing site, say i , in a linear chain. When only nearest-neighbor transitions are considered, and when the particle starts at a site $k < i$, the first transition to the trapping site occurs from site $i - 1$. Hence the conditional probability $P(i - 1, t | \bar{i})$ of finding the particle at this neighbor site is required, under the condition that i was not visited until time t . The transition to site i then takes place with rate Γ . The method of images constructs these conditional probabilities in such a way that the boundary condition of vanishing probability at the absorbing sites is satisfied. If i is the only trapping site in the uniform chain, the method of images is applied as follows. The paths of continuous-time random walk on the uniform chain are divided into allowed paths which do not reach i , and forbidden paths, cf. fig. 9.1. The contribution of the forbidden paths are subtracted in form of their mirror images, in an unrestricted RW these would occur with equal probabilities. One has

$$P(j, t | \bar{i}) = P(j, t) - P(2i - j, t), \quad (j \leq i). \quad (9.5)$$

The initial condition of start at say $k = 0$ has not been noted explicitly. The probability density of first passage to site i is then given by (set $j = i - 1$)

$$\chi_{i,0}(t) = \Gamma[P(i - 1, t) - P(i + 1, t)]. \quad (9.6)$$

The conditional probability $P(i \pm 1, t)$ is expressed by modified Bessel functions, as in eq. (8.1), and the recurrence relation [194] is applied,

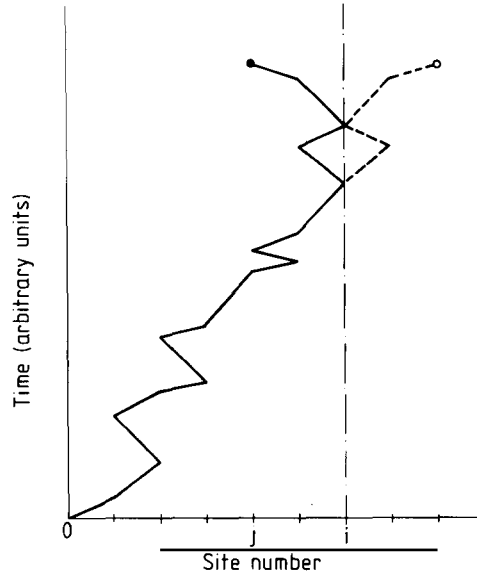


Fig. 9.1. The method of images applied to the trapping site i . Paths that go through i are forbidden. These contributions are subtracted by using their mirror images.

$$I_{i-1}(2\Gamma t) - I_{i+1}(2\Gamma t) = \frac{2i}{2\Gamma t} I_i(2\Gamma t). \tag{9.7}$$

The final result for $i = 1$ is eq. (9.4).

One could argue that the probability density of first passage to the trapping site i should follow from the convolution of the probability $P(i - 1, t' | \bar{i})$ of finding the particle at site $i - 1$ at time t' , and the waiting-time distribution for a transition to site i , $\Gamma \exp[-2\Gamma(t - t')]$. This reasoning leads to a wrong result. The derivation is rectified by using the probability density $Q(i - 1, t' | \bar{i})$ of a transition to site $i - 1$ at time t' , and by convoluting this probability density with the waiting-time distribution for the direct transition from $i - 1$ to i . $P(i - 1, t | \bar{i})$ is related to $Q(i - 1, t' | \bar{i})$ by the probability of sojourn at site $i - 1$, as discussed in section 3.2, cf. eq. (3.12). If this relation is taken into account, eq. (9.4) is regained. Continuous-time random walk requires sometimes careful analysis!

The method of images can be readily extended to two absorbing sites at, say, $-k$ ($k > 0$) and i ; this is already the general case in $d = 1$. The particle is assumed to start at site 0 at $t = 0$, the boundary condition of vanishing probability at the two absorbing sites. By this method the following relation is used

$$P(j, t | -\bar{k}, \bar{i}) = P(j, t | -\bar{k}, 2\bar{i} + \bar{k}) - P(2i - j, t | -\bar{k}, 2\bar{i} + \bar{k}).$$

This is iterated to obtain

$$P(j, t | -\bar{k}, \bar{i}) = \sum_{l=0}^{\infty} \{P(j + 2l(i + k), t | -\bar{k}) - P(2i - j + 2l(i + k), t | -\bar{k})\}.$$

Again by the method of images,

$$P(j, t | -\bar{k}) = P(j, t) - P(j + 2k, t),$$

and using symmetry the sum can be written as:

$$P(j, t | -\bar{k}, \bar{i}) = \sum_{l=-\infty}^{\infty} \{P(j + 2l(i + k), t) - P(2i - j + 2l(i + k), t)\}. \quad (9.8)$$

This equation may serve as a starting point for the trapping problem in $d = 1$. The infinite sum eq. (9.8) can be reduced to a finite sum (as many terms as the number of free sites between the traps); these manipulations are described in [7] for discrete RW, but they are the same for CTRW.

In this section the individual transitions were assumed to form a Poisson process. First-passage time probability densities with more general WTD were considered, e.g., by Balakrishnan and Khanta [222].

9.2. Relation between first-passage time distribution and conditional probability and applications

There exists a fundamental relation between the first-passage time distribution to a site and the conditional probability of finding the particle at this site at time t . The relation expresses essentially the fact that for a Markov process the probability of occurrence of an event at step ν is composed of the probability of the *first* occurrence at step ν , and of the probability of first occurrence at step $\nu' < \nu$, times the probability that the event again occurs after the remaining $\nu - \nu'$ steps. Schroedinger [223] applied this reasoning to the first-passage time problem on a line. As in the previous section, the relation will be formulated from the outset in continuous time. Since the Laplace transform of the continuous-time problem is equivalent to the generating function of the discrete-time description [24], both formulations are equivalent.

A uniform lattice of arbitrary dimensionality is considered. Let $F(\mathbf{n}, t)$ be the probability density of first arrival at site \mathbf{n} at time t ; the particle starts at site $\mathbf{n} = \mathbf{0}$ at $t = 0$. The start is not counted as an arrival event, hence $F(\mathbf{n} = \mathbf{0}, 0) = 0$. In other words, for $t > 0$ $F(\mathbf{0}, t)$ describes the first *return* to the origin. $P(\mathbf{n}, t)$ is the conditional probability of finding the particle at site \mathbf{n} at time t with $P(\mathbf{n}, 0) = \delta_{\mathbf{n}, \mathbf{0}}$. Then the following relation holds

$$P(\mathbf{n}, t) = \Psi(t) \delta_{\mathbf{n}, \mathbf{0}} + \int_0^t dt' F(\mathbf{n}, t') P(\mathbf{0}, t - t'). \quad (9.9)$$

For lattices with non-uniform transition rates, the start and end sites must be noted explicitly in the derivations. Laplace transformation of eq. (9.9) yields

$$\tilde{F}(\mathbf{n}, s) = \frac{\tilde{P}(\mathbf{n}, s) - \tilde{\Psi}(s) \delta_{\mathbf{n}, \mathbf{0}}}{\tilde{P}(\mathbf{0}, s)}. \quad (9.10)$$

The usefulness of the relation relies on two facts: i) The conditional probability is more readily available than the first-passage time distribution, especially in higher dimensions, and ii) the conditional probability can be calculated without considering the point under question as a special one. To demonstrate the use of this relation eq. (9.3) will be rederived, taking $n = 1$,

$$\tilde{\chi}_{1,0}(s) = \tilde{P}(1, s) / \tilde{P}(0, s). \quad (9.11)$$

The quantities $\tilde{P}(1, s)$ and $\tilde{P}(0, s)$ can be taken from eq. (2.33). Their quotient is identical with eq. (9.3).

One consequence which can be drawn from eq. (9.10) is the well-known dependence of the probability of return to the origin on dimensionality. It is given by the time integral of the waiting-time distribution for return; hence in continuous time the question arises whether this waiting-time distribution is normalized or not. From eq. (9.10) follows

$$\tilde{F}(\mathbf{0}, 0) = 1 - \bar{t} \tilde{P}(\mathbf{0}, 0). \tag{9.12}$$

Here \bar{t} is the mean residence time of the particle at a lattice site. The last term contains the inverse of the time integral over the probability of finding the particle at the origin; after dividing the integral by \bar{t} the mean number of visits at the origin is obtained. The calculation of this quantity is discussed in detail in the two reviews [7, 8]; only the result is quoted. $\bar{t}^{-1} \tilde{P}(\mathbf{0}, 0)$ is infinite for $d = 1, 2$ and finite for $d \geq 3$. Hence the waiting-time distribution for return to the origin is normalized in $d = 1, 2$, or the probability of return is unity. In $d \geq 3$ the probability of return is less than unity and the particle can escape to infinity without further returns. Explicit numbers for the return probabilities in various 3-dimensional lattices are found in the literature [86].

The mean time until trapping at a given point or return to the origin can also be discussed starting from eq. (9.10). First the mean time of return to the origin in $d = 1$ and 2 is considered. It follows from the waiting time distribution for the first return,

$$\int_0^\infty dt t F(\mathbf{0}, t) = - \left. \frac{\partial \tilde{F}(\mathbf{0}, s)}{\partial s} \right|_{s=0}. \tag{9.13}$$

For $n = 0$, eq. (9.10) reads

$$\tilde{F}(\mathbf{0}, s) = 1 - \tilde{\Psi}(s) / \tilde{P}(\mathbf{0}, s). \tag{9.14}$$

For Poissonian random walk in $d = 1$

$$\tilde{\Psi}(s) = (s + 2\Gamma)^{-1},$$

and

$$\tilde{P}(\mathbf{0}, s) = [s(s + 4\Gamma)]^{-1/2}.$$

Hence the small- s expansion reads

$$\tilde{F}(0, s) = 1 - (s/\Gamma)^{1/2} + \dots, \tag{9.15}$$

and no first moment of $F(0, t)$ exists. Consequently the mean time until return to the origin is infinite, as already deduced in section 9.1. A similar result holds in $d = 2$, where for the square lattice

$$\tilde{\Psi}(s) = (s + 4\Gamma)^{-1},$$

and $\tilde{P}(\mathbf{0}, s)$ is given as an elliptic integral [24]. Its expansion for small s is

$$\tilde{P}(\mathbf{0}, s) \xrightarrow{s \rightarrow 0} \frac{1}{4\pi\Gamma} \ln\left(\frac{32\Gamma}{s}\right). \quad (9.16)$$

Hence

$$\tilde{F}(\mathbf{0}, s) \xrightarrow{s \rightarrow 0} 1 - \frac{\pi}{\ln(32\Gamma/s)}, \quad (9.17)$$

and the first moment of $F(\mathbf{0}, t)$ diverges.

In three dimensions the same method can be used to derive the mean time until return at least for the lattices where the lattice Green functions $\tilde{P}(\mathbf{0}, s)$ are explicitly known, including their expansions for small s . This derivation would yield the mean time until trapping under the condition that the particle is actually trapped. The particle escapes to infinity with finite probability; hence the complete mean time until return to the origin should diverge. Montroll and Weiss [24] performed a calculation which exhibits these effects by considering finite, large lattices. They calculated the mean time until trapping at a general point \mathbf{n} and evaluated the leading term which they found proportional to the number of lattice sites N in $d = 3$. If each site is a trapping site with finite probability c , a *mean* trapping rate can be deduced. The result is identical to the result of the Rosenstock approximation which will be discussed in the next section. Therefore no explicit expressions are presented here. A very careful investigation of the average number of steps until trapping for several classes of RW's and arbitrary dimensions was made recently by den Hollander [224].

Next the mean number of *distinct* sites visited until time t is considered in a random walk on a d -dimensional uniform lattice. This important quantity follows quite easily from the probability density of first return to a site, $F(\mathbf{n}, t)$. As before, the calculations are performed in continuous time with the hope that this variant of the usual description may be useful in some cases. The derivation is an adaptation of the procedure of Montroll [225] to continuous time.

One defines

$$\Delta(t) = \sum_{\mathbf{n} \neq \mathbf{0}} F(\mathbf{n}, t). \quad (9.18)$$

After normalization with the number N of sites this is the probability density of arrival at time t at an arbitrary not yet visited site. Hence $\Delta(t) dt$ is the average increase of newly visited sites in the interval $[t, t + dt)$. The mean number of distinct points visited until time t is related to $\Delta(t)$,

$$\langle S(t) \rangle = 1 + \int_0^t dt' \Delta(t'). \quad (9.19)$$

or in the Laplace domain

$$\langle \tilde{S}(s) \rangle = [1 + \tilde{\Delta}(s)]/s. \quad (9.20)$$

In this relation eq. (9.18) and the expression eq. (9.10) for $\tilde{F}(\mathbf{n}, s)$ is introduced. The sum $\sum_{\mathbf{n}} \tilde{P}(\mathbf{n}, s)$ gives $1/s$ because of normalization. Hence

$$\langle \tilde{S}(s) \rangle = 1/[s^2 \tilde{P}(\mathbf{0}, s)]. \tag{9.21}$$

It is quite easy to deduce the known asymptotic results in $d = 1$ and 3 from (9.21). For instance, in $d = 1$

$$\tilde{P}(\mathbf{0}, s) \xrightarrow{s \rightarrow 0} (4\Gamma s)^{-1/2}. \tag{9.22}$$

Hence

$$\langle \tilde{S}(s) \rangle \xrightarrow{s \rightarrow 0} (4\Gamma)^{1/2} s^{-3/2}, \tag{9.23}$$

and

$$\langle S(t) \rangle \xrightarrow{t \rightarrow \infty} \left(\frac{16\Gamma t}{\pi} \right)^{1/2}. \tag{9.24}$$

Identifying $2\Gamma t$ with the number of steps n the usual result in discrete time [7] is recovered. The asymptotic result in $d = 2$ is less readily obtained since the inverse Laplace transform involves Volterra type functions whose asymptotic properties are not easily accessible.

The approximate asymptotic behavior of $\langle S(t) \rangle$ in $d = 2$ can be conjectured from the corresponding asymptotic behavior of $\langle S_n \rangle$ for discrete RW which is now known as a series [226]. The leading asymptotic term of $\langle S(t) \rangle$ can be obtained from the leading term of that series by the substitution $n = t/\bar{t}$, cf. also [24]. For the square lattice

$$\langle S(t) \rangle \xrightarrow{t \rightarrow \infty} \frac{\pi t}{t \ln(8t/\bar{t})}. \tag{9.25}$$

A more complete derivation of $\langle S(t) \rangle$ including more than the asymptotic term in CTRW is desirable.

The dimensionality 3 is simple again, since $\tilde{P}(\mathbf{0}, s)$ approaches a constant value in the limit $s \rightarrow 0$. Hence

$$\langle \tilde{S}(s) \rangle \xrightarrow{s \rightarrow 0} 1/[s^2 \tilde{P}(\mathbf{0}, 0)], \tag{9.26}$$

or

$$\langle S(t) \rangle \xrightarrow{t \rightarrow \infty} t/[\tilde{P}(\mathbf{0}, 0)]. \tag{9.27}$$

The result will be rewritten as

$$\langle S(t) \rangle \xrightarrow{t \rightarrow \infty} (1 - p_r)t/\bar{t}$$

where eq. (9.12) was used and p_r is an abbreviation for the return probability $\tilde{F}(\mathbf{0}, 0)$.

It is easy to extend the results presented in this chapter on first-passage time distributions to random walks with internal states, in the sense discussed in chapter 3. The basic relation between the first-passage time distribution and the conditional probability holds irrespective of the internal structure of the random walk. $\tilde{P}(\mathbf{n}, s)$ must be interpreted as the summary probability of finding the particle at

site \mathbf{n} , after the internal states have been summed over. Of course, the quantitative behavior of $\tilde{P}(\mathbf{0}, s)$ depends on the nature of the random walk under consideration.

This point will be illustrated for the correlated random walk in $d = 1$ discussed in section 4.2. It can be derived from the expression $\tilde{P}(k, s)$, eq. (4.6) that $\tilde{P}(0, s)$ is given by

$$\tilde{P}(0, s) = \frac{(\Gamma_b + \Gamma_f)[s^2 + 2s(\Gamma_b + \Gamma_f) + 4\Gamma_b\Gamma_f] + (\Gamma_f - \Gamma_b)\tilde{Q}(s)}{2\Gamma_f(s + \Gamma_b + \Gamma_f)\tilde{Q}(s)}, \quad (9.28)$$

$$\tilde{Q}(s) = [s(s + 2\Gamma_b)(s + 2\Gamma_f)(s + 2\Gamma_b + 2\Gamma_f)]^{1/2}.$$

In the limit $s \rightarrow 0$ this quantity behaves as

$$\tilde{P}(0, s) \xrightarrow{s \rightarrow 0} \left(\frac{\Gamma_b}{2\Gamma_f(\Gamma_b + \Gamma_f)s} \right)^{1/2} + \frac{\Gamma_f - \Gamma_b}{2\Gamma_f(\Gamma_f + \Gamma_b)} + \dots \quad (9.29)$$

This behavior can now be used to deduce from eq. (9.21) the mean number of distinct sites visited by the correlated random walk. The result is

$$\langle S(t) \rangle \xrightarrow{t \rightarrow \infty} [8(\Gamma_b + \Gamma_f)ft/\pi]^{1/2} + 1 - f + \dots, \quad (9.30)$$

where f is the correlation factor,

$$f = \Gamma_f/\Gamma_b. \quad (9.31)$$

The asymptotic result for correlated walk is obtained by rescaling the time in (9.24) with the correlation factor f . This result was obtained by Keller [227]. The correction to the asymptotic behavior was derived by Kehr and Argyrakis for discrete RW [228]; it does not obey scaling. Numerical simulations verify the correction term, cf. fig. 9.2.

The mean number of sites visited by correlated walk in higher dimensions was also investigated in ref. [228]. The model with restricted reversals and the forward stepping model were studied for discrete RW in $d = 2$ and 3. Asymptotic expressions could be analytically derived for the model of restricted reversals. The leading term in $d = 2$ can be obtained by scaling the step number with f ; again there appear corrections that do not fulfil scaling. In $d = 3$ the form obtained by scaling and the correction term are of the same order.

9.3. Survival probability of particles diffusing in the presence of traps

In this section the survival probability of a particle is examined that is put randomly on a lattice with a random distribution of traps and then performs a random walk. The waiting-time distribution is requested for first arrival at a trap where the particle is assumed to be annihilated or permanently trapped. This waiting-time distribution may be expressed in discrete time, ψ_n , or in continuous time, $\psi(t)$. The survival probability Ψ_n after n steps or $\Psi(t)$ after time t is related to ψ_n or $\psi(t)$ by

$$\Psi(n) = 1 - \sum_{m=0}^n \psi_m, \quad (9.32)$$

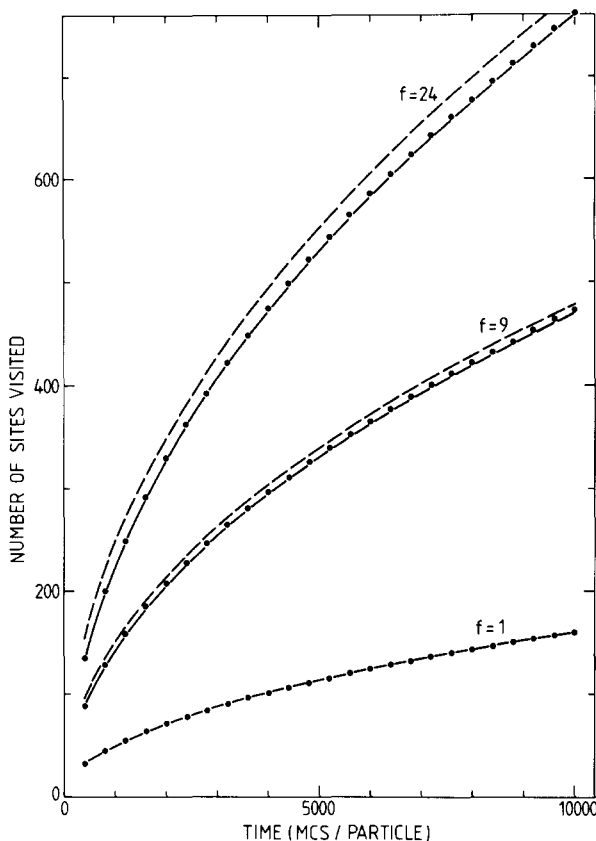


Fig. 9.2. The mean number of sites visited by a correlated random walk on a linear chain versus time. The solid circles are Monte Carlo simulations. The solid lines represent the asymptotic expression with the term $1 - f$ in eq. (9.30), whereas the dashed curves neglect this term.

or

$$\Psi(t) = 1 - \int_0^t dt' \psi(t'). \tag{3.1}$$

The waiting-time distributions ψ_n or $\psi(t)$ include a double average over the random-trap distributions and over the different possible random walks. The combination of the two averages led to some surprising results, which found much attention recently.

The permanent traps are assumed to be randomly distributed over an infinite lattice, with probability c of finding a trap at any site, and no correlations between different sites. Let S_n be the number of distinct sites visited in an n -step random walk. The survival probability after n steps is evidently given by

$$\Psi_n = \langle (1 - c)^{S_n} \rangle. \tag{9.33}$$

In this expression only an average over different random walks must be taken; the average over the random-trap distribution has already been performed in the expression given above. Stanley et al. [229]

verified eq. (9.33) by performing explicitly the average over different trap configurations; they also elaborated the role of the weight factor $p = 1 - c$.

To perform the average eq. (9.33) it suffices to know the probability distribution $p_n(S)$ of the number S of distinct sites visited by an n -step RW. It is also convenient to define

$$p = (1 - c) = \exp(-\lambda). \quad (9.34)$$

The survival probability is thus given by the average

$$\Psi_n = \sum_{S=1}^{\infty} p_n(S) e^{-\lambda S} = \langle e^{-\lambda S} \rangle, \quad (9.35)$$

i.e., each walk is counted in the average with a weight factor $\exp(-\lambda S)$. The case $n = 0$ where $p_0(S) = \delta_{S,1}$ and $\Psi_0 = 1 - c$ is included.

The same reasoning as above can be made in continuous time. Thus, when the survival probability is requested in continuous time, the following average must be studied

$$\Psi(t) = \langle (1 - c)^{S(t)} \rangle, \quad (9.36)$$

where $S(t)$ is the number of distinct sites visited up to time t . Also this average can be understood as an average over the probability distribution $p_t(S)$ of the number of distinct sites visited up to time t . Applications of the previous expressions were mainly made for discrete RW.

An approximate evaluation of the survival probability will be given now in continuous time. The approximation, done in continuous time, consists in replacing $S(t)$ in eq. (9.36) by its average value

$$\Psi_R(t) = (1 - c)^{\langle S(t) \rangle}. \quad (9.37)$$

This approximation is due to Rosenstock [230] who calculated essentially a waiting-time distribution for luminescence using this approximation. Later work by him and Straley [231, 232] was mainly concerned with the mean time until trapping, which can be derived from the survival probability. The asymptotic behavior of the mean number of distinct sites $\langle S(t) \rangle$ visited up to time t was reviewed in the preceding section. Using these expressions, the asymptotic behavior of the survival probability is obtained in the Rosenstock approximation, in continuous time

$$\Psi_R(t) = \begin{cases} \exp[-\lambda(8t/\pi\bar{t})^{1/2}], & d = 1, \\ \exp\{-(\lambda\pi t)/[\bar{t} \ln(8t/\bar{t})]\}, & d = 2, \\ \exp[-\lambda(1 - p_r)t/\bar{t}], & d \geq 3. \end{cases} \quad (9.38)$$

The result for $d = 2$ is valid for the square lattice. In the Rosenstock approximation, the survival probability decays exponentially with time in 3 and more dimensions, and a time-independent capture rate can be identified from eq. (9.38). It is given by

$$\Gamma_t = \lambda(1 - p_r)/\bar{t}. \quad (9.39)$$

For small c the capture rate is proportional to c , as expected. The result eq. (9.39) represents the

capture rate for diffusion-limited trapping where the diffusion occurs on a discrete lattice. For small c , it is identical to the result in eq. (7.35) of the average T -matrix approximation for the random trap model.

One may ask whether the Rosenstock approximation made in continuous time is equivalent to the analogous approximation in discrete time, when the step number is identified with $n = t/\bar{t}$. When the CTRW is Poissonian the equivalence can be justified by the arguments given in section 2.3. The simple transcription of the discrete into the continuous-time result may no longer be possible when the elementary jump process is described by a more complicated waiting-time distribution. For instance, non-exponential waiting-time distributions may occur as a result of multipolar long-range transfer, as considered in ref. [233].

The survival probability can be derived beyond the Rosenstock approximation by employing cumulant expansion techniques [233, 234]. In fact, the average eq. (9.35) can be expressed in the form

$$\Psi_n = \exp \left[\sum_{j=1}^{\infty} \kappa_{j,n} (-\lambda)^j \frac{1}{j!} \right], \tag{9.40}$$

where the $\kappa_{j,n}$ are the cumulants of order j of the distribution $p_n(S)$. Restriction to the first cumulant is identical to the Rosenstock approximation. Zumofen and Blumen [234] have numerically determined some cumulants from simulations of $p_n(S)$. Figure 9.3 shows their results for the survival probability (normalized to one) derived from the numerical cumulants, in $d = 1$. There is good agreement between an exact expression (see below) and the direct simulations of the survival probability. The successive inclusion of higher cumulants yields survival probabilities that approximate successively better the correct Ψ_n , but the expansion always breaks down for larger steps numbers. These results also demonstrate that Rosenstock's approximation is very poor in $d = 1$. $d = 1$ is the least favorable case; in

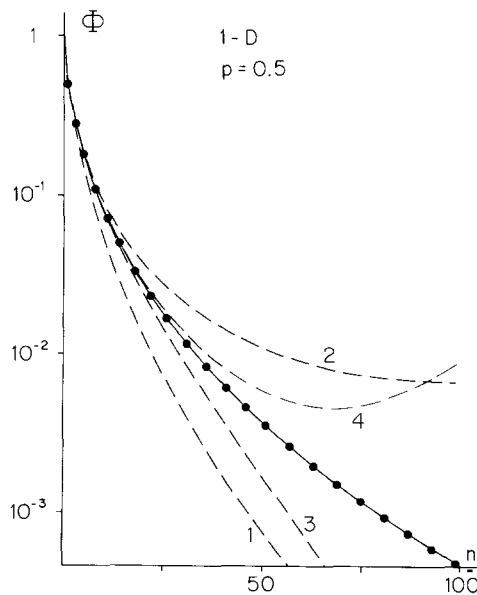


Fig. 9.3. The survival probability, Φ , in one dimension as a function of step number, n , calculated using Monte-Carlo data (solid circles) and numerically determining successive cumulants of order $j = 1, 2, 3$ and 4 (from Zumofen and Blumen [234]).

$d = 2$ already the inclusion of 2 cumulants gives good results for intermediate step numbers, while in $d = 3$ already the Rosenstock approximation gives a useful description of the decay laws [234]. A related work is the article of Weiss [235] in which he derived Ψ_n in $d = 3$ from the distribution $p_n(S)$ of distinct sites visited. In accordance with results of Jain and Pruitt [236] a Gaussian form of $p_n(S)$ was used, with specified mean and standard deviation. Hence this procedure is equivalent to a second-order cumulant expansion.

It became clear in recent years that the survival probability does not behave asymptotically as predicted by the Rosenstock approximation or its extensions. The correct asymptotic behavior of $\Psi(t)$ in continuous time and for a continuous diffusion for small trap concentrations $c \ll 1$ and long times was found by Balagurov and Vaks [237]. They found

$$\Psi(t) \sim \begin{cases} 8 \left(\frac{2c^2t}{3\pi t} \right)^{1/2} \exp \left[-\frac{3\pi^{2/3}}{2} (c^2t/\bar{t})^{1/3} \right], & d = 1, \\ \exp[-\sqrt{\pi}\mu_0(ct/\bar{t})^{1/2}], & d = 2, \\ \exp \left[-\left(\frac{\pi}{3} \right)^{8/5} \frac{5}{2^{1/5}} (c^{2/3}t/\bar{t})^{3/5} \right], & d = 3, \end{cases} \quad (9.41)$$

where μ_0 is the first zero of the Bessel function $J_0(z)$. Balagurov and Vaks solved in $d = 1$ the diffusion equation for a particle on a finite segment of a line, bounded by traps, with the boundary condition of vanishing probabilities at the traps. The solution of the diffusion equation was then averaged over the *distribution* of the lengths of these segments. While the survival probability decays exponentially in a given, fixed, segment the average over the distribution of the lengths leads to the anomalous behavior. There are large trap-free segments, although with small probabilities, and the particles may survive abnormally long in those segments. Similar considerations were made in higher dimensions. There is a close analogy of the trapping problem to the problem of the density of states of an electron in a medium with random impurities; this problem was extensively discussed by Lifshitz [238].

The work of Balagurov and Vaks [237] did not reach general attention. Some time thereafter Donsker and Varadhan [239, 240] proved rigorously that the survival probability behaves asymptotically in a way consistent with eq. (9.41). They gave their proof first for continuous diffusion in continuous time [239] and they extended it later to random walk in discrete time [240]. For the random walk the theorem requires no bias of the walk and a finite second moment. It reads, specialized to nearest-neighbor jumps, and for $\lambda > 0$,

$$\lim_{n \rightarrow \infty} \frac{\ln \langle \exp(-\lambda S) \rangle}{n^{d/(d+2)}} = -k(\lambda, d), \quad (9.42)$$

where

$$k(\lambda, d) = \lambda^{2/(d+2)} \frac{d+2}{-2} \left(\frac{2\mu_d}{d} \right)^{d/(d+2)}$$

and μ_d is the smallest eigenvalue of the Laplace operator $\Delta/2$ in d dimensions on a unit sphere with

Dirichlet boundary conditions. For instance, in one dimension $\mu_1 = \pi^2/2$ and

$$\Psi_n \sim \exp[-\frac{3}{2}(\pi\lambda)^{2/3}n^{1/3}]. \tag{9.43}$$

$\lambda = c$ for small c and one recognizes the asymptotic equivalence with (9.41). Also the rigorous proof of Donsker and Varadhan remained largely unnoticed up until recently [241].

The trapping problem obtained general attention through the work of Grassberger and Procaccia [242]. They considered Brownian motion in continuous time and a random distribution of traps. They started from the physical consideration of fluctuations of the trap densities and were able to derive the asymptotic behavior

$$\Psi(t) \sim \exp(-\alpha t^{d/(d+2)}), \tag{9.44}$$

from the contributions of the trap-free regions of different size. Below an adaptation of their argument to random walk in discrete time will be given. The derivation of Grassberger and Procaccia gives a lower bound to $\Psi(t)$; an upper bound for $\Psi(t)$ was established by Kayser and Hubbard [243] for Brownian motion in continuous time in the presence of random spherical traps. It was found that asymptotically both bounds were identical.

The following qualitative derivation can be given [244] for the non-integer exponent of the asymptotic behavior of the survival probability. Consider start of the particle in a trap-free region with S sites. The probability to find such a region is $p^S = \exp(-\lambda S)$ with λ defined in eq. (9.34). The linear extension of a (compact) region is up to numerical factors $R = S^{1/d}$ (lattice constant is unity). This quantity is a measure for the distance to be traversed by a random walk until capture. The mean number of steps necessary for traversal by a random walk is thus given by $\langle n \rangle = R^2 = S^{2/d}$. For a fixed configuration of traps an exponential decay of the survival probability is obtained, with $f_n \propto \exp(-n/\langle n \rangle)$. The configuration-averaged survival probability is

$$\Psi_n = \sum_S \exp(-\lambda S) \exp(-n/\langle n \rangle); \tag{9.45}$$

or, after replacing the sum by an integral and inserting $\langle n \rangle$

$$\Psi_n \simeq \int_0^\infty dS \exp[g(S)], \tag{9.46}$$

where

$$g(S) = -\lambda S - nS^{-2/d}.$$

The maximum of $g(S)$ is at

$$S_m = (2n/d\lambda)^{d/(d+2)}, \tag{9.47}$$

and saddle-point integration yields

$$\Psi_n \sim \exp\left[-\frac{d+2}{2} \lambda^{2/(d+2)} \left(\frac{2n}{d}\right)^{d/(d+2)}\right]. \quad (9.48)$$

Apart from a numerical factor this estimate is equivalent to the result of Donsker and Varadhan.

Explicit expressions are to be expected in $d = 1$ where random-walk problems can be solved exactly to a large extent. Movaghar et al. [246] derived the solution of the random-walk problem between two absorbing traps by scattering methods and averaged it over the trap distributions. To obtain a closed expression they introduced an approximation valid for small c only; their result is identical to the one derived by Balagurov and Vaks in $d = 1$, cf. (9.41).

Anlauf pointed out in his work [244, 245] that the asymptotic behavior of the survival probability can be deduced from the published asymptotic representations of $p_n(S)$. Two different forms have been given in the literature [7] in the form of infinite sums. It is important to realize that the weight factor $\exp(-\lambda S)$ in eq. (9.35) favors the small S values. In fact, $p_n(S)$ has a maximum at $S \propto n^{1/2}$ while the combined quantity $p_n(S) \exp(-\lambda S)$ has its maximum at $S \propto n^{1/3}$, cf. fig. 9.4. Hence that representation of $p_n(S)$ should be used which converges most rapidly for small S values. Only a few (one or two) terms are necessary to obtain an excellent approximation for $p_n(S)$ for S values left of the maximum, cf. however the discussion below. Anlauf deduced the leading asymptotic behavior and the corrections to it from the first term of $p_n(S)$. The following scaling variable can be introduced

$$x = [\pi\lambda]^{2/3} n^{1/3}, \quad (9.49)$$

where λ is defined in eq. (9.34). The survival probability was derived including corrections up to relative order x^{-4} . It is given by

$$\Psi_n = \frac{8}{\pi} \left(\frac{2}{3\pi}\right)^{1/2} x^{3/2} \exp\left[-3x/2 + \frac{a_1}{x} + \frac{a_2}{x^2} + \frac{a_3}{x^3} + \frac{a_4}{x^4} + \dots\right],$$

where

$$a_1 = \frac{17}{18}, \quad a_2 = -\frac{7}{54}, \quad a_3 = -\frac{26}{243} \quad \text{and} \quad a_4 = \frac{167}{942}. \quad (9.50)$$

The leading term coincides with the one given above. The numerical simulations agree well with eq. (9.50) for concentrations up to 0.5, cf. fig. 9.5; for details see refs. [244, 245]. Also the scaling property eq. (9.49) could be verified by the simulations.

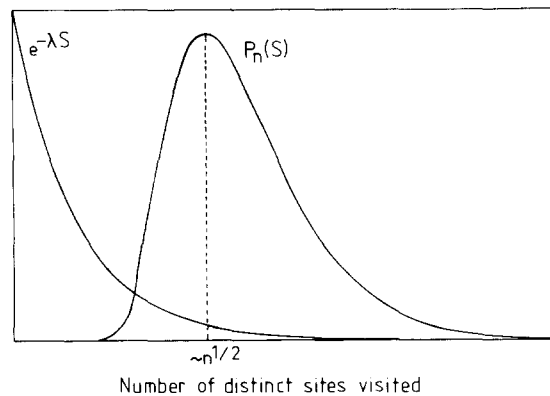


Fig. 9.4. Illustration of the distribution of distinct sites visited $p_n(s)$ and the exponential factor appearing in eq. (9.35).

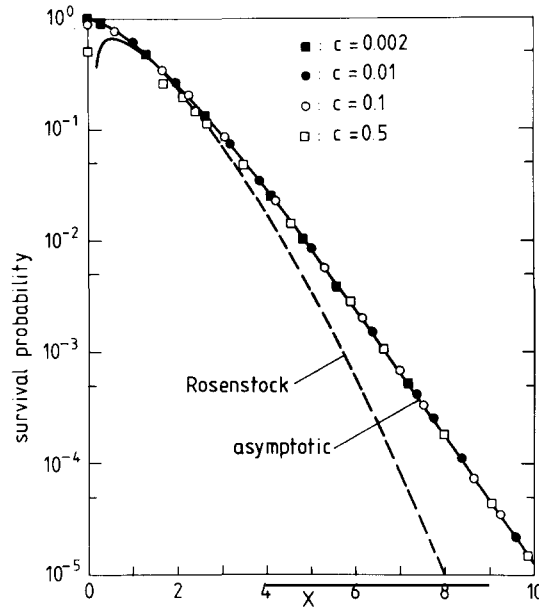


Fig. 9.5. Numerical simulation of the survival probability in $d = 1$ versus scaled step number for several concentrations. The dashed curve shows Rosenstock's first cumulant approximation; the solid curve is eq. (9.50). Figure from J.K. Anlauf [245].

Thus far results were considered following from the asymptotic expansion of $p_n(S)$. At very large trap concentrations where the survival probability becomes small for small step numbers, yet another type of corrections must be taken into account. These corrections arise from the difference between asymptotic and exact expressions for $p_n(S)$. Exact representations for $p_n(S)$ can be obtained by the transfer matrix method, the results are equivalent to those following from the method of images. Evaluation of the exact expressions in the asymptotic limit (i.e. for large x) leads to a modification of the result eq. (9.50) by the factor $[\lambda = -\ln(1 - c)]$:

$$C = \frac{c^2}{(1 - c)[-\ln(1 - c)]^2}, \tag{9.51}$$

and correction terms in the coefficients of a_1, a_2, \dots . For example, the coefficient a_1 is modified to

$$a_1 \rightarrow \left[\frac{17}{18} - \frac{\pi^2 \ln^2(1 - c)}{12} \right]. \tag{9.52}$$

The higher-order coefficients are modified in a similar manner. The c -dependent additional factor C deviates from 1 in the limit $c \rightarrow 0$ as

$$C = 1 + \frac{c^2}{12} + O(c^3); \tag{9.53}$$

hence it is near to one for small and intermediate c . Even at $c = 0.5$ a deviation of only 4% has to be

considered. Exact numerical enumeration techniques confirm [244] the correction terms discussed above in the case of large trap concentrations.

Presently not much work has been done on the trapping problem in higher dimensions. According to Zumofen and Blumen [234] in $d = 3$ the Rosenstock approximation and its improvement by the next cumulant seems to represent well the survival probability for moderate step numbers. Lubensky [247] studied the trapping problem by path-integral methods. Using an instanton technique, he could derive a general form of the survival probability in arbitrary dimensions. The exponent contains a series in powers of $n^{d/(d+2)}$, $n^{(d-1)/(d+2)}$, \dots . Of course, the coefficient of the first term must coincide with the result of Donsker and Varadhan. The following coefficient can only be calculated approximately for $d > 1$. The form of the survival probability obtained in $d = 1$, cf. eq. (9.50), agrees with the general result found by Lubensky [247]. Recently Havlin et al. [248] did numerical work by exact enumeration techniques on the survival probability of particles in 2 and 3-dimensional lattices with moderate and large trap concentrations. They showed that their data scaled as the asymptotic behavior of Donsker and Varadhan for step numbers where already $\Psi_n \leq 10^{-13}$. It is not known how in $d = 3$ the changeover from the exponential decay at smaller step number to the asymptotic decay $\propto \exp(-\alpha n^{3/5})$ occurs quantitatively. Investigation of the changeover as a function of trap concentration is a pressing problem. Since in many instances simple exponential WTDs for trapping and the accompanying concept of a time-independent trapping rate has been used in $d = 3$, the range of validity of these ideas must be critically examined.

9.4. Reemission and recapture

In the last section the waiting-time distribution was studied for the first capture of a particle which performs a random walk in the presence of randomly distributed traps. In many applications reemission processes of trapped particles must be taken into account, in particular particles may escape from the traps by thermal excitation. Typically this process is an activated transition process over a barrier. It may be described by a waiting-time distribution for escape $\psi_r(t)$. In the simplest case this waiting-time distribution is exponential,

$$\psi_r(t) = \gamma_r \exp(-\gamma_r t), \quad (9.54)$$

where γ_r is the escape rate. Some discrete stochastic models for deriving more complicated waiting-time distributions were considered in section 5.3. After the particle escaped from the trap, it may be recaptured by the same, or by another, randomly located trap. One should note that the two-state model of section 5.1 *assumes* that the waiting-time distribution for recapture is exponential,

$$\psi_r(t) = \gamma_r \exp(-\gamma_r t), \quad (9.55)$$

where γ_r is a rate for (re)capture. Almost no explicit determinations of the precise average waiting-time distribution for recapture have been made. Anlauf [244] pointed out how the waiting-time distributions for capture at the same trap and for capture at the other traps can be calculated by the same formalism as used for deriving the waiting-time distribution for random implantation. This formalism leads in principle to waiting-time distributions with the same leading asymptotic behavior as the previous ones. Intuitively one expects a strong tendency for recapture at the same trap after a few steps and a behavior similar to the waiting-time distribution for random implantation after a long time.

Den Hollander and Kasteleyn [249] have provided a theory that effectively relates the summary waiting-time distribution for first recapture at an arbitrary trap to the waiting-time distribution for first capture after random implantation. This theory is formulated in discrete time. It will be reviewed here with suitable simplifications for the present purpose.

Den Hollander and Kasteleyn consider a regular lattice with two kinds of points ('white' and 'black' points). The colors of the points shall be randomly distributed over the lattice, with c the probability of finding a black point. The random walk of a test particle on the lattice is assumed to be independent of the color of the points, i.e., one has random walk on a regular lattice. Two different processes are considered, (0) the particle starts at an arbitrary site, and (1) the particle starts at a black site. Consider first process (0) and introduce P_{n,n_1,\dots,n_i} as the joint probability that the particle is at a black point after step n and that it again is at a black point after n_1 steps, after n_2 steps, etc. and the i th time after n_i steps. Similarly, F_{n,n_1,\dots,n_i} is the joint probability of *first* reaching a black point after n steps and performing i returns to black points with the step numbers n_1, \dots, n_i . Process (1) is characterized by F_{0,n_1,\dots,n_i} since the particle starts at a black point. Den Hollander and Kasteleyn deduce from the translation invariance of the probability distribution of black points that

$$P_{n,n_1,\dots,n_i} = P_{0,n_1,\dots,n_i}. \tag{9.56}$$

In particular

$$P_n = P_0 = c. \tag{9.57}$$

The following relation between P and F can be established

$$P_{n,n_1,\dots,n_i} = F_{n,n_1,\dots,n_i} + \sum_{m=1}^n P_{n-m,m,n_1,\dots,n_i}. \tag{9.58}$$

The argument leading to eq. (9.58) is similar to the one used for eq. (9.9) in section 9.2, i.e., the particle arrives at a black point either first at step n , or it was already on a black point at a prior step. Here no product terms are necessary because the definition of the quantities P_{n,n_1,\dots,n_i} includes repeated visits at black sites before step n , in the first index. Equation (9.56) is used to simplify the relation between F and P ,

$$F_{n,n_1,\dots,n_i} = P_{0,n_1,\dots,n_i} - \sum_{m=1}^n P_{0,m,n_1,\dots,n_i}. \tag{9.59}$$

Now F_n is the discrete analog of the waiting-time distribution for a first visit to a black point, or first arrival at a trap, if black points are identified with temporary traps. Hence ($P_0 = c$)

$$F_n = c - \sum_{m=1}^n P_{0,m}. \tag{9.60}$$

Setting $n = 0$ and $i = 1, n_1 = m$ in eq. (9.59) one obtains

$$F_{0,m} = P_{0,m}; \tag{9.61}$$

and thus

$$F_n = c - \sum_{m=1}^n F_{0,m}. \quad (9.62)$$

The quantity $F_{0,m}$ can be interpreted as the waiting-time distribution for first recapture at a black point, given that the particle started at a black point at step 0, multiplied by the probability of start at a black point, $P_0 = c$. Hence eq. (9.62) gives the relation between the discrete waiting-time distributions for the first capture in a random situation and for recapture after release. Note that $F_{0,n}$ includes the return to the same black point and arrival at other black points.

Relation eq. (9.62) is given in discrete time. Transcription of this relation to continuous time would give

$$\psi(t) = c \left[1 - \int_0^t dt' \psi_R(t') \right], \quad (9.63)$$

where $\psi(t)$ is the waiting-time distribution for first capture after random implantation and $\psi_R(t)$ is the waiting-time distribution for return to any trap after release. However, in eq. (9.63) retardation effects are neglected, resulting from longer stays in the traps. If one would consider different waiting-time distributions for steps originating on white points or on the black points one should correct for this difference in the derivation of eq. (9.63). This appears to be simple for exponential waiting-time distributions.

Den Hollander and Kasteleyn [249] have discussed how the moments of process (0) (random start) and process (1) (start at a black point) are related. Generally the moments of process (1) are related to the moments of (0) of one order less. Analogous derivations can be made in continuous-time random walk. For instance, eq. (9.63) shows that the mean time until recapture at a black point is given by the zeroth moment of the left-hand side, which is one because of normalization. Hence the mean time until recapture is proportional to the inverse concentration of the black points. Of course, this argument must be modified if the escape from the black points is governed by a different waiting-time distribution.

In summary, the behavior of the WTD for capture of a particle by random traps after random implantation appears to be closely related to the behavior of the WTD for recapture after release from the traps. If no anomalous time dependencies are brought in by the WTD for release, the WTD considered above should exhibit similar asymptotic time dependencies.

10. Biased random walks

10.1. Introduction

During a biased random walk the particle drifts in a preferential direction. The field causing the biased drift may be local, i.e. restricted to a few lattice sites, or it may be global, extending over the whole lattice. An applied static electric field or a static elastic deformation of the sample can be used to induce a drift in a preferential direction on the whole lattice. Whereas, local charge centers or defects in the lattice can cause a local drift into a region of lower potential energy.

These random walks can be important in understanding significant physical properties of materials. For example, static electric fields in microelectronic circuitry result in large electric fields in gate connections and welds; as smaller gate sizes are sought and higher densities of gates on chips are achieved, there is a corresponding larger current density in the wires and solder connections. The atoms in the solders are mobile and they can be swept from the contact region by a process called electromigration [250–252]. Internal structures, such as atomic impurities, dislocations or vacancies can locally distort the lattice over several lattice sites. Evidence for this internal elastic deformation is found in Huang scattering experiments and Zwischenreflex scattering [253, 254]. The extended internal structures cause a local drift as the particle falls into and again climbs out of the distorted regions. The understanding of the interrelationship between both of these types of bias mechanisms could very well advance the stability and lifetime of the microchips.

Bias appears quite naturally when general models with disordered transition rates are considered, i.e. when the restrictions of symmetry of transitions between sites (chapter 6) or of the transitions originating at the site (chapter 7) are relaxed. The transition rates $\Gamma_{n,n'}$ between nearest-neighbor sites are thus considered as independent random numbers. A one-dimensional potential leading to such transition rates is depicted in fig. 10.1. One recognizes regions with local drift; also global drift is present in the general situation.

The simplest version of a biased random walk is a single-state CTRW with constant transition rates on a d -dimensional hypercubic lattice. This example serves to illustrate the biased random walks. Suppose that the static field is applied along the positive axis in the d direction. The transition rates in the master equation for the directions $\nu = 1, 2, \dots, d-1$ are set equal to Γ . For the $\nu = d$ axis the transition rate is $\Gamma = \Gamma b^{-1}$, when the transition is to a neighbor in the negative direction and it is $\Gamma_+ = \Gamma b$, when the jump is in the positive direction. The factors $b^{\pm 1} = \exp(\pm \beta E)$ are due to the relative changes in the potential barrier as seen from the central site and E is the static applied field with unit distance between neighboring sites.

The conditional probability in the Fourier–Laplace representation is:

$$\tilde{P}(\mathbf{k}, s | \mathbf{0}) = \{s + \gamma[1 - p(\mathbf{k})]\}^{-1}, \quad (10.1)$$

where the structure function of the biased random walk is

$$p(\mathbf{k}) = \left[\sum_{\nu=1}^d \cos k_{\nu} + (\exp(-ik_d)b + \exp(ik_d)b^{-1})/2 \right] / [d - 1 + (b + b^{-1})/2] \quad (10.2)$$

and γ is the summary transition rate,

$$\gamma = \Gamma[2(d-1) + (b + b^{-1})]. \quad (10.3)$$

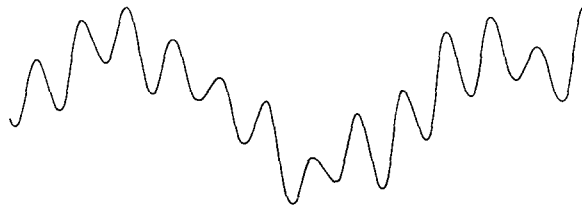


Fig. 10.1. Schematic representation of a model with random transition rates. A portion of a one-dimensional potential on a lattice is shown where both the maxima and minima are random.

The first moment is non-zero only in the direction of the applied field and it is along the positive axis:

$$\langle x_d \rangle(t) = \Gamma(b - b^{-1})t. \quad (10.4)$$

This is the first new property of biased random walks. It is a first-order effect, i.e. linear in the field at small field values. It is easy to calculate the diffusion tensor from the expression for the conditional probability, and the second new property of biased random walks is the field-induced asymmetry of the diffusion tensor:

$$D_{\nu\nu}^0 = \begin{cases} \Gamma, & \nu = 1, 2, \dots, d-1, \\ \Gamma(b + b^{-1})/2, & \nu = d. \end{cases} \quad (10.5)$$

This is a second-order effect in the applied field, i.e. quadratic in the field at small fields. The mean-square displacement has the following behavior:

$$\langle r^2 \rangle(t) = \gamma t + \Gamma^2(b - b^{-1})^2 t^2. \quad (10.6)$$

The first term expresses the field-dependent diffusion and the last term is the square of the drift caused by the application of the field. The expression eq. (10.1) can be transformed back to the space-time coordinates ($\mathbf{n} = n_1 \mathbf{e}_1 + \dots + n_d \mathbf{e}_d$)

$$P(\mathbf{n}, t | \mathbf{0}, 0) = \exp(-\gamma t) I_{n_1}(2\Gamma t) I_{n_2}(2\Gamma t) \cdots I_{n_d}(2\Gamma t) b^{n_d}, \quad (10.7)$$

where $I_n(z)$ is a modified Bessel function [194]. The occupation of the initial site asymptotically falls off as an exponential function of time, rather than as an algebraic power of the time. This model is so simple that no frequency dependence could be expected for the diffusion coefficient; it is interesting to speculate as to whether this situation is altered if the waiting-time distributions are not exponential, even when the first jump is treated as an equilibrium renewal process. This question is taken up and answered in the following section.

10.2. Biased CTRW models

Consider now the problem of bias using the CTRW description when the waiting-time distributions are not exponential. Here it is assumed that the system is in a steady state. This is possible by considering a finite lattice of N sites with periodic boundary conditions. In this situation, if each site is equivalent on the lattice, then they have equal occupation probabilities, even in a field. All translation invariant models satisfy this criterion; in particular, two models which satisfy the criterion of equal occupation probabilities on each site are the trapping models in chapter 5. As in the previous section, transition probabilities to nearest-neighbor sites are altered by the factors $b^{\pm 1}$. It is assumed that the spatial effect of the bias on the RW is incorporated in the structure function in eq. (10.2). The WTD $h(t)$ and $\psi(t)$ describe the temporal behavior of the first, and all other transitions to neighboring sites, respectively. The derivations in chapter 3 can then be utilized without any modification; in particular, the conditional probability $\tilde{P}(\mathbf{k}, s | \mathbf{0})$ is represented by eq. (3.15) where $p(\mathbf{k})$ is given by eq. (10.2). From that equation the average displacement along the α th axis is:

$$\langle x_\alpha \rangle(s) = \frac{i\tilde{h}(s)}{s(1 - \tilde{\psi}(s))} \left. \frac{\partial p(\mathbf{k})}{\partial k_\alpha} \right|_{\mathbf{k}=\mathbf{0}}. \quad (10.8)$$

The mean-square displacement is:

$$\langle x_\alpha^2 \rangle(s) = \frac{-\tilde{h}(s)}{s(1-\psi(s))} \left. \frac{\partial^2 p(\mathbf{k})}{\partial k_\alpha^2} \right|_{\mathbf{k}=\mathbf{0}} - \frac{2\tilde{\psi}(s)\tilde{h}(s)}{s(1-\psi(s))^2} \left(\left. \frac{\partial p(\mathbf{k})}{\partial k_\alpha} \right|_{\mathbf{k}=\mathbf{0}} \right)^2. \tag{10.9}$$

In eqs. (10.8) and (10.9) the first-jump waiting-time distribution appears explicitly. For an equilibrium renewal process $\tilde{h}(s) = [1 - \tilde{\psi}(s)]/s\bar{t}$. In this case the moment equations simplify to:

$$\langle x_\alpha \rangle(s) = \frac{i}{s^2\bar{t}} \left. \frac{\partial p(\mathbf{k})}{\partial k_\alpha} \right|_{\mathbf{k}=\mathbf{0}} \tag{10.10}$$

and

$$\langle x_\alpha^2 \rangle(s) = -\frac{1}{s^2\bar{t}} \left. \frac{\partial^2 p(\mathbf{k})}{\partial k_\alpha^2} \right|_{\mathbf{k}=\mathbf{0}} - \frac{2\tilde{\psi}(s)}{s^2(1-\psi(s))\bar{t}} \left(\left. \frac{\partial p(\mathbf{k})}{\partial k_\alpha} \right|_{\mathbf{k}=\mathbf{0}} \right)^2. \tag{10.11}$$

From eq. (10.10) it is evident that the mean displacement is a linear function of time in the direction of the applied field. The result is the same as for a CTRW with Poissonian WTD, eq. (10.6), with $\gamma = \bar{t}^{-1}$. The first term in eq. (10.11) contains the diffusion tensor in the presence of a field; again, with the identification of γ with the inverse of the mean stay time this term is equivalent to eq. (10.4). The last term in eq. (10.11) contains two contributions; one is the drift contribution to the mean-square displacement and this is proportional to t^2 . This contribution can be subtracted by using the Laplace transform of the square of the mean displacement. The remaining portion provides a frequency dependence to the diffusion tensor. The components of the tensor are frequency independent in the directions orthogonal to the field. In the direction of the field the diffusion coefficient is:

$$\tilde{D}_{dd}(s) = \frac{b + b^{-1}}{2[2(d-1) + b + b^{-1}]\bar{t}} + \frac{1}{\bar{t}} \left(\frac{b - b^{-1}}{2(d-1) + b + b^{-1}} \right)^2 \left(\frac{\tilde{\psi}(s)}{1 - \tilde{\psi}(s)} - \frac{1}{s\bar{t}} \right). \tag{10.12}$$

In linear response there is no frequency dependence of the diffusion coefficient and the field-dependent diffusion coefficient eq. (10.12) is unchanged by a reversal of the field. It is of interest to note that if $\tilde{h}(s) = \tilde{\psi}(s)$, as is appropriate for transient experiments, then the mean displacement is no longer a linear function of time. The linear time dependence is appropriate for the steady state.

The results of this section have been developed by Tunaley [255]. Nelkin and Harrison [256] used these results as a basis for the discussion of the origin of $1/f$ noise [257, 258]. In particular, they have taken the multiple trapping models (chapter 5) as a particular realization of single-state CTRW. A quantity of interest to experimentalists studying $1/f$ noise is the current noise spectral density given by [255]:

$$P(f) = -\frac{2ne^2A\omega^2}{l} \int_0^\infty dt \langle (x_d(t) - x_d(0))^2 \rangle \cos(\omega t), \tag{10.13}$$

where $f = \omega/2\pi$, A is the samples cross-sectional area, e is the carrier charge, n is the carrier density, and l is the length of the medium in the direction of the field.

For the stationary state the noise spectral density is expressed as ($x_d(0) = 0$):

$$P(f) = -\frac{2ne^2A\omega^2}{l} \operatorname{Re}\{\langle x_d^2 \rangle(s = i\omega)\}. \quad (10.14)$$

Equation (10.14) shows the simple connection between the mean-square displacement in eq. (10.11) and the quantity $P(f)$. Within the framework of these models, the appearance of $1/f$ noise can be achieved by appropriately modelling trapping states and determining the corresponding waiting-time distribution [256]. The first term in eq. (10.11) is related to the background current fluctuations and is equivalent to the Nyquist theorem [255]. The origin of $1/f$ noise in these models is attributed to the excess noise following from the last term of eq. (10.11) or equivalently, the second term in eq. (10.12).

It was noted in chapter 2 that the diffusion coefficient is constant for an unbiased CTRW with $h(t)$ chosen from an equilibrium renewal process; nevertheless, the fourth moment of the displacement (super Burnett coefficient) has a complicated time and frequency dependence. This was used by Stanton and Nelkin [259] to study the band-limited noise power, as suggested by Voss and Clarke [260]. This quantity is related to a fourth moment of the displacement and the modelling of $1/f$ noise is again reduced, using these models, to a calculation of the WTD for a distribution of traps.

As previously mentioned, it is possible that the trap and release rates are also affected by the bias field. Such models were considered by Boettger and Bryksin [261] (in a different formalism) and by Barma and Dhar [262]. The physical motivation for this generalization by Barma and Dhar was the percolation problem introduced in the previous chapters. The backbone (i.e. infinite) cluster is simplified to a one-dimensional lattice. There are many branches on the backbone which can be assumed to be finite for the moment; these branches resemble the trapping sites on the ladder trap model, but the trapping rates are affected by the bias field as they may lie partially in the field direction.

The two-state model in one dimension is sufficient to demonstrate the salient features which bias-dependent trapping and release rates has on the results. In these models the trap rate is increased by $\gamma_t^* = b\gamma_t$, and the release rate from the trap is reduced by $\gamma_r^* = \gamma_r/b$. Using the results of chapter 5, the WTD for this model is (eq. (5.22)):

$$\tilde{\psi}(s) = \frac{\gamma}{\gamma + s[1 + \gamma_t b/(s + \gamma_t b^{-1})]} \quad (10.15)$$

and the first-jump WTD is:

$$\tilde{h}(s) = \frac{\gamma[1 + \gamma_t b/(s + \gamma_t b^{-1})]}{\{\gamma + s[1 + \gamma_t b/(s + \gamma_t b^{-1})]\}(1 + \gamma_t b^2/\gamma_t)}, \quad (10.16)$$

where γ is the unbiased summary transition rate to nearest-neighbor sites, see fig. 5.1. The average waiting time is given by the expression:

$$\bar{t} = (\gamma_r + \gamma_t b^2)/\gamma\gamma_r. \quad (10.17)$$

It is a straightforward matter to calculate the average steady-state drift velocity for this two-state model. The result is:

$$V = \frac{1}{\bar{t}} \frac{b - b^{-1}}{b + b^{-1}}. \quad (10.18)$$

The velocity increases for small applied fields, but it vanishes as $1/b$ for sufficiently large field amplitudes. The reason for this behavior is the increased steady-state occupation of the traps in very high fields. The diffusion coefficient is frequency dependent. In the Laplace domain

$$\tilde{D}(s) = \frac{1}{2t} + \frac{1}{t^2} \left(\frac{b - b^{-1}}{b + b^{-1}} \right)^2 \frac{\gamma_l b^2 / \gamma_r}{s + \gamma_r b^{-1} + \gamma_l b}. \quad (10.19)$$

As $b \rightarrow \infty$ the diffusion coefficient also vanishes.

The above results provide qualitative explanations of field-induced trapping treated by other authors (White and Barma [263], Barma and Dhar [262], Boettger and Bryksin [261], Pandey [264]). The generalization to a random number of trapping states at each site has been treated by White and Dhar [263]. They found that, when the maximum number of trapping states on a site was allowed to become infinite, the average velocity identically vanishes above a threshold value of the applied field. Precisely, how the diffusion coefficient vanishes in high fields for these models remains an open problem. It is worth reminding the reader that the diffusion coefficient would be obtained from the coefficient for linear growth in time of the mean-square displacement at long times. Clearly though, these models warrant further investigation in higher dimensions.

10.3. Random lattices with a constant bias

The previous section has demonstrated that an applied field can cause a frequency-independent diffusion coefficient to become frequency dependent even without introducing a statistical treatment of the randomness. Now, it is appropriate to return to the previously considered models of random media and investigate the changes in the dynamical properties when a field is applied.

Most of the results developed with bias and randomness apply to the random barrier model in one dimension [265, 266]. However, some results in higher dimensions have been reported and the lattices with random traps have also been treated [267–269].

The model for the one-dimensional infinite random-barrier problem discussed in section 6.3 has been extended to include an applied field by Khantha and Balakrishnan [270]. They use the stationary solution of the N -site chain with reflecting boundary conditions at the end of each segment which is given as:

$$P^{st}(m) = b^{2m-1} (1 - b^2) / (1 - b^{2N}), \quad (10.20)$$

for $1 \leq m \leq N$. The diagonalization of the tridiagonal matrix is performed analytically and the results for the N -site chain diffusion coefficient $D_N(i\omega)$ are presented. Two special limits of interest are the high-frequency limit:

$$\begin{aligned} \tilde{D}_N(i\omega) = & \Gamma \frac{b + b^{-1}}{2} \left\{ 1 - \frac{1}{N} + \frac{2}{N} \left[2(N-2) \left(\frac{b - b^{-1}}{b + b^{-1}} \right)^2 - 1 \right] \frac{\Gamma(b + b^{-1})}{2i\omega} \right. \\ & \left. + \frac{2}{N} \left[1 - 9 \left(\frac{b - b^{-1}}{b + b^{-1}} \right)^2 \right] \left[\frac{\Gamma(b + b^{-1})}{2i\omega} \right]^2 + \dots \right\} \end{aligned} \quad (10.21)$$

and the low-frequency limit:

$$\tilde{D}_N(i\omega) = i\omega \left[\frac{N^2}{6} - \frac{N}{4} \frac{(1+b^2)}{(1-b^2)} \frac{(1+b^{2N})}{(1-b^{2N})} + \frac{(1+10b^2+b^4)}{12(1-b^2)^2} \right] + O(\omega^2), \quad (10.22)$$

where b has been defined above eq. (10.1). The calculation of the diffusion coefficient, after properly weighting and summing the coefficients $D_N(i\omega)$ is discussed in their article. In the strong-field regime simple analytical results are given; otherwise, the expressions are suitable for numerical summation.

The next step in considering models with a bias is the solution of the random-barrier model and the random-trap model. For these models analytic results are also available. Consider the master equation with arbitrary jump rates:

$$\frac{dP(n, t)}{dt} = [\Gamma_{n, n+1} P(n+1, t) - \Gamma_{n+1, n} P(n, t)] + [\Gamma_{n, n-1} P(n-1, t) - \Gamma_{n-1, n} P(n, t)]; \quad (10.23)$$

define the probability current over the barrier between site n and site $n+1$ as:

$$j_n(t) = \Gamma_{n+1, n} P(n, t) - \Gamma_{n, n+1} P(n+1, t). \quad (10.24)$$

The master equation can now be written in the shortened form:

$$dP(n, t)/dt = j_{n-1}(t) - j_n(t). \quad (10.25)$$

In the steady state $dP(n, t)/dt = 0$, the time independence of the solutions requires that the current over each barrier be a constant independent of the position on the lattice:

$$j_n = v, \quad (10.26)$$

where v is identified as the average value of the current. Instead of a lattice with an infinite number of sites, a lattice is considered which is restricted to N sites and periodic boundary conditions. Otherwise source and sink terms may be added at the ends. The limit of an infinite lattice is taken after the calculations are performed. A recursive solution of eq. (10.24) is:

$$P^{\text{st}}(n) = \frac{v}{\Gamma_{n+1, n}} + \frac{\Gamma_{n, n+1}}{\Gamma_{n+1, n}} P^{\text{st}}(n+1); \quad (10.27)$$

continuing the recursion relation and using the periodic boundary condition, the solution is:

$$P^{\text{st}}(n) = \left[\frac{v}{\Gamma_{n+1, n}} + v \sum_{j=1}^{N-1} \frac{1}{\Gamma_{n+1+j, n+j}} \prod_{i=1}^j \frac{\Gamma_{n+i-1, n+i}}{\Gamma_{n+i, n+i-1}} \right] / \left[1 - \prod_{j=1}^N \frac{\Gamma_{j, j+1}}{\Gamma_{j+1, j}} \right]. \quad (10.28)$$

The constant v can, under restricted circumstances to be discussed below, be explicitly calculated.

To calculate the average velocity in the biased random-barrier model [266], set

$$\Gamma_{n, n+1} = b^{-1} \Gamma_n \quad \text{and} \quad \Gamma_{n+1, n} = b \Gamma_n. \quad (10.29)$$

The stationary solution eq. (10.28) is:

$$P^{st}(n) = vb \sum_{j=0}^{N-1} \frac{b^{2j}}{\Gamma_{n+j}} / (1 - b^{2N}). \quad (10.30)$$

In this case it is assumed that $b < 1$; however, if $b > 1$, then it is a simple matter to rewrite the series to obtain an expression in powers of b^{-2} . Summing eq. (10.30) over n and dividing by N , the left-hand side is set equal to unity. Finally, taking the limit $N \rightarrow \infty$, the average velocity can be determined:

$$v = (b - b^{-1}) \langle 1/\Gamma \rangle^{-1}. \quad (10.31)$$

This expression has the same form as the average velocity calculated from the CTRW model in eq. (10.4).

For the biased random-trap model the rates are:

$$\Gamma_{n+1,n} = b\Gamma_n \quad \text{and} \quad \Gamma_{n-1,n} = b^{-1}\Gamma_n. \quad (10.32)$$

The result for the average velocity is the same as in eq. (10.31). Short-time dynamical properties are calculated by using the solution of the master equation in powers of the time:

$$P(n, t) = P(n, 0) + t[\Gamma \cdot P(0)]_n + \frac{t^2}{2} [\Gamma \cdot \Gamma \cdot P(0)]_n + \dots, \quad (10.33)$$

and for the initial condition $P(n, 0)$, the steady-state solution is used. For the random-barrier model, the distribution when the particle is initially at $n = 0$ is ($b < 1$):

$$P(n, 0) = \delta_{n,0} \frac{(1 - b^2)}{\langle 1/\Gamma \rangle} \sum_{p=0}^{\infty} \frac{b^{2p}}{\Gamma_{-(1+p)}}. \quad (10.34)$$

The diffusion coefficient calculated for short times is [266]:

$$\tilde{D}(s) = b \langle \Gamma \rangle + \frac{(b^{-1} - b)}{2 \langle 1/\Gamma \rangle} + \frac{1}{s} \{ 2b^2 \langle \Gamma \rangle^2 - b(b + b^{-1}) \langle \Gamma^2 \rangle + b(b^{-1} - b) \langle \Gamma \rangle \langle 1/\Gamma \rangle^{-1} \} + \dots. \quad (10.35)$$

The next term in the expansion can be found in Biller's article [266]. It is interesting to note here that the diffusion coefficient at short times has terms with $\langle \Gamma \rangle$, as well as $\langle 1/\Gamma \rangle$, the latter dependence occurs because of the complicated steady-state occupation probabilities given in eq. (10.34).

This method can also be extended to calculate the dynamical properties at low frequencies; the equation of motion used by Biller [266] is:

$$dw(n, t)/dt = -j_n(t) + v \quad (10.36)$$

where j_n is the probability current and v is the average velocity. The set of functions $\{w(n, t)\}$ are

related to the conditional probabilities by

$$P(n, t) = w(n, t) - w(n-1, t). \quad (10.37)$$

The functions $w(n, t)$ are summary probabilities for the particle to be in the range $\{-\infty, n\}$. The initial condition is $P(0, 0) \theta(n)$, where $P(0, 0)$ is given in eq. (10.34) and $\theta(n)$ is the Heavyside function.

The equations of motion in eq. (10.36) are solved by using Laplace transforms and the average Green function for the system. Assuming the particle is initially on site m , the average unperturbed Green function satisfies the equation ($\bar{\Gamma} = \langle 1/\Gamma \rangle^{-1}$):

$$s \tilde{G}_{n,m}^0(s) - \bar{\Gamma} \left[b (\tilde{G}_{n+1,m}^0(s) - \tilde{G}_{n,m}^0(s)) - \frac{1}{b} (\tilde{G}_{n,m}^0(s) - \tilde{G}_{n-1,m}^0(s)) \right] = \delta_{n,m}. \quad (10.38)$$

The solutions of these coupled equations are calculated in a manner identical to the development of eq. (2.33):

$$\tilde{G}_{n,m}^0(s) = \frac{1}{(\lambda_+ - \lambda_-)} \begin{cases} \lambda_+^{(n-m)}, & n \geq m, \\ \lambda_-^{(n-m)}, & n \leq m, \end{cases} \quad (10.39)$$

where

$$\lambda_{\pm} = \frac{1}{2} [\langle s/\Gamma \rangle + b + b^{-1} \pm \{ \langle s/\Gamma \rangle^2 + 2(b + b^{-1}) \langle s/\Gamma \rangle + (b - b^{-1})^2 \}^{1/2}].$$

This solution is found, as in section 2.2, cf. eq. (2.33), by simple contour integration. The perturbation series, now in real space, is similar to the calculations in section 6.2, and the diffusion coefficient for small s is:

$$\tilde{D}(s) = \frac{\langle \frac{1}{\Gamma} \rangle^{-1}}{\left[\frac{b + b^{-1}}{2} \left\langle \left(\frac{1}{\Gamma} - \left\langle \frac{1}{\Gamma} \right\rangle \right)^2 \right\rangle \right] \langle \frac{1}{\Gamma} \rangle^{-1}} \frac{bs}{(\lambda_+ - \lambda_-)} \frac{(1 - \lambda_-)}{(1 - b^2 \lambda_-)} + \dots \quad (10.40)$$

The frequency behavior of the diffusion coefficient depends on the field strength. At high fields, i.e. $\langle s/\bar{\Gamma} \rangle \ll (b - b^{-1})^2 / 2(b + b^{-1})$, the expansion of $\tilde{D}(s)$ has integral powers of s . Whereas, there are intermediate frequencies (or correspondingly small field strengths), where the half-integral powers of s are approximately recovered.

Similar results were discussed in the weak disorder expansion by Derrida and Orbach [265]. Their method has been generalized to higher dimensions by Derrida and Luck [271]. They use a weak disorder expansion of the master equation with the ordered state being the zeroth order result. The average velocity V_0 and the diffusion coefficient D_0 of the unperturbed system are used in the expansion. The disorder is measured by the second moments of the transition rate fluctuations ($\delta\Gamma_{n,n'}$):

$$C = \sum_n (n_d - n'_d)^2 [\langle \delta\Gamma_{n,n'}^2 \rangle - \langle \delta\Gamma_{n,n'} \delta\Gamma_{n',n} \rangle]. \quad (10.41)$$

They find the disordered systems possess an upper critical dimension $d_u = 2$. Above this dimension, the average velocity vanishes linearly as $|V_0| \rightarrow 0$:

$$V = V_0(1 + K_d C + \dots). \quad (10.42)$$

However, at $d = 2$ and below anomalous behavior of the velocity is observed. The disorder is important even if it is weak. Their average velocity for $d = 2$ is:

$$V = V_0(1 - \eta + 3\eta^2 + \dots), \quad (10.43)$$

where $\eta = C \ln(D_0^2/V_0^2)/4\pi D_0$. For $1 < d < 2$ the average velocity is:

$$V = V_0[1 - K_d C V_0^{-(2-d)}], \quad (10.44)$$

and the average velocity for $d = 1$ is:

$$V = V_0 - \text{sgn}(V_0)[C/2D_0 + \dots]. \quad (10.45)$$

A field-theoretical renormalization group approach [272] gives the average velocity in $d = 2$ as:

$$V \sim \frac{V_0}{C \ln(K_2/V_0^2)}. \quad (10.46)$$

Comparison with eq. (10.43) shows that the parameter η now appears in the denominator, indicating importance of the higher-order terms in the series in eq. (10.42) as $d \rightarrow 2$.

These results show the importance of the disorder is qualitatively different in dimensions higher than 2. The effect of strong disorder, i.e., transition-rate distributions with diverging inverse moments, and a more detailed analysis of these systems remain as open problems.

Results for the biased random-trap model have quite recently appeared [190, 267, 268]. The diffusion coefficient and the super Burnett coefficient have been calculated in d dimensions. Nieuwenhuizen and Ernst [268] have studied distributions where all moments of the transition rates exist and also the strong-disorder case. In the first case where all the inverse moments of the transition rates exist, they calculate the dynamical properties using the response-function method described in chapter 7. The strong-disorder case was treated using an effective medium theory, the occupation probabilities of the initial sites was, of course, not the equilibrium stationary state. This model has $1/f$ noise when the distribution function for the transition rates has a non-zero value for very deep traps, i.e., $f \gg \gamma_t$.

10.4. Models with a random bias

Models which have not been considered in this review so far are those containing a random bias [273–278]. Models of this type have been formulated to analyze replication of polymer chains [273], and the diffusion of vacancies in alloys [274, 275]. The results have mostly been obtained for one-dimensional systems (see Kalikow for results in higher dimensions [276]).

As an example of this class of systems, consider the stationary probability distribution eq. (10.28) and take the transition rates to be

$$\Gamma_{n+1,n} = b_n \Gamma \quad \text{and} \quad \Gamma_{n,n+1} = b_n^{-1} \Gamma. \quad (10.47)$$

The bias fields b_n are assumed to be independently distributed. The stationary probability density is:

$$P^{\text{st}}(n) = \left[\frac{v}{b_n \Gamma} + \frac{v}{\Gamma} \sum_{j=1}^{N-1} \prod_{i=0}^{j-1} \frac{1}{b_{n+i}^2 b_{n+j}} \right] / \left(1 - \prod_{j=1}^N b_j^{-2} \right). \quad (10.48)$$

The model is restricted to the case, $\langle \ln(b_j^{-1}) \rangle < 0$; this requirement insures that the denominator converges to unity in the limit $N \rightarrow \infty$. This can be seen as writing the product as a sum over $\ln b_j$ in an exponential function. Summing the result and using the normalization of the stationary probability distribution the result is:

$$1 = \frac{v}{\Gamma} \left\langle \frac{1}{b} \right\rangle \sum_{j=0}^{\infty} \left\langle \frac{1}{b^2} \right\rangle^j. \quad (10.49)$$

When it is assumed that the series, i.e., $\langle b^{-2} \rangle < 1$, the average velocity is then:

$$v = \frac{\Gamma(1 - \langle 1/b^2 \rangle)}{\langle 1/b \rangle}. \quad (10.50)$$

If the average $\langle b^{-2} \rangle$ is greater than unity, the inverse moment $\langle b^2 \rangle$ may be less than unity and the series analogous to eq. (10.48) can again be summed. However, it is easy to create distributions where both of these moments are greater than unity; in this case the velocity vanishes [277]. The long-time asymptotic behavior of the mean displacement has been analyzed by Sinai [279], Derrida and Pomeau [280], Derrida [281] and Bernasconi and Schneider [282]. Their models and methodology differ from that presented here; only the results will be discussed.

Derrida [281] has calculated the velocity and diffusion for the model where the transition rates have the distribution:

$$\rho(\Gamma_{n+1,n}, \Gamma_{n,n+1}) = (1-c) \delta(\Gamma_{n+1,n} - \Gamma^<) \delta(\Gamma_{n,n+1} - \Gamma) + c \delta(\Gamma_{n+1,n} - \Gamma) \delta(\Gamma_{n,n+1} - \Gamma^<). \quad (10.51)$$

This distribution has regimes where the velocity is finite and where the velocity is zero. As long as the condition:

$$\langle \Gamma_{n+1,n} / \Gamma_{n,n+1} \rangle < 1 \quad \text{or} \quad \langle \Gamma_{n,n+1} / \Gamma_{n+1,n} \rangle < 1 \quad (10.52)$$

is satisfied, the velocity is non-zero and its expression is (assuming the first inequality holds):

$$v = \langle 1 / \Gamma_{n,n+1} \rangle^{-1} [1 - \langle \Gamma_{n+1,n} / \Gamma_{n,n+1} \rangle]^{-1}, \quad (10.53)$$

eq. (10.52) is violated for concentrations c :

$$\frac{1}{2} \leq c \leq \Gamma / (\Gamma + \Gamma^<) = c_1, \quad (10.54)$$

where $\Gamma^< < \Gamma$.

The diffusion coefficient for this model is given by the expression:

$$D = \frac{(1 - \langle \Gamma_{n+1,n} / \Gamma_{n,n+1} \rangle^2) \langle 1 / \Gamma_{n,n+1} \rangle^{-3}}{(1 - \langle (\Gamma_{n+1,n} / \Gamma_{n,n+1})^2 \rangle)} * \left[\left\langle \frac{1}{\Gamma_{n,n+1}} \right\rangle \left\langle \frac{\Gamma_{n+1,n}}{\Gamma_{n,n+1}^2} \right\rangle + \frac{1}{2} \left\langle \frac{1}{\Gamma_{n,n+1}^2} \right\rangle \left(1 - \left\langle \frac{\Gamma_{n+1,n}}{\Gamma_{n,n+1}} \right\rangle \right) \right]. \tag{10.55}$$

This holds as long as the condition:

$$\langle (\Gamma_{n+1,n} / \Gamma_{n,n+1})^2 \rangle < 1, \tag{10.56}$$

is satisfied. Otherwise the diffusion coefficient diverges. The concentration interval where eq. (10.56) is violated is:

$$\frac{1}{2} \leq c \leq \Gamma^2 / (\Gamma^2 + \Gamma^{<2}) = c_2. \tag{10.57}$$

This concentration interval is different from that for the vanishing of the velocity, see fig. 10.2. It is to be expected that higher moments have anomalous behavior at other concentrations, as well.

Bernasconi and Schneider have considered a diode model [282]; these models are a variant of the usual random barrier model. They have the property that the particle can jump across certain barriers only in one direction; the reverse direction acts like an infinite barrier. There is an anomalous regime in this model and the particle's average position grows with a non-integral power of time, t^ν , where $\nu < 1$ (see also Solomon [277]). Also, the asymptotic time dependence of the average position is modulated by a function of $\ln(t)$.

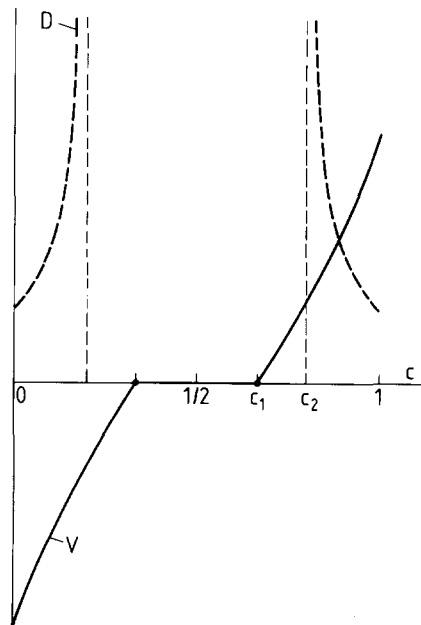


Fig. 10.2. The diffusion coefficient and the velocity in the model of Derrida versus concentration of right-biased transition rates. The diffusion coefficient (dashed lines) diverges and the velocity (solid lines) vanishes at different concentrations. Figure adapted from Derrida [281].

The discrete-time models of Solomon [277], Kesten [278] and Derrida and Pomeau [280] have a bias in the right transitions, p_n , and the left transitions, q_n , from the site n . The distribution of values of $p_n = 1 - q_n$ is:

$$\rho(p_n) = c \delta(p_n - p) + (1 - c) \delta(p_n - (1 - p)). \quad (10.58)$$

Figure 10.1 is representative of this model; the barriers fluctuate according to a random walk displacement with a global bias when $c \neq \frac{1}{2}$. For $\frac{1}{2} < c < p$, the average displacement is [278, 280]

$$\langle x \rangle(t) \sim t^\nu, \quad (10.59)$$

where $\nu = \ln\{c/(1-c)\}/\ln\{p/(1-p)\}$. The velocity in the long-time regime vanishes even though a global bias has been imposed on the particle. This special feature occurs because the typical barrier height is not representative of the highest barriers. As fig. 6.2 illustrates, the average velocity of a particle is limited by the highest obstacles and not by the average barrier heights.

In the special case of no global bias $c = \frac{1}{2}$ Sinai [279] showed that the displacement divided by the square of $\ln t$:

$$y = x/(\ln t)^2, \quad (10.60)$$

has a limit distribution.

The case without global bias resembles a random walk on a random-walk set by the potential on the lattice and the result in eq. (10.60) can be heuristically explained as follows. The average potential difference ΔU from one point on the lattice to another point separated by a distance L is

$$\Delta U = K\sqrt{L}, \quad (10.61)$$

where K is constant. The time required to diffuse the distance L on the lattice is

$$t \sim \exp(\beta \Delta U) = \exp(\beta\sqrt{L} K). \quad (10.62)$$

Since L is taken to be the average distance covered by the particle in time t , the solution of eq. (10.62) for $L(t)$ has the dependence found in eq. (10.60). Marinari et al. [283] showed that the power spectrum defined by:

$$P(f) = \lim_{T \rightarrow \infty} \frac{1}{T} \left| \int_0^T dt e^{ift} x(t) \right|^2, \quad (10.63)$$

by the same heuristic arguments used above, has approximately a $1/f$ behavior as $f \rightarrow 0$. This dependence is modified by logarithms of the frequency:

$$P(f) \sim (\ln^4 f)/f. \quad (10.64)$$

They further studied a random bias model in two dimensions by Monte-Carlo simulation and found a behavior which was consistent with the one-dimensional model.

The review ends here, but it is hoped that this presentation has whetted the reader's appetite for these problems and she/he will penetrate deeper into the subject. The emphasis of the review was necessarily restricted in order to keep the presentation reasonably coherent and pedagogical. This restriction has meant that omissions were made; for instance, field theoretic renormalization group methods have not been discussed in detail, although there are publications in this area [272, 284–286]. Furthermore quantum-mechanical lattice models also have a large literature [44], but very little progress has been made on these models with disordered transition rates. The theoretical problems are many in this field, so be bold and take up the challenge!

Acknowledgments

Thanks are due to many colleagues for their comments and assistance, especially to J.K. Anlauf, A. Blumen, R. Czech, F. den Hollander, H.B. Huntington, K. Kitahara, R. Kutner, D. Richter, H. van Beijeren and J. Villain. The award of NATO Grant No. RG 85/0119, which accelerated the completion of this review, is also gratefully acknowledged.

References

- [1] H.A. Kramers, *Physica* 7 (1940) 284.
- [2] G.H. Vineyard, *J. Phys. Chem. Sol.* 3 (1957) 121.
- [3] G. Leibfried and N. Breuer, in: *Springer Tracts in Mod. Phys.*, ed. G. Hoehler, 81 (1978) 1; P.H. Dederichs and R. Zeller, *ibid.* 87 (1980) 1.
- [4] H. Haken, *Laser Theory* (Springer, Berlin, 1984).
- [5] L. Arnold and R. Lefever, eds., *Stochastic Nonlinear Systems in Physics, Chemistry and Biology*, Springer Series in Synergetics Vol. 8 (Springer, Berlin, 1981).
- [6] I. Oppenheim, K.E. Schuler and G.H. Weiss, eds., *Stochastic Processes in Chemical Physics: The Master Equation* (MIT Press, Cambridge, Mass., 1977).
- [7] G.H. Weiss and R.J. Rubin, *Adv. in Chem. Phys.* 52 (1983) 363.
- [8] E.W. Montroll and B.J. West, in: *Fluctuation Phenomena*, eds. E.W. Montroll and J.L. Lebowitz (North-Holland, Amsterdam, 1979); M.F. Shlesinger and B.J. West, eds., *Random Walks and Their Applications in the Physical and Biological Sciences*, AIP Conf. Proc. 109 (1984).
- [9] R.L. Stratonovich, *Topics in the Theory of Random Noise*, Vols. 1 and 2 (Gordon and Breach, New York, 1963 and 1967).
- [10] W. Feller, *An Introduction to Probability Theory*, Vols. 1 and 2 (Wiley, New York, 1968 and 1971).
- [11] F. Spitzer, *Principles of a Random Walk* (Van Nostrand, Princeton, NJ, 1964).
- [12] M.N. Barber and B.W. Ninham, *Random and Restricted Walks, Theory and Applications* (Gordon and Breach, New York, 1970).
- [13] N.S. Goel and N. Richter-Dyn, *Stochastic Models in Biology* (Academic Press, New York, 1974).
- [14] N.G. Van Kampen, *Stochastic Processes in Physics and Chemistry* (North-Holland, Amsterdam, 1981).
- [15] S. Chandrasekhar, *Rev. Mod. Phys.* 35 (1943) 1, reprinted in: *Selected Papers on Noise and Stochastic Processes*, ed. N. Wax (Dover, New York, 1954).
- [16] F. Reif, *Fundamentals of Statistical and Thermal Physics* (McGraw-Hill, New York, 1965).
- [17] The Chapman-Kolmogoroff equation was first derived by Bachelier. See the review of Montroll and West in ref. [8] for references on this equation.
- [18] L. van Hove, *Phys. Rev.* 95 (1954) 249.
- [19] C.T. Chudley and R.J. Elliott, *Proc. Phys. Soc. Lond.* 77 (1961) 353.
- [20] J.M. Rowe, J.J. Rush, L.A. de Graaf and G.A. Ferguson, *Phys. Rev. Lett.* 29 (1972) 1250.
- [21] T. Springer, *Springer Tracts in Modern Physics* 64 (Springer, Berlin, 1972).
- [22] D. Richter, *Springer Tracts in Modern Physics* 101 (1983) 85.
- [23] T. Springer and D. Richter, in: *Methods of Experimental Physics*, eds. K. Sköld and D.L. Price (Academic, New York, 1987) Chap. 10.
- [24] E.W. Montroll and G.H. Weiss, *J. Math. Phys.* 6 (1965) 167.
- [25] W. Gissler and H. Rother, *Physica* 50 (1970) 380.
- [26] R. Kutner, I. Sosnowska and W. Kley, *Phys. Stat. Sol. (b)* 89 (1978) K29.

- [27] V. Lottner, J.W. Haus, A. Heim and K.W. Kehr, *J. Phys. Chem. Solids* 40 (1979) 557.
- [28] R. Kutner and I. Sosnowska, *J. Phys. Chem. Solids* 38 (1977) 747.
- [29] J.M. Rowe, K. Skold, H.F. Flotow and J.J. Rush, *J. Phys. Chem. Solids* 32 (1971) 41.
- [30] G. Blaesser and J. Peretti, *Juel-Conf-2, Vol. II* (1968) p. 886.
- [31] V. Lottner, U. Buchenau and W.J. Fitzgerald, *Z. Phys. B35* (1979) 35.
- [32] K.W. Kehr, D. Richter and R.H. Swendsen, *J. Phys. F8* (1978) 433.
- [33] R. Kutner and I. Sosnowska, *J. Phys. Chem. Solids* 38 (1977) 741.
- [34] C.H. Wu and E.W. Montroll, *J. of Nonmetals and Semiconductors* 2 (1973) 153.
- [35] I.S. Anderson, A. Heideman, J.E. Bonnet, D.K. Ross, S.K.P. Wilson and M.W. McKergow, *J. Less Common Met.* 101 (1984) 405.
- [36] See Vol. II of Feller [10].
- [37] M. Lax and H. Scher, *Phys. Rev. Lett.* 39 (1977) 781.
- [38] J.K.E. Tunaley, *Phys. Rev. Lett.* 33 (1974) 1037.
- [39] J.K.E. Tunaley, *J. Stat. Phys.* 11 (1974) 397; 12 (1975) 1; 14 (1976) 461.
- [40] H. Scher and M. Lax, *Phys. Rev. B7* (1973) 4491.
- [41] H. van Beijeren, *Rev. Mod. Phys.* 54 (1982) 195.
- [42] D. Bedeaux, K. Lakatos-Lindenberg and K. Shuler, *J. Math. Phys.* 12 (1971) 2116.
- [43] V.M. Kenkre, E.W. Montroll and M.F. Shlesinger, *J. Stat. Phys.* 9 (1973) 45.
- [44] V.M. Kenkre, *Springer Tracts in Modern Physics* 94 (Springer, Berlin, 1982) p. 1.
- [45] V.M. Kenkre and R.S. Knox, *Phys. Rev. B9* (1974) 5279;
V.M. Kenkre and T.S. Rahman, *Phys. Lett. A* 50 (1974) 170;
V.M. Kenkre, *Phys. Rev. B12* (1975) 2150.
- [46] W.J. Shugard and H. Reiss, *J. Chem. Phys.* 65 (1976) 2827.
- [47] U. Landman, E.W. Montroll and M.F. Shlesinger, *Proc. Natl. Acad. Sci. USA* 74 (1977) 430;
U. Landman and M.F. Shlesinger, *Phys. Rev. B19* (1979) 6207, 6220.
- [48] J.W. Haus and K.W. Kehr, unpublished preprint (1977).
- [49] U. Landman and M.F. Shlesinger, *Phys. Rev. B16* (1977) 3389.
- [50] D.T. Gillespie, *Phys. Lett. A64* (1977) 22.
- [51] M.O. Caceres and H.S. Wio, *Z. Phys. B54* (1984) 175.
- [52] J. Jeans, *Phil. Mag.* 8 (1904) 692.
- [53] M. von Smoluchowski, *Ann. d. Phys.* 21 (1906) 756 (in German).
- [54] R. Fuerth, *Z. Phys.* 2 (1920) 244 (in German).
- [55] G.J. Taylor, *Proc. London Math. Soc.* 20 (1922) 196.
- [56] W. Kuhn, *Kolloid-Z.* 76 (1936) 258; 87 (1939) 3 (in German).
- [57] J. Bardeen and C. Herring, in: *Imperfections in Nearly Perfect Crystals*, ed. W. Shockley (Wiley, New York, 1952) p. 261.
- [58] K. Compaan and Y. Haven, *Trans. Faraday Soc.* 52 (1956) 786.
- [59] J.W. Haus and K.W. Kehr, a) *Solid State Commun.* 26 (1978) 753, b) *J. Phys. Chem. Solids* 40 (1979) 1019.
- [60] Y. Okamura, E. Blaisten-Barojas, S.V. Godoy, S.E. Ulloa and S. Fujita, *J. Chem. Phys.* 76 (1982) 601.
- [61] M.O. Caceres and H.S. Wio, *Z. Phys. B58* (1985) 329.
- [62] C. Domb and M.E. Fisher, *Proc. Camb. Phil. Soc.* 54 (1958) 48.
- [63] J. Gillis, *Proc. Camb. Phil. Soc.* 51 (1955) 639.
- [64] S. Goldstein, *Quart. J. Mech. and Applied Math.* 4 (1951) 129.
- [65] J. Jeulink, L.A. DeGraaf, M.R. Ypma and L.M. Caspers, *Delft Progr. Rep. Series A* 1 (1975) 115.
- [66] Y. Okamura, E. Blaisten-Barojas, S. Fujita and S.V. Godoy, *Phys. Rev. B22* (1980) 1638.
- [67] S.V. Godoy, *J. Chem. Phys.* 78 (1983) 6940.
- [68] W. Zwerger and K.W. Kehr, *Z. Phys. B40* (1980) 157.
- [69] K.W. Kehr, R. Kutner and K. Binder, *Phys. Rev. B23* (1981) 4931.
- [70] E.W. Montroll, *J. Chem. Phys.* 18 (1950) 734.
- [71] C.M. Tchen, *J. Chem. Phys.* 20 (1952) 214.
- [72] R. Kutner, *Solid State Ionics* 9&10 (1983) 1409; *J. Phys. C18* (1985) 6323.
- [73] R.J. Rubin, *J. Chem. Phys.* 20 (1952) 1940.
- [74] P.J. Flory, *Statistical Mechanics of Chain Molecules* (Interscience, New York, N.Y., 1969).
- [75] S. Fujita, Y. Okamura and J.T. Chen, *J. Chem. Phys.* 72 (1980) 3993.
- [76] M.F. Thorpe and W.K. Schroll, *J. Chem. Phys.* 75 (1981) 5143.
- [77] W.K. Schroll, A.B. Walker and M.F. Thorpe, *J. Chem. Phys.* 76 (1982) 6384.
- [78] P.G. deGennes, *Scaling Concepts in Polymer Physics* (Cornell University Press, Ithaca, N.Y., 1979).
- [79] J.W. Halley, H. Nakanishi and S. Sundararajan, *Phys. Rev. B31* (1985) 293.
- [80] P. Argyrakis and R. Kopelman, a) *Phys. Rev. B22* (1980) 1830; b) *Chem. Phys.* 57 (1981) 29; 78 (1983) 251.
- [81] M.F. Shlesinger, *Solid State Commun.* 32 (1979) 1207.

- [82] S. Fujita, Y. Okamura, E. Blaisten and S.V. Godoy, *J. Chem. Phys.* 73 (1980) 4569.
- [83] S. Fujita, E. Blaisten-Barojas, M. Torres and S.V. Godoy, *J. Chem. Phys.* 75 (1981) 3097.
- [84] J.R. Manning, *Diffusion Kinetics for Atoms in Solids* (Van Nostrand, Princeton, N.J., 1968).
- [85] G.L. Montet, *Phys. Rev.* B7 (1973) 650.
- [86] M. Koiwa and S. Ishioka, *J. Stat. Phys.* 30 (1983) 477.
- [87] P. Benoist, J.L. Bocquet and P. LaFore, *Acta Met.* 25 (1977) 265.
- [88] G.V. Kidson, *Phil. Mag.* A37 (1978) 305.
- [89] M. Koiwa, *J. Phys. Soc. Jpn.* 45 (1978) 781.
- [90] H. van Beijeren and K.W. Kehr, *J. Phys. C* 19 (1986) 1319.
- [91] M. Eisenstadt and A.G. Redfield, *Phys. Rev.* 132 (1963) 635.
- [92] D. Wolf, *Phys. Rev.* B10 (1974) 2710; *Solid State Commun.* 23 (1977) 853.
- [93] H. van Beijeren, K.W. Kehr and R. Kutner, *Phys. Rev.* B28 (1983) 5711.
- [94] O. Bender and K. Schroeder, *Phys. Rev.* B19 (1979) 3399.
- [95] G.E. Murch, in: *Diffusion in Crystalline Solids*, eds. G.E. Murch and A.S. Nowick (Academic, Orlando, FL, 1984) p. 379.
- [96] K.W. Kehr and K. Binder, in: *Applications of the Monte Carlo Method in Statistical Physics*, ed. K. Binder, *Topics in Current Physics* 36 (1984) p. 181.
- [97] P.A. Fedders and O.F. Sankey, *Phys. Rev.* B15 (1977) 3580;
O.F. Sankey and P.A. Fedders, *ibid.* 15 (1977) 3586;
P.A. Fedders and O.F. Sankey, *ibid.* 18 (1978) 5938.
- [98] K. Nakazato and K. Kitahara, *Prog. Theor. Phys.* 64 (1980) 2261.
- [99] R.A. Tahir-Kheli and R.J. Elliott, *Phys. Rev.* B27 (1983) 844.
- [100] R.A. Tahir-Kheli, *Phys. Rev.* B27 (1983) 6072.
- [101] R. Kutner, H. van Beijeren and K.W. Kehr, *Phys. Rev.* B30 (1984) 4382.
- [102] H. van Beijeren and R. Kutner, *Phys. Rev. Lett.* 55 (1985) 238.
- [103] J.E. Lennard-Jones, *Trans. Faraday Soc.* 28 (1932) 333.
- [104] J.E. Lennard-Jones, *Proc. Phys. Soc. (London)* 49 (extra part) (1937) 140.
- [105] J.R. Cann, J.G. Kirkwood and R.A. Brown, *Arch. Biochem. Biophys.* 72 (1957) 37.
- [106] J.C. Giddings, *J. Chem. Phys.* 31 (1959) 1462.
- [107] W.P. Helman and K. Funabashi, *J. Chem. Phys.* 71 (1979) 2458.
- [108] M. Lax and P. Mengert, *J. Phys. Chem. Solids* 14 (1960) 248.
- [109] W. van Roosbroeck, *Phys. Rev.* 123 (1961) 474.
- [110] W.E. Teft, *J. Appl. Phys.* 38 (1967) 5265.
- [111] W.D. Lakin, L. Marks and J. Noolandi, *Phys. Rev.* B15 (1977) 5834.
- [112] F.W. Schmidlin, *Solid State Commun.* 22 (1977) 451; *Phys. Rev.* B16 (1977) 2362; *Phil. Mag.* B41 (1980) 535.
- [113] J. Noolandi, *Solid State Commun.* 24 (1977) 477.
- [114] J. Noolandi, *Phys. Rev.* B16 (1977) 4466, 4474.
- [115] G. Pfister and H. Scher, *Adv. Phys.* 27 (1978) 747.
- [116] J. Mort, *Adv. Phys.* 29 (1980) 367.
- [117] K.S. Singwi and A. Sjolander, *Phys. Rev.* 119 (1960) 863.
- [118] A. McNabb and P.K. Foster, *Trans. Met. Soc. AIME* 227 (1963) 618.
- [119] D. Richter, K.W. Kehr and T. Springer, in: *Proc. Conf. on Neutron Scattering*, Gatlinburg, TN, USA, June 6–10, 1976, Vol. 1, ed. R.A. Moon, ORNL and ERDA (1976) p. 568.
- [120] K.W. Schroeder, *Z. Phys.* B25 (1976) 91.
- [121] D. Richter and T. Springer, *Phys. Rev.* B18 (1978) 126.
- [122] V. Balakrishnan and S. Dattagupta, *Z. Phys.* B42 (1981) 13.
- [123] M. Nelkin and A. Harrison, *Phys. Rev.* B26 (1982) 6696.
- [124] M. Borghini, T.O. Niinikoski, J.C. Soulie, O. Hartmann, E. Karlsson, L.O. Norlin, K. Pernestal, K.W. Kehr, D. Richter and E. Walker, *Phys. Rev. Lett.* 40 (1978) 1723.
- [125] K.W. Kehr, G. Honig and D. Richter, *Z. Phys.* B32 (1978) 49.
- [126] K.W. Kehr and J.W. Haus, *Physica* 93A (1978) 412.
- [127] D.R. Cox, *Renewal Theory* (Methuen, London, 1962).
- [128] G.H. Weiss, *J. Stat. Phys.* 8 (1973) 221.
- [129] G.H. Weiss, *J. Stat. Phys.* 15 (1976) 157.
- [130] H. Sillescu, *Adv. Mol. Relax.* 3 (1972) 91.
- [131] K. Lindenberg and R.I. Cukier, *J. Chem. Phys.* 62 (1975) 3271.
- [132] R.S. Hayano, Y.J. Uemura, J. Imazato, N. Nishida, T. Yamazaki and R. Kubo, *Phys. Rev.* B20 (1979) 850.
- [133] J. Bernasconi, S. Alexander and R. Orbach, *Phys. Rev. Lett.* 41 (1977) 185.
- [134] J. Bernasconi, H.U. Beyeler, S. Strassler and S. Alexander, *Phys. Rev. Lett.* 42 (1979) 819.

- [135] J. Bernasconi, W.R. Schneider and W. Wyss, *Z. Physik* B37 (1980) 175.
- [136] S. Alexander, J. Bernasconi, W.R. Schneider and R. Orbach, *Rev. Mod. Phys.* 53 (1981) 175.
- [137] S. Alexander, J. Bernasconi, W.R. Schneider, R. Biller and R. Orbach, *Mol. Cryst. & Liq. Cryst.* 85 (1982) 121.
- [138] R. Zwanzig, *J. Stat. Phys.* 28 (1982) 127.
- [139] P.J.H. Denteneer and M.H. Ernst, *J. Phys.* C16 (1983) L961.
- [140] P.J.H. Denteneer and M.H. Ernst, *Phys. Rev.* B29 (1984) 1755.
- [141] F.J. Dyson, *Phys. Rev.* 92 (1953) 1331;
H. Schmidt, *Phys. Rev.* 105 (1957) 425; reprinted in: E.H. Lieb and D.C. Mattis, *Mathematical Physics in One Dimension* (Academic Press, New York, 1966).
- [142] A. Igarashi, *Prog. Theor. Phys.* 69 (1983) 1031.
- [143] M.J. Stephen and R. Kariotis, *Phys. Rev.* B26 (1982) 2917.
- [144] T.M. Nieuwenhuizen and M.H. Ernst, *Phys. Rev.* B31 (1985) 3518.
- [145] P.M. Richards and R.L. Renken, *Phys. Rev.* B21 (1980) 3740.
- [146] J. Heinrichs, *Phys. Rev.* B22 (1980) 3093; B25 (1982) 1388.
- [147] T. Odagaki and M. Lax, *Phys. Rev. Lett.* 45 (1980) 847; *Mol. Cryst. & Liq. Cryst.* 85 (1982) 129; *Phys. Rev.* B25 (1982) 1392.
- [148] S. Alexander, J. Bernasconi and R. Orbach, *Phys. Rev.* B17 (1978) 4311;
see also J. Bernasconi, *Phys. Rev.* B25 (1982) 1394.
- [149] V.V. Bryksin, *Fiz. Tverd. Tela* 22 (1980) 2048 [English translation: *Sov. Phys.-Solid State* 22 (1980) 1194].
- [150] S. Summerfield, *Sol. St. Commun.* 39 (1981) 401.
- [151] T. Odagaki and M. Lax, *Phys. Rev.* B24 (1981) 5284;
T. Odagaki, M. Lax and A. Puri, *Phys. Rev.* B28 (1983) 2757.
- [152] I. Webman, *Phys. Rev. Lett.* 47 (1981) 1496.
- [153] J.W. Haus, K.W. Kehr and K. Kitahara, *Phys. Rev.* B25 (1982) 4918.
- [154] I. Webman and J. Klafter, *Phys. Rev.* B26 (1982) 5950.
- [155] J.W. Haus, K.W. Kehr and K. Kitahara, *Z. Physik* B50 (1983) 161.
- [156] M. Sahimi, B.D. Hughes, L.E. Scriven and H.T. Davis, *J. Chem. Phys.* 78 (1983) 6849.
- [157] S. Katsura, T. Morita, S. Inawashiro, T. Horiguchi and Y. Abe, *J. Math. Phys.* 12 (1971) 892;
T. Horiguchi, *J. Math. Phys.* 13 (1972) 1411.
- [158] P.B. Visscher, *Phys. Rev.* B29 (1984) 5472.
- [159] R. Kariotis, *J. Phys.* A17 (1984) 2889.
- [160] J.P. Clerc, G. Giraud, J. Rousseny, R. Blanc, J.P. Carton, E. Guyon, H. Ottavi and D. Stauffer, *Ann. Phys. (France)* 8 (1983) 5 (in French).
- [161] S. Kirkpatrick, *Rev. Mod. Phys.* 45 (1973) 574.
- [162] J.W. Essam, in: *Phase Transitions and Critical Phenomena*, Vol. 2, eds. C. Domb and M.S. Green (Academic, New York, 1972).
- [163] P.G. de Gennes, *La Recherche* 7 (1976) 919.
- [164] D. Stauffer, *Phys. Reports* 54 (1979) 1; *Introduction to Percolation Theory* (Taylor and Francis, London, 1985).
- [165] J.M. Ziman, *J. Phys.* C1 (1968) 1532.
- [166] G.N. Watson, *Quart. J. Math.* 10 (1939) 266.
- [167] P.C. Hohenberg and B.I. Halperin, *Rev. Mod. Phys.* 49 (1977) 435.
- [168] R. Bausch, H.K. Janssen and W. Wagner, *Z. Phys.* B24 (1976) 113.
- [169] F. Haake, M. Lewenstein and M. Wilkens, *Z. Phys.* B54 (1984) 333 and references therein.
- [170] J. Machta, *Phys. Rev.* B24 (1981) 5260; *J. Stat. Phys.* 30 (1983) 305.
- [171] P.B. Visscher, *Phys. Rev.* B29 (1984) 5462.
- [172] R.A. Guyer, *Phys. Rev.* A29 (1984) 2114.
- [173] C.E.T. Goncalves de Silva and B. Koiller, *Solid State Commun.* 40 (1981) 215.
- [174] P.W. Anderson, in: *La Matière Mal Condensée – III Condensed Matter*, eds. R. Balian, R. Maynard and G. Toulouse (North-Holland, Amsterdam, 1979) p. 159.
- [175] See Vol. 2 of Feller [10].
- [176] J.W. Haus and K.W. Kehr, *Phys. Rev.* B28 (1983) 3573.
- [177] J. Klafter and R. Silbey, *Phys. Rev. Lett.* 44 (1980) 55.
- [178] R. Zwanzig, in: *Lectures in Theoretical Physics*, eds. W.E. Brittin, B.W. Downs and J. Downs (Interscience, New York, 1961) Vol. 3, p. 106.
- [179] F. Haake, *Springer Tracts in Modern Physics* 66 (1973) 98.
- [180] H. Scher and M. Lax, *J. Non-Crystalline Solids* 8–10 (1972) 497.
- [181] Further discussion can be found in: S. Kivelson, *Phys. Rev.* B21 (1980) 5755.
- [182] J.W. Haus, K.W. Kehr and J.W. Lyklema, *Phys. Rev.* B25 (1982) 2905.
- [183] K. Schroeder, *Proc. Intern. Conf. on Fundamental Aspects of Radiation Damage in Metals*, ERDA CONF751006, Vol. 1, eds. M.T. Robinson and F.W. Young Jr. (1975) p. 525.
- [184] T.M. Nieuwenhuizen and M.H. Ernst, *Phys. Rev.* B31 (1985) 3518.
- [185] K.W. Kehr and D. Richter, *Solid State Commun.* 20 (1976) 477.

- [186] R.J. Elliott, J.A. Krumhansl and P.L. Leath, *Rev. Mod. Phys.* 46 (1974) 465.
- [187] K.W. Kehr, D. Richter and K. Schroeder, in: *Neutron Inelastic Scattering 1977* (International Atomic Energy Agency, Vienna, 1978), Vol. II, p. 399.
- [188] P.A. Fedders, *Phys. Rev.* B16 (1977) 4769.
- [189] V. Halpern, *J. Stat. Phys.* 30 (1983) 373.
- [190] J. Machta, M. Nelkin, T.M. Nieuwenhuizen and M.H. Ernst, *Phys. Rev.* B31 (1985) 7636.
- [191] S. Alexander, *Phys. Rev.* B23 (1981) 2951.
- [192] J. Machta, *J. Phys.* A18 (1985) L531.
- [193] H. van Beijeren, *Rev. Mod. Phys.* 54 (1982) 195.
- [194] M. Abramowitz and I.A. Stegun, eds., *Handbook of Mathematical Functions* (US Government Printing Office, Washington, DC, 1965).
- [195] K.W. Kehr and R. Kutner, *Physica* 110A (1982) 535.
- [196] R. Kutner, *J. Phys.* C18 (1985) 6323.
- [197] H. van Beijeren and R. Kutner, *Phys. Rev. Lett.* 55 (1985) 238.
- [198] R.A. Tahir-Kheli and R.J. Elliott, *Phys. Rev.* B27 (1983) 844.
- [199] K. Kaski, R.A. Tahir-Kheli and R.J. Elliott, *J. Phys.* C15 (1982) 209.
- [200] T. Keyes and J.W. Lyklema, *J. Stat. Phys.* 27 (1982) 487.
- [201] R.F. Loring, H.C. Anderson and M.D. Fayer, *Phys. Rev. Lett.* 50 (1983) 1324.
- [202] C.R. Gochanour, H.C. Anderson and M.D. Fayer, *J. Chem. Phys.* 70 (1979) 4254.
- [203] S.W. Haan and R. Zwanzig, *J. Chem. Phys.* 68 (1978) 1879.
- [204] R.A. Tahir-Kheli, *Phys. Rev.* B28 (1983) 3049.
- [205] D. Stauffer, *Phys. Reports* 54 (1979) 1.
- [206] R. Kutner and K.W. Kehr, *Phil. Mag.* A48 (1983) 199.
- [207] B.B. Mandelbrot, *The Fractal Geometry of Nature* (Freeman, San Francisco, 1983).
- [208] S. Alexander and R. Orbach, *J. Phys. (Paris) Lett.* 43 (1982) L625.
- [209] Y. Termonia, *Phys. Rev. Lett.* 53 (1984) 1356.
- [210] Y. Gefen, A. Aharony, B.B. Mandelbrot and S. Kirkpatrick, *Phys. Rev. Lett.* 47 (1981) 1771.
- [211] S. Harlin and D. Ben-Avraham, *J. Phys.* A15 (1982) L311;
D. Ben-Avraham and S. Havlin, *J. Phys.* A15 (1982) L691.
- [212] P. Argyrakis and R. Kopelman, *Phys. Rev.* B29 (1984) 511.
- [213] R. Hilfer and A. Blumen, *J. Phys.* A17 (1984) L537.
- [214] D. Dhar, *J. Math. Phys.* 18 (1977) 577; 19 (1978) 5.
- [215] R. Rammal and G. Toulouse, *J. Phys. (Paris) Lett.* 44 (1983) L13.
- [216] R.A. Guyer, *Phys. Rev.* A29 (1984) 2751; A30 (1984) 1112.
- [217] A. Blumen, J. Klafter, B.S. White and G. Zumofen, *Phys. Rev. Lett.* 53 (1984) 1301.
- [218] B. Derrida, R. Orbach and K.-W. Yu, *Phys. Rev.* B29 (1984) 6645;
R. Orbach, *J. Stat. Phys.* 36 (1984) 735.
- [219] S. Kelham and R. Rosenberg, *J. Phys.* C14 (1981) 1737;
M.P. Zaitlin and A.C. Anderson, *Phys. Rev.* B12 (1975) 4475.
- [220] G.H. Weiss, *J. Stat. Phys.* 24 (1981) 587.
- [221] F. Oberhettinger and L. Badii, *Tables of Laplace Transforms* (Springer, Berlin, 1973).
- [222] V. Balakrishnan and M. Khanta, *Pramana* 21 (1983) 187.
- [223] E. Schroedinger, *Phys. Zeits.* 16 (1915) 289 (in German);
see also, A.J.F. Siegert, *Phys. Rev.* 81 (1951) 617;
D.A. Darling and A.J.F. Siegert, *Ann. Math. Stat.* 24 (1953) 624.
- [224] W.Th.F. den Hollander, *J. Stat. Phys.* 37 (1984) 331.
- [225] E.W. Montroll, *J. Soc. Ind. Appl. Math.* 4 (1956) 241; in: *Proc. Sixteenth Symp. in Applied Mathematics*, Vol. 16 (1964) p. 193.
- [226] F.S. Henyey and V. Seshadri, *J. Chem. Phys.* 76 (1982) 5530.
- [227] J.U. Keller, *Z. Naturf.* 26a (1971) 1539 (in German).
- [228] K.W. Kehr and P. Argyrakis, *J. Chem. Phys.* 84 (1986) 5816.
- [229] H.E. Stanley, K. Kang, S. Redner and R.L. Blumberg, *Phys. Rev. Lett.* 51 (1983) 1223.
- [230] H.B. Rosenstock, *Phys. Rev.* 187 (1969) 1166.
- [231] H.B. Rosenstock, *J. Math. Phys.* 21 (1980) 1643.
- [232] H.B. Rosenstock and J.P. Straley, *Phys. Rev.* B24 (1981) 2540.
- [233] A. Blumen and G. Zumofen, *J. Stat. Phys.* 30 (1983) 487.
- [234] G. Zumofen and A. Blumen, *Chem. Phys. Lett.* 88 (1982) 63.
- [235] G.H. Weiss, *Proc. Natl. Acad. Sci. USA* 77 (1980) 4391.
- [236] N.C. Jain and W.E. Pruitt, *J. d'Analyse Math.* 24 (1971) 369.
- [237] B.Ya. Balagurov and V.G. Vaks, *Zh. Eksp. Teor. Fiz.* 65 (1973) 1939 [English translation: *Sov. Phys.-JETP* 38 (1974) 968].

- [238] I.M. Lifshitz, *Usp. Fiz. Nauk* 83 (1964) 617 [English translation: *Sov. Phys.-Uspekhi* 7 (1965) 549].
- [239] M.D. Donsker and S.R.S. Varadhan, *Commun. Pure Appl. Math.* 28 (1975) 525.
- [240] M.D. Donsker and S.R.S. Varadhan, *Commun. Pure Appl. Math.* 32 (1979) 721.
- [241] F. Delyon and B. Souillard, *Phys. Rev. Lett. (Comments)* 51 (1983) 1720.
- [242] P. Grassberger and I. Procaccia, *J. Chem. Phys.* 77 (1982) 6281.
- [243] R.F. Kayser and J.B. Hubbard, *Phys. Rev. Lett.* 51 (1983) 79.
- [244] J. Anlauf, Diploma thesis, Universitaet zu Koeln, unpublished (in German).
- [245] J. Anlauf, *Phys. Rev. Lett.* 52 (1984) 1845.
- [246] B. Movaghar, G.W. Sauer and D. Wuertz, *J. Stat. Phys.* 27 (1982) 473;
B. Movaghar, G.W. Sauer, D. Wuertz and D.L. Huber, *Solid State Commun.* 39 (1981) 1179.
- [247] T. Lubensky, *Phys. Rev.* A30 (1984) 2657.
- [248] S. Havlin, M. Dishon, J.E. Kiefer and G.H. Weiss, *Phys. Rev. Lett.* 53 (1984) 407.
- [249] W.Th.F. den Hollander and P.W. Kasteleyn, *Physica* 117A (1983) 179.
- [250] C.K. Hu and H.B. Huntington, *Phys. Rev.* B26 (1982) 2782.
- [251] P.A. Totta and R.P. Sopher, *IBM J. Res. and Develop.* 13 (1969) 226.
- [252] W.K. Warburton and D. Turnbull, in: *Diffusion in Solids: Recent Developments*, eds. A.S. Nowick and J.J. Burton (Academic, New York, 1975) p. 125.
- [253] H.G. Haubold, *Rev. Phys. Appl.* 11 (1976) 73.
- [254] W. Schmatz, in: *A Treatise on Materials Science and Technology*, 2, ed. H. Hermans (Academic, New York, 1973).
- [255] J.K.E. Tunaley, *J. Stat. Phys.* 15 (1976) 149.
- [256] M. Nelkin and A.K. Harrison, *Phys. Rev.* B26 (1982) 6696.
- [257] P. Dutta and P.M. Horn, *Rev. Mod. Phys.* 53 (1981) 497.
- [258] F.N. Hooge, T.G.M. Kleinpenning and L.K.J. Vandamme, *Rep. Prog. Phys.* 44 (1981) 479.
- [259] C.J. Stanton and M. Nelkin, *J. Stat. Phys.* 37 (1984) 1.
- [260] R.F. Voss and J. Clarke, *Phys. Rev. Lett.* 36 (1976) 42.
- [261] H. Boettger and V.V. Bryksin, *Phys. Status Solidi* 113 (1982) 9.
- [262] M. Barma and D. Dhar, *J. Phys.* C16 (1983) 1451 and references therein.
- [263] S.R. White and M. Barma, *J. Phys.* A17 (1984) 2995.
- [264] R.B. Pandey, *Phys. Rev.* B30 (1984) 489.
- [265] B. Derrida and R. Orbach, *Phys. Rev.* B27 (1983) 4694.
- [266] R. Biller, *Z. Phys.* B55 (1984) 7.
- [267] W. Lehr, J. Machta and M. Nelkin, *J. Stat. Phys.* 36 (1984) 15.
- [268] T.M. Nieuwenhuizen and M.H. Ernst, in: *Kinetics of Aggregation and Gelation*, eds. F. Family and D.P. Landau (Elsevier, Amsterdam, 1984) p. 249.
- [269] T.M. Nieuwenhuizen and M.H. Ernst, *Phys. Rev.* B33 (1986) 2824.
- [270] K. Khantha and V. Balakrishnan, *Phys. Rev.* B29 (1984) 4679.
- [271] B. Derrida and J.M. Luck, *Phys. Rev.* B28 (1983) 7183.
- [272] J.M. Luck, *Nucl. Phys.* B225 (1983) 169.
- [273] A.A. Chernov, *Biofizika* 12 (1967) 297 [English translation: *Biophysics* 12 (1967) 336].
- [274] D.E. Tempkin, *Dokl. Akad. Nauk SSSR* 206 (1972) [English translation: *Sov. Math. Dokl.* 13 (1972) 1172].
- [275] D.E. Tempkin, *Fiz. Tverd. Tela* 13 (1971) 3381 [English translation: *Sov. Phys.-Solid State* 13 (1972) 2840].
- [276] S.A. Kalikow, *Ann. of Probability* 9 (1981) 753.
- [277] F. Solomon, *Ann of Probability* 3 (1975) 1.
- [278] H. Kesten, M.V. Kozlov and F. Spitzer, *Compositio Math.* 30 (1975) 145.
- [279] Ya. G. Sinai, *Lecture Notes in Physics* 153 (Springer, Berlin, 1982) p. 12; *Teop. Bepo.* 27 (1982) 247 (in Russian).
- [280] B. Derrida and Y. Pomeau, *Phys. Rev. Lett.* 48 (1982) 627.
- [281] B. Derrida, *J. Stat. Phys.* 31 (1983) 433.
- [282] J. Bernasconi and W.R. Schneider, *J. Phys.* A15 (1983) L729.
- [283] E. Marinari, G. Parisi, D. Ruelle and P. Windey, *Phys. Rev. Lett.* 50 (1983) 1223; *Commun. Math. Phys.* 89 (1982) 1.
- [284] J.L. Cardy, *J. Phys.* A16 (1983) L355.
- [285] D.S. Fisher, *Phys. Rev.* A30 (1984) 960.
- [286] D.S. Fisher, D. Friedan, Z. Qiu, S.J. Shenker and S.H. Shenker, *Phys. Rev.* A31 (1985) 3841.

Notes added in proof

The flow of publications on the subject of the review does not diminish, although the emphasis on particular topics is shifting. Below some references on developments will be given which we found interesting. Of course, we could not be complete. Another review with emphasis on complementary topics, e.g., percolation, many diffusing particles, etc., is in preparation [287]. Applications of stochastic hopping models to the calculation of correlation functions are described in the book [288].

More complicated jump models for two-dimensional diffusion were considered in [289] and the diffusion coefficient for models with multiple transition rates was derived in [290].

The fact that multistate CTRW does exhibit a frequency-dependent diffusion coefficient was demonstrated in a quasi-one-dimensional model [291]. A model equivalent to non-Poissonian WTD was treated in [292] and correlated-jump models with general WTD were considered in [293]. An interesting extension of multistate random walk to networks where partial summations on internal states are performed is given in [294]. New results for correlated random walks that are continuous in space and discrete in time are found in [295].

Experiments on photoconductivity in amorphous materials over many decades in time showed a transition from dispersive to nondispersive transport [296]. This is consistent with models discussed in chapter 5 if a finite maximal trap depth is assumed. The two-state model was used in the analysis of quasielastic neutron-scattering experiments on hydrogen diffusion in a metglass [297].

A simplified treatment of the low-frequency conductivity of the one-dimensional random-barrier model was given in [298]. An anomalous long-time behavior of the diffusion process of the broken-bond model was found in [299], after averaging over the distribution of the segment lengths. The random-resistor network, corresponding to two different transition rates, was studied in a systematic density expansion in [300]. Quasi-one-dimensional models with a power-law distribution of the conductivities were considered in [301]. An interesting extension is the case where one transition rate becomes infinite; this gives the ‘termite models’. They were studied, e.g., in [302] when the other transition rate is zero, and in [303] when this rate is a random quantity. The frequency dependence of the diffusion coefficient of such models was studied in the frame of the EMA in [304].

It was recently asserted [305] that there are oversights in the proof [182] of the strictly linear behavior of the mean-square displacement in the random-trap model. Reference [182] establishes this behavior for infinite lattices, including the case of periodic boundary conditions. It is obvious that corrections appear for reflecting boundary conditions and they are derived in [305]. A previous article is concerned with nonstationary initial conditions [306].

The model of random walk on a random walk was applied to diffusion in channels in [307]. A model of diffusion of hierarchical lattices was studied in [308]. The problem of diffusion in the model with randomly blocked sites and bonds was treated exactly in a low-density expansion by the Utrecht group [309, 310]. A subject matter of recently growing interest is random walk in ultrametric spaces, here the reader is referred to [311–314] as examples.

First-passage time properties such as probability of return to the origin and mean number of distinct sites visited were investigated in [315] for multistate random walk. The application to correlated random walk was made in [316]. The exponential decay of the survival probability in a finite lattice with a single trap was established in [317, 318]; these references contain also other useful exact results. The survival probability of a particle diffusing by correlated walk in the presence of traps was derived in [319]. An important numerical technique for studying the trapping problem in higher dimensions was devised in [320]. The survival probability and trapping probability on a site were calculated for partially

absorbing traps in [321]. The survival probability of a particle diffusing in medium with connected traps was considered in [322]. Also the influence of bias on the survival probability of a particle on a linear chain has been discussed, cf., e.g., ref. [323].

The frequency-dependent conductivity in a model with random barriers, random sites energies, and a static bias field was investigated in [324]. A Monte-Carlo study of similar models was undertaken in [325]. Diffusion in one-dimensional models with attached random ladders and a 'topological bias' were considered in [326, 327]. 'Anomalous ballistic diffusion' was found in a superconducting linear chain model with randomly inserted resistors [328]. We reiterate that these references represent only a selection of some recent developments in this field.

- [287] S. Havlin and D. Ben-Avraham, in preparation for *Adv. Phys.* (1987).
- [288] S. Dattagupta, *Relaxation Phenomena – Spectroscopy, Correlation Functions and Stochastic Models* (Academic Press, New York, 1987).
- [289] A. Magerl, H. Zabel and I.S. Anderson, *Phys. Rev. Lett.* 55 (1985) 222.
- [290] S. Ishioka and M. Koiwa, *Phil. Mag.* A52 (1985) 267.
- [291] T. Odagaki, M. Lax and R.S. Day, *Phys. Rev. B*30 (1984) 6911.
- [292] S.D. Druger, M.A. Ratner and A. Nitzan, *Phys. Rev. B*31 (1985) 3939.
- [293] R. Kutner, *Phys. Stat. Sol. (b)* 135 (1986) 535.
- [294] I. Goldhirsch and Y. Gefen, *Phys. Rev. A*33 (1986) 2583.
- [295] T.M. John and K.P.N. Murthy, *J. Stat. Phys.* 45 (1986) 753.
- [296] E. Mueller-Horsche, D. Haarer and H. Scher, *Phys. Rev. B*35 (1987) 1273.
- [297] D. Richter, G. Driesen, R. Hempelmann and I.S. Anderson, *Phys. Rev. Lett.* 57 (1986) 731.
- [298] R. Biller, *Phys. Rev. B*29 (1984) 2277.
- [299] B. Pohlmann, D. Wuertz and B. Movaghar, unpublished preprint (1982).
- [300] M.H. Ernst, P.F.J. van Velthoven and Th.M. Nieuwenhuizen, *J. Phys. A* (in the press).
- [301] S. Havlin, A. Bunde, H. Weissman and A. Aharony, *Phys. Rev. B*35 (1987) 397.
- [302] D.C. Hong, H.E. Stanley, A. Coniglio and A. Bunde, *Phys. Rev. B*33 (1986) 4564.
- [303] S. Havlin, A. Bunde and J. Kiefer, *J. Phys. A*19 (1986) L419.
- [304] T. Odagaki, *Phys. Rev. B*33 (1986) 544.
- [305] K. Kundu, P. Phillips, I. Oppenheim and K. Kassner, preprint (1987).
- [306] K. Kundu and P. Phillips, *Phys. Rev. A*35 (1987) 857.
- [307] D.A. Huckaby and J.B. Hubbard, *Physica* 122A (1983) 602.
- [308] S.H. Liu and A. Liu, *Phys. Rev. B*34 (1986) 343.
- [309] Th.M. Nieuwenhuizen, P.F.J. van Velthoven and M.H. Ernst, *Phys. Rev. Lett.* 57 (1986) 2477.
- [310] M.H. Ernst and P.F.J. Velthoven, *J. Stat. Phys.* 45 (1986) 1001.
- [311] B.A. Huberman and M. Kerszberg, *J. Phys. A*18 (1985) L331.
- [312] A.T. Ogielski and D.L. Stein, *Phys. Rev. Lett.* 55 (1985) 1634.
- [313] S. Teitel and E. Domany, *Phys. Rev. Lett.* 55 (1985) 2176.
- [314] A. Blumen, G. Zumofen and J. Klafter, *J. Phys. A*19 (1986) L861.
- [315] J.B.T.M. Roerdink and K.E. Shuler, *J. Stat. Phys.* 40 (1985) 205; 41 (1985) 581.
- [316] J.B.T.M. Roerdink, *J. Appl. Prob.* 22 (1985) 951.
- [317] G.H. Weiss, S. Havlin and A. Bunde, *J. Stat. Phys.* 40 (1985) 191.
- [318] W. Th. F. den Hollander, *J. Stat. Phys.* 40 (1985) 201.
- [319] J.K. Anlauf, K.W. Kehr and S. Reulein, submitted to *J. Stat. Phys.*
- [320] H. Meirovitch, *Phys. Rev. A*32 (1985) 3699.
- [321] G.H. Weiss, *J. Stat. Phys.* 44 (1986) 933.
- [322] A.R. Kerstein, *Phys. Rev. B*32 (1985) 3361.
- [323] B. Movaghar, B. Pohlmann and D. Wuertz, *Phys. Rev. A*29 (1984) 1586.
- [324] S.K. Lyo, *Phys. Rev. B*33 (1986) 2179.
- [325] K.W. Wu and P.M. Hui, *Phys. Rev. A*33 (1986) 2745.
- [326] A. Bunde, S. Havlin, H.E. Stanley and G.H. Weiss, *Phys. Rev. B*34 (1986) 8129.
- [327] S. Havlin, A. Bunde, Y. Glaser and H.E. Stanley, *Phys. Rev. A*34 (1986) 3492.
- [328] S. Havlin, A. Bunde and H.E. Stanley, *Phys. Rev. B*34 (1986) 445.